Nature and Origin of Black Carbon in Ireland

A thesis submitted to

THE NATIONAL UNIVERSITY OF IRELAND, CORK

for the degree of

DOCTOR OF PHILOSOPHY

by

Paul Christopher Buckley

Based on research carried out at

School of Chemistry

&

Environmental Research Institute

Supervisor

Professor John Wenger

Head of Department

Dr Humphrey Moynihan

University College Cork _____ December 2019

Contents

Declaration

This is to certify that the work I am submitting is my own and has not been submitted for another degree, either at University College Cork or elsewhere. All external references and sources are clearly acknowledged and identified within the contents. I have read and understood the regulations of University College Cork concerning plagiarism.

_____

Paul Buckley

Dedication

For my family, past and present

Quotation

"*Fly the rank city, shun its turbid air,*

Breathe not the chaos of eternal smoke

And volatile corruption"

John Armstrong, *The Art of Preserving Health*, 1744

Funding Statement

The research presented in this thesis is supported by a Government of Ireland Postgraduate Scholarship (GOIPG/2015/3051) titled “The Nature and Origin of Black Carbon in Ireland”.

This project, which is administered by the Irish Research Council is funded by the EPA Research Programme 2014-2020. The EPA Research Programme, which has the statutory function of co-ordinating and promoting environmental research is a Government of Ireland initiative funded by the Department of Communications, Climate Action and Environment.

Preface

The work presented in this thesis belongs to a body of research carried out at University College Cork (UCC) and incorporates field studies conducted in Killarney, Enniscorthy, Birr and Dublin, Ireland. This work is linked to two projects funded by the Environmental Protection Agency (EPA); Source Apportionment of Particulate Matter in Urban and Rural Areas of Ireland (SAPPHIRE), project ID 2013-EH-MS-15, and Source Apportionment of airborne pollutants transported too and across Ireland using Aerosol Mass Spectrometry and Positive Matrix Factorization Techniques (AEROSOURCE), project ID 2016-CCRP-MS-31.

In co-operation with Dr Stig Hellebust, Dr Ian O'Connor, Dr Eoin McGillicuddy, and Dr Jovanna Arndt, this author was responsible for the operation and maintenance of a wide range of UCC owned instruments during the SAPPHIRE campaign. Specifically this author was responsible for day-to-day running of the campaign in Birr, while Dr O'Connor and Dr McGillicuddy managed the campaigns in Killarney and Enniscorthy. As part of the AEROSOURCE campaign, run in co-operation with Dr Chunshui Lin, Dr Jurgita Ovadnevaite and Dr Darius Ceburnis, from the National University of Ireland, Galway (NUIG), this author was in charge of operating and maintaining UCC's aethalometer instrument. The analysis of the aethalometer data presented and discussed in this work was carried out by the author, with advice from Dr Gary Fuller (King's College London, UK) and Dr Griša Močnik (Aerosol d.o.o., Slovenia). The analysis of the ATOFMS data collected during the SAPPHIRE campaigns was initially carried out by Dr Jovanna Arndt, and was repeated by the author during this study. The analysis of the data gathered by the ACSM during the AEROSOURCE project was carried out by Dr Chunshui Lin (NUIG). The historical air pollution data presented in this thesis was provided by Martin Fitzpatrick (Dublin City Council), Prof Pat Goodman (Technological University Dublin) and Dr Gary Fuller. The author collated and analysed this data with some guidance from Dr Gary Fuller.

Acknowledgements

My time in the CRAC lab has been a period of many changes for myself, the group and the lab. There have been two constants however in this period. Prof John Wenger has been an ever present source of advice, support and encouragement, and I will be eternally grateful to him for everything. He took me in as a summer intern and I think it has worked out very well for us both! The second constant has been Prof John Sodeau, who has not changed in the six years I have known him. The "Old Man" provided welcome comic relief, sage advice, and a couple of scares along the way… It is safe to say my experience would not have been the same without him. Most of my insight into the world of data analysis came from Dr Stig Hellebust, from our nights in Birr, to discussions in the office, Stig opened my eyes to the world of code writing and for that I am sincerely grateful. To Dr Dean Venables, thank you for taking the time to assess and advise for the last number of years. Finally to Dr Trevor Carey, your help, advice, and continued friendship means a great deal to me. Our tour of Munster's best carvery restaurants provided many welcome breaks from the writing process.

I have had the pleasure of working with many great people in the CRAC lab. When I started as a summer intern Jovanna, Eoin Mc, Eoin Wilson, Dave and Ian made me feel welcome and helped me settle in. When I started on my postgrad journey, all of the advice about instruments, data analysis, and simply how to be a good researcher was greatly appreciated. I was sad to see you all move on but the continued support has meant a lot to me. Of course as one era ends a new one begins and Paddy, Mike and Shane certainly made years 1 and 2 more enjoyable. From visiting a composting site, to judging the CRAC lab Master Chef in Valentia, we always had a laugh and it was always interesting. As the lads left for pastures new, some fresh faces arrived; Meheal, Niall, Eimear, Elena and most recently Hayley and Julien, who have made the last couple of years easier. The sporting commentary and Simpsons references have made the many early mornings and late nights more manageable. To Eimear, your continued support, patience and love has made a hard journey significantly more enjoyable. You have stuck with me and I look forward to what the future holds.

I would also like to thank those from outside the group who have helped me. In particularly I must mention Dr Gary Fuller and Dr Griša Močnik, the insight and

advice you have given me has been invaluable and has helped me gain a better understanding of my work.

I have had the pleasure of travelling to many new places during the last few years; Kyoto, Zurich, Ljubljana, Leipzig, Vienna, Gothenburg, Birmingham and, the most glamourous of all… Birr, Co. Offaly! All of these trips have been made infinitely better by the company of many CRAC members and the memories will last a lifetime!

Finally I would like to thank my family and friends. To my friends, you have kept me grounded over the last few years and stopped me from losing the run of myself! To all of my family, especially Mam, Dad, my sister Jen, and my grandparents, your lasting love and support have helped me navigate the tough road that is completing a PhD. It has not always been easy, but we got there and I hope I've made you all proud. I love you all.

Now, on to the next adventure…

Abstract

Black carbon (BC) particles are important atmospheric radiative forcing agents and also have a negative effect on human health. In this study, a seven wavelength, dual spot aethalometer, was used to determine the equivalent BC (eBC) concentrations at four locations in Ireland; Killarney, Enniscorthy, Birr and Dublin. The aethalometer data were combined with other measurements and meteorological parameters to determine the sources of the particles observed at the monitoring sites.

The mean eBC concentrations measured in Killarney and Enniscorthy were higher than those in Dublin during the winter months, while the concentrations in Birr were only marginally lower. The aethalometer source apportionment model was used to show that domestic solid fuel burning accounted for 61%, 81% and 63% of eBC mass in Killarney, Enniscorthy and Birr respectively. The average diurnal profiles for eBC at these three locations showed a minor peak during morning hours attributed to traffic and a very large peak during the evening due to solid fuel burning. Results from two years of continuous measurements at an urban background location in Dublin, showed a strong seasonal variation in eBC. Higher concentrations were measured during winter due to solid fuel burning, which accounted for 57% of eBC during the winter of 2016/2017, and 50% during the winter of 2017/2018. The diurnal profile for Dublin during winter was similar to that observed at the other three sites. During summer, eBC levels were much lower and dominated by traffic emissions.

The parameters used in the source apportionment model were explored and site-specific absorption Ångström exponents (α) and Mass Absorption Cross-section (MAC) values were also derived to provide an indication of the different aerosol properties at each location. The results of the source apportionment at all four sites correlate strongly with those from other instruments deployed during the campaigns.

The BC levels recorded in Dublin were compared to historical measurements of black smoke in Dublin, Belfast, London and Paris, from 1963 to 2003. Large decreases in BS concentrations (over 90%) have been observed in each city and are related to legislative changes introduced in each jurisdiction over the decades.

Overall, this work has highlighted the ability of the aethalometer to measure eBC concentrations in real-time and derive contributions from both solid fuel burning and traffic emissions.

List of Abbreviations and Acronyms

AEROSOURCE	Source Apportionment of airborne pollutants transported too and across Ireland using Aerosol Mass Spectrometry and Positive Matrix Factorization Techniques
ACSM	Aerosol Chemical Speciation Monitor
AMS	Aerosol Mass Spectrometer
APHEA	Air Pollution and Health: A European Approach
AQEG	Air Quality Expert Group
ARIMA	Auto-regressive Integrated Moving Average
ATN	Attenuation
ATOFMS	Aerosol Time of Flight Mass Spectrometer
BB	Biomass Burning
BBOA	Biomass Burning Organic Aerosol
BC	Black Carbon
BrC	Brown Carbon
BS	Black Smoke
BSI	Black Smoke Index
CARB	California Air Resources Board
CC	Closed Combustion
CCN	Cloud Condensation Nuclei
CF	Coating Factor
CFC	Chlorofluorocarbon
Chl	Chloride
CLRTAP	Convention on Long-range Transboundary Air Pollution
COA	Cooking Organic Aerosol
COH	Coefficient of Haze
COPD	Chronic Obstructive Pulmonary Disorder
COSMOS	Continuous Soot Monitoring System
DCC	Dublin City Council
DEFRA	Department for Environment, Food and Rural Affairs
D_p	Particle Diameter
DSF	Domestic Solid Fuel

D_{ve}	Volume Equivalent Diameter
eBC	Equivalent Black Carbon
eBC_{SF}	Solid Fuel Burning related equivalent Black Carbon
eBC_{Tr}	Traffic related equivalent Black Carbon
EC	Elemental Carbon
ECLIPSE	Evaluating the Climate and Air Quality Impacts of Short-lived Pollutants
EEA	European Environment Agency
EEC	European Economic Community
EMEP	European Monitoring and Evaluation Programme
ENCHILADA	Environmental Chemistry through Intelligent Atmospheric Data Analysis
EPA	Environmental Protection Agency
ERFaci	Effective Radiative Forcing due to aerosol – cloud interactions
EUSAAR	European Supersites for Atmospheric Aerosol Research
FF	Fossil Fuel
GDP	Gross Domestic Product
HAP	Household Air Pollution
HCFC	Hydrochlorofluorocarbon
HOA	Hydrocarbon-like Organic Aerosol
HR-ToF-AMS	High Resolution Time-of-Flight Aerosol Mass Spectrometer
IMPROVE	Interagency Monitoring of Protected Visual Environments
IN	Ice Nuclei
IPCC	Intergovernmental Panel on Climate Change
IR	Infra-red
LED	Light Emitting Diode
LII	Laser Induced Incandescence
LMI	Laser Modulated Incandescence
LPG	Light Petroleum Gas
LV-OOA	Low-volatility Oxygenated Organic Aerosol
MAAP	Multi-angle Absorption Photometer
MAC	Mass Absorption Cross-section

MEGAPOLI	Megacities: Emissions, urban, regional and Global Atmospheric Pollution and climate effects, and integrated tools for assessment and mitigation
NDIR	Non-disperse Infrared
Nd:YAG	Neodymium doped Yttrium Aluminium Garnet
NIOSH	National Institute for Occupational Safety and Health
NJDEP	New Jersey Department of Environmental Protection
NMVOC	Non-Methane Volatile Organic Compound
NOA	Nitrogen-enriched Organic Aerosol
NOAA	National Oceanic and Atmospheric Administration
NSMC	North South Ministerial Council
OA	Organic Aerosol
OB	Open Burning
OC	Organic Carbon
OECD	Organisation for Economic Cooperation and Development
OOA	Oxygenated Organic Aerosol
OPS	Optical Particle Sizer
Org	Organic
PAS	Photoacoustic Spectrometer
PCA	Principal Component Analysis
PCOA	Peat and Coal Oxygenated Aerosol
PEACE	Pollution Effects on Asthmatic Children in Europe
PFC	Perfluorocarbon
PM	Particulate Matter
PMF	Positive Matrix Factorization
POA	Primary Organic Aerosol
PSAP	Particle Soot Absorption Photometer
PTFE	Polytetrafluoroethylene
QUARG	Quality of Urban Air Review Group
rBC	Refractory Black Carbon
RF	Radiative Forcing
SAPPHIRE	Source Apportionment of Particulate Matter in Urban and Rural Areas of Ireland
SD	Standard Deviation

SEAI	Sustainable Energy Authority of Ireland
SF	Solid Fuel
SFB	Solid Fuel Burning
SMPS	Scanning Mobility Particle Sizer
SOA	Secondary Organic Aerosol
SP2	Single Particle Soot Photometer
SP-AMS	Soot Particle Aerosol Mass Spectrometer
SV-OOA	Semi-volatile Oxygenated Organic Aerosol
T2S	Thermal-2-Step
TC	Total Carbon
TEOM	Tapered Element Oscillating Microbalance
TMS	Thermal Multi Step
TOT	Total Optical Transmittance
TSP	Total Suspended Particles
UNECE	United Nations Economic Commission for Europe
UV	Ultra-violet
VAT	Value Added Tax
VOC	Volatile Organic Compound
WB	Wood Burning
WHO	World Health Organisation

1. Introduction

Contents

1.1. Atmospheric Aerosol Particles

An aerosol is defined as a suspension of liquid or solid particles in a gas (Finlayson-Pitts and Pitts, 2000), but does not include cloud and rain droplets (Mészáros, 1999). The particle content of aerosols, more commonly referred to as particulate matter (PM), ranges in size from approximately 0.002–100 μm. The size of the individual particles plays a key role in determining their behaviour in the atmosphere, i.e. their lifetime, the interactions they have with other particles and removal processes (Calvo *et al.*, 2013). Particles that are less than ten micrometres in size (PM_{10}) and less than 2.5 μm in size ($PM_{2.5}$) are key metrics in air pollution monitoring and legislative action is routinely taken to limit their respective concentrations (European Environment Agency, 2018). Particle size, along with the chemical, physical, and optical properties, is strongly influenced by the source, which can be natural or anthropogenic (Monks *et al.*, 2009), and the extent of atmospheric processing or ageing. Particles are also classified as being primary or secondary in origin. Primary particles are emitted directly into the atmosphere, while secondary particles are formed in situ by gas to particle conversion, nucleation or condensation of gaseous species onto existing particles (Finlayson-Pitts and Pitts, 2000; Pöschl, 2005; Calvo *et al.*, 2013).

Important natural sources of primary aerosols are sea spray, volcanoes, pollen, fungal spores and wind-blown mineral dust (O'Dowd *et al.*, 1997; Finlayson-Pitts and Pitts, 2000; Hobbs, 2000; Bond *et al.*, 2004; Seinfeld and Pandis, 2006). Major anthropogenic sources of primary aerosols include industrial processes, domestic emissions from cooking and heating, motor vehicles and the re-suspension of dust (Castro *et al.*, 1999; Finlayson-Pitts and Pitts, 2000). Combustion processes are the principal source of the secondary inorganic components, nitrate and sulfate, while agricultural activities are responsible for the release of ammonia which results in the formation of particulate ammonium (AQEG, 2005). Finally, secondary organic aerosols can be produced from the atmospheric processing of volatile organic compounds from both biogenic and anthropogenic sources (Hallquist *et al.*, 2009).

The main focus of this work is the carbonaceous component of atmospheric aerosols, which can be divided into three types, as shown in *Figure 1.1*. The first type is black carbon or elemental carbon (BC or EC) (Bond *et al.*, 2004), which is largely made up of graphite-like material. The second is non-light absorbing organic carbon (OC) and the third type is light absorbing organic carbon, commonly referred to as brown carbon (BrC) (Laskin *et al., 2015)*. This chapter will present a brief introduction to the sources, physical properties and effects of atmospheric black carbon (BC) aerosols, expanding on the comprehensive review by Bond *et al.* (2013).

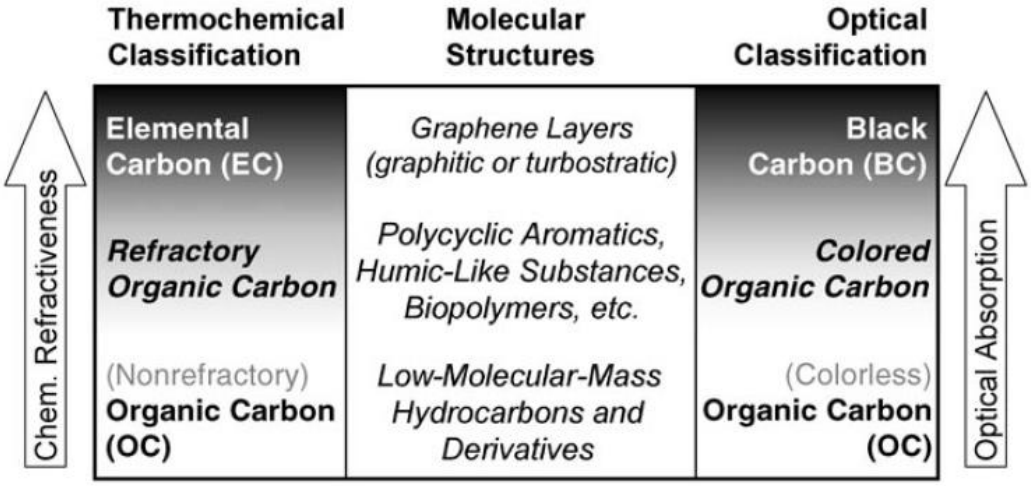

Figure 1.1. Optical and thermochemical classifications of the different types of carbonaceous aerosols and the molecular structures of each type (Pöschl, 2005).

1.2. Properties of Black Carbon (BC)

Historically, BC has been defined as black carbon particles produced during combustion processes that have a graphite-like microstructure (Novakov, 1984), or "an impure form of carbon produced by the incomplete combustion of fossil fuels and biomass. It contains over 60% carbon with the major accessory elements hydrogen, oxygen, nitrogen, and sulfur (Goldberg, 1985). In a more recent publication, the term BC was defined as "a useful qualitative description when referring to light-absorbing carbonaceous substances in atmospheric aerosol", it is also stated that in order to make a quantitative measurement, the method used to determine the concentration must also be provided (Petzold *et al.*, 2013). BC concentrations determined using optical

methods, coupled with a suitable mass absorption cross-section (MAC) value, should be referred to as *equivalent black carbon* (*eBC*). BC concentrations derived from incandescence methods, like laser-induced incandescence and single particle soot photometry (SP2), should be referred to as *refractory black carbon* (*rBC*). Finally, the term *elemental carbon* (*EC*) should be used when the analysis method is specific to the carbon content of carbonaceous aerosols, e.g. thermal/optical analysis performed using the OCEC instrument (Petzold *et al.*, 2013).

BC particles are characterized by a number of distinct properties, as defined by Bond *et al.* (2013); (i) they strongly absorb light in the visible and infra-red (IR) regions of the electromagnetic spectrum, and freshly produced BC particles have a mass absorption cross-section (MAC) value greater than 5 m^2/g at a wavelength (λ) of 550 nm; (ii) they are refractory, with a volatilization temperature of approximately 4000 K; (iii) they are insoluble in water, organic solvents, including methanol and acetone, and other atmospheric aerosol components; (iv) the particles are made up of small carbon spherules with diameters between approximately 10 and 50 nm; (v) BC particles contain a high fraction of graphite-like sp^2-bonded carbon atoms. These properties of BC particles contribute to a wide variety of atmospheric interactions (*Figure 1.2*). *Figure 1.3* shows three examples of fractal aggregates, generated using different types of types of algorithms that include different fractal dimensions (Sorensen, 2001). Fresh soot particles are generally chain agglomerates while particles that have been processed in the atmosphere exhibit a more compact, almost spherical form (Zhang *et al.*, 2008).

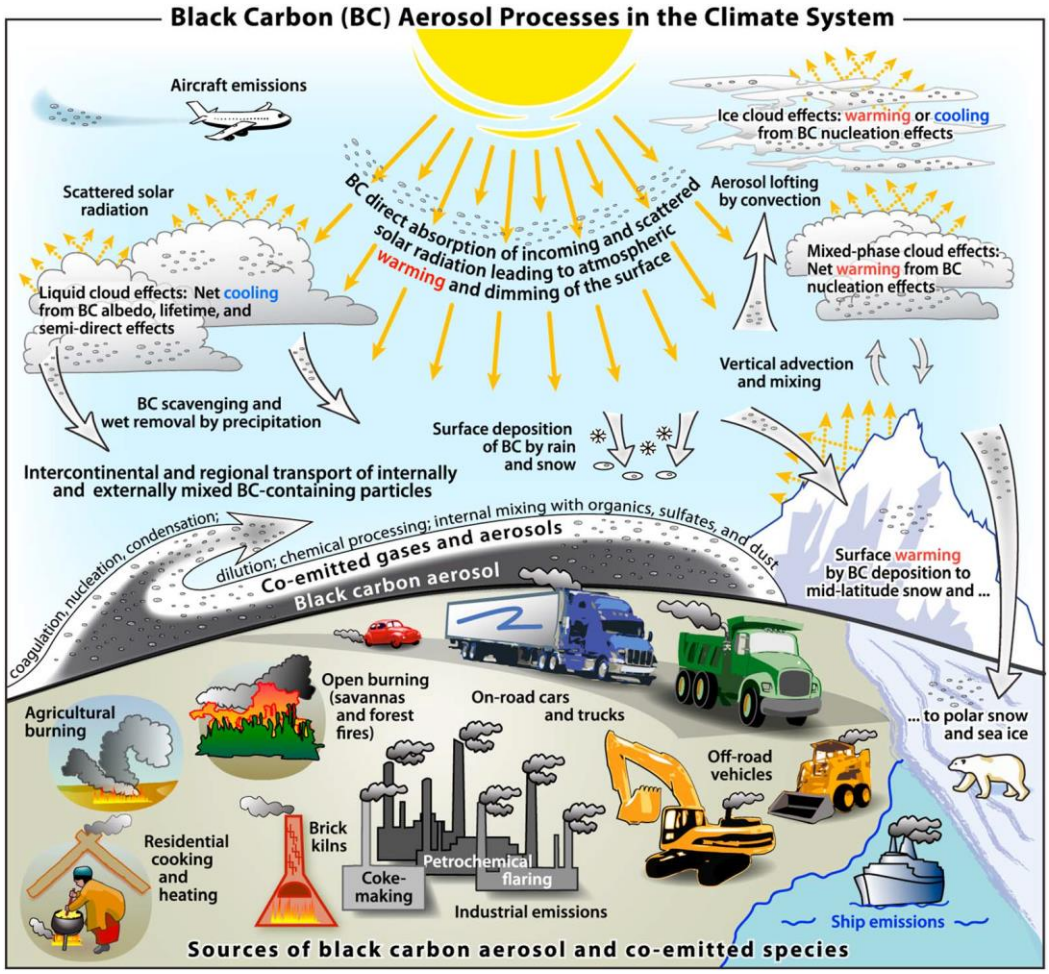

Figure 1.2. Summary of BC particle sources and climate impacts compiled by Bond *et al.* (2013).

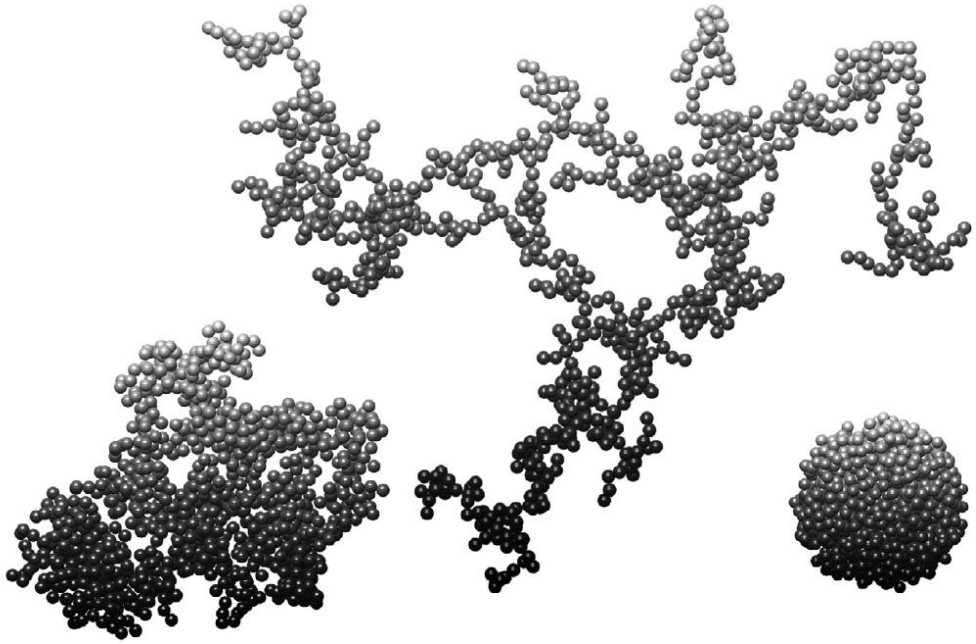

Figure 1.3. Examples of numerically generated BC aggregates containing 1000 monomers, with fractal dimensions of 1.8, 2.3, and 2.8 respectively (C. Liu *et al.*, 2019).

The microphysical properties of BC particles, including the density, refractive index, particle size, shape and mixing state, have a strong influence on the optical properties, specifically the MAC and the single scattering albedo (ω_0) (Bond *et al.*, 2013). The MAC of a BC particle describes the amount of absorption per particle mass (Knox *et al.*, 2009), while the ω_0 value is the aerosol scattering divided by the total extinction, *i.e.* the scattering plus absorption (Montilla *et al.*, 2011). A wide variety of densities have been calculated for BC particles, for both freshly emitted agglomerates and mixed BC particles. A density value of 1.8 g/cm^3 for mixed BC particles (Bond and Bergstrom, 2006) has been used on several occasions for modelling BC optical properties (e.g. Knox *et al.*, 2009; Scarnato *et al.*, 2013; Radney *et al.*, 2014; Zhang *et al.*, 2016; H. Liu *et al.*, 2019; Pan *et al.*, 2019). The refractive index expresses how light interacts with the material in the particle (Bond and Bergstrom, 2006) and is vitally important for calculating the scattering and absorption coefficients of particles (e.g. Marley *et al.*, 2001; Kim *et al.*, 2015). As stated above, the size of the BC monomers contained in the agglomerates generally have diameters between 10 and 50 nm. The size of the agglomerates is highly dependent on the source and the types of co-emitted species that combine with the particles. However, more than 90% of BC particles fall into the $PM_{2.5}$ size fraction (Wang *et al.*, 2011a). The presence and mixing state of other particulate components can greatly influence the MAC and ω_0 of BC particles by altering the other parameters listed above. BC can be internally mixed with other components, *i.e.*, where a shell is formed on the outside of the particles, or it can be externally mixed, *i.e.*, where BC exists on the surface of the particle, (Sedlacek III *et al.*, 2012). When the BC agglomerate is coated with a non-absorbing shell, it can be transformed into a tightly packed sphere, for example Zhang *et al.* (2008) found that the density of BC particles increased from 0.56 to 1.60 g/cm^3 after coating with sulfuric acid (H_2SO_4), which increases the refractive index of the particle (Zhang *et al.*, 2016). The coating of BC particles with absorbing species can greatly affect the absorption Ångström exponent (α), a property describing the wavelength dependence of absorption (Liu *et al.*, 2018). The removal of coatings from fresh and semi-aged particles alters the MAC value. Knox *et al.* (2009) found that the average MAC value for freshly emitted BC particles was (9.3 ± 1.8) m^2/g but following the removal of the coating this value was reduced to (7.7 ± 2.2) m^2/g. The magnitude of the measured absorption enhancement varies with the coating, *Figure 1.4*, which can be dependent on combustion conditions and fuel type (You *et al.*, 2016). The highest

absorption enhancement was observed when BC particles were mixed with humic acid, a proxy for BrC.

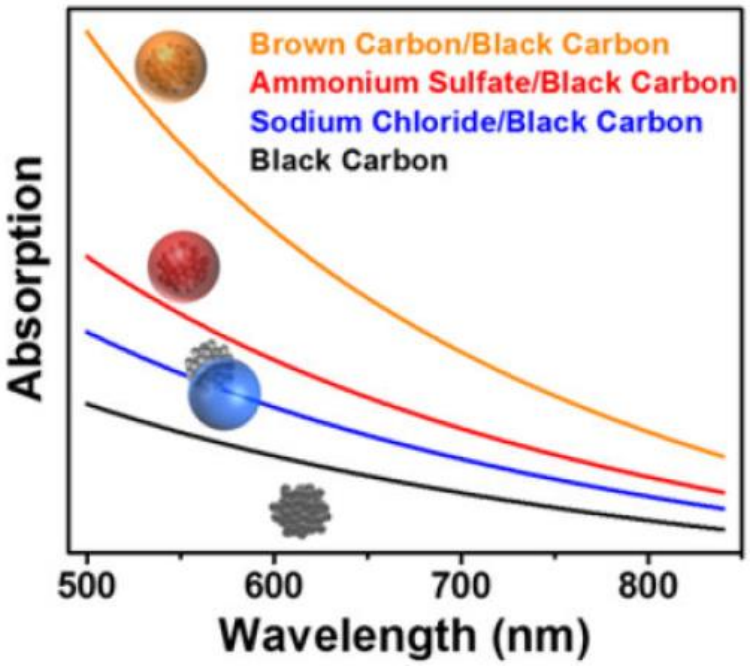

Figure 1.4. Variation of light absorption as a function of wavelength for uncoated BC particles and BC particles coated with different absorbing and non-absorbing species (You *et al.*, 2016).

1.3. Climate Effects of Black Carbon (BC)

The climate effects of BC particles can be divided into direct, indirect and semi-indirect effects. The direct effect is a result of the absorption or scattering of solar radiation (Penner *et al.*, 1998; Bahadur *et al.*, 2012), while the indirect and semi-indirect effects are related to the interaction of BC particles with clouds (Bond *et al.*, 2013).

BC is now recognised as one of the most significant positive radiative forcing agents in our atmosphere due to its strong absorbance in the IR region (Bond and Bergstrom, 2006), with an estimated radiative forcing contribution of +0.71 W/m^2 with an uncertainty of 90% (+0.08 W/m^2 – 1.27 W/m^2), second only to carbon dioxide (CO_2) (IPCC, 2013). The large amount of uncertainty associated with the magnitude of the positive forcing attributed to these particles, illustrated in *Figure 1.5*, is due to uncertainties associated with measurement techniques and climate model results. In this estimate, BC, both suspended in the atmosphere and deposited on the Earth's

surface, has a large positive, or warming effect. Due to the significantly shorter lifetime of BC, approximately six to seven days (Cape *et al.*, 2012), relative to CO_2, a reduction in BC concentrations would provide a more immediate impact on global radiative forcing and has been identified as a crucial goal in the efforts to limit global warming to less than 1.5 ºC (IPCC, 2018).

As BC is chemically inert and insoluble in water, it remains intact as it is removed from the atmosphere via wet and dry deposition (Begam *et al.*, 2016; Bibi *et al.*, 2017; Barrett *et al.*, 2019). Therefore BC particles continue to absorb solar radiation when deposited on the Earth's surface. The deposition of BC particles can reduce the Earth's albedo by accelerating the melting of snow and ice cover by darkening these white surfaces and thus enhancing absorption (Yang *et al.*, 2015; Dou and Xiao, 2016) which can result in further warming via a snow-albedo feedback loop (Flanner *et al.*, 2009).

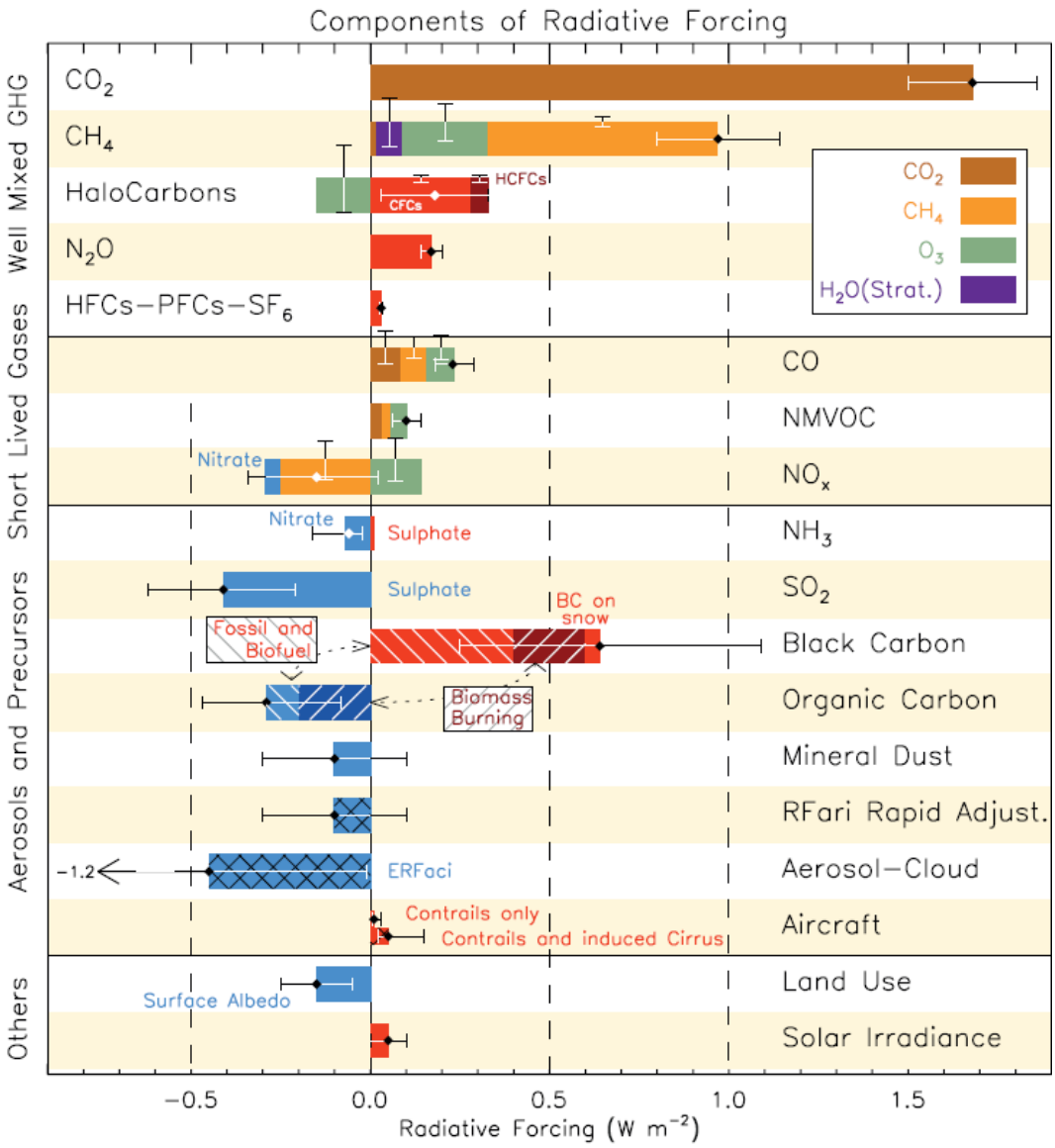

Figure 1.5. Radiative forcing (RF) of emitted pollutants during the industrial era, 1750 to 2011. The horizontal bars indicate overall uncertainty, while the vertical bars show the uncertainty of individual components. (CFCs = chlorofluorocarbons, HCFCs = hydrochlorofluorocarbons, PFCs = perfluorocarbons, NMVOC = non-methane volatile organic compounds, BC = black carbon, ERFaci = effective radiative forcing due to aerosol-cloud interactions). Adapted from IPCC, 2013.

The indirect and semi-direct effects of BC are related to the impacts of particles on cloud formation in the atmosphere. The BC particles can act as cloud condensation nuclei (CCN) or ice nuclei (IN), increasing the number of water droplets or ice particles in the atmosphere, potentially leading to an increased number of clouds, increased lifetimes and changing the amounts of precipitation (Koch *et al.*, 2011; Cherian *et al.*, 2017 and references therein). The clouds reflect incoming solar radiation away from the Earth's surface, causing a cooling effect, known as cloud-

albedo. BC particles can also act to dissipate clouds by increasing their temperature via the absorption of incoming solar radiation (Ackerman *et al.*, 2000). This reduces the overall cloud-albedo and results in net warming of the atmosphere.

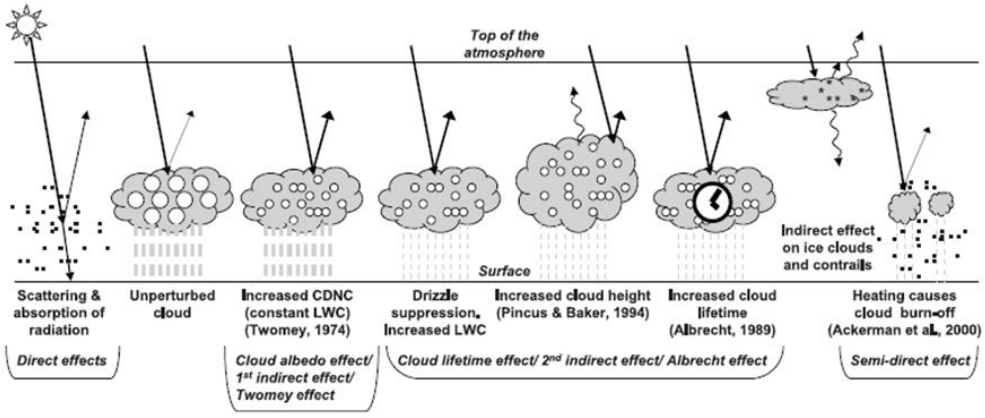

Figure 1.6. Schematic diagram of the radiative mechanisms associated with clouds in the atmosphere (Haywood and Boucher, 2000; IPCC, 2007).

BC in the atmosphere can have additional effects that lead to further atmospheric and health impacts, for example BC particles can catalyse the formation of nitrous acid in polluted air masses, which is an important precursor for the hydroxyl radical, Earth's main tropospheric oxidising agent (Ammann *et al.*, 1998).

1.4. Health Effects of Black Carbon (BC)

In recent years, a significant amount of research has been conducted into the health effects of particulate matter (e.g. Anderson *et al.*, 2012; Bell, 2012; Hoek *et al.*, 2013; Kim *et al.*, 2015; WHO, 2016; Wu *et al.*, 2018). The World Health Organisation (WHO) estimate that exposure to $PM_{2.5}$ is responsible for approximately seven million premature deaths worldwide annually, with three million of these deaths attributable to ambient air pollution (WHO, 2016). The WHO also estimates that over 90% of the global population is exposed to levels of $PM_{2.5}$ over the recommended level. The majority of the premature deaths attributed to indoor air pollution occur in Asia, *Figure 1.7*, where there are high levels of solid fuel use for home heating and cooking purposes (Balmes, 2019).

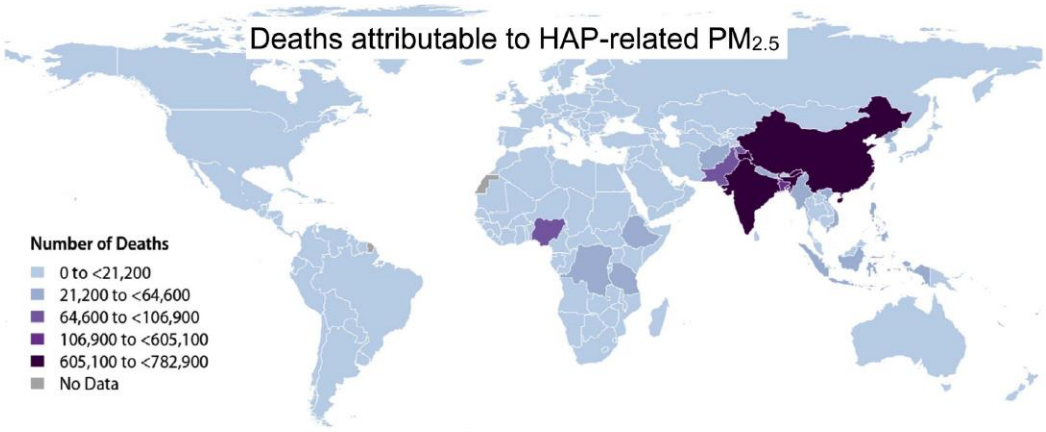

Figure 1.7. Global distribution of annual deaths related to household air pollution (HAP)-related $PM_{2.5}$ (Balmes *et al.*, 2019).

Particles of this size are capable of penetrating deep into the respiratory system, often reaching as far as the alveoli in the lungs, *Figure 1.8* (Guarieiro and Guarieiro, 2013). Acute exposure to $PM_{2.5}$ is associated with the exacerbation of some existing respiratory illnesses, for example asthma (Peden, 2005), cause eye irritation (Mirabelli *et al.*, 2009), and lead to the development of skin irritation in the form of acne, psoriasis, and atopic dermatitis, particularly in children (Kim *et al.*, 2016). Exposure to $PM_{2.5}$ is also associated with diabetes, lung cancer and cardiovascular disease (Pearson *et al.*, 2010; Pope III *et al.*, 2016).

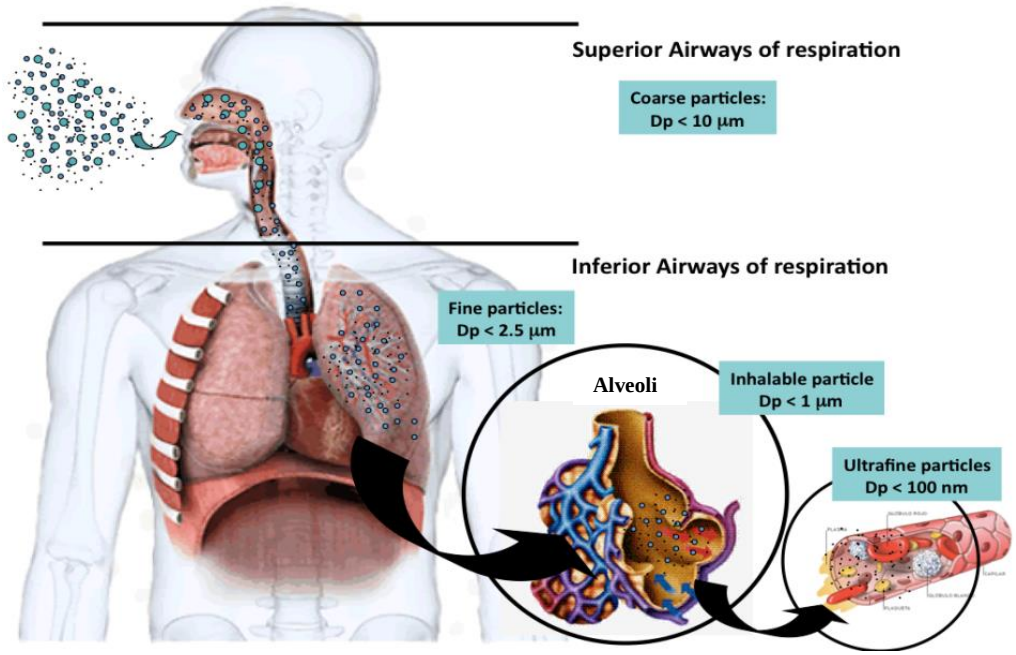

Figure 1.8. Penetration of particulate matter into the respiratory system as a function of size (Guarieiro and Guarieiro, 2013).

The health effects of nanoparticles have also been subject to many studies in recent years (e.g. Donaldson *et al.*, 1998, 2005; Rönkkö and Timonen, 2019). Particles of this size are capable of penetrating further into the respiratory system, potentially even passing through the gaseous exchange region of the alveoli. If particles are able to enter the blood stream, they can be transported through the body and be deposited in any organ, as illustrated by *Figure 1.9*.

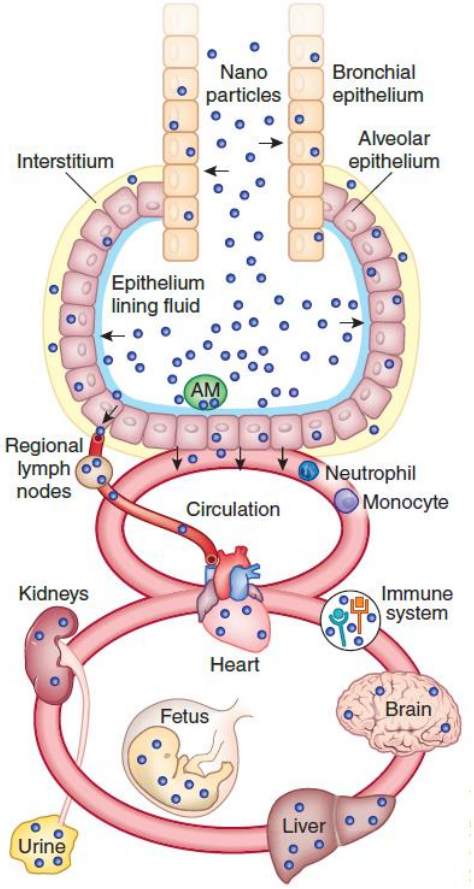

Figure 1.9. Potential deposition sites for nanoparticles, i.e. particles < 100 nm in diameter, that penetrate the gaseous exchange region in the lungs and are transported through the bloodstream (Kreyling *et al.*, 2010).

As the vast majority of BC particles are in the $PM_{2.5}$ size range, the general health effects that are associated with $PM_{2.5}$ can also be attributed to BC particles. Given the small size of BC particles and high levels in well-populated areas, investigations into the specific health effects of BC particles are of critical importance. Studies have indicated that particles produced by combustion processes are potentially more toxic than particles originating from other sources (Janssen *et al.*, 2011, 2012). This is possibly due to the BC particles acting as a vector for other toxic components of combustion emissions (Cassee *et al.*, 2013; WHO, 2015). It has been shown that

exposure to high concentrations of BC can reduce the health benefits of exercise (Jereb *et al.*, 2018; Laeremans *et al.*, 2018). The effects of exposure to BC from traffic sources can cause inflammation of the epithelial cells (Mazzarella *et al.*, 2012), elevated blood pressure (Delfino *et al.*, 2010), and lead to increased incidences of cardiovascular disease (Gong *et al.*, 2019). Traffic related pollution, including BC particles, has also been shown to cause changes in DNA methylation levels (Baccarelli *et al.*, 2009). Lower levels of DNA methylation is related to increased oxidative stress, cell aging and atherosclerosis. DNA damage resulting from exposure to mutagenic and carcinogenic chemicals transported into the body can induce cardiovascular and reproductive effects (Lewtas, 2007). Similar health effects have been observed in emissions from domestic solid fuel combustion (Chen *et al.*, 2017; Krapf *et al.*, 2017; Li *et al.*, 2017; Balmes, 2019). BC particles have also been identified on the foetal side of the human placenta (Bové *et al.*, 2019). BC particles present in a developing foetus can potentially lead to reduced birth weight, premature birth, and slower rates of foetal growth in the womb. The authors postulate that BC particles are delivered to the placenta from the mother's lungs.

1.5. Measurement Techniques

For over 60 years, the concentration of light absorbing carbonaceous particles in the atmosphere has been determined by measuring the darkness of particulate material collected on filter papers. This is achieved by measuring the proportion of white light reflected from sample filter papers and using an empirical relationship to convert this reflectance into a mass concentration of black smoke (BS) (Christolis *et al.*, 1992). This method became standardised during the 1960s (OECD, 1964) and was deployed at a large scale in black smoke monitoring networks around the world. As a result, black smoke and its main co-pollutant, sulfur dioxide, were the principal indicators of ambient air quality all the way through to the early 2000s, before the introduction of PM_{10} and $PM_{2.5}$ as standard metrics for particulate matter (Richter and Williams, 1998; Fuller and Connolly, 2012; European Environment Agency, 2013). The black smoke method is rarely used nowadays and many of the old BS monitoring stations measure Black Carbon instead, typically using an aethalometer.

The first aethalometer instrument measured the attenuation of light at 530 nm by particles deposited on a cellulose fibre filter (Hansen *et al.*, 1984). The absorption coefficient associated with the particles deposited on the filter was then used to calculate the concentration of BC particles. As this is not a direct measure of BC concentration, the calculated term is labelled "equivalent black carbon" (eBC) (Petzold *et al.*, 2013). Aethalometer instruments have evolved over the years and have been deployed as part of large monitoring networks for long-term measurements of eBC (Fuller and Connolly, 2012; European Environment Agency, 2013; Hessey *et al.*, 2017; von Schneidemesser *et al*., 2017).

The latest aethalometer model (AE33) incorporates light of seven different wavelengths, ranging from the near-IR to the near-UV, which are passed through an automatically advancing filter paper. A second spot, used as a reference, is also incorporated to allow for the real-time correction of errors associated with filter based measurements (Drinovec *et al.*, 2015). The eBC concentration is determined using a pre-selected MAC value and the proportion of eBC originating from fossil fuel burning and biomass burning sources is calculated (Zotter *et al.*, 2017). A more complete description of the AE33 instrument and the source apportionment method is provided in Chapter 2.

A number of other light absorption methods are also used to calculate the concentration of eBC (Moosmüller *et al.*, 2009; Cross *et al.*, 2010; Petzold *et al.*, 2013). The multi-angle absorption photometer (MAAP) instrument determines the light absorption of aerosols deposited on a filter paper by measuring the radiation which passes through and is scattered by the particles on the filter. Measurements are performed at three different angles in order to account for the light scattered and to measure the angular distribution of back scattered radiation as a function of aerosol type. The absorption is then determined using a radiative transfer model (Petzold and Schönlinner, 2004). The photoacoustic spectrometer (PAS) technique uses a modulated laser beam and microphones to measure the acoustic signal produced by the absorption of light by the aerosol species. The laser beam power is converted into an acoustic pressure through absorption-induced gas expansion. The magnitude of the acoustic signal produced provides an indication of the amount of light absorbed by the sample (Arnott *et al.*, 1999). The particle soot absorption photometer (PSAP) technique works by continuously monitoring the change in transmittance across a filter using a 567 nm LED (Bond *et al.*, 1999; Virkkula *et al.*, 2005). The continuous soot

monitoring system (COSMOS) measures the changes in transmittance across an automatically advancing quartz fibre filter tape using a 565 nm LED (Miyazaki *et al.*, 2008). Cavity ring-down systems, in conjunction with instruments that measure the scattering of light by particles, e.g. the nephalometer, can also be used to determine the absorption of light by particles, e.g. Smith and Atkinson, 2001. The absorption coefficients determined by each of these techniques can then be converted to an equivalent BC (eBC) concentration using an appropriate mass absorption cross-section (MAC) value (Petzold *et al.*, 2013).

A number of refractory instruments have been developed to determine the concentration of refractory BC (rBC) in recent years. Laser modulated or induced incandescence (LMI or LII) methods have been deployed to determine the size distribution and volume fraction of the soot particles (Melton, 1984). The LII measurement technique has been adapted for atmospheric measurements of soot volume (Snelling *et al.*, 2005) and single particle analysis (Stephens *et al.*, 2003; Schwarz *et al.*, 2006). Measurement of the soot volume was based on determining the incandescence of soot deposited on a filter paper at two different wavelengths. This allowed for the quantitative measurement of soot volumes without the need for *ex situ* calibration of the instrument. The single particle soot photometer (SP2) technique developed by Stephens *et al*. (2003) allows for the determination of the laser induced incandescence, size and composition of individual particles based on the amount of light scattered by the particle. This techniques deploys a diode-pumped Nd:YAG laser which is used to vapourize the particles in a single particle beam. The scattered and incandescent light are then detected by an array of detectors contained in the chamber of the instrument. This technique can also detect individual elements present in particles, such as tungsten and silicon. The SP2 technique has also been used to quantify the concentration of BC particles deposited on snow and ice (Schwarz *et al.*, 2006, 2012). The SP2 instrument has been incorporated into an aerosol mass spectrometer to provide chemical and physical properties of particles that contain refractory BC (rBC) (Onasch *et al.*, 2012). The soot particle aerosol mass spectrometer (SP-AMS) is comprised of a high resolution time-of-flight aerosol mass spectrometer (HT-ToF-AMS) and the SP2 instrument with an intracavity Nd:YAG laser.

The other main methods for determining the carbonaceous content of ambient particles are based on thermal and thermal-optical methods, which can determine the total carbon fraction of atmospheric aerosols, including elemental carbon (EC) and

organic carbon (OC) (Birch and Cary, 1996; Cavalli *et al.*, 2010). Several different analytical protocols have been developed for the analysis of carbonaceous aerosols collected on filter media in Sunset OCEC analyser instruments, IMPROVE (Chow *et al.*, 1993), NIOSH (Birch, 2003), EUSSAR_2 (Cavalli *et al.*, 2010), in addition to the VDI-2, thermal-2-step (T2S) oxidation, thermal multi-step (TMS) oxidation and thermal-optical transmittance (TOT) analysis procedures (ten Brink *et al.*, 2004). These analysis methods involve a multi-step heating procedure, with the initial heating step removing OC deposited on the filter, followed by the oxidation of the EC deposited on the filter using an oxygen rich atmosphere. In the Sunset OCEC instrument, the EC is pyrolyzed and the concentration of CO_2 produced during this reaction is measured using an non-disperse infrared (NDIR) detector system (Sunset Laboratory Inc., 2005). This signal measured by the NDIR system is then converted to the EC concentration.

Finally, online mass spectrometry techniques can be used to determine both organic and elemental carbon mass concentrations. The aerosol mass spectrometer (AMS, Aerodyne Inc.) has been widely deployed over the last 15 years to determine the mass of organic aerosol in PM_1 and its sources (Zhang *et al.*, 2011; Crippa *et al.*, 2014). More recently, a smaller, more affordable version of the AMS, called the Aerosol Chemical Speciation Monitor (ACSM) has been deployed as part of air quality monitoring networks alongside aethalometer instruments to measure the total carbonaceous content of PM_1 (Petit *et al.*, 2015; Lin *et al.*, 2019b). Single particle mass spectrometry techniques, such as the aerosol time-of-flight mass spectrometer (ATOFMS, TSI Inc.), can also be used for organic and elemental carbon source apportionment based on fingerprint mass spectra collected during combustion experiments. For example (Healy *et al.*, 2012) determined the source and mixing state of EC particles in Paris using an ATOFMS instrument. The results correlated well with BC measurements made by co-located MAAP, aethalometer, and Sunset OCEC instruments. Strong correlations were also observed between the AMS and ATOFMS source apportionment results in Paris (Healy *et al.*, 2013).

1.6. Sources of Black Carbon (BC)

BC particles are generated through the incomplete combustion of hydrocarbons in fossil fuel or biomass. They are predominantly generated through anthropogenic processes, but can also originate from natural wildfires (Bond *et al.*, 2004). Information on the sources of BC is can be obtained using two different approaches; (i) in-situ measurements coupled with source apportionment methods that are scaled up to regional or global levels (Johnson *et al.*, 2011; Briggs and Long, 2016); and (ii) "bottom-up" models based on emission inventories including data relating to fuel consumption and land use (Chow *et al.*, 2010; Bond *et al.*, 2013), which can be used to model past and future concentrations (Junker and Liousse, 2008; Wang *et al.*, 2012; Liousse *et al.*, 2014).

1.6.1. Emissions Inventories and Models

In the absence of global long-term measurements and source apportionment of BC, computer models have been employed to determine the contributions of individual sources to global BC emissions, e.g. Schaap *et al.*, 2004; Streets *et al.*, 2004; Rao *et al.*, 2005; Cao *et al.*, 2006; Lamarque *et al.*, 2010; Chow *et al.*, 2011; Ni *et al.*, 2014; Wang *et al.*, 2014. It has been shown however, that the estimated concentrations of BC can vary significantly between different models and inventories (Koch *et al.*, 2009; Vignati *et al.*, 2010).

Historical emissions of BC and OC have been estimated for the period 1850 to 2000 based on fossil fuel and biofuel combustion (Bond *et al.*, 2007). This work was based on reconstructed fossil fuel consumption per sector, and on historical estimates of biofuel consumption. The authors found that BC emissions increased from approximately 1000 Gg in 1850, to 2200 Gg in 1900, to 3000 Gg in 1950, to 4400 Gg in 2000 (*Figure 1.10*). Coal combustion contributed the most to BC emissions between 1880 and 1975, and while consumption increased after 1975, improving technologies resulted in decreasing emissions overall. BC emissions from biofuel and diesel combustion have become the most important factors since 1990.

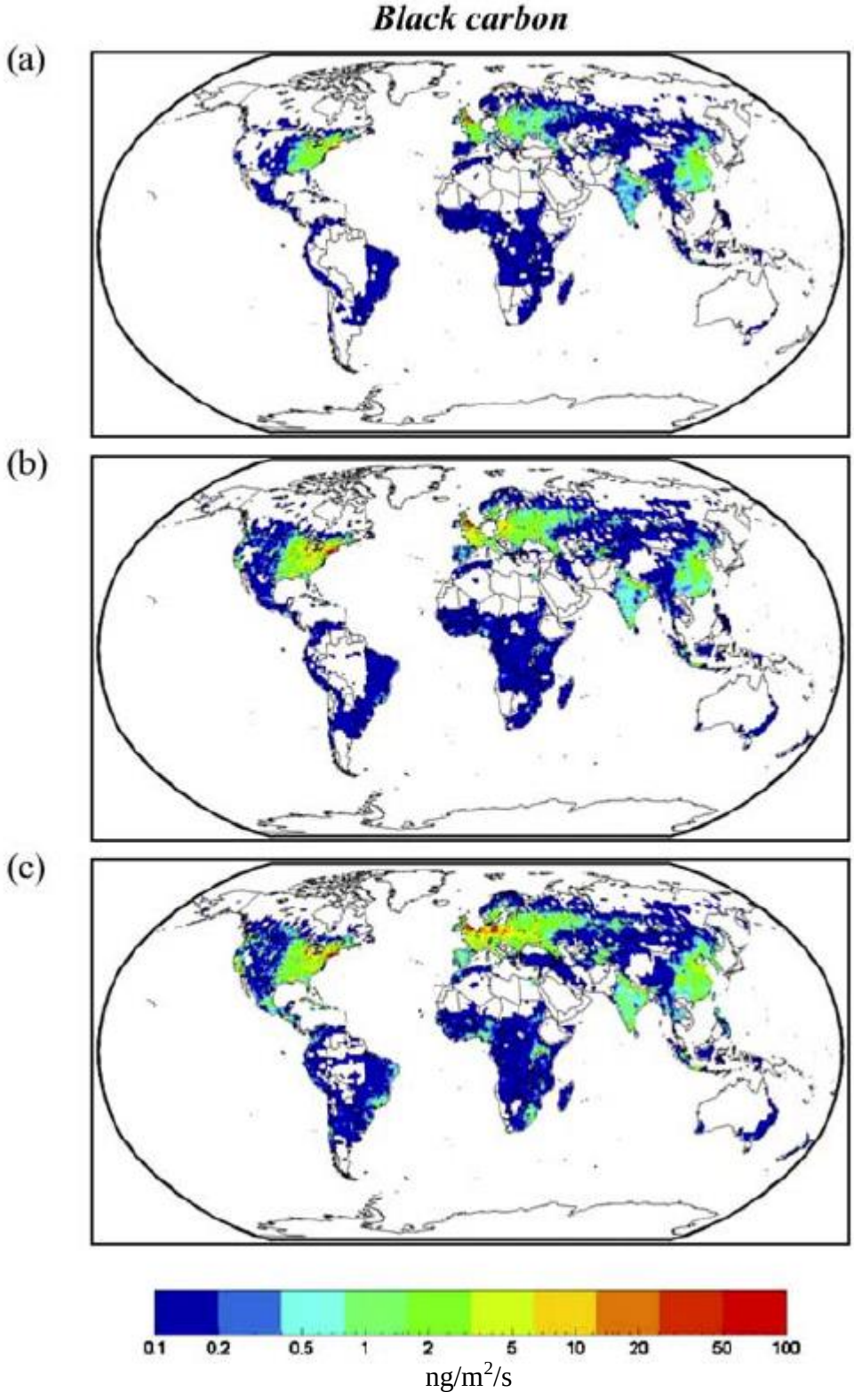

Figure 1.10. Global distribution of BC emissions from fossil fuel and biofuel combustion in (a) 1850, (b) 1900 and (c) 1950 (units: ng/m^2/s) (adapted from Bond *et al.*, 2007).

The trends in global black carbon emissions per region were analysed by Wang *et al.* (2014). The authors found that for 1960 to 2007 the annual BC emissions increased from approximately 5.1 Tg/yr to approximately 9.1 Tg/yr, with higher contributions from Europe, North America and the former USSR at the beginning of the study period. In the latter half of the 20th century, the emissions from China and other Asian countries increased significantly, *Figure 1.11*.

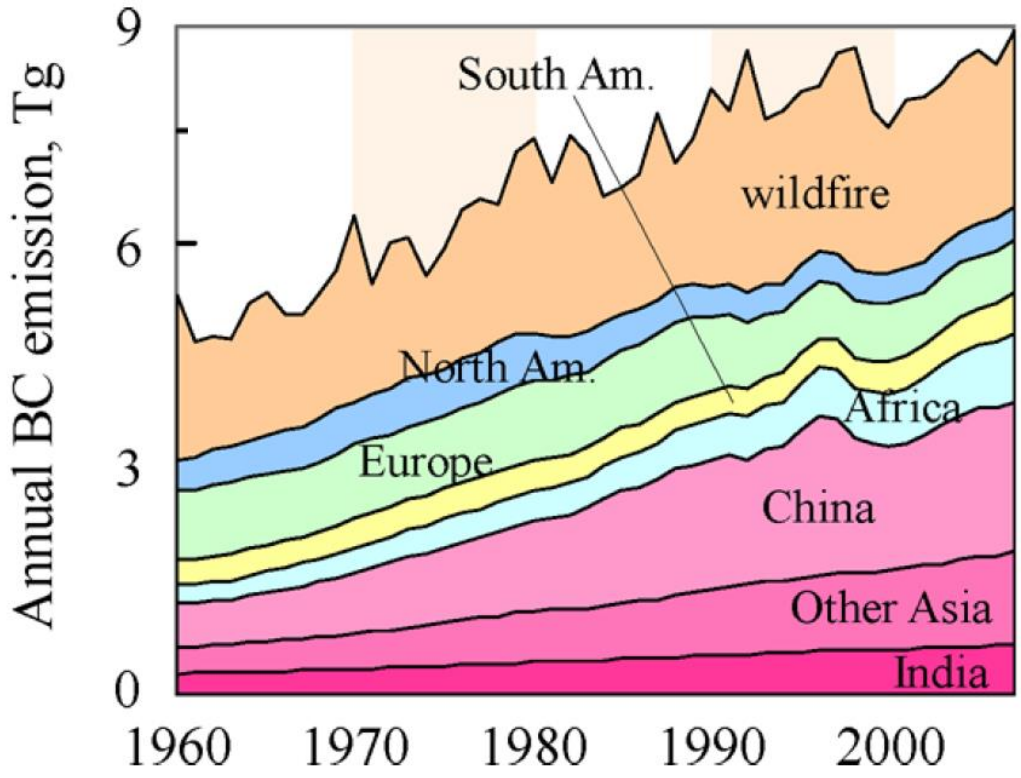

Figure 1.11. Annual emissions of BC in various regions/countries from 1960 to 2007 (Wang *et al.*, 2014).

BC emissions can be subdivided into different source categories, originating from either closed combustion (CC) or open burning (OB) (Bond *et al.*, 2004). Closed combustion sources include all industrial sources, power generation, vehicle emissions and residential combustion involving stoves and boiler systems. The open burning category encompasses most outdoor burning of solid fuels and agricultural by-products. This category also includes naturally occurring forest and savannah fires (Ni *et al.*, 2014). A breakdown of world-wide BC emissions by source category for the year 1996 is shown in *Figure 1.12*.

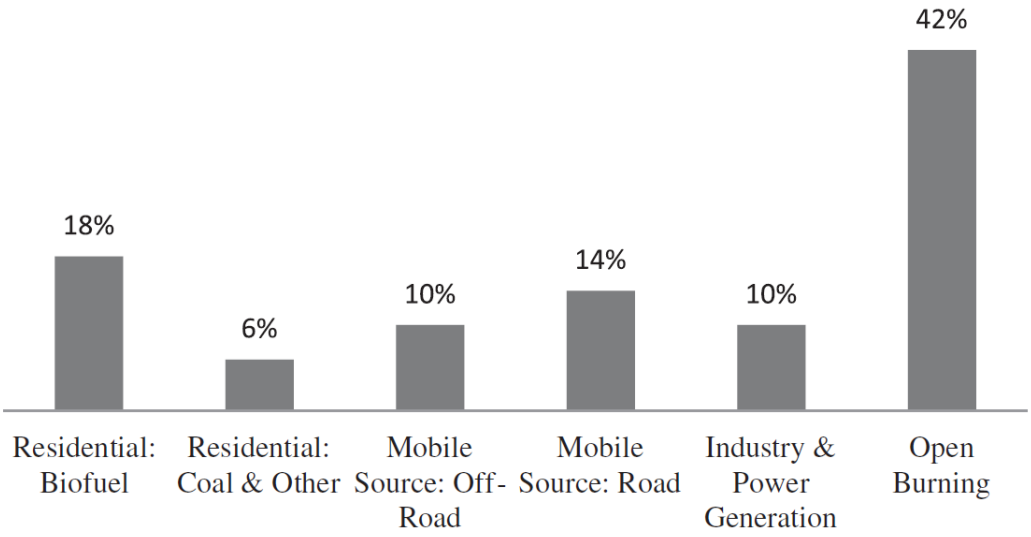

Figure 1.12. Global breakdown of BC emissions in 1996 (Ni *et al.*, 2014, adapted from Bond *et al.*, 2004).

BC emissions in India, modelled by Sahu *et al.* (2008) showed significant increases in the emitted BC between 1991 and 2001. Employing a finely gridded emission inventory, the authors found that the BC emissions increased by approximately 61% over the Indian geographical region. The vehicular emissions of BC increased by approximately 112% during the study period but the emissions from coal were still dominant. The contribution from biomass declined as more efficient energy sources were introduced into the Indian market.

A more recent study conducted by Klimont *et al.* (2017), using data from the ECLIPSE project (Evaluating the Climate and Air Quality Impacts of Short-lived Pollutants), showed that in 2010, approximately 76% of emitted BC originated from anthropogenic sources, with the remainder originating from forest and savannah fires. Anthropogenic BC accounted for approximately 9% of total $PM_{2.5}$ mass in 2010, and 15% of anthropogenically generated $PM_{2.5}$. Roughly 57% of anthropogenic BC originated from residential combustion, while approximately 25% was attributed to transport related sources, including international shipping and aviation (*Figure 1.13).*

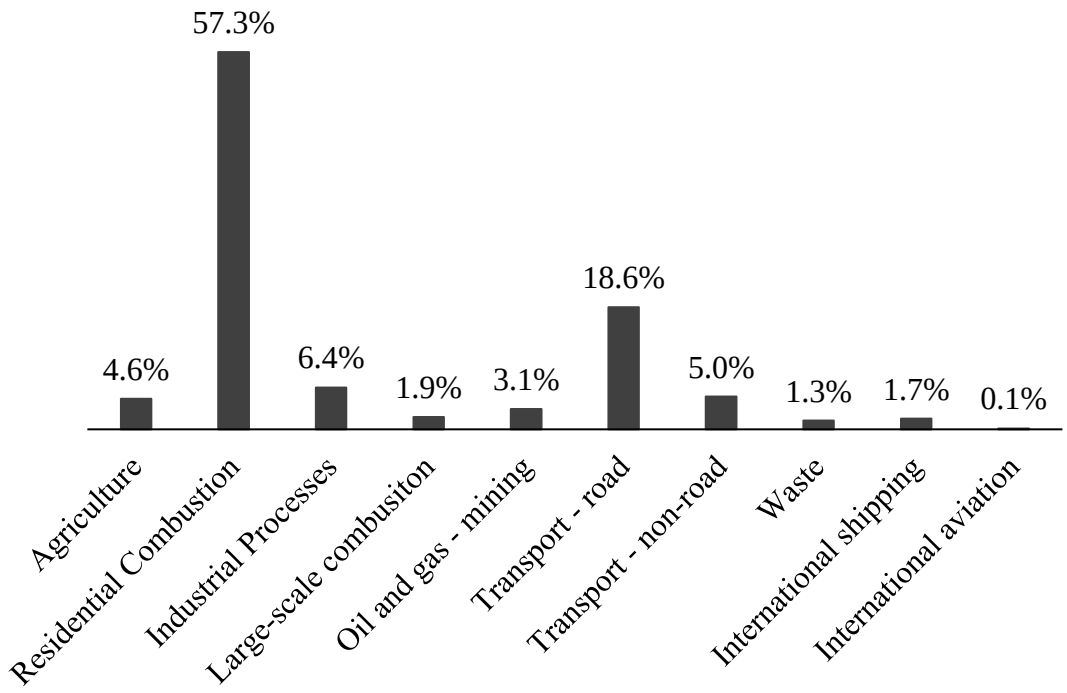

Figure 1.13. Contribution to global anthropogenic BC mass (Gg/year) in 2010 from each source, adapted from Klimont *et al.* (2010), calculated using data from ECLIPSE *V5a*.

The region contributing the most to global anthropogenic BC emissions in 2010 was Asia, accounting for 59.3%. This is comprised of the East Asia region (36.1%) and the South-west and Central Asia region (23.2%), *Figure 1.14*. However, it was found that BC contributed the most to $PM_{2.5}$ mass in North America (20%), and the least to $PM_{2.5}$ mass in East Asia (13%) (Klimont *et al.*, 2017).

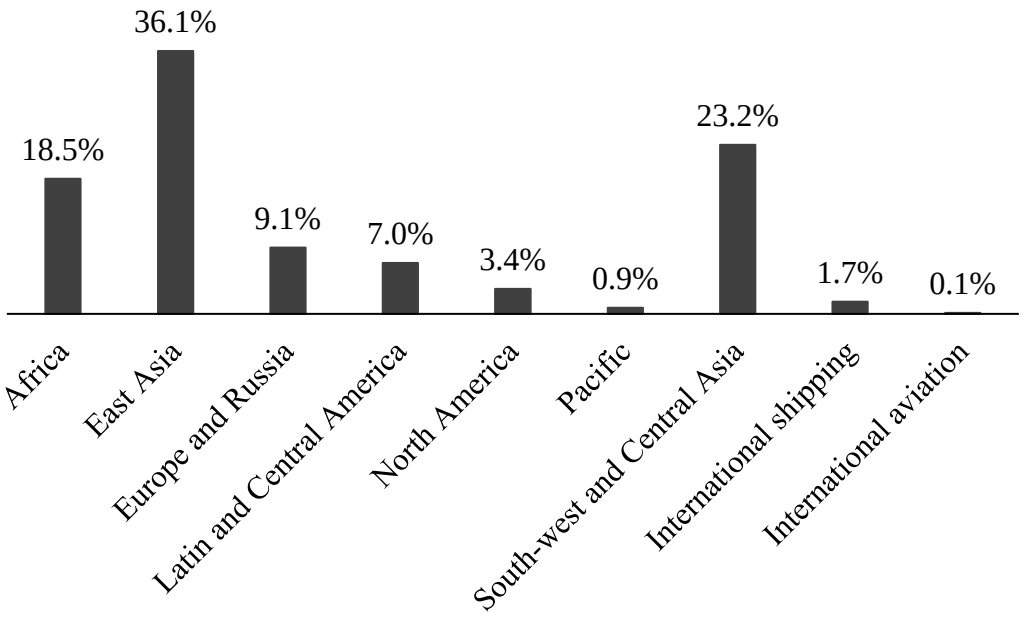

Figure 1.14. Contribution to global anthropogenic BC mass (Gg/year) in 2010 from each region and international shipping and aviation, adapted from Klimont *et al.* (2010), calculated using data from ECLIPSE *V5a*.

1.6.2. Source Apportionment Based on Measurements

Over the last decade, source apportionment of BC based on ambient measurements, also referred to as receptor modelling, has become increasingly used to quantify contributions from fossil fuels and wood (or biomass) burning. Most are performed using multi-wavelength aethalometer which uses the different light absorption characteristics of BC produced from these two sources (Sandradewi *et al.*, 2008a; Drinovec *et al.*, 2015; Zotter *et al.*, 2017). This approach has become very popular, as the measurement is quite simple and is suited to routine monitoring applications. A detailed review of work in this area is provided in Chapter 4.

BC source apportionment can also be conducted using other instruments, for example the combination of the single particle soot photometer (SP2) instrument and aerosol mass spectrometers (AMS) has previously been used to estimate the source contributions to BC in London (Liu *et al.*, 2014). It was shown that the results of the aethalometer source apportionment model correlated quite well with the results from the SP2 and AMS instruments but the relationship broke down during extreme pollution events. This could potentially be due to the selection of inappropriate model

parameters for the aethalometer model. Other instruments used to measure BC concentrations and identify the sources are detailed in section 1.6.

Radiocarbon (^{14}C) analysis has also been used for source apportionment purposes over the last number of decades. This technique exploits the fact that ambient aerosols generally have different $^{14}C/^{12}C$ ratios. This ratio is dependent on the chemical composition of the aerosol, which is dependent on the source. As ^{14}C has a half-life of approximately 5730 years, higher amounts are observed in biomass burning emissions. The contributions from different sources can be quantitatively determined using the accelerator mass spectrometry (AMS) technique (Currie, 2000, 2004).

1.7. Overview

1.7.1. Aim of this Work

The overall aim of this study can be summarised as follows:

- Identify the diurnal, weekday, and seasonal patterns in BC concentration in Dublin, and determine the seasonal source contributions to BC mass using the aethalometer source apportionment model.
- Determine the source contributions to BC mass concentrations in rural areas of Ireland using the aethalometer source apportionment model and refine the model parameters to provide more tailored source apportionment at each location.
- Validate the results from the aethalometer source apportionment model with those obtained using other instruments, such as the Aerosol Time of Flight Mass Spectrometer (ATOFMS), and the Aerosol Chemical Speciation Monitor (ACSM).
- Determine the origin and nature of BC particles in the atmosphere using parameters from the aethalometer and other instruments deployed at each monitoring location.
- Conduct a comprehensive review of historical black smoke (BS) and sulfur dioxide (SO_2) concentrations in Dublin, Belfast, London and Paris and to track changes in concentrations with respect to legislative changes in each region.

1.7.2. Overview of Thesis

Chapter 1 presents a brief introduction to atmospheric aerosols, with a more specific focus on black carbon (BC) aerosol sources, physical properties, and the climate and health effects of BC. A brief review of the measurement techniques used to measure BC aerosol is also provided.

Chapter 2 provides an overview of the operating principles of the aethalometer and the data analysis techniques used during the work described in this thesis. In addition, a brief description of the other instruments deployed alongside the aethalometer during the measurement campaigns is included.

Chapter 3 provides details of the SAPPHIRE monitoring campaigns, which saw a large suite of instruments deployed at three rural locations in Ireland during winter months. Source apportionment was performed on the eBC data collected by the aethalometer and the results of this analysis were compared to the results from the other instruments.

Chapter 4 describes the deployment of the aethalometer alongside the aerosol chemical speciation monitor in Dublin, Ireland, during the AEROSOURCE project, and the results of the source apportionment analysis carried out on the two year dataset.

Chapter 5 describes the analysis of historical black smoke (BS) and sulfur dioxide (SO_2) concentrations measured in Dublin, Belfast, London, and Paris. A comprehensive list of legislative changes implemented during the study period is also described.

Chapter 6 presents a short summary of the work performed during this thesis and future perspectives.

2. Instrumentation and Methodology

Contents

2.1. Model AE33 Aethalometer

The instrument deployed during the SAPPHIRE and AEROSOURCE campaigns for the measurement of black carbon is the seven wavelength, dual spot Aethalometer (Magee Scientific, model AE33), supplied by Aerosol d.o.o., Ljubljana, Slovenia. The instrument is based on the original design developed by Hansen *et al.* (1984), which employed a single wavelength (530 nm) to measure the attenuation of light by a sample of particles collected on a filter paper. The AE33 aethalometer operates using seven wavelengths, ranging from the near-ultraviolet (UV) region to the near-infrared (IR) region (370, 470, 520, 590, 660, 880, and 950 nm respectively). The AE33 model also utilizes a second measurement spot to eliminate some errors that occur with filter based optical measurements (Drinovec *et al.*, 2015).

The basic layout of the instrument is shown in *Figure 2.1* and *Figure 2.2*. The front section of the instrument consists of two mounts for the measurement tape, the optical chamber, and the bypass filter, which is used to remove particles from ambient air for performing clean air tests. The filter medium is made of glass fibres coated with polytetrafluoroethylene (PTFE). The type of tape used influences two different parameters that must be pre-set once the tape is replaced and the sampling begins again. These parameters are the optical enhancement factor (*C*), and the tape tangential leakage factor (*Z*), which are set in the "*Advanced*" section of the "*Operations*" tab on the instrument front panel. In the "General" section of the "*Operations*" tab, several other parameters can be changed, namely the time base, the flow rate, the time and date, the time zone, the maximum attenuation limit prior to a tape advance, or the time interval between tape advances. The instrument operates using a pre-set flow rate, ranging from 2 litres per minute to 5 litres per minute.

Figure 2.1. Rear view of the model AE33 aethalometer (left) and inside view of the instrument from the front (right), with labels of relevant components (NOAA, 2016).

2.1.1. Aerosol Sampling

Ambient aerosol is drawn through an air inlet at the back of the instrument (shown in *Figure 2.1* and *Figure 2.2*). The sample line is often connected to a size selective inlet to limit the size range of the sampled aerosol. The aerosol passes through the initial ball valve (valve 4 in *Figure 2.3*) which determines whether the air flows to the filter tape or through the bypass filter. The bypass filter is used during the clean air tests. If valve 4 is in position "0", the sampled aerosol passes through the filter tape spots "S1", "S2", and "Ref". Different flows pass through spots S1 and S2, these are modulated by the orifice "O2", and are determined by the flowmeters "F1" and "FC". Finally, the "CRC" or "Pulse Damper" minimizes perturbations in the airflow, which would impact the optical measurements. The filter tape advances from left to right as shown in the diagram. It is advanced by the "Tape Advance Mechanism", and the duration of the advance is determined by the tape sensors located on either side of the optical chamber.

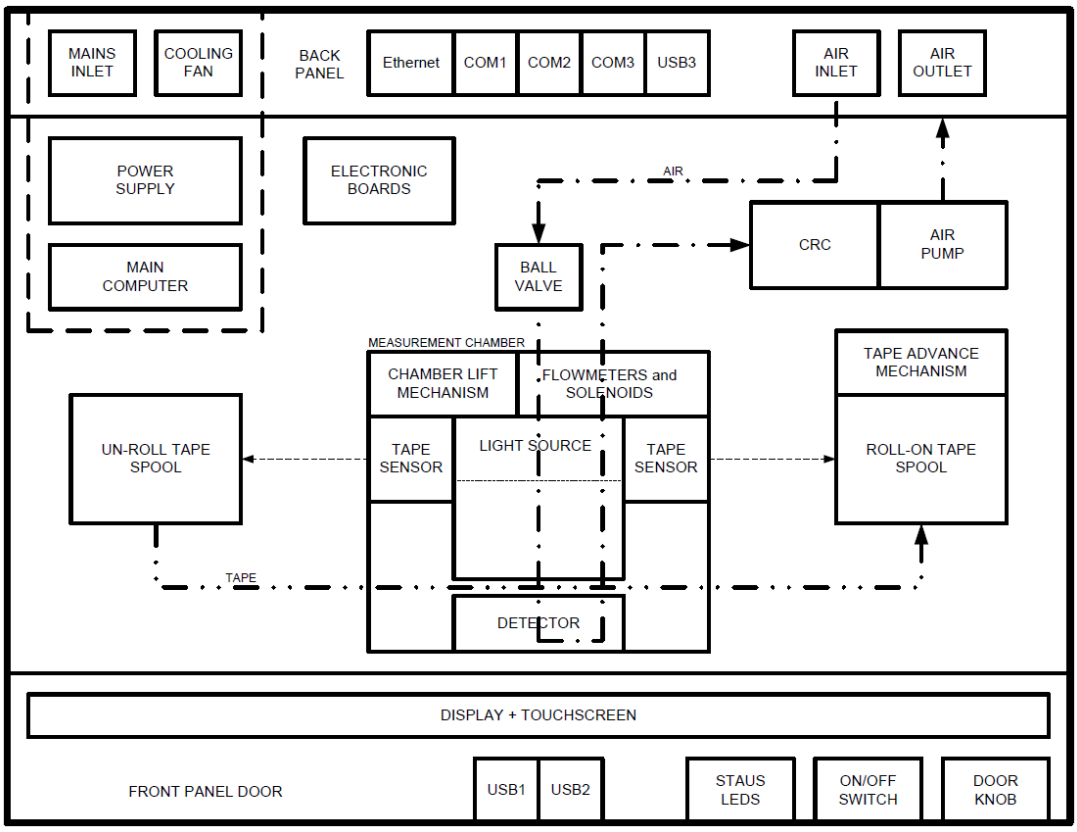

Figure 2.2. Block diagram of AE33 instrument (Magee Scientific Inc., 2016).

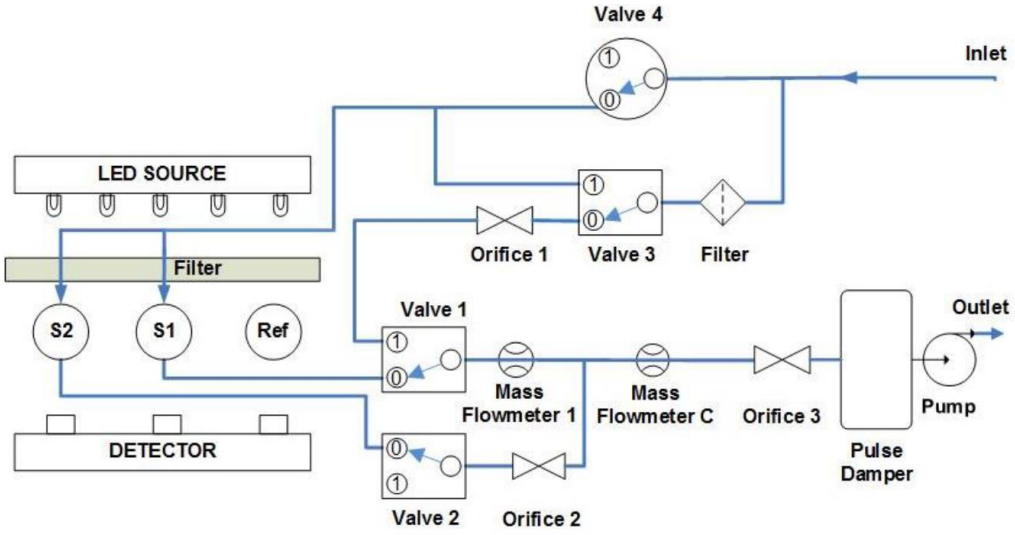

Figure 2.3. Flow diagram of AE33 instrument (Drinovec *et al.*, 2015).

2.1.2. Measurement of Attenuation and Calculation of Mass Concentration

The operating principles of the optical chamber in the AE33 instrument are shown in *Figure 2.4.* The attenuation (*ATN*) of light by the filter is calculated using the intensity of light that passes through the sampling spots and the reference spot using the following equation:

$$ATN = 100 * \ln(\frac{I_0}{I_x})$$

where I_0 is the intensity of the light emitted from the light source, I_x is the intensity of light measured after it has passed through the aerosol collected on spot 1 (I_1) or spot 2 (I_2) (Sandradewi *et al.*, 2008a). The calculated attenuation is then used to derive an attenuation coefficient (b_{atn}):

$$b_{atn} = \frac{S * (\frac{\Delta ATN}{100})}{F_{in} \Delta t}$$

where S is the spot area, ΔATN is the change in the attenuation over time (t), and F_{in} is the flow. The flow is calculated using the equation $F_{in} = F_{out} * (1 - \zeta)$, where F_{out} is the measured flow, and ζ is the leakage factor, predefined by the user (Z). The attenuation coefficient is used to calculate an absorption coefficient (b_{abs}):

$$b_{abs} = \frac{b_{atn}}{C}$$

where C is the multiple scattering parameter, also predefined by the user. This absorption coefficient is converted to an equivalent black carbon (eBC) mass concentration:

$$eBC = \frac{b_{abs}}{\sigma_{air}}$$

where σ_{air} is the mass absorption cross-section (MAC). The MAC value is set by the manufacturer for each wavelength. The channel used to calculate the eBC concentration is at 880 nm, in the near-IR region. The pre-set MAC value at 880 nm is 7.77 m^2/g (Magee Scientific Inc., 2016).

The eBC concentration is then corrected using the filter loading correction parameter, *k*, using the equation:

$$eBC^{\lambda}{}_{compensated} = \frac{eBC^{\lambda}{}_{non-compensated}}{(1 - k_{\lambda} * ATN_{\lambda})}$$

where $eBC^{\lambda}{}_{compensated}$ is the eBC value calculated for the different wavelengths (λ), $eBC^{\lambda}{}_{non\text{-}compensated}$ is the eBC value calculated without accounting for the loading compensation effect, k_{λ} is the compensation parameter for each wavelength (Drinovec *et al.*, 2017). Combining all of the above equations gives the final calculation for eBC concentration:

$$eBC = \frac{S * (\frac{\Delta ATN}{100})}{F_1(1 - \zeta) * \sigma_{air} * C * (1 - k * ATN_{\lambda}) * \Delta t}$$

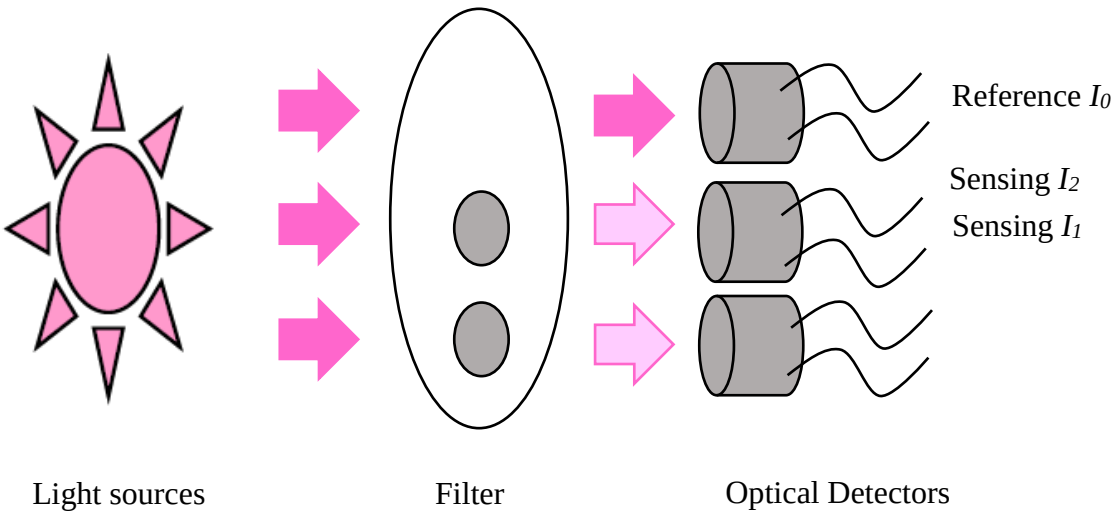

Figure 2.4. Schematic diagram of optical chamber operation, adapted from AE33 User Manual (Magee Scientific Inc., 2016).

2.2. AE33 Data Handling and Analysis

2.2.1. Aethalometer Outputs

The AE33 instrument is equipped with software produced by the manufacturer. This software controls all operations of the instrument and provides an easy-to-use interface for controlling the instrument. During sampling, the instrument saves a total of 67 different parameters to internal memory. The raw data is exported in the "*.dat*" format. A new file is created at the beginning of every day. In addition to the data file, a log file is also created, detailing the parameters selected by the user, and any changes to the status over the course of the day. The main parameters in the exported data file are; i) the attenuation (ATN) measurements for the three spots (spot 1, spot 2, and the reference spot); ii) the calculated eBC mass concentration values for each spot, and iii) the filter loading correction parameter (*k*), for the seven wavelengths. Additional parameters contained in the raw data file exported from the instrument include date, time, time base, flow rates, temperature, pressure and the status of the instrument. The instrument also performs a basic source apportionment of the measured eBC, splitting it into two sources, biomass burning related (eBC_{bb}), also referred to as wood burning (eBC_{wb}), and fossil fuel related (eBC_{ff}), also referred to as traffic ($eBC_{traffic}$). This two source model is based on the approach developed by (Sandradewi *et al.*, 2008b). The source apportionment uses the attenuation coefficients (b_{abs}) at 470 nm and 950 nm, as well as Ångström absorption coefficient (α) values for biomass burning (α_{bb}) and fossil fuel (α_{ff}). These α values are pre-set in the instrument, and can be changed by the user. The default values used in the Sandradewi model are 1 for α_{ff}, and 2 for α_{bb}. The equations used for the model are:

$$\frac{b_{abs}(470\ nm)_{ff}}{b_{abs}(950\ nm)_{ff}} = (\frac{470}{950})^{-\alpha_{ff}}$$

$$\frac{b_{abs}(470\ nm)_{bb}}{b_{abs}(950\ nm)_{bb}} = (\frac{470}{950})^{-\alpha_{bb}}$$

$$b_{abs}(470\ nm) = b_{abs}(470\ nm)_{ff} + b_{abs}(470\ nm)_{bb}$$

$$b_{abs}(950\ nm) = b_{abs}(950\ nm)_{ff} + b_{abs}(950\ nm)_{bb}$$

where $b_{abs}(\lambda)$ is the absorption coefficient for a particular wavelength (λ), $b_{abs}(\lambda)_{ff}$ is the fraction attributed to fossil fuel, and $b_{abs}(\lambda)_{bb}$ is the fraction attributed to biomass burning. The amount of biomass burning is calculated by:

$$BB(\%) = \frac{b_{abs}(950\ nm)_{bb}}{b_{abs}(950\ nm)}$$

The concentration of eBC attributed to biomass burning and fossil fuel are calculated using:

$$BC_{bb} = BB * BC$$

$$BC_{ff} = (1 - BB) * BC$$

2.2.2. *R*-script Analysis

The "*.dat*" files downloaded from the instrument are imported directly into the freeware *Openair* package developed using the *R* computer language (Carslaw and Ropkins, 2012; Carslaw, 2015). The use of *R* allows for the swift analysis of large amounts of data and the *Openair* package was specifically developed for the analysis of data generated by air quality monitoring instruments. The scripts used for analysis of the data collected during the SAPPHIRE and AEROSOURCE measurement campaigns are detailed in *Appendix I*.

The script can be broken down into several different sections. The first section imports the individual raw files into the workspace and concatenates them into a single file. The date and time stamp are formatted to Coordinated Universal Time (UTC). The rolling mean of the eBC concentrations for each wavelength are then calculated over a 15 minutes period in order to smooth any noise that may have occurred during measurement. This procedure removes the negative values that occur, and the corresponding positive value that results, thus avoiding potential biases. The filter loading correction parameters (*k*) for each wavelength are then imported into the database. The rolling mean procedure was repeated, with a time base of 15 minutes.

The next section of the script calculates the alpha (α) value associated with the ambient aerosol sampled on the filter tape. This calculation is based on the equations above, using the absorption coefficient (b_{abs}), eBC concentration, and the mass absorption cross-section (MAC) values associated with each wavelength. The MAC,

or σ, values associated with each wavelength are 18.47, 14.54, 13.14, 11.58, 10.35, 7.77, and 7.19 m^2/g respectively. While many previous studies have used different pairs of wavelengths to calculate the α value, for example Perron *et al.*, 2010; Herich *et al.*, 2011; Fuller *et al.*, 2014, in this study, the α value was calculated using only six wavelengths in order to maximise the use of the wavelengths available from the AE33 aethalometer. The 370 nm wavelength was excluded from the analysis due to potential interferences from volatile organic compounds deposited on the filter tape and non-BC light absorbing particles deposited on the filter such as secondary organic aerosols (Lack *et al.*, 2008; Vecchi *et al.*, 2014; Zotter *et al.*, 2017).

The next section of the script is the source apportionment section. The initial eBC source apportionment studies by Sandradewi *et al.* (2008a, 2008b) were conducted in an environment with two principal sources of BC; traffic and wood burning. However, there are several different fuels used for domestic combustion in Ireland, namely peat, coal, and wood. Therefore it was necessary to change the labelling from "wood burning" to "solid fuel burning". Using the two wavelengths defined by Sandradewi *et al*. (470 and 950 nm), the model is run to split the eBC mass concentrations into traffic related and solid fuel related fractions. This section allowed for modification of the original model, changing the α values assigned to traffic and biomass burning, or changing the wavelength pair used.

The final section of the script contains the functions that allow for manipulation of the processed data. The data can be time averaged to match the other instruments employed during the measurement campaigns. The data collected during the SAPPHIRE and AERSOURCE campaigns was converted to hourly averaged concentrations, two hourly averaged concentrations and daily averaged concentrations as required. Various functions for visualising the data are also contained in this section.

2.2.3. Additional Parameters Investigated

A variety of parameters obtained directly from the AE33 and also after some processing were used to ascertain the sources of eBC at rural and urban locations around Ireland. Firstly, the temporal and diurnal trends of eBC concentrations were calculated using the b_{abs} value from the 880 nm wavelength channel. The eBC concentrations from the 370 nm wavelength channel and the 880 nm channel were then used to calculate the ΔC value.

$$\Delta C = eBC_{370\,nm} - eBC_{880\,nm}$$

ΔC is an indicator of the level of wood or biomass burning particles in the ambient aerosol (Wang *et al.*, 2011b).

The temporal and diurnal patterns of the filter loading parameter (k) and the calculated α value were also investigated. The variation in the α value was investigated for all locations. The source apportionment analysis requires the input of two preselected α values, one for traffic and one for solid fuel burning. The values used for this study are taken from the Zotter *et al*. (2017) study, 0.9 for traffic (α_{Tr}) and 1.68 for solid fuel combustion (α_{SF}). The diurnal and seasonal variation in α provides information on particle composition and the dominant source of particles during different hours of the day, days of the week, and months of the year. Frequency distributions of the calculated α value show the differences in source contributions during the different seasons.

2.3. Additional Instrumentation During the SAPPHIRE Campaign

In addition to the AE33, eight other instruments were deployed during the measurement campaigns in Killarney, Enniscorthy, and Birr. An Optical Particle Sizer (OPS) (TSI Inc., Model 3300), and a Scanning Mobility Particle Sizer (SMPS) (TSI Inc., Model 3080), were deployed for measuring particle number and size distributions. A Tapered Element Oscillating Microbalance (TEOM) (Thermo Electron, Model 1400a) was deployed to measure $PM_{2.5}$ mass concentration. A nitrogen oxides (NO_x) monitor (Teledyne, Model T200) was used to measure concentrations of NO, NO_2, and NO_x. A high volume sampler (DIGITEL, Model DHA-80) was deployed to collect filter samples for offline chemical analysis. These instruments are described in more detail in Chapter 3. The main instruments that provided complementary data for analysis of the carbonaceous aerosol content were the Aerosol Time of Flight Mass Spectrometer (ATOFMS) and the OCEC analyser.

2.3.1. Aerosol Time of Flight Mass Spectrometer (ATOFMS)

The ATOFMS (TSI Inc., Model 3800) measures the size and chemical composition of single particles with diameters ranging from 100 – 3000 nm (Prather *et al.*, 1994; Gard *et al.*, 1997; Healy *et al.*, 2010; Arndt *et al.*, 2017). This instrument can detect a range of species, including elemental and organic carbon, sodium chloride, transition metals, and secondary species such as sulfate, ammonium and nitrate. Interpreting the chemical composition of particles, temporal profiles of the different classes, size distributions and meteorological information enables the user to perform a type of source apportionment, where the observed particle classes are attributed to different natural and anthropogenic sources (Healy *et al.*, 2010).

The ATOFMS consists of three different operating regions, shown in the schematic diagram below (*Figure 2.5*). In the sampling region, ambient aerosol is drawn through the inlet and aerodynamic lens, where the single particle beam is generated. In the sizing region, the single particle passes through two lasers (λ = 532 nm) that determine the aerodynamic diameter of the particle. Finally, the particle

moves through to the mass spectrometer region, where it is ablated by a pulsed ultraviolet laser (λ = 266 nm). The timing of the pulse from this laser is calculated using the aerodynamic diameter of each particle. The pulsed laser produces gaseous ions that enter the time-of-flight mass spectrometers to yield a positive and negative mass spectrum of the single particle.

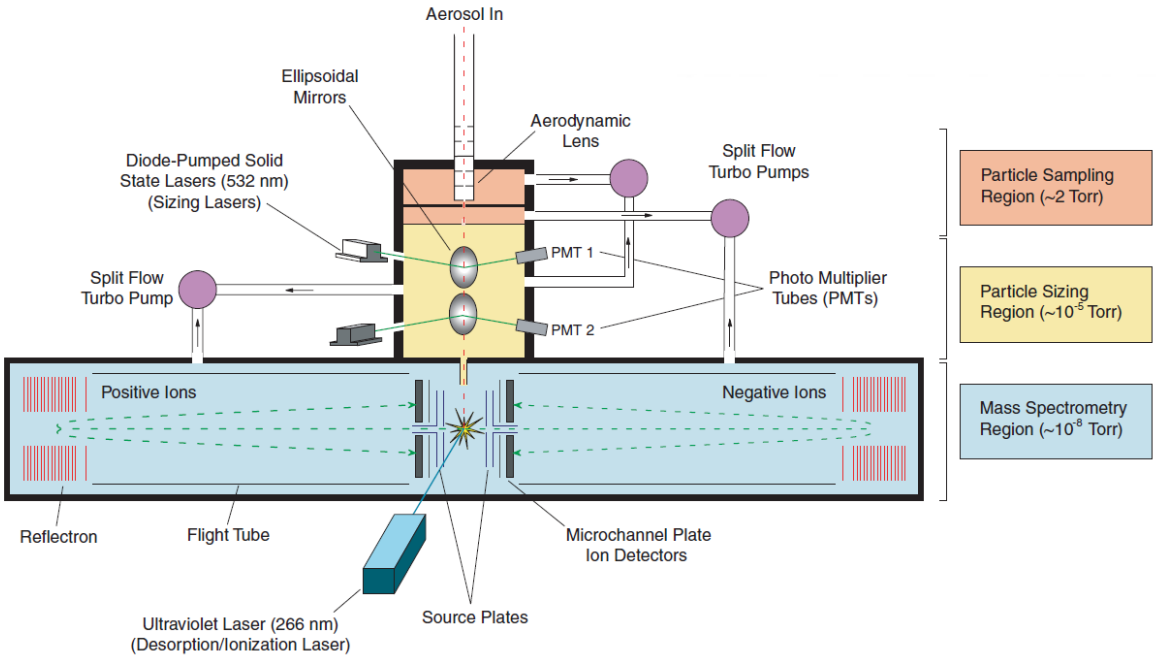

Figure 2.5. Schematic of the aerosol time-of-flight mass spectrometer (ATOFMS) (TSI, 2007).

The data collected by the ATOFMS during the SAPPHIRE measurement campaigns was analysed by Dr Jovanna Arndt of the Centre for Research into Atmospheric Chemistry at University College Cork. Details of the analysis procedure are provided elsewhere (Arndt, 2015; Arndt *et al.*, 2017). In brief, analysis of the data was carried out using ENCHILADA (ENvironmental CHemistry through InteLligent Atmospheric Data Analysis), a freeware SQL-based computer programme (Gross *et al.*, 2010). The programme uses the *K*-means algorithm (Macqueen, 1967), that clusters single particle mass spectra into a user defined number of clusters (*K*) based on their similarity (Anderson *et al.*, 2005). The user defined number of clusters is increased until no significant changes are observed in the dataset. Clusters with similar average mass spectra and temporal trends were grouped together. The identification of the different particle classes was based on "fingerprint" spectra identified for different pollution sources, for example by Healy *et al.* (2010). While the ATOFMS

is a powerful tool for source apportionment, it does not quantify the mass concentrations of the different particle classes. In order to produce meaningful mass concentrations for the identified particle classes, a scaling procedure is required. For the SAPPHIRE campaign, this scaling procedure was performed using the number concentrations measured by the OPS and SMPS instruments. The mass concentrations are derived from the scaled number concentrations based on the equation from Reinard *et al.*, (2007);

$$m_p = \frac{\pi}{6}\rho_p d_{ve}^3$$

where ρ_p is the particle density, and d_{ve} is the volume equivalent diameter. This scaling procedure used an assigned density for each particle class based on the chemical composition and also relied on the assumption that all measured particles were spherical. Although these assumptions are subject to some uncertainty, the approach has been successful in previous studies (Healy *et al.*, 2012, 2013), i.e. the mass concentrations for each ATOFMS particle class derived using this scaling procedure do compare well with direct quantitative measurements of $PM_{2.5}$ and eBC.

2.3.2. OCEC Analyser

Organic and elemental carbon (OC and EC) concentrations were measured using the semi-continuous OC/EC instrument, Model 4L (Sunset Laboratory Inc., 2005), shown in *Figure 2.6*.

Particulate matter samples are collected on a quartz fibre filter that is contained in a glass tube that has been inserted into the instrument. Ambient aerosol is drawn through an inlet with a 2.5 μm cut-off for 108 minutes and deposited on a quartz fibre filter punch contained in the instrument. Once sample collection is complete, a 12 minute analysis period is enacted.

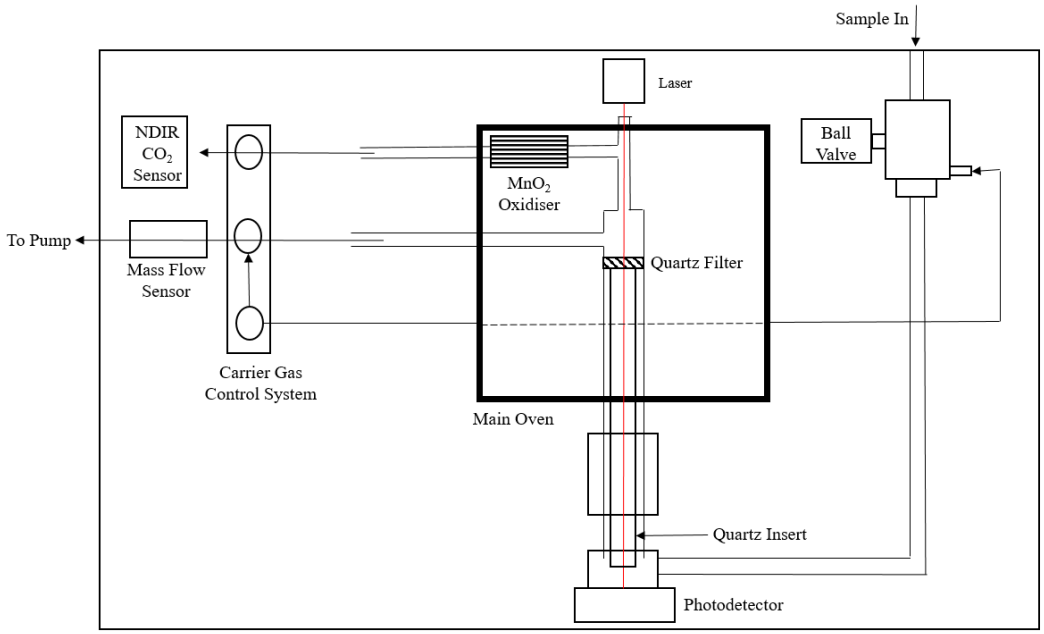

Figure 2.6. Flow schematic of Sunset OC/EC instrument (adapted from O'Connor, 2012).

The instrument was operated using the NIOSH protocol (Birch, 2003), in order to allow for comparison to previous measurements made in Ireland (for example Yin *et al.*, 2005; Dall'Osto *et al.*, 2013). Firstly, the oven is purged with helium and a stepped-temperature increase is initiated, rising to a temperature of 850 ºC. Organic compounds on the filter are thermally desorbed during this period, and, in addition to any pyrolysis products, pass into an oxidizing oven containing manganese dioxide (MnO_2). The carbon fragments are converted to CO_2 as they flow through the oxidising oven. The CO_2 gas is then measured by a non-dispersive infrared (NDIR) detector system. The concentration of CO_2 gas is directly related to the amount of organic carbon and pyrolysis products. After a brief cool down period, a second temperature ramp protocol is initiated using oxidising gases, methane (CH_4) and oxygen (O_2). This removes any elemental carbon deposited on the filter, which is oxidised and passed through the oxidising oven and NDIR in the same fashion as the organic carbon fraction.

The software provided by the manufacturer is designed to run in conjunction with the instrument and analyse the data as it is measured by the NDIR. The software also facilitates analysis of the collected data. The OC and EC concentrations are calculated automatically based on the response of the NDIR during the different stages of the protocol. Also factored into the calculation are the baseline response of the NDIR when no aerosol is deposited on the filter, and the results of weekly calibrations.

The post sampling processing of the data involved ensuring the split point between OC and EC occurred at the correct time in each sample. This split point was occasionally moved from the standard position due to charring that can occur on the filter during the heating stage of the protocol.

2.4. Additional Instrumentation During the AEROSOURCE campaign

In addition to the AE33, an Aerosol Chemical Speciation Monitor (ACSM, Aerodyne Research Inc.) was deployed to measure the organic carbon contribution to PM_1 mass. The instrument was operated and maintained by colleagues from the School of Physics and Centre for Climate and Air Pollution Studies, in the National University of Ireland Galway.

A schematic diagram of the ACSM is shown in *Figure 2.7* and a complete description of the ACSM instrument can be found in Ng *et al*. (2011). In brief, the instrument operates by sampling ambient aerosol, passing it through an aerodynamic lens and into a hot oven, where the particles are vapourized. This vapour is then analysed using an electron impact ionization quadrupole mass spectrometer. The instrument measures an average mass spectrum that reflects the bulk composition of the ambient aerosol and is divided between different chemical components; organic aerosol (OA), sulfate, nitrate, chloride and ammonium. Source apportionment of the OA fraction can be achieved using positive matrix factorization (Paatero and Tapper, 1994; Paatero, 1997) and comparing the mass spectrum for each factor to fingerprint spectra for specific sources. Typical OA types can be split into two different classes; primary organic aerosol (POA) and secondary organic aerosol (SOA). POA compounds are released directly in particulate form from the combustion of fuels, biomass and from other mechanical processes, while SOA compounds are formed in the atmosphere through the oxidation of volatile organic compounds (VOCs) (Zhang *et al.*, 2011). OA types can include hydrocarbon-like OA (HOA), biomass burning OA (BBOA), cooking OA (COA), semi-volatile oxygenated OA (SV-OOA), low volatility oxygenated OA (LV-OOA), and nitrogen-enriched OA (NOA) (Zhang *et al.*, 2011;

Crippa *et al.*, 2014). Fingerprint spectra for different OA sources, such as wood burning, coal burning, cooking, have been previously identified (Schneider *et al.*, 2006; Alfarra *et al.*, 2007; Weimer *et al.*, 2008; Slowik *et al.*, 2010; Wang *et al.*, 2013; Zhang *et al.*, 2015). A recent study by Lin *et al.* (2017) identified fingerprint spectra for the various solid fuel types used in Ireland, i.e. coal, peat and wood, based on a series of combustion experiments. These fingerprint spectra were then used to isolate the contribution from each fuel type to ambient pollution levels in Galway, Ireland (Lin *et al.*, 2019a).

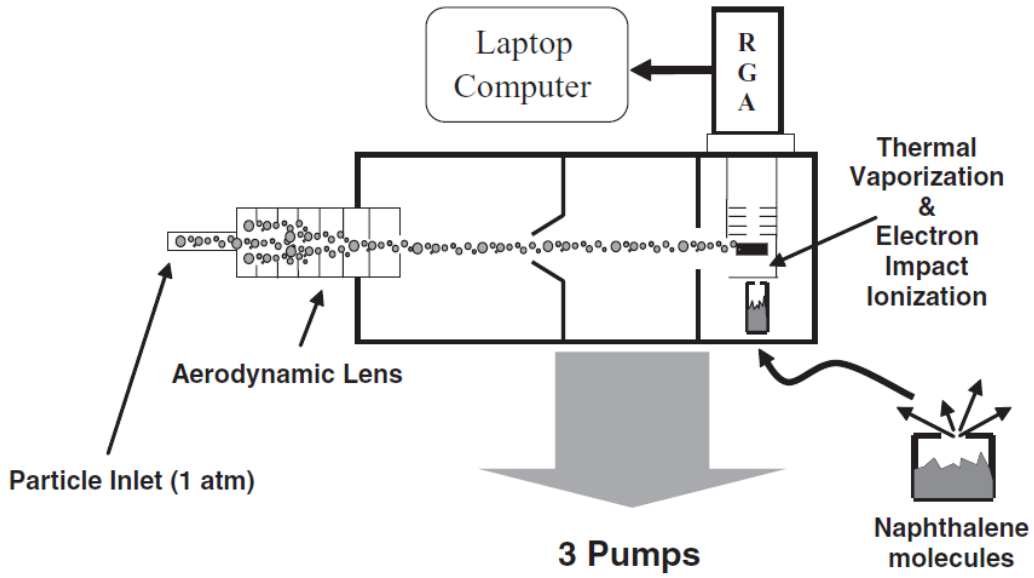

Figure 2.7. Schematic of the aerosol chemical speciation monitor (ACSM) (Ng *et al.*, 2011).

The data collected by the ACSM was analysed by Dr Chunshui Lin, of the School of Physics and Centre for Climate and Air Pollution Studies, in the National University of Ireland Galway (Lin *et al.*, 2017; Lin, 2019). The instrument measures an average mass spectrum for the ambient aerosol, which is divided between different chemical components; organic aerosol (OA), sulfate, nitrate, chloride and ammonium. Source apportionment of the OA fraction was based on "fingerprint" spectra measured for each fuel type during a series of combustion experiments (Lin *et al.*, 2017), in addition to temporal trends of particle classes and meteorological conditions. Using the "fingerprint" spectra, the OA fraction was separated into contributions from wood, peat, and coal for the AEROSOURCE measurement campaign at University College Dublin (UCD).

2.5. Analysis of Historical Black Smoke and SO_2 Data

The analysis of black smoke (BS) concentrations measured in Dublin since the 1960s, was an additional objective of the AEROSOURCE campaign. These original black smoke measurements were made in accordance with methods detailed by the Organization for Economic Cooperation and Development (OECD, 1964), and is described in the British Standards Institute document BS 1747-2 (1969): Determination of concentration of suspended matter (British Standards Institute, 1969a). The apparatus used to measure BS concentrations is shown in *Figure 2.8*. In brief, air was passed through a Whatman No. 1 filter paper at a set flow rate. The reflectance of the particulate matter collected on the filter was measured using a reflectometer and converted into $\mu g/cm^2$ using the equation detailed in Christolis *et al.* (1992). Reflectance measurements were also converted into a Black Smoke Index (BSI) value using a standard table based on International Standards Organisation (ISO) document 9835: Ambient air – Determination of a black smoke index (ISO, 1993) . Irish, British and European measurements were made in accordance with this procedure (Goodman, 1999; Goodman *et al.*, 2009; Quincey *et al.*, 2009).

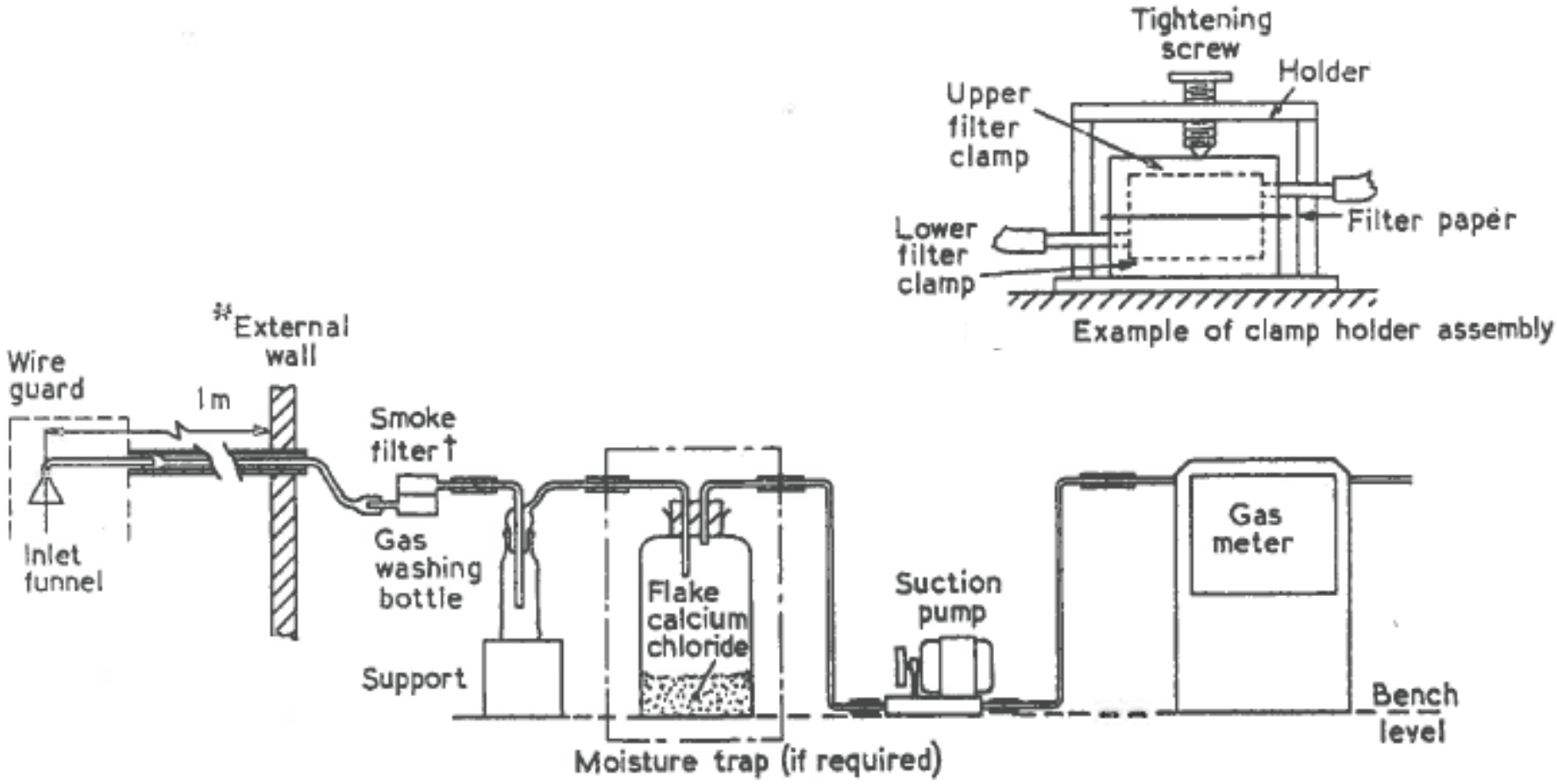

Figure 2.8. Schematic of measurement system used to measure BS concentrations (adapted from British Standards Institute, 1969a).

SO_2 measurements were made in accordance with the ISO document 4219:1979, "Air quality – Determination of gaseous sulfur compounds in ambient air – Sampling equipment" (ISO, 1979). This method is summarised by the British Standards Institute document BS 1747-3 (1969): Determination of sulfur dioxide (British Standards Institute, 1969b). In brief, the concentration of sulfur dioxide was determined by passing a sample of filtered air through a bubbler containing an acidified solution of hydrogen peroxide, pH ~4.5. The SO_2 is absorbed into the acidified solution, the solution is then titrated against a standard basic solution to determine how much SO_2 has been absorbed (AFA Technology, 1999).

3. Source Apportionment of eBC During the SAPPHIRE Project

Contents

3.1. Introduction

3.1.1. Global and Regional Impacts of Solid Fuel Burning

The combustion of solid fuels (coal, peat, and wood) and biomass emits significant amounts of particles and other pollutants into the atmosphere. A reduction of these emissions would significantly benefit human health and reduce climate warming (Butt *et al.*, 2016). Solid fuel is used globally for both residential heating and cooking purposes. Modelling studies have shown that the percentage of households around the world using solid fuels for cooking decreased from 1980 to 2010, however the number of people exposed to pollution remained relatively stable at approximately 2.8 billion (Bonjour *et al.*, 2013; Bruce *et al.*, 2013). During this period, it is estimated that the number of households in Africa utilising solid fuel increased, with 646 million people exposed to the corresponding rise in air pollution. In contrast, most other regions around the world, including Europe, showed a reduction in the percentage of households using solid fuels over this period.

In 2018, the number of people affected by air pollution from solid fuel burning was estimated to be approximately 2.45 billion (Shupler *et al.*, 2018). The rural and poorer areas of low and middle income countries in Africa, Asia, Central and South America were, again, identified as being markedly affected by this type of air pollution. Using 419 source apportionment studies from around the globe, Karagulian *et al.* (2015) reviewed local source contributions in different countries. Based on the global averages, 25% of $PM_{2.5}$ in urban areas originated from traffic sources, 15% from industrial activity, 20% from domestic fuel burning, 18% from natural dust and sea spray, and 22% from non-specific human activities. Domestic solid fuel burning was identified as the major source of $PM_{2.5}$ in Africa (34%) and in Central and Eastern Europe (32%). It was also a significant contributor in South America (25%, excluding Brazil), North Western Europe (22%), Southern China (21%), South Eastern Asia (19%) and India (16%). Domestic solid fuel was also a significant contributor to PM_{10} concentrations in Central and Eastern Europe (45%), North Western Europe (24%), Africa (21%), and Northern China (19%). Vicente and Alves (2018) performed a comprehensive review of studies focused on all aspects of residential biomass

combustion. The economic crisis of 2008 resulted in an increase in household biomass burning in the EU, for example, in Thessaloniki, Greece $PM_{2.5}$ concentrations increased by 30% due to a higher prevalence of residential wood combustion (Saffari *et al.*, 2013). Studies showed that in the cooler months, biomass burning emissions significantly increased the levels of $PM_{2.5}$ measured at all locations. Overall, residential biomass burning contributed approximately 40–60% of the measured PM fractions in Europe (Vicente & Alves, 2018 and references therein) and is also the largest source of organic aerosol (Denier Van Der Gon *et al.*, 2015). Modelling studies have predicted that the amount of $PM_{2.5}$ emitted by residential fuel burning, both biomass and fossil fuel, will decrease in Europe up to 2030. However, it is also estimated that the relative contribution to $PM_{2.5}$ mass will increase as other major sources, such as traffic, decrease due to improving technology and mitigation strategies (WHO, 2015). The trend of decreasing $PM_{2.5}$ mass is observed in emission inventory estimates published by the European Environment Agency (EEA), shown below in *Figure 3.1.* It is estimated that the commercial, institutional and residential sector (blue) contributed 56% of the emitted $PM_{2.5}$ in 2017 (EEA, 2019).

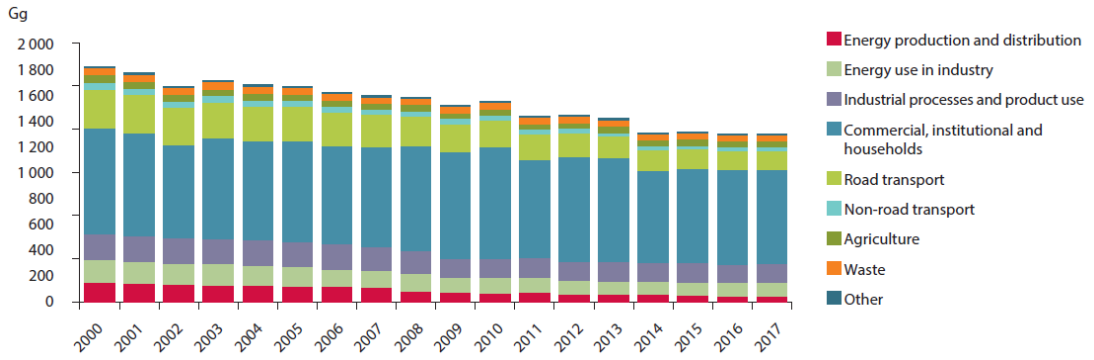

Figure 3.1. Sectoral contributions to $PM_{2.5}$ mass emissions in Europe from 2000 to 2017 (EEA, 2019).

Source apportionment of PM_{10} and $PM_{2.5}$ in order to identify the major contributions to air pollution in different European cities has been carried out using the SHERPA modelling tool (Thunis *et al.*, 2018) and an urban $PM_{2.5}$ atlas has been produced by the Joint Research Centre (Thunis *et al.*, 2017). The average contribution from the residential sector, including emissions from fireplaces, boilers, cookers and heating stoves, across the 150 monitoring locations was 13%. The highest contributions from the residential sector were observed in eastern European countries - Poland in particular, as well as some cities in Italy - with the highest values occurring

in Warsaw (48%) and Krakow (40%). The model did not show high contributions from the residential sector in Northern European countries such as the UK, Ireland and Germany.

3.1.2. Solid Fuel Burning in Ireland

There is a long history of solid fuel use in Ireland for domestic purposes, which has often led to air pollution issues around the country. Airborne particles were measured in the Dublin city area during the mid-1920s (Boylan, 1926), and the influence of domestic solid fuel burning during the winter months was established in the 1940s (Leonard *et al.*, 1950). A network of monitoring stations was established in Dublin in 1963 to provide continuous, long-term measurements of black smoke (BS) and SO_2. This network, which operated until 2009, captured many winter time pollution events that were related to solid fuel burning during particularly cold and/or still periods. The high use of solid fuels in the Dublin area was curtailed with the introduction of a ban on the sale of bituminous coal in 1990, which subsequently led to a 70% reduction in measured BS concentrations (Clancy *et al.*, 2002). Over the next two decades, this ban was gradually extended to the main cities and more populated towns across Ireland. Data presented in the North South Ministerial Report of 2016 shows that between 2000 and 2013, the residential sector was the largest single contributor to $PM_{2.5}$ emissions in Ireland, accounting for 50.02% and 56.65% in 2000 and 2013 respectively (Abbott *et al.*, 2016). It was estimated that in 2013, approximately 99.2% of the residential $PM_{2.5}$ emissions originated from the combustion of solid fuels, including bituminous coal, anthracite and manufactured ovoids, lignite, petroleum coke and biomass. The other 0.8% of emissions originated from the combustion of kerosene, light petroleum gas (LPG), gasoline/diesel and natural gas. In a more recent report from the Sustainable Energy Authority of Ireland (SEAI) in 2018, it was estimated that the energy demand from the residential sector in Ireland decreased by 11% between 2005 and 2017 (SEAI, 2018). During this period, fossil fuel use decreased by 18.1%, owing to an increased use of electricity (+ 6.0%) and renewable energy sources (+ 228.7%), and to the decreased use of coal, peat, oil and gas, with reductions of 39.5%, 31.0%, 15.5% and 8.5% respectively.

Detailed information on the contribution of solid fuel burning to ambient levels of particulate pollution are best obtained from measurements of the chemical composition of the particles. The first detailed study of the chemical composition and sources of PM in Ireland was published by Yin *et al*. (2005). Measurements of PM_{10} and $PM_{2.5}$ were made at five locations around Ireland; two sites in Dublin, and one location in Cork, Galway, and Wicklow. The main contributors to PM mass were identified as primary marine aerosol, secondary inorganic materials, primary anthropogenic combustion materials, primary and secondary organic materials, and re-suspended dusts. The composition of atmospheric aerosols also varied by location. The major components of $PM_{2.5}$ mass at urban locations (79–84%), were organic compounds, elemental carbon, ammonium sulfate/nitrate. At the rural and coastal locations, $PM_{2.5}$ was dominated by ammonium sulfate/nitrate and organic matter (65%). The main contributor to PM_{10} mass at all locations was sea salt, 56–66% in urban areas, 39% in rural areas, and 56% in coastal areas. An intensive two month monitoring campaign was also conducted during this time, with size-segregated mass, soluble ions, elemental carbon (EC) and organic carbon (OC) all being measured (Ceburnis *et al.*, 2006). Results showed that urban pollution in Ireland was dominated by local emissions from within a 20–30 km radius, with carbonaceous compounds accounting for roughly 90% of the particle mass in the 0.066–0.61 μm range. OC varied by season, with significantly higher levels measured during the summer owing to biogenic emissions. In the winter, elemental carbon emissions were substantially elevated due to solid fuel burning.

Source apportionment of PM has also been conducted in several studies around Cork. One study of the air quality in Cork city and harbour used data from five different locations coupled with Principal Component Analysis (PCA) to show that high levels of marine aerosol and naturally re-suspended dusts existed at all locations (Byrd *et al*. 2010), accounting for up to 56% of the 2010 EU annual PM_{10} limit (20 $\mu g/m^3$). In an alternative approach, Hellebust *et al*. (2010) used real-time measurements of eight pollutants to identify the major sources of $PM_{2.5}$ using Principal Component Analysis (PCA) and Positive Matrix Factorization (PMF). The largest contributors to $PM_{2.5}$ mass, accounting for a combined 80%, were identified as sea salt, shipping, crustal material, and secondary organic aerosols. It should be noted that these studies were limited as they did not measure the carbonaceous content of PM which typically represents a large and often dominant component of the PM mass.

Kourtchev *et al*. (2011) performed source apportionment of OC in ambient $PM_{2.5}$ aerosol at Tivoli Docks in Cork's inner harbour. Filter samples collected every 6-12 hours were analysed for polar organic compounds that act as markers for biomass burning emissions, fungal spores and secondary organic aerosol (SOA). The markers for fungal spores and biogenic SOA were only detected during summer months, while biomass burning markers, in particular levoglucosan, were present in all of the collected samples. The seasonal domestic solid fuel (DSF) burning contribution to the measured OC mass concentration was estimated as follows; summer (10.8%), autumn (50%), late autumn (66.4%), and winter (74.9%). This study further highlighted the fact that despite a ban on the sale of bituminous (smoky) coal in the city, DSF burning is still the major source of OC during autumn and winter months, making a large contribution to $PM_{2.5}$ mass concentrations. The collection of filters for this type of source apportionment, while useful, has some inherent disadvantages; i) the highest time resolution possible to achieve the required sensitivity is at least six hours, and ii) this method is unable to distinguish between different solid fuel types, since the particles emitted by each of the fuels contain the same marker compounds (levoglucosan, mannosan, galactosan). These issues were overcome with the deployment of an Aerosol Time of Flight Mass Spectrometer (ATOFMS) for source apportionment study at the same inner harbour location in August 2008 (Healy *et al.*, 2010). The major advantage of the ATOFMS during this campaign was the one hour time resolution coupled with the ability to distinguish between the different solid fuel classes. ATOFMS results, along with data from several other on-line instruments, were used to determine source contributions to $PM_{2.5}$ mass using Positive Matrix Factorisation. The six factors identified and their respective contributions to $PM_{2.5}$ mass were; vehicular traffic (23%), marine (14%), long range transport (13%), industrial combustion (11%), domestic solid fuel combustion (5%) and shipping emissions (1.5%).

A further measurement campaign conducted in Cork at the inner harbour location involved the co-deployment of an ATOFMS and aerosol mass spectrometer (AMS) for three weeks in February 2009. The contributors to non-refractory PM_1 mass were identified as organic aerosol (62%), nitrate (15%), sulfate (9%), ammonium (9%) and chloride (5%). Five factors were identified using PMF, "hydrocarbon-like" organic aerosol (HOA), "low-volatility" oxygenised organic aerosol (LV-OOA), "biomass burning" organic aerosol (BBOA), "peat and coal" organic aerosol (PCOA)

and "cooking" organic aerosol (COA), contributing 20%, 18%, 23%, 21% and 18% to PM_1 mass respectively (Dall'Osto *et al*., 2013). PMF analysis was also performed using a combination of all the instruments deployed during the monitoring campaign (Dall'Osto *et al*., 2014). In this complementary study, five factors were also identified; regional domestic solid fuel burning (24–27%), local urban domestic solid fuel burning (22–23%), road vehicle emissions (15–20%), secondary aerosols from regional anthropogenic sources (9–13%) and secondary aged/processed aerosols related to urban anthropogenic sources (21–26%). Results from this analysis were in good agreement with the earlier study of Kourtchev *et al.* (2011) showing that solid fuel burning was the major source of $PM_{2.5}$ in the wintertime in Cork (46–50%).

In recent years, the chemical composition of PM_1 has also been investigated using an Aerosol Chemical Speciation Monitor (ACSM) instrument. As a more compact version of the AMS, this instrument also allows for the analysis of the organic aerosol fraction of PM. Initially, ambient measurements were conducted at the Centre of Climate and Air Pollution Studies in NUI Galway from 17/10/15 to 23/11/15 (Lin *et al.*, 2017). The results of the source apportionment analysis show that domestic solid fuel burning is the dominant contributor to evening and night-time particulate pollution, despite reported low use. Summer time measurements in Galway were made using the ACSM from 01/06/16 to 22/06/16 at the same location as the winter time campaign (Lin *et al.*, 2019a). It was found that the average PM_1 concentration, 2.7 ± 2.3 $\mu g/m^3$, was lower than the concentration measured during the winter campaign and also lower than reported for other European locations. In this study, 54% of the PM_1 mass was attributed to organic aerosol, 84% of which was attributed to secondary production. The remaining 16% was attributed to primary emissions from peat burning.

As part of the AEROSOURCE monitoring campaign, presented in Chapter 4, the ACSM was deployed on the campus of University College Dublin, an urban background location in the city of Dublin. During periods of extremely high pollution in the winter of 2016/17, organic aerosol accounted for over 60% of the measured PM_1 mass (Lin *et al.*, 2018). During the evening and night-time hours, significant contributions from coal, peat, wood and oil combustion were measured.

3.1.3. The SAPPHIRE Project

A number of field measurement campaigns over the last decade have identified domestic solid fuel burning as a major source of air pollution in Ireland, particularly during winter months. However, these studies were conducted in the largest cities, i.e. Cork, Galway and Dublin, where there is a ban on the sale and distribution of bituminous or "smoky" coal. The smoky coal ban is also in place in "Large Towns" with a population over 15,000 (O'Dwyer, 2013), but not in other parts of the country, *Figure 3.2*. There are over 800 "Small Towns" in Ireland with a population of less than 15,000 and despite high levels of PM observed in some rural locations (EPA, 2019a), there has been no source apportionment studies performed outside of the main cities. Therefore the principal aim of the SAPPHIRE project was to determine the sources of particulate pollution in residential areas of rural towns in Ireland.

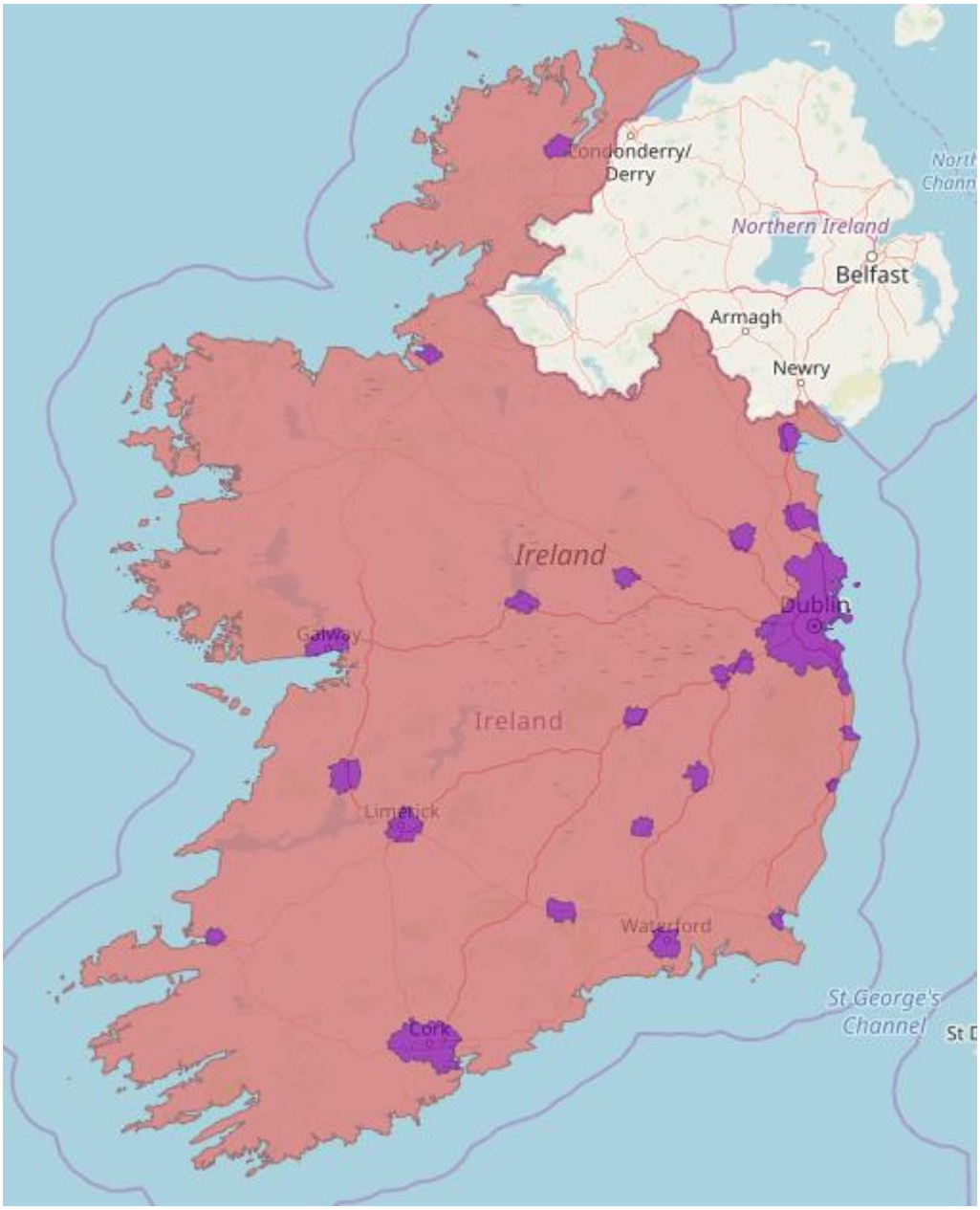

Figure 3.2. Map of areas (in purple) covered by "smoky" coal ban in Ireland as of 2015 (EPA, 2019b).

Measurements were made during winter time in three small towns, Killarney in Co. Kerry, Enniscorthy in Co. Wexford, and Birr in Co. Offaly, using a suite of instruments for monitoring PM mass, size and chemical composition. The results were used to conduct a source apportionment study of $PM_{2.5}$ at the selected monitoring locations and quantify the contributions of major sources, especially residential solid fuel burning. Particular efforts were made to quantify the contribution that each solid fuel type (coal, peat and wood/biomass) made to the measured $PM_{2.5}$.

Real-time monitoring of PM chemical composition using an ATOFMS showed that domestic solid fuel burning was the dominant source category at all three

locations, accounting for 64%, 70% and 54% of $PM_{2.5}$ measured in Killarney, Enniscorthy and Birr respectively, *Figure 3.3* (Arndt *et al.*, in preparation). The results showed that peat burning was the main contributor, followed by wood and coal. Some unassigned DSF burning particles were also observed in each location. Traffic and sea spray were minor sources of $PM_{2.5}$, while evidence was found to suggest that gaseous amines and ammonia released from the agricultural sector can effectively combine with combustion aerosols to accelerate particle growth and increase $PM_{2.5}$.

These results were used to draw conclusions about the sources of $PM_{2.5}$ in rural and urban residential areas of Ireland and provide policy makers with relevant scientific information to support the development of effective strategies for reducing particulate pollution.

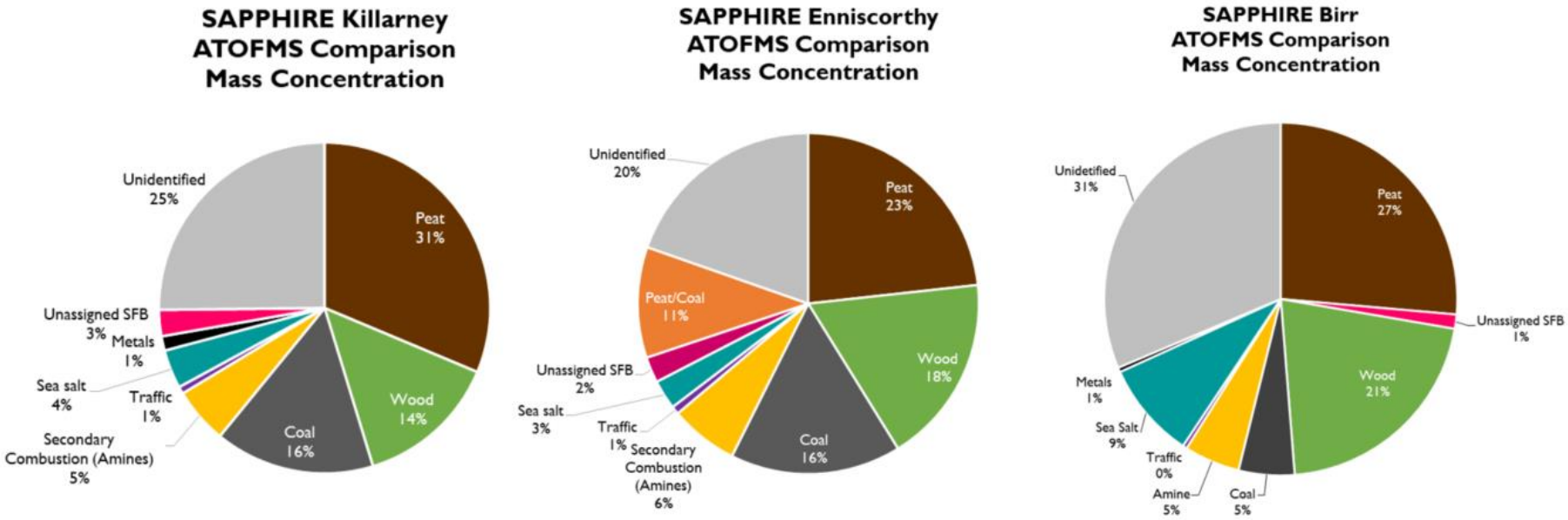

Figure 3.3. Contributions of ATOFMS particle categories to $PM_{2.5}$ mass concentration during the three SAPPHIRE measurement campaigns (Arndt *et al*., in preparation).

3.1.4. Aim of this Work

The aim of the work presented in this chapter is to examine the carbonaceous content of $PM_{2.5}$ measured at each of the three monitoring locations involved in the SAPPHIRE campaign. The main instrument used for this work is the AE33 seven wavelength dual-spot aethalometer (Drinovec *et al.*, 2015). The data collected during the monitoring campaigns are used to assess the concentrations of black carbon in rural locations around Ireland. Source apportionment using the model developed by Sandradewi *et al.* (2008b) is initially used to determine the contributions of traffic and wood-burning sources to BC concentrations. The model however is not suitable for the multi-fuel Irish environment and alterations to the parameters are made to provide a more accurate source apportionment of BC in rural Ireland. The new, optimised, parameters are then compared to the parameters recently proposed by Zotter *et al.* (2017). Site specific mass absorption cross section (MAC) values are also determined for the monitoring sites, using data from the aethalometer and an OCEC carbon analyser. The optimisation of the source apportionment model is validated using other data acquired from the aethalometer instrument, such as the ΔC value. The variation in ΔC, calculated α value, and MAC provide an indication of the different compositions of the ambient aerosol at each site. The results of the optimised source apportionment model are compared to those obtained from other instruments that were deployed during the campaigns, including the ATOFMS instrument, which allows for classification of the chemical composition of single particles.

3.2. Methodology

3.2.1. Sampling Sites

Sampling and measurements for the SAPPHIRE project took place in three rural towns in Ireland. The criteria for selection of sites for this project were; i) the location had to be outside of existing smoke control areas (meaning a population of less than 15,000); ii) no access to the national natural gas supply; iii) expected high use of solid fuel for domestic heating purposes, taken from relevant census data gathered by the Central Statistics Office (CSO, 2011). The towns selected for measurements were Killarney in Co. Kerry, Enniscorthy in Co. Wexford, and Birr in Co. Offaly, as shown in *Figure 3.4* and *Table 3.1*. Killarney had been the location for a previous EPA funded air quality study (McNally, 2013). PM_{10} mass concentrations in Enniscorthy are among the highest in Ireland based on EPA air quality reports (EPA, 2015). Finally, Birr was selected based on a number of exploratory measurements using a portable optical particle sizer (Model 3330, TSI Inc.) at several locations in Co. Offaly.

The reported solid fuel use detailed in *Table 3.1* is taken from the data gathered during the Irish Census of 2011. Further data is available from a Quarterly National Housing Survey (QNHS) performed in 2014, with a focus on household environmental behaviour (CSO, 2016). In this survey, questions were asked about secondary heating sources used by households, and the fuel used in these open fires and/or stoves.

Table 3.1. Key criteria for SAPPHIRE measurement locations (CSO, 2011).

Location	Population	Number of Households	Solid Fuel Use (%) for Central Heating
Killarney, Co. Kerry	12740	4168	10
Enniscorthy, Co. Wexford	2842	1245	28
Birr, Co. Offaly	4428	1664	30

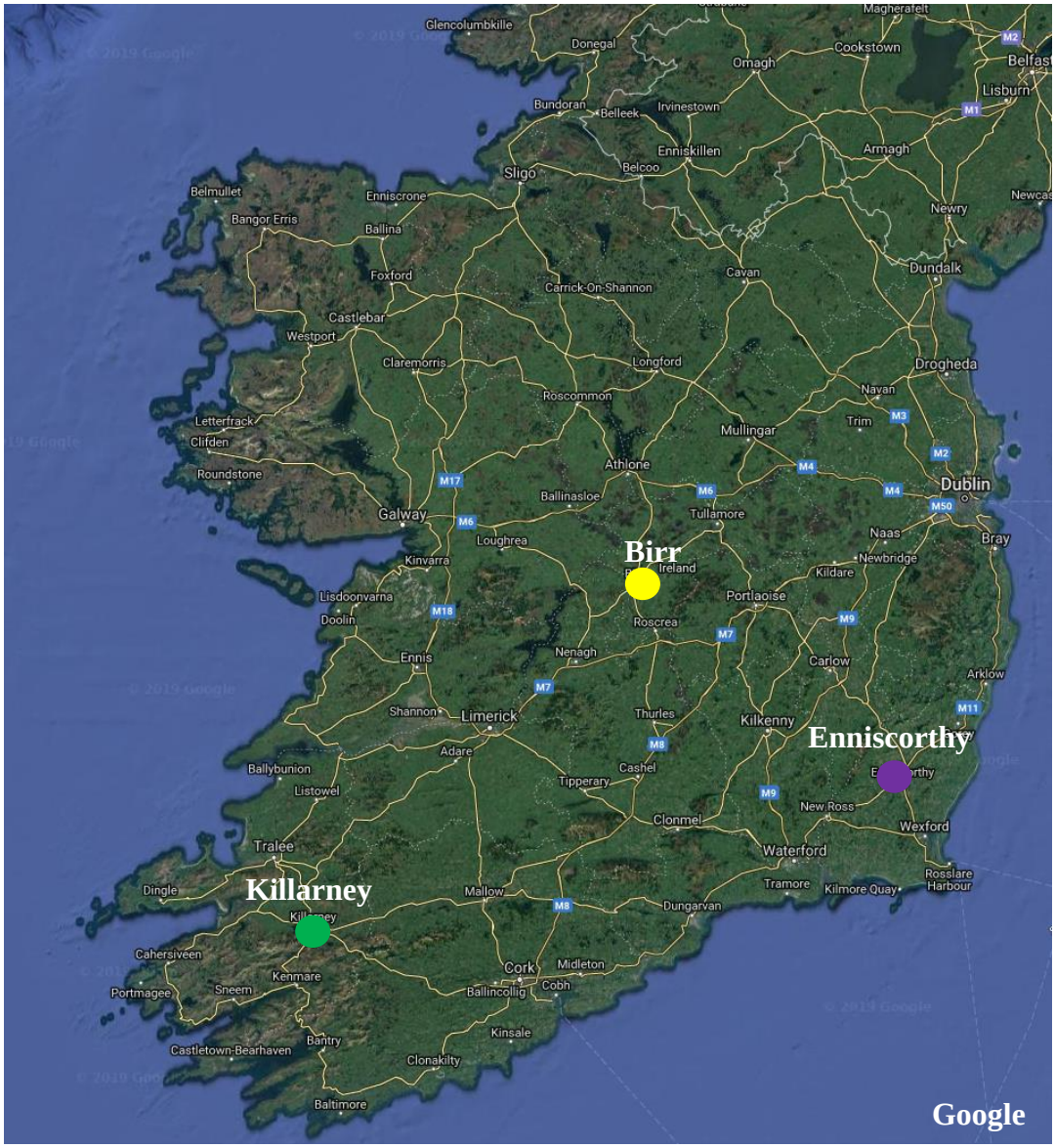

Figure 3.4. Locations of SAPPHIRE monitoring sites, Killarney (green), Enniscorthy (purple), and Birr (yellow).

The site in Killarney, located on the grounds of Killarney Community Hospital (52º 03’ 56.5” North, 9º 31’ 00.4” West), is mainly surrounded by residential (blue) and urban (grey) areas, *Figure 3.5*. The site is located to the north west of the town centre, and roughly 200 m from the N71 national road. It is also potentially influenced by biogenic emissions from the nearby Killarney national park (green) to the west, and by emissions from farmland and forestry land around the town, not highlighted on the map.

Figure 3.5. Overview of zones in Killarney: Blue – residential; Grey – urban; Green – national park.

The site in Enniscorthy, positioned at the rear of Enniscorthy public library (52º 30’ 01.8” North, 6º 34’ 13.0” West), is located near the centre of the Enniscorthy urban area. Directly east of the site is the town centre, marked in grey in *Figure 3.6*, and the main national road through the town, the N30, is roughly 0.5 km west of the monitoring location, with the N11 located across the river. In addition, Enniscorthy train station is located to the North East of the site. All farmlands surrounding the monitoring site are not marked on the map, but are visible in the figure. The town of Enniscorthy is also located in a valley, and the monitoring location is roughly 150 m above the level of the river flowing through the bottom of the valley.

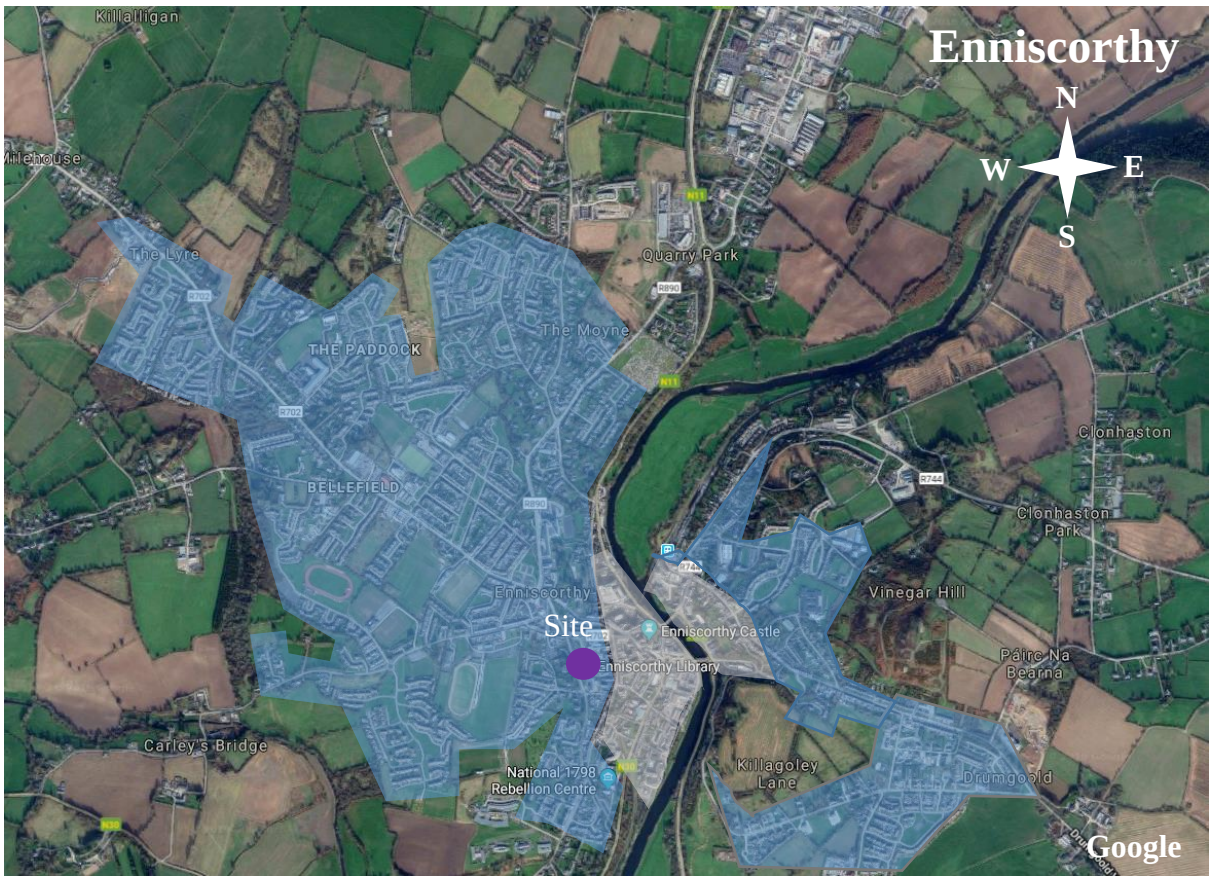

Figure 3.6. Overview of zones in Enniscorthy. Blue – residential; Grey – urban.

The site in Birr, located at the rear of John's Mall, in a local council yard (53º 05' 47.1" North, 7º 54' 29.9" West), is in the middle of the town, marked in yellow in *Figure 3.7*, with the town centre directly to the west. The monitoring site is surrounded by residential areas, marked in blue on the map. The main national road through the town, the N52, is located roughly 100 m from the site to the south east. Approximately 0.5 km to the north-west is a park on the grounds of Birr Castle, in addition to farmland not marked on the map. Also visible on the map is the edge of a large, commercially farmed, peat bog, located roughly 3.5 km to the north-east of the town, and shown in brown in the top right corner.

Figure 3.7. Overview of zones in Birr. Blue – residential; Grey – urban; Green – park.

The measurement periods for each of the field campaigns are:

Killarney:	12 November – 20 December 2014
Enniscorthy:	8 January – 18 February 2015
Birr:	18 November 2015 – 14 January 2016.

3.2.2. Instrumentation and Analysis

A wide range of instruments was deployed during the field campaigns to measure the chemical and physical properties of atmospheric particles, *Table 3.2*. The instruments were located in a van and a specially designed container, fitted with size selective sampling inlets. All instruments were operated on a continuous basis, with occasional downtime for instrument maintenance, particularly for the ATOFMS and TEOM. The measured parameters were analysed to yield hourly values, with the exception of the OCEC analyser, which provided average concentrations over a two hour period. Wind speed, wind direction and rainfall data were obtained from the closest synoptic Met Éireann weather stations, located ~59 km (Valentia Island Observatory), 26 km (Johnstown Castle) and 12 km (Gurteen College) from the Killarney, Enniscorthy and Birr sampling sites respectively.

Table 3.2. Instrumentation deployed during the field campaigns.

Instrument	Parameter(s) measured	Temporal resolution
Scanning mobility particle sizer (SMPS, TSI Inc. Model 3081)	Particle number concentration (10-480 nm)	3 min
Optical Particle Sizer (OPS, TSI Inc. Model 3330)	Particle number concentration (300-10000 nm)	3 min
Tapered element oscillating microbalance (TEOM, Thermo Electron Model 1400a)	$PM_{2.5}$ mass concentration	30 min
Thermal-optical carbon (OCEC) analyser (Sunset Inc. Model, 3rd generation)	Elemental and organic carbon mass concentrations	2 h
Seven Wavelength aethalometer (Model AE33, Magee Scientific)	Black carbon concentration	1 min
NO_x analyser (Teledyne T200)	NO and NO_x mixing ratio	1 min
High volume sampler (DIGITEL Model DHA 80)	Collection of particulate matter ($PM_{2.5}$)	6 h
Aerosol time-of-flight mass spectrometer (ATOFMS, TSI Inc., Model 3800)	Single particle size and chemical composition (100-3000 nm)	1 min

Black carbon concentrations were calculated using the absorption measurements from an AE33 dual-spot aethalometer (Drinovec *et al.*, 2015). A detailed description of the aethalometer instrument and analysis technique is provided in Chapter 2. In brief, particles are collected on a filter tape, the attenuation of light at seven different wavelengths is measured. The attenuation at 880 nm is directly proportional to black carbon concentrations. The attenuation measurements are used to calculate the equivalent black carbon (eBC) concentrations based on the equations detailed in Zotter *et al*. (2017). Analysis of the data from the AE33 was performed using the *Openair* software package. Model parameters ($\alpha_{WB} = 2$, $\alpha_{FF} = 1.0$) initially chosen for source apportionment were based on previous studies performed in central

Europe (Sandradewi *et al.*, 2008b; Drinovec *et al.*, 2015; Zotter *et al.*, 2017). The MAC value selected was 7.77 m^2/g. The optimum α values and MAC for each monitoring location were determined by comparing the AE33 results to those obtained by other instruments co-deployed at the monitoring sites. The α values selected for the final analysis were 1.68 for solid fuel burning related BC, and 0.9 for traffic related BC (Zotter *et al.*, 2017).

Thermal elemental carbon (EC) and organic carbon (OC) measurements were derived using a modified version of the NIOSH 0540 analysis protocol (Birch, 2003; Birch and Cary, 1996). This procedure consisted of 108 minutes of sampling followed by 12 minutes of heating and analysis, delivering average values for EC and OC on a 2 hour basis.

$PM_{2.5}$ mass concentration was measured continuously using a tapered element oscillating microbalance (TEOM). Particle size distributions and number concentrations were measured using a scanning mobility particle sizer (SMPS) and optical particle sizer (OPS). The SMPS provides particle size and number concentration in the range of 10 nm to 480 nm. The OPS provides particle size and number concentration in the range of 300 nm to 10 μm. In Enniscorthy, this information was used to correct the TEOM data upon the conclusion of the campaign. A full explanation of this procedure is provided in *Appendix II*.

Single particle chemical composition was determined in real-time using an aerosol time of flight mass spectrometer (ATOFMS). A detailed description of the ATOFMS can be found elsewhere (Gard *et al.*, 1997). In brief, particles are sampled directly from the ambient aerosol and focused into a single particle stream using an aerodynamic focusing lens. The particles pass through a sizing region which contains two orthogonally arranged lasers (λ = 532 nm), this region provides information on particle size and number. The particles are then desorbed/ionised using a pulsed Nd:YAG laser (λ = 266 nm). Positive and negative ion mass spectra of the individual particles are obtained allowing for the identification of the chemical constituents of the particles.

Table 3.3 summarizes the percentage data capture achieved by the instruments used during the SAPPHIRE campaigns. The AE33 instrument performed well throughout all campaigns, with downtime only required for tape advancement and routine maintenance. Data capture for the TEOM decreased after Killarney due to maintenance required in Enniscorthy and Birr. The OPS instrument experienced a

malfunction in Birr on 20 December 2015. As a result, all data collected after that date was deemed invalid. The OPS malfunction also accounts for the lower data capture of the ATOFMS in Birr, as the OPS and SMPS instruments are used for calculating the ATOFMS mass concentrations (Healy *et al.*, 2012; Arndt *et al.*, 2017). In addition, routine maintenance procedures required during each campaign resulted in periods of downtime for the ATOFMS instrument, further lowering the amount of data collected

Table 3.3. Percentage data capture for each instrument during the SAPPHIRE campaigns.

Instrument	**Killarney** 12/11/14 – 20/12/14	**Enniscorthy** 08/01/15 – 18/02/15	**Birr** 18/11/15 – 14/01/16
SMPS	78.5	85.0	100.0
OPS	74.0	92.4	58.5
TEOM	98.9	81.3	72.4
OCEC	90.8	94.1	90.1
AE33	98.2	99.7	99.9
NO_x analyser	99.1	89.8	100.0
ATOFMS	54.4	92.7	36.1

3.3. Results and Discussion

3.3.1. Meteorological Parameters

Figure 3.8. shows the time series of rainfall (mm), temperature (ºC), and wind speed (m/s), for each measurement campaign. These measurements were taken from the closest available synoptic Met Éireann weather station. For Killarney this was Valentia Island Observatory (~59 km away), for Enniscorthy it was Johnstown Castle (~26 km away), and for Birr it was Gurteen College (~12 km away). The observed variations in wind speed, temperature and rainfall are summarised in *Table 3.4*.

Table 3.4. Summary of hourly averaged meteorological parameters at SAPPHIRE sites.

Parameter	**Killarney**		**Enniscorthy**		**Birr**	
	Mean	Range	Mean	Range	Mean	Range
Wind speed (m/s)	5.0	0.0–14.9	5.0	0.5–13.9	5.7	0.5–15.4
Temperature (ºC)	8.9	1.9–14.5	4.5	-1.6–11.8	9.0	1.1–14.8
Rainfall (mm)	0.21	0–8.3	0.06	0–3.7	0.23	0–8

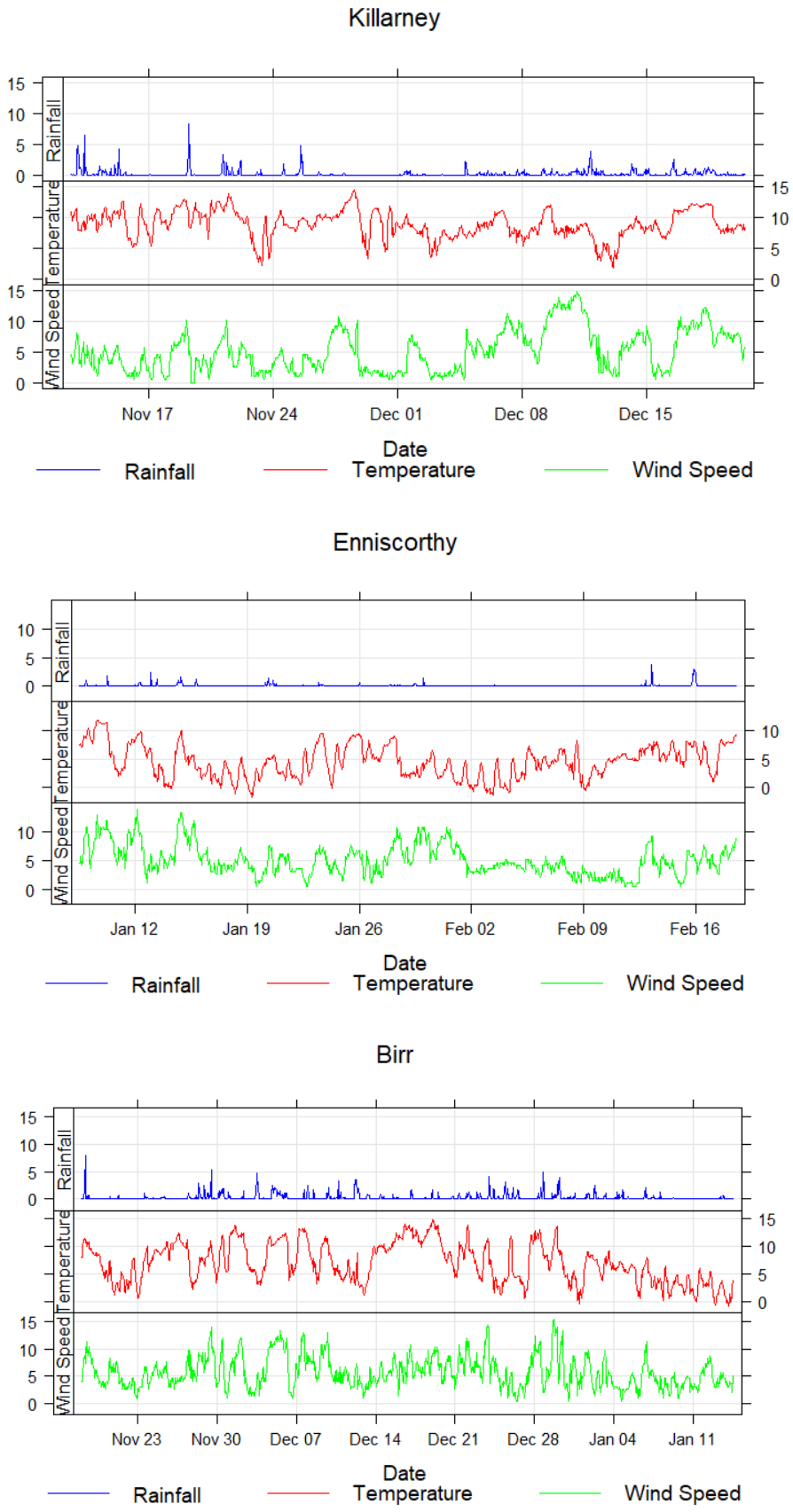

Figure 3.8. Rainfall (mm), temperature (°C), and wind speed (m/s), for Killarney, Enniscorthy, and Birr during the SAPPHIRE campaign.

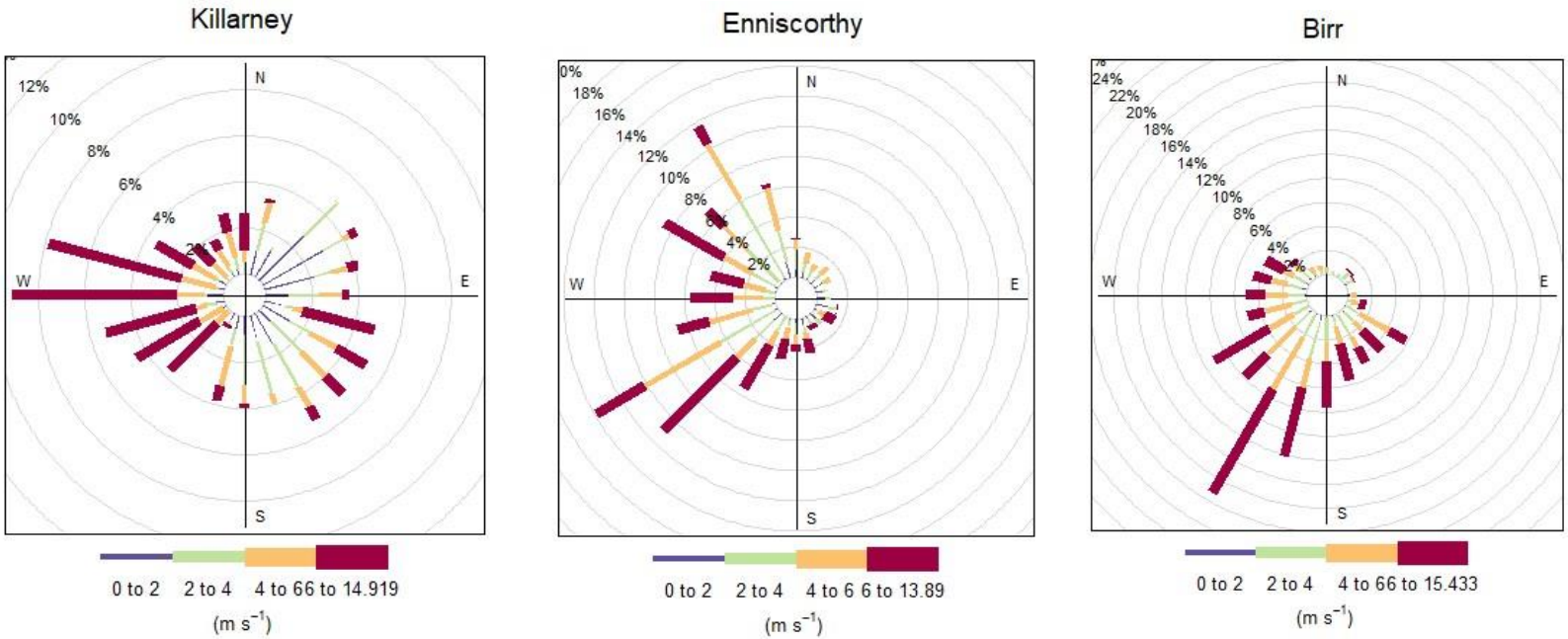

Figure 3.9. Wind rose plots for Killarney, Enniscorthy and Birr during the SAPPHIRE campaign.

The highest wind speeds at each site mainly originated from the southerly and westerly direction (*Figure 3.9*), which are the predominant wind directions in Ireland. It should be noted that several periods of high wind speed were designated as storms during the measurement campaigns. The naming convention came into effect during 2015, covering the campaign conducted in Birr. The storms recorded during the measurement period were Storm Barney (17–18 November 2015), Storm Clodagh (29 November 2015), Storm Desmond (4–6 December 2015), Storm Eva (23–24 December 2015) and Storm Frank (29–30 December 2015) (UK Met Office, 2016).

3.3.2. Particle Size, Number and Mass Concentrations

$PM_{2.5}$ mass concentration profiles for each of the measurement campaigns are shown in *Figure 3.10*. The $PM_{2.5}$ mass for Killarney and Birr were directly taken from the TEOM, however, this instrument malfunctioned in Enniscorthy and the values obtained at this location were subject to corrections, as outlined in *Appendix II*. The $PM_{2.5}$ mass and number concentrations, summarized in *Table 3.5*, show a broad range for all three sites. The highest hourly average concentrations were observed in Enniscorthy, where a value of 236.6 $\mu g/m^3$ was recorded during the evening of 02 February 2015. Evening concentrations frequently exceeded 50 $\mu g/m^3$ in Killarney and Enniscorthy, and exceeded 50 $\mu g/m^3$ once in Birr. The average $PM_{2.5}$ mass concentration in Enniscorthy was 29.2 $\mu g/m^3$, which is comparable to winter-time levels previously measured at a rural location in China, 31.4 $\mu g/m^3$ (Zhao *et al.*, 2009). Levels in Killarney and Enniscorthy were comparable or higher than winter-time $PM_{2.5}$ concentrations observed in the United Kingdom over a three year period, at kerbside, urban background, and rural locations (Harrison *et al.*, 2001). The average $PM_{2.5}$ concentrations in Killarney and Enniscorthy are also comparable to winter-time concentrations measured in several large European cities including Madrid, Athens, Barcelona, Marseille, Genoa and Thessaloniki (Kassomenos *et al.*, 2012; Salameh *et al*., 2015).

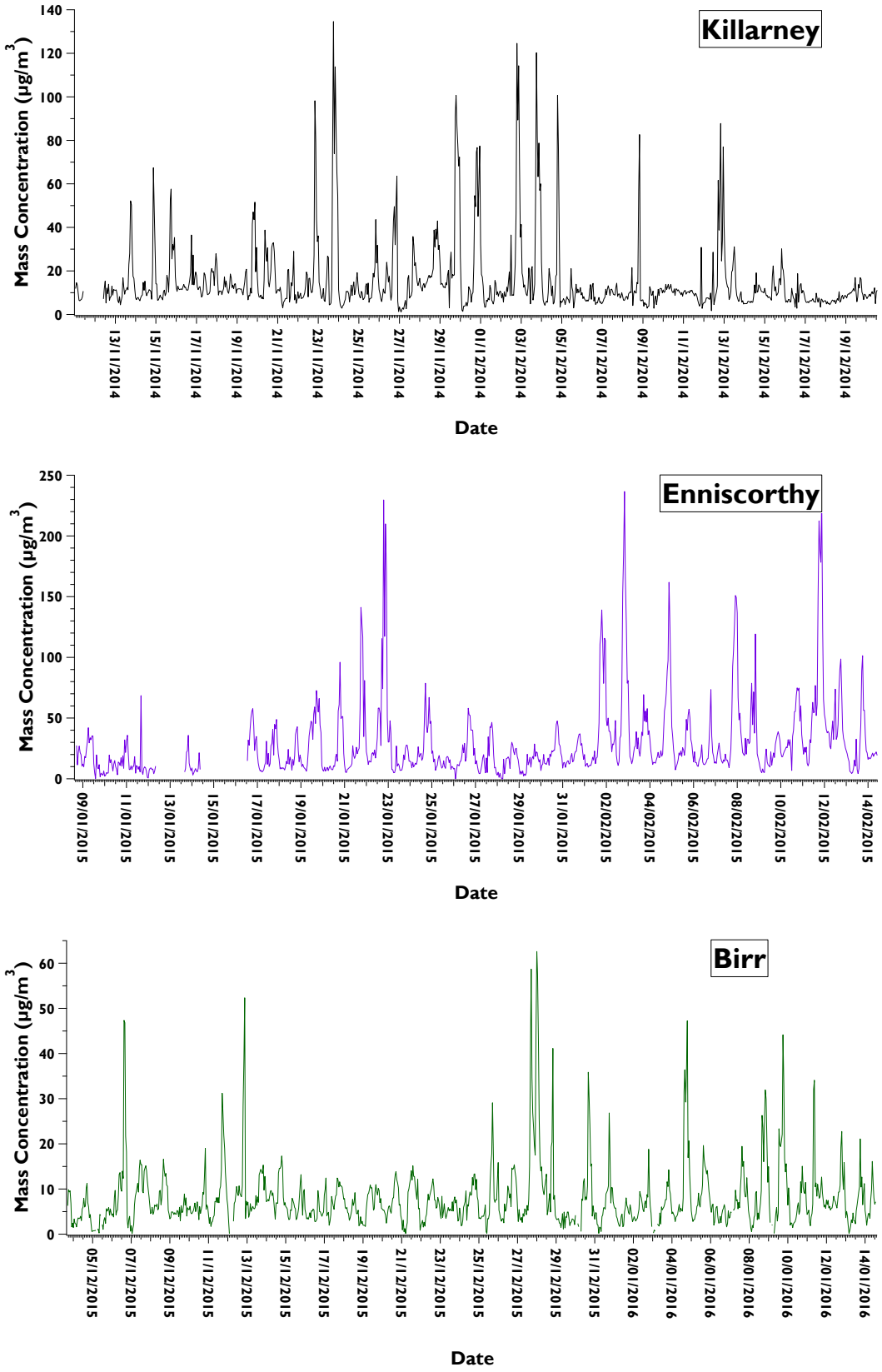

Figure 3.10. $PM_{2.5}$ mass concentration profiles for Killarney, Enniscorthy, and Birr during the SAPPHIRE project. Data for Killarney and Birr were provided directly by the TEOM. Data for Enniscorthy was obtained by applying corrections derived from the particle sizing instruments to the TEOM measurements (*Appendix II*).

A strong diurnal trend was observed at all three locations, with elevated levels of pollution between 17:00 and 23:00 (*Figure 3.11*), a pattern consistent with emissions from domestic solid fuel burning. A small increase in $PM_{2.5}$ mass was also observed between 08:00 and 10:00 at each location, related to emissions from motor vehicles. As expected, similar trends were observed for particle number concentrations (*Figure 3.12*). Gradual increases in particle numbers were observed during the daytime at each location (07:00 – 15:00) followed by a rapid increase peaking between 18:00 and 20:00. The SMPS data indicates a larger number of smaller particles in Birr than Killarney (*Figure 3.12)*. The size distributions for Killarney and Enniscorthy are extremely similar with the majority of particles in the 70 – 100 nm range, which is typical for fresh combustion particles and similar to the size distributions observed in Dublin during winter-time pollution events (Lin *et al.*, 2018). While the Birr data shows this size range is present, an intense signal is also apparent in the smaller mode, up to 30 nm in size (*Figure 3.13*).

Table 3.5. Hourly averaged concentrations of $PM_{2.5}$ and particle number at SAPPHIRE sites.

Parameter	**Killarney**		**Enniscorthy**		**Birr**	
Date	11/11/14–20/12/14		08/01/15–14/02/15		03/12/15–14/01/16	
	Mean (± SD)	Range	Mean (± SD)	Range	Mean (± SD)	Range
$PM_{2.5}$ ($\mu g/m^3$)[a]	15.3 (± 16.7)	1.2–134.6	29.2 (± 31.9)	0–236.6	7.9 (± 7.2)	0.1–62.6
Number ($\#/cm^3$)[b]	4394 (± 6762)	40–40896	8096 (± 10349)	105–75855	5922 (± 7184)	70–48965
Number ($\#/cm^3$)[c]*	195 (± 407)	1.0–2552	404 (± 522)	0–4646	63 (± 101)	0–1112

[a] mean hourly $PM_{2.5}$ measured by TEOM. Data for Enniscorthy is corrected (see text).

[b] mean hourly particle numbers determined by SMPS (10 – 480 nm).

[c] mean hourly particle numbers determined by OPS (0.3 – 2.5 μm).

* OPS malfunctioned in Birr on 21/12/15, measurements ceased at that point.

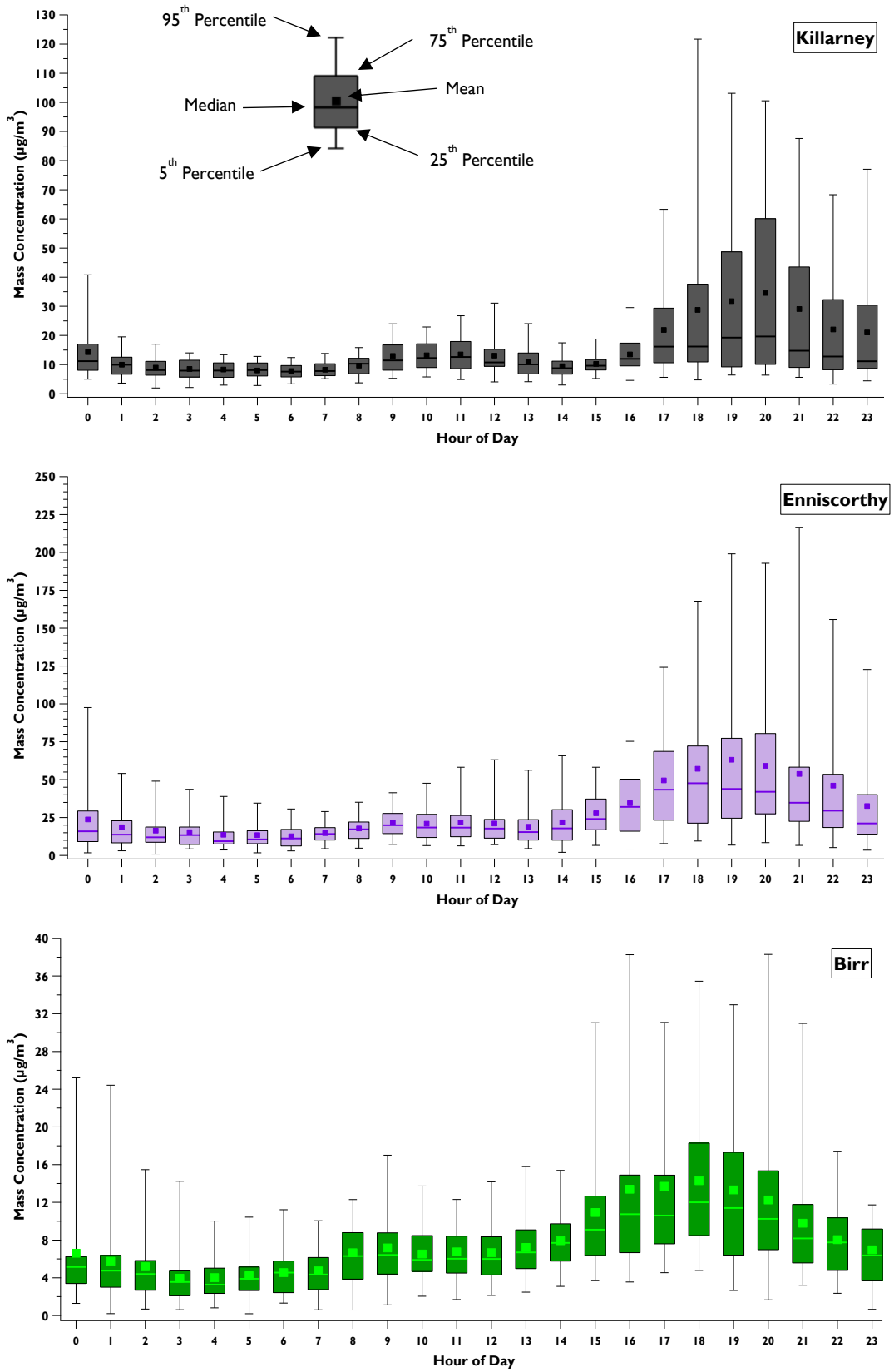

Figure 3.11. Diurnal variation in mass concentration of $PM_{2.5}$ during the field measurement campaigns in Killarney, Enniscorthy and Birr.

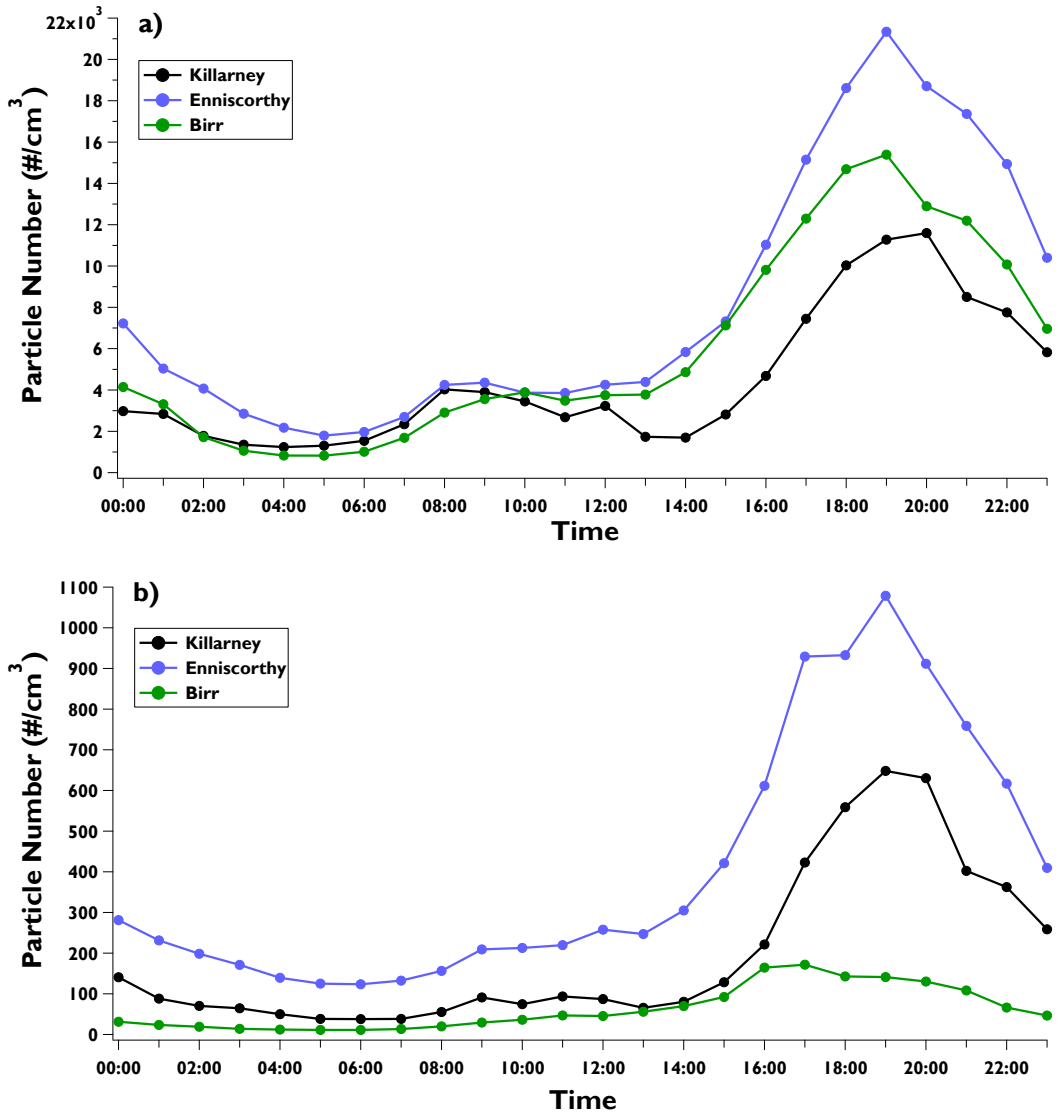

Figure 3.12. Diurnal distributions of particle numbers measured by the SMPS (a), and the OPS (b), during the field campaigns in Killarney, Enniscorthy, and Birr.

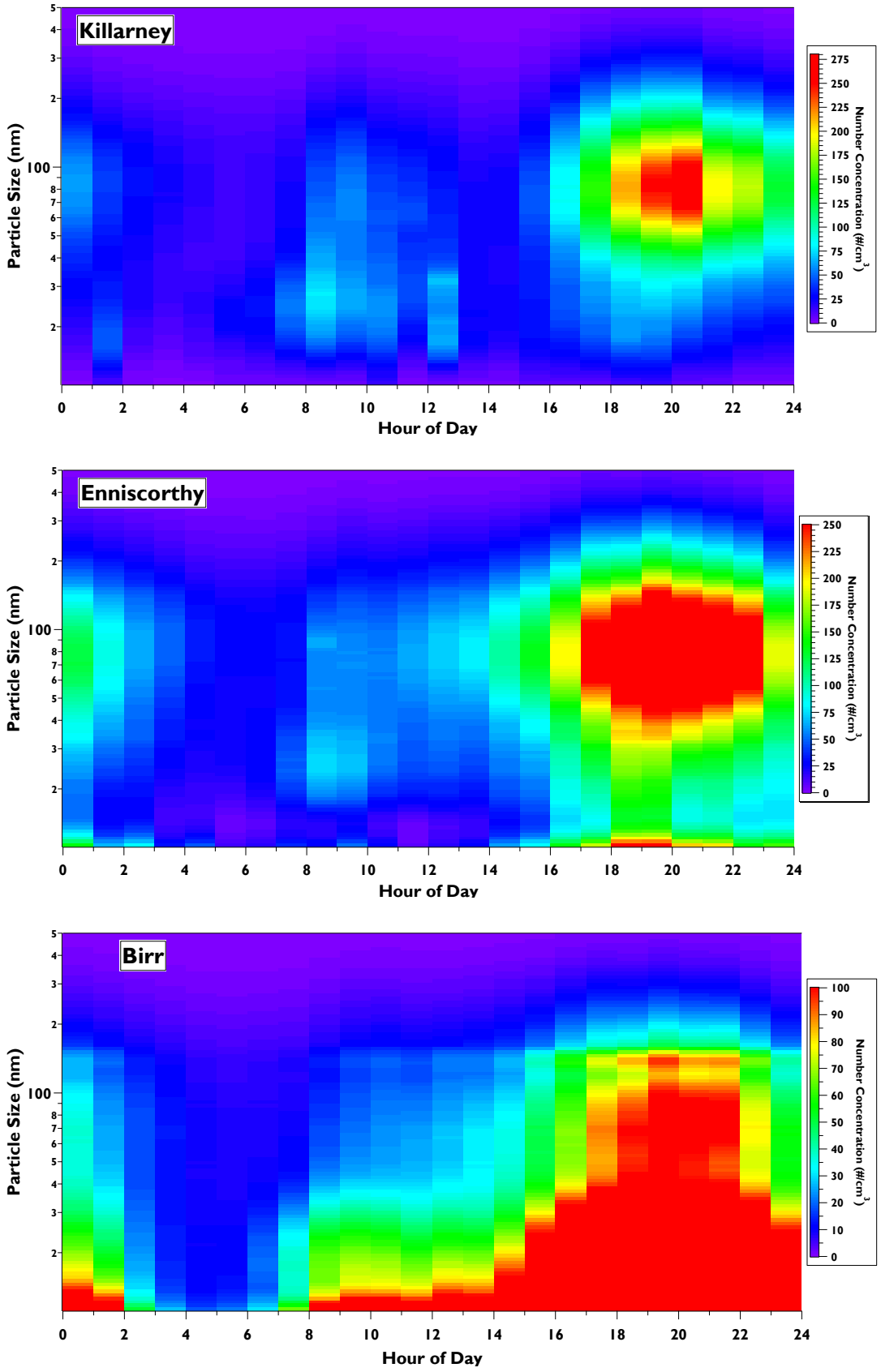

Figure 3.13. Diurnal variation in average size-resolved particle number concentrations measured by SMPS during the field campaigns in Killarney, Enniscorthy and Birr.

3.3.3. Elemental Carbon (EC) and Organic Carbon (OC)

The temporal profiles of EC and OC mass concentrations during each of the campaigns are shown in *Figure 3.14*. A summary of the OC and EC concentrations, and the contribution to $PM_{2.5}$ mass is given in *Table 3.6.* The diurnal variation of EC and OC in each location is quite similar, *Figure 3.15*, with larger OC peaks in the evening hours, corresponding to domestic solid fuel burning hours. Analysis shows that on average, total carbon (OC + EC) accounts for 35 – 59% of the measured $PM_{2.5}$ at the three sites. This is comparable to the 55% of $PM_{2.5}$ accounted for by total carbon in Cork Harbour by Dall'Osto *et al*. (2013). It is also comparable to the 53 – 66% contribution of OC + EC at urban locations in Ireland reported by Yin *et al.* (2005). OC and EC concentrations measured at the Cork inner harbour site were lower than those measured at the SAPPHIRE monitoring locations (O'Connor, 2012). The average OC concentration was 5.2 ± 4.9 $\mu g/m^3$, while the average EC concentration was 1.9 ± 1.8 $\mu g/m^3$. OC and EC accounted for 34.1 ± 7.7% and 13.7 ± 5.1% of reconstructed $PM_{2.5}$ mass respectively at the harbour site, while the average winter-time OC/EC ratio was 3.0 ± 1.1, slightly lower than the values obtained in Killarney and Enniscorthy.

At each location, the OC/EC ratio is at its lowest in the morning hours, corresponding to rush hour traffic (*Figure 3.15*). The average OC/EC ratio values from each location are indicative of the influence of biomass and fossil fuel burning sources. A comprehensive review by Ni *et al*. (2018) proposed an OC/EC ratio of 5 is indicative of biomass burning, and OC/EC ratio of 2.38 is indicative of coal burning. OC/EC ratios obtained for this study, listed in *Table 3.6*, indicate that Birr is likely dominated by biomass burning, while Killarney and Enniscorthy are likely influenced by both biomass and coal burning. Similar values were observed around Ireland during winter-time measurements by Ceburnis *et al*. (2006). Crilley *et al.* (2015) recorded winter-time OC/EC ratios of between 2.3 ± 0.8 and 3.9 ± 1.8 at different locations around London. Thermal EC measurements from the OCEC instrument were also used to calculate site specific Mass Absorption Cross-Section (MAC) values. This provides information on the aging of BC particles and mixing state (Knox *et al*., 2009 and references therein). The calculation of site specific MAC values for the SAPPHIRE sites are discussed in Section 3.3.4.

Table 3.6. Two hourly average concentrations of OC and EC at SAPPHIRE sites and comparison to $PM_{2.5}$ mass.

Parameter	**Killarney**		**Enniscorthy**		**Birr**	
Dates	22/11/14–20/12/14		09/01/15–14/02/15		03/12/15–14/01/16	
	Mean (± SD)	Range	Mean (± SD)	Range	Mean (± SD)	Range
OC (μg/m^3)	5.9 (± 9.5)	0.6–52.6	9.6 (± 12.2)	0.5–75.8	4.1 (± 3.5)	0.81–27.4
EC (μg/m^3)	1.8 (± 2.9)	0.0–16.6	2.9 (± 3.5)	0.0–22.1	0.7 (± 0.61)	0.0–3.7
OC/EC Ratio	3.8	0.9–60.3	4.0	0.5–71.1	6.3	1.7–39.6
$PM_{2.5}$ (μg/m^3)	15.6 (± 16.7)	1.7–104.2	29.5 (± 30.7)	0.7–205.2	7.9 (± 7.2)	0.1–60.1
OC+EC/$PM_{2.5}$	0.35	0.07–1.0	0.37	0.06–1.0	0.59	0.05–1.0
OC/$PM_{2.5}$	0.28	0.07–0.89	0.29	0.05–0.88	0.51	0.05–1.0
EC/$PM_{2.5}$	0.08	0–0.26	0.08	0–0.48	0.08	0–0.35

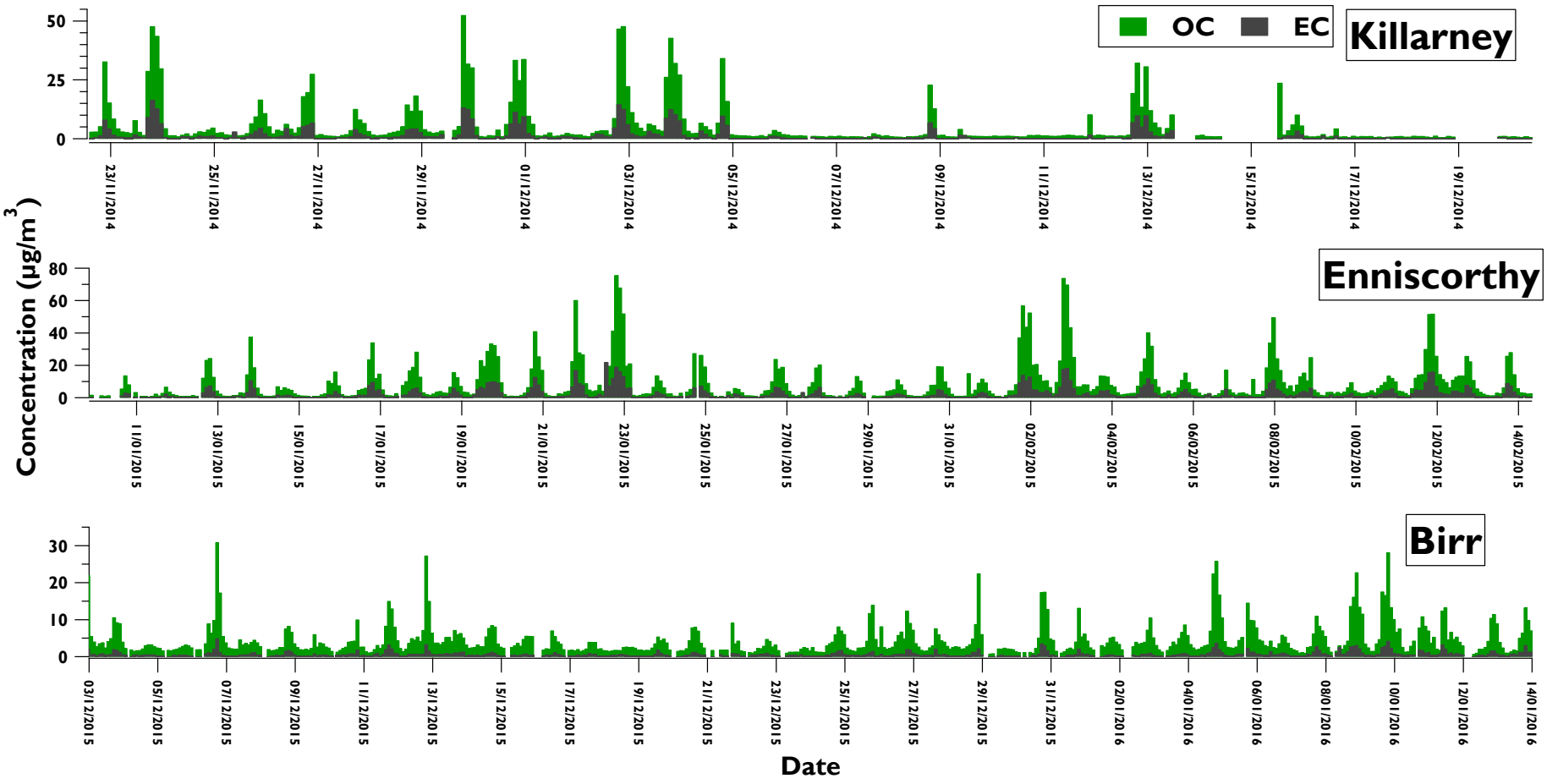

Figure 3.14. Temporal profiles of OC and EC mass concentrations in Killarney, Enniscorthy and Birr.

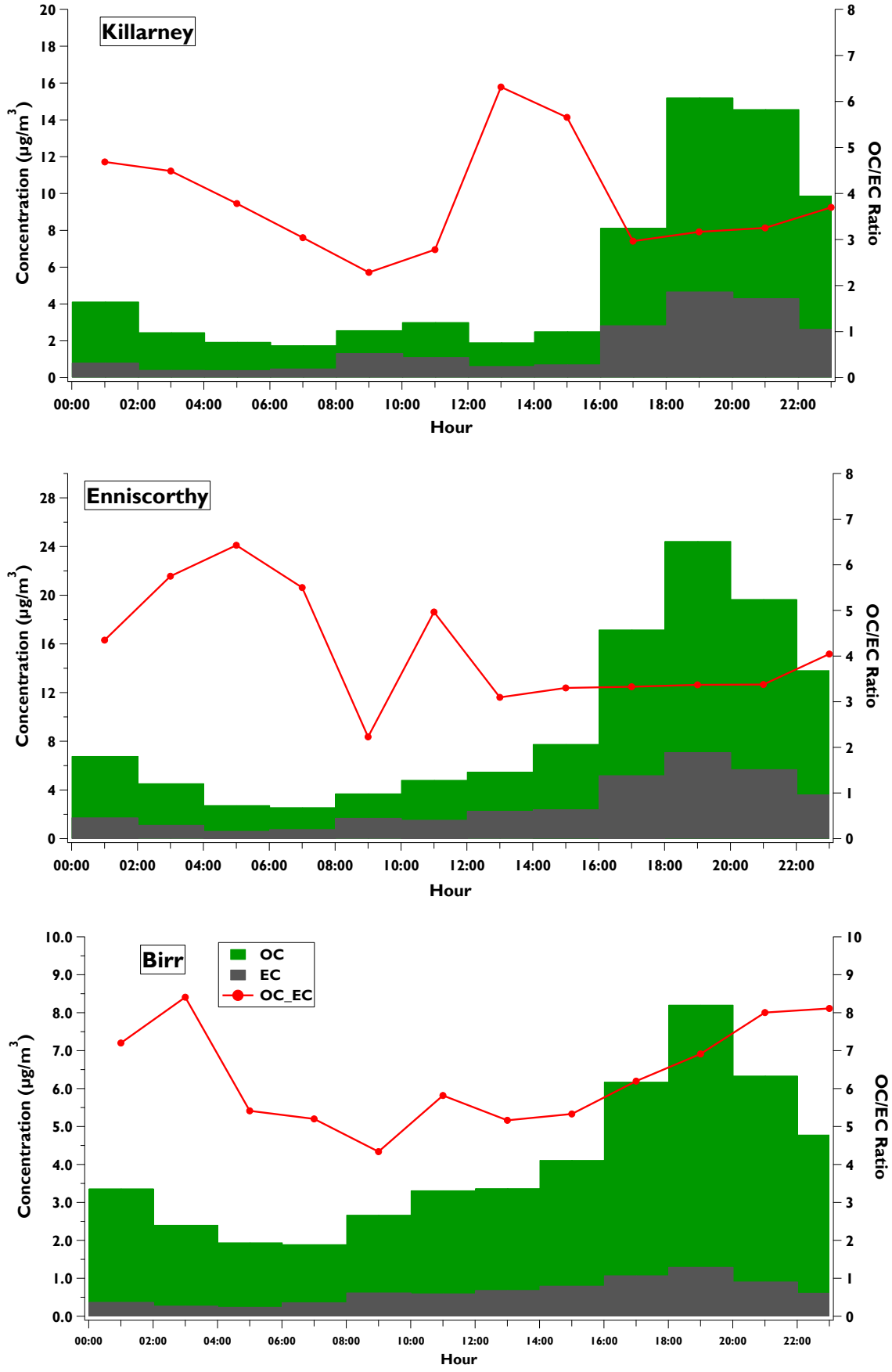

Figure 3.15. Diurnal variation of mean OC, EC and OC/EC ratio during SAPPHIRE.

3.3.4. Equivalent Black Carbon (eBC)

Equivalent black carbon (eBC) values determined by the aethalometer also followed the EC, OC, particle number measured by the SMPS, and $PM_{2.5}$ mass concentrations very closely throughout each of the measurement campaigns, *Figure 3.16*. Overall, good correlations were observed between the eBC concentrations and PM mass and number concentration. The lowest R^2 value (0.74) was obtained for the regression of eBC versus particle number concentration in Birr. This is potentially due to poorer performance of the SMPS over the course of the monitoring period. A summary of the calculated eBC mass concentration for each location, in addition to the percentage contribution from eBC to $PM_{2.5}$ mass, is provided in *Table 3.7*. The highest eBC contribution to $PM_{2.5}$ mass was observed in Enniscorthy (13.2%), indicating a greater contribution from local combustion sources. eBC contributes approximately 9.9% and 11.4% of $PM_{2.5}$ mass in Killarney and Enniscorthy respectively.

In the UK, the contribution of eBC to $PM_{2.5}$ mass concentrations is variable and depends on location (Hessey *et al.*, 2017). At the roadside site on Marylebone Road, eBC accounts for 31% of $PM_{2.5}$ mass. In less polluted areas, for example at Auchencorth Moss, in the Glasgow area, eBC contributes 3% of $PM_{2.5}$ mass. In Belfast city centre, an area designated as a solid fuel influenced location, eBC contributes 8% of $PM_{2.5}$ mass. In New Delhi, eBC accounted for approximately 6% of winter-time $PM_{2.5}$ mass during 2011 (Tiwari *et al.*, 2013). In Finland, the estimated winter-time contribution of eBC to $PM_{2.5}$ mass between October 2015 and March 2017 was 21 ± 18% for a street canyon location, and 18 ± 20% at a detached house location (Helin *et al.*, 2018).

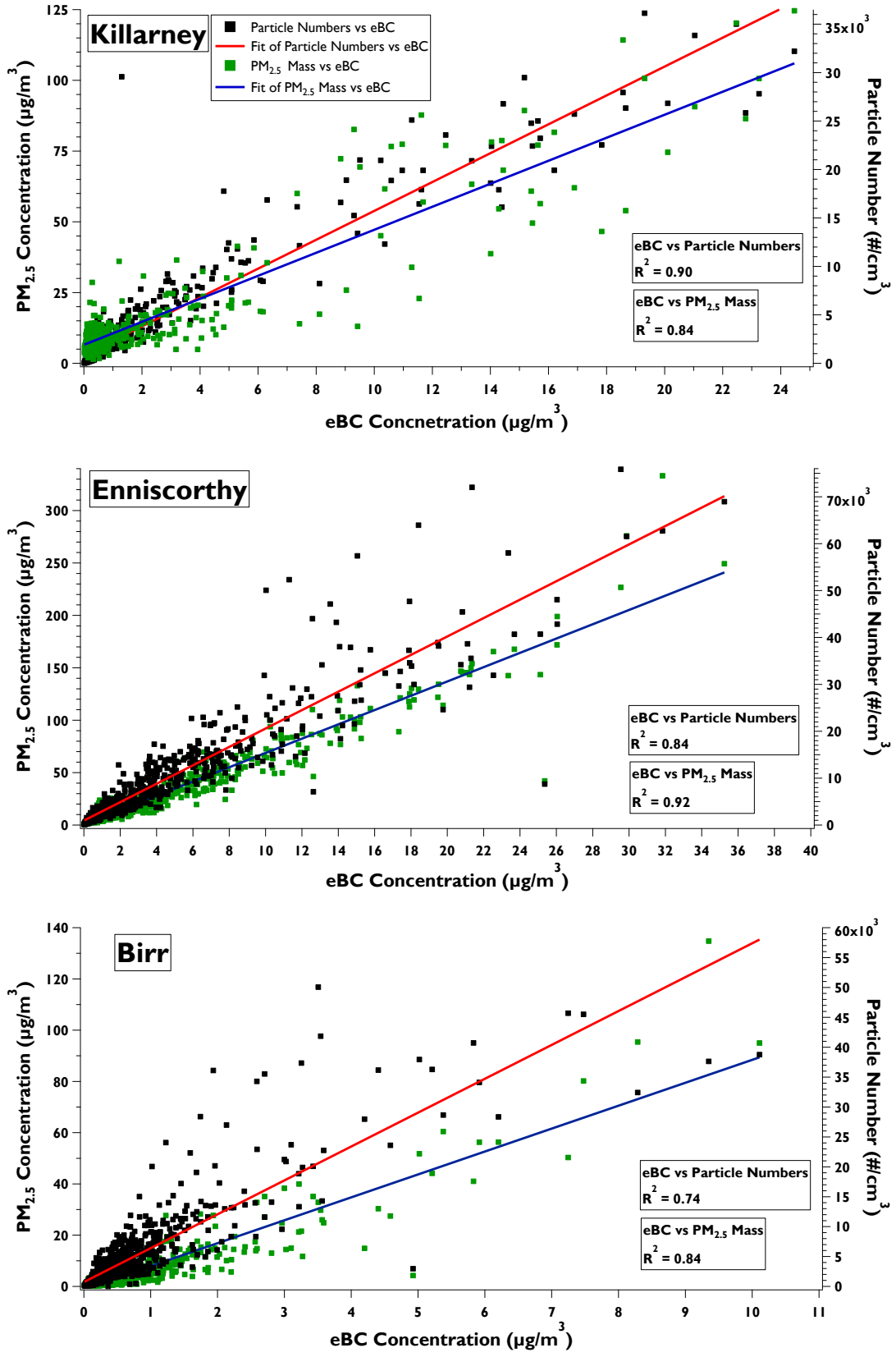

Figure 3.16. Comparison of eBC concentration, $PM_{2.5}$ mass concentration, measured by the TEOM, and number concentration, measured by SMPS (< 500 nm) for the SAPPHIRE monitoring sites.

Table 3.7. Hourly average eBC concentrations at the SAPPHIRE monitoring locations and comparison to $PM_{2.5}$ mass concentration.

Parameter	**Killarney**		**Enniscorthy**		**Birr**	
Dates	12/11/14–20/12/14		08/01/15–14/02/15		03/12/15–14/01/16	
	Mean (± SD)	Range	Mean (± SD)	Range	Mean (± SD)	Range
eBC ($\mu g/m^3$)	2.06 (± 3.8)	0.01–25.2	3.6 (± 4.8)	0.01–35.2	0.8 (± 0.9)	0.01–6.35
$PM_{2.5}$ ($\mu g/m^3$)	15.4 (± 16.8)	1.2–134.6	29.2 (± 31.9)	0–236.6	7.9 (± 7.2)	0.1–62.6
% eBC/$PM_{2.5}$	9.9	0.3–79.9	13.2	0.07–90.0	11.4	0.2–97.5

The two parameters which had the most pronounced effect on eBC concentrations were the amount of rainfall and wind speed. As expected, an increase in rainfall decreased the amount of eBC measured due to the washing out of particles from the atmosphere. Increases in wind speed also decreased the observed concentrations of eBC (*Figure 3.17*). *Figure 3.18* shows that the mean concentration of eBC was not dependent on wind direction. The largest concentrations of eBC were observed at lower speeds. With the exception of Killarney, the highest concentrations were observed in the immediate vicinity of the measurement site. In Killarney, the highest concentrations were observed during periods of low wind speed, originating from the North East, potentially the result of a plum of pollution, originating from a residential area in that direction, which passed over the monitoring site. No significant relationship was observed between temperature and eBC concentrations, indicating that the use of solid fuel for domestic heating during the monitoring periods occurred regardless of temperature. This habitual burning was observed during site visits to all three locations, and was corroborated by anecdotal evidence provided by local residents.

Figure 3.19 shows the daily profiles of hourly averaged equivalent black carbon (eBC) concentrations in Killarney, Enniscorthy, and Birr respectively. The maximum concentrations observed were 24.5, 35.25, and 10.1 $\mu g/m^3$, respectively, with mean concentrations of 2.1, 3.6, and 0.81 $\mu g/m^3$. These diurnal profiles show similar patterns for all three locations, with small peaks in the morning hours, and

larger peaks in the evening. Further analysis of the eBC daily pattern over the course of a week indicates only slight differences between the weekdays and weekends (*Figure 3.20*). There is no strong evidence for the "weekend effect", in which increased emissions are observed at weekends due to so-called "recreational burning" (Fuller *et al.*, 2014; Petit *et al.*, 2015). Thus, the field observations during SAPPHIRE indicate that solid fuel combustion is a daily activity at the selected locations, and is not necessarily more popular at the weekend.

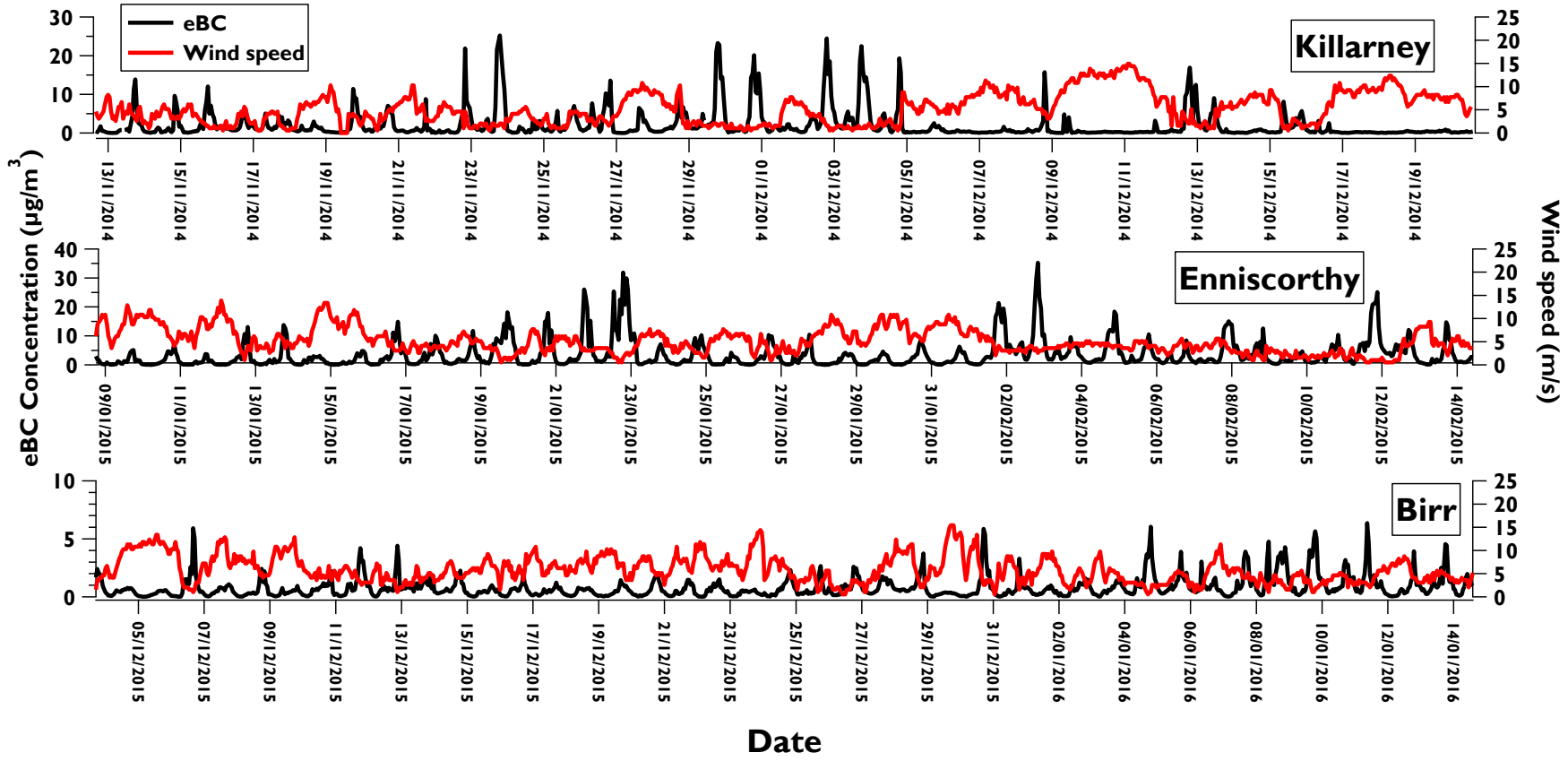

Figure 3.17. Relationship between wind speed (m/s) and eBC mass concentrations (µg/m^3) for the SAPPHIRE measurement sites.

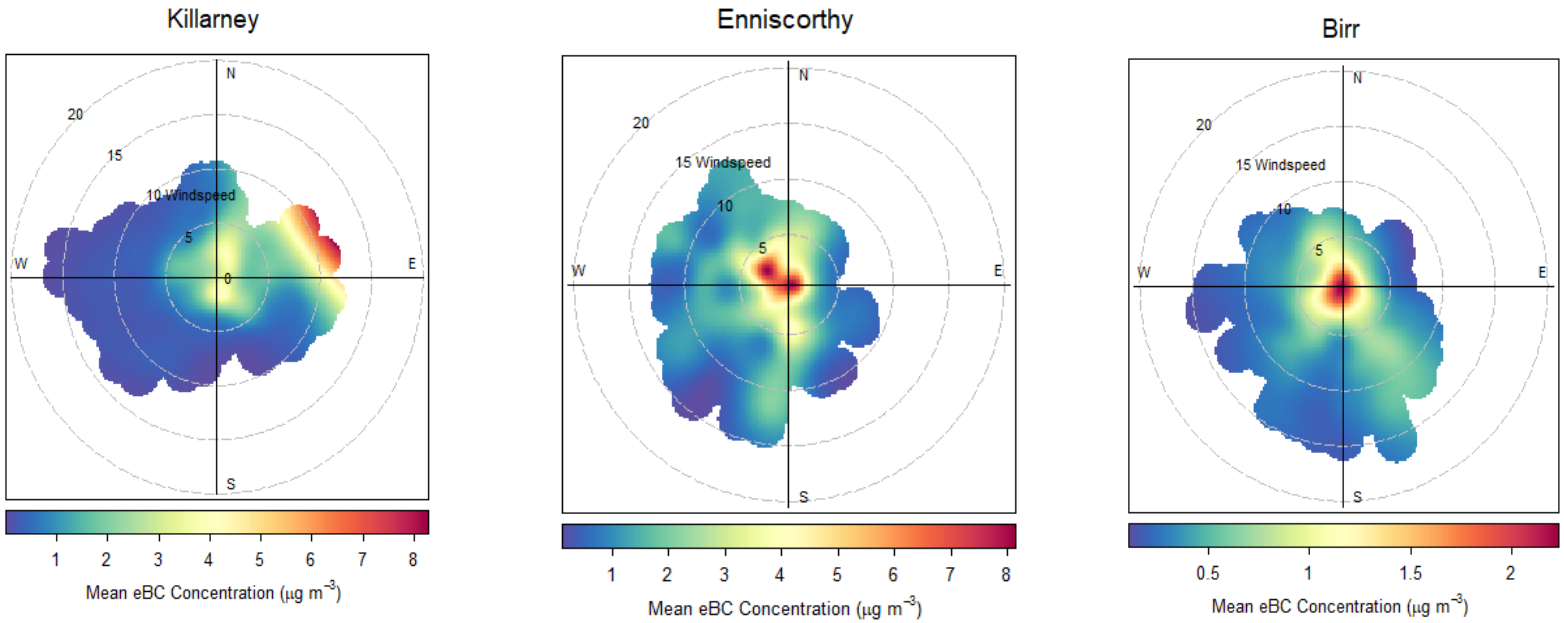

Figure 3.18. Wind rose plots describing wind dependence of eBC mass concentration during SAPPHIRE measurement campaigns.

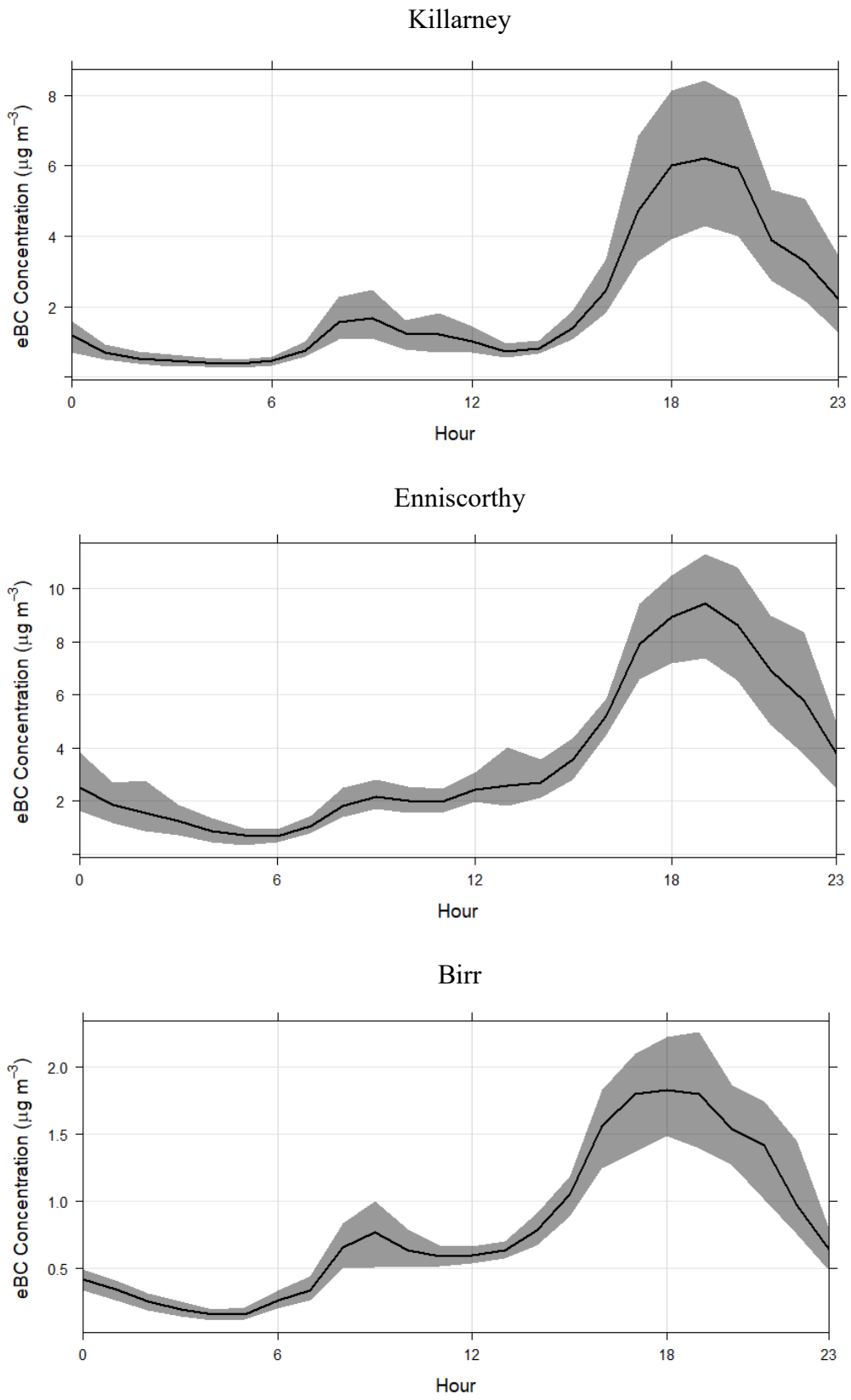

Figure 3.19. Mean daily eBC profiles for Killarney, Enniscorthy and Birr with 95% confidence intervals.

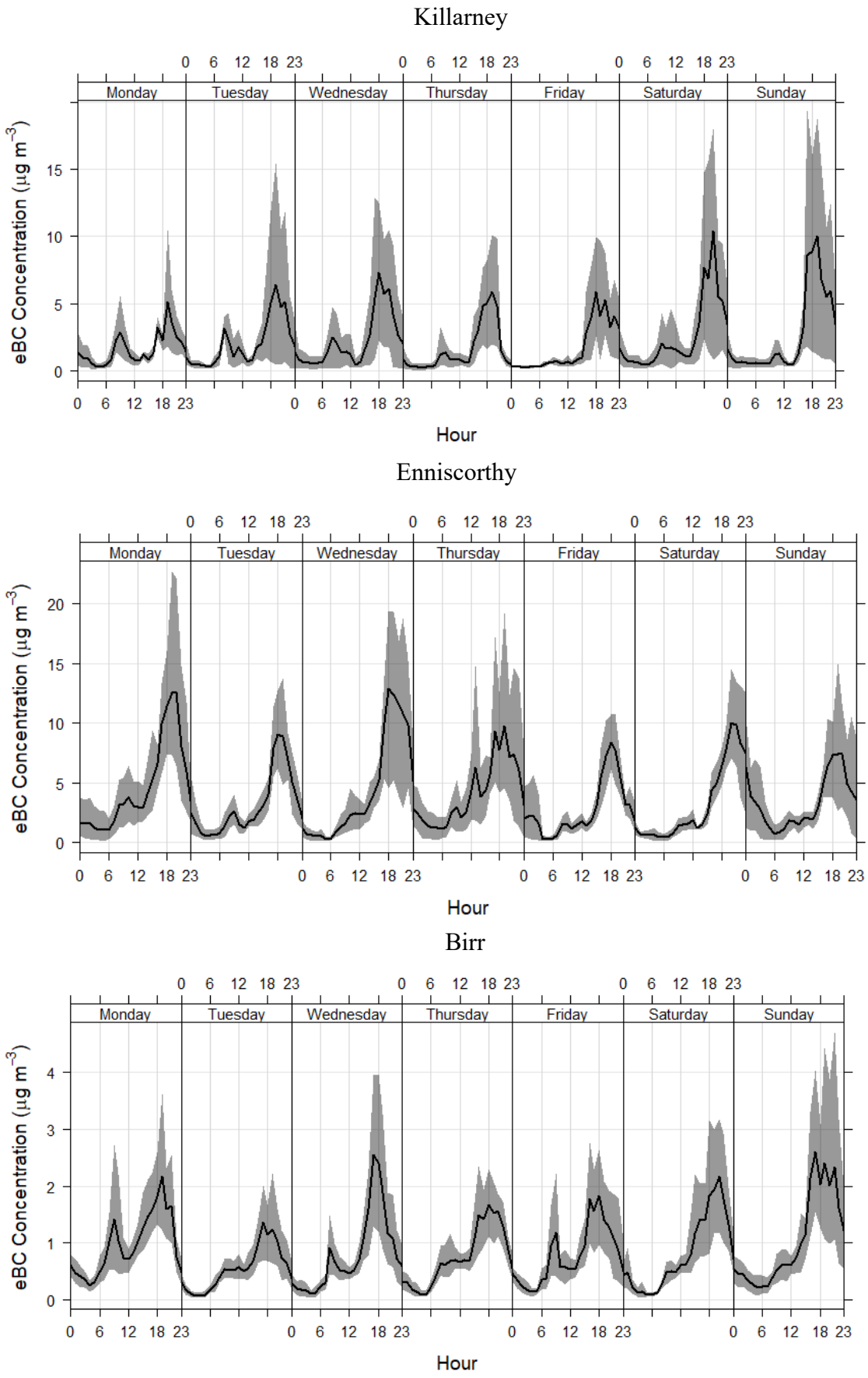

Figure 3.20. Mean weekly eBC profiles for Killarney, Enniscorthy and Birr with 95% confidence intervals.

The relationship between the eBC from the AE33 and the thermal EC measured by the OCEC instrument was also investigated. The regressions of eBC versus thermal EC (*Figure 3.21*) show excellent correlations for each site. Similar relationships have been observed previously at a variety of locations, for example in Canada (Healy *et al.*, 2017), the UK (Hessey *et al.*, 2017), and Switzerland (Herich *et al.*, 2011; Zotter *et al.*, 2017). However, the two measurements are not exactly matched, owing to the different measurement techniques employed. The variation in the measurements could be due to deviation of the true MAC value from the assumed value of 7.77 m^2/g for the 880 nm channel. Therefore it was decided to calculate site specific MAC values using the regression of the absorption coefficient (b_{abs}) derived from the AE33 measurements using the equation detailed in Chapter 2, and the Thermal EC mass concentration from the OCEC instrument (Presler-jur *et al.*, 2017). As the OCEC instrument measures with a time resolution of 2 hours, the data from the AE33 was averaged to the same time period. The MAC for each site was derived from the slope of the regression line obtained for each site (*Figure 3.22*). The R^2 value for each location was > 0.9, highlighting the excellent agreement between the AE33 and OCEC instruments. The calculated MAC value was 11.08 ± 0.09 m^2/g for Killarney, 10.72 ± 0.07 m^2/g for Enniscorthy, and 8.34 ± 0.14 m^2/g for Birr. These values are within the range of values that have been derived at a variety of locations across Europe (Herich *et al.*, 2011; Zanatta *et al.*, 2016; Zotter *et al.*, 2017).

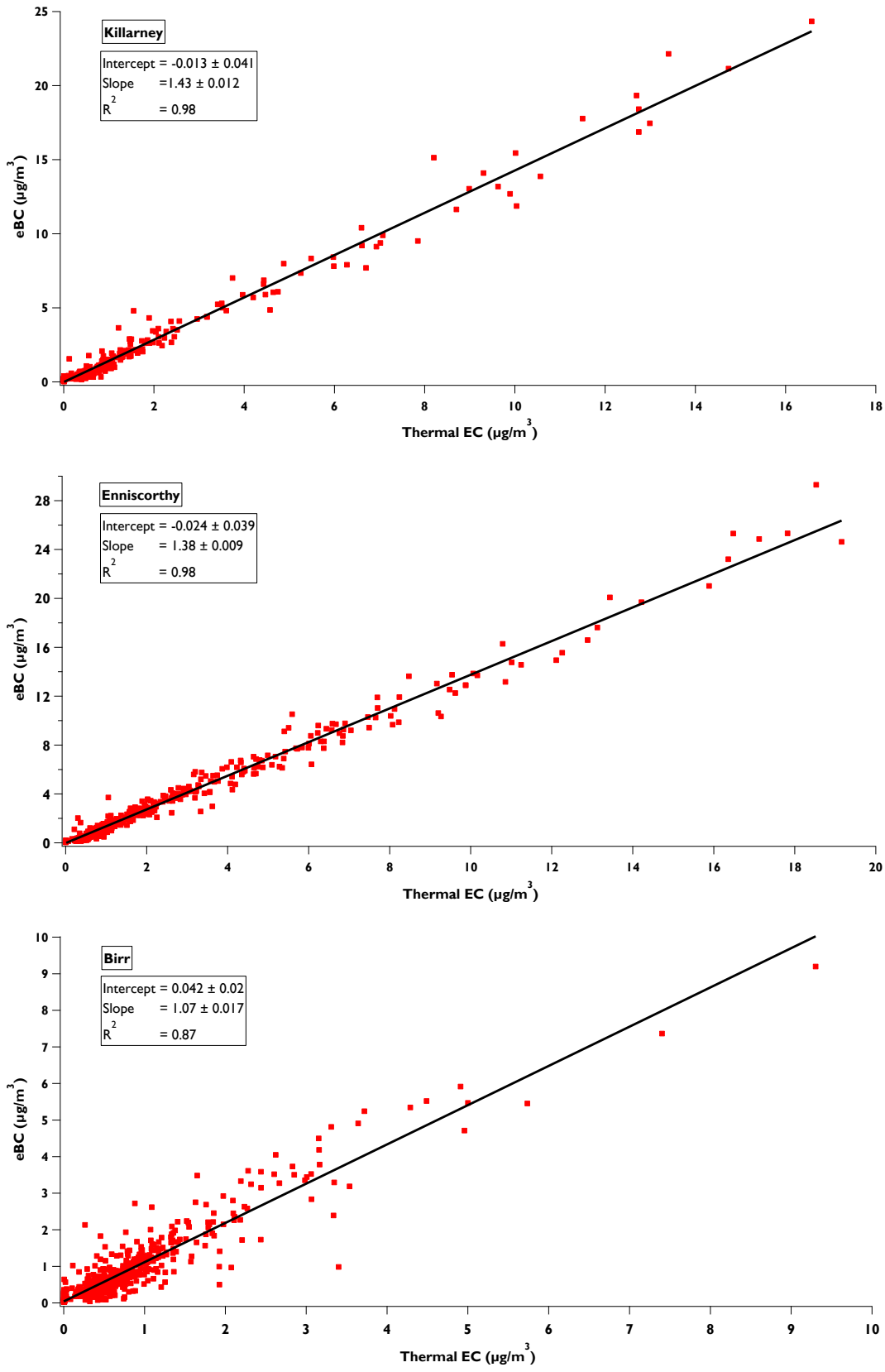

Figure 3.21. Comparison of Thermal EC from OCEC and eBC calculated using the standard MAC value of 7.77 m^2/g, for Killarney, Enniscorthy, and Birr.

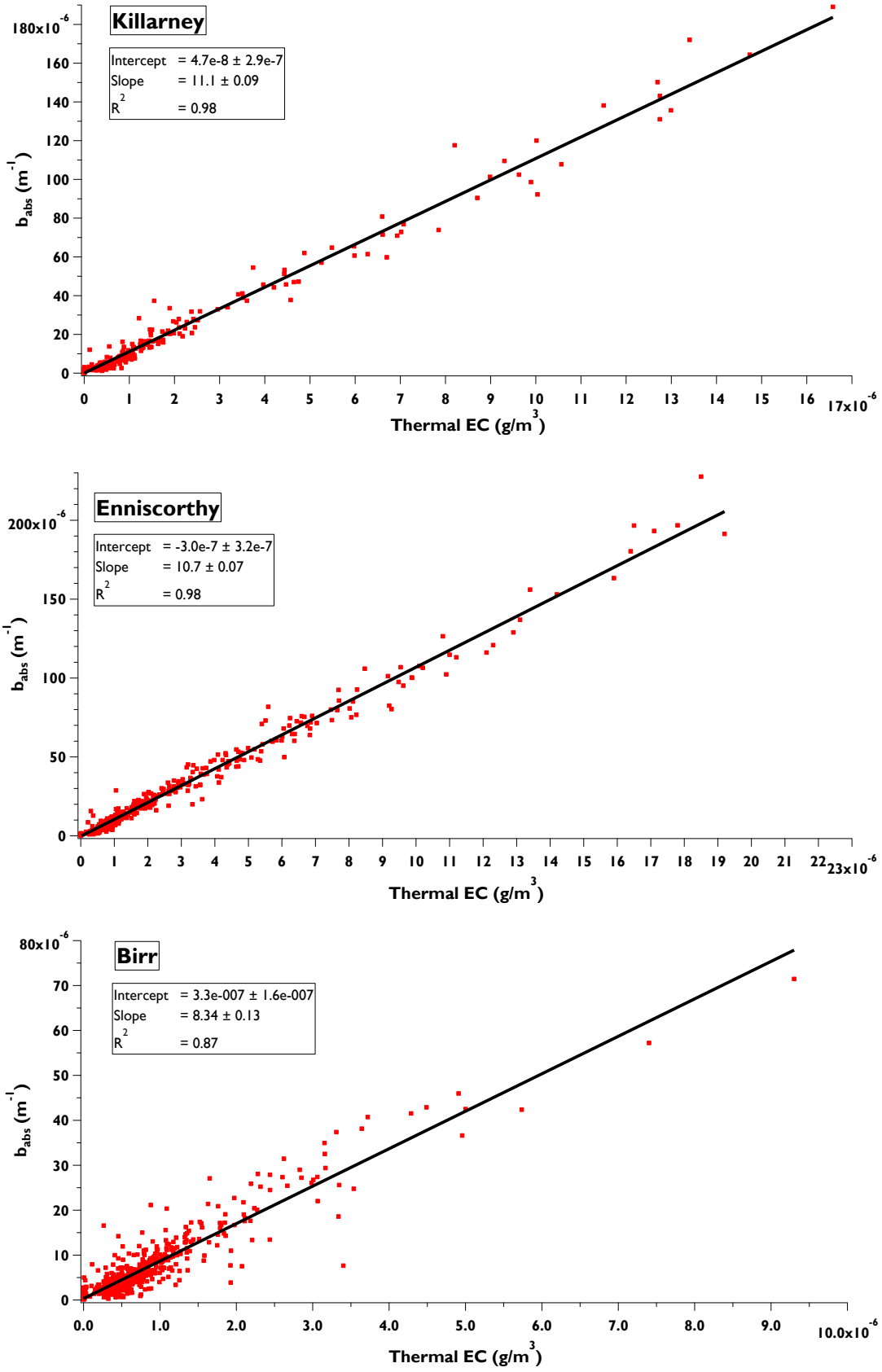

Figure 3.22. Regression of absorption coefficient (b_{abs}) measured by the AE33 and Thermal EC measured by the OCEC for Killarney, Enniscorthy and Birr.

The site-specific MAC values allowed for the recalculation of the eBC concentrations using the b_{abs} values from the AE33. Using the new MAC values to calculate eBC improved the relationship between the Thermal EC and the eBC (*Figure 3.23*). The slopes of the regression lines improved from 1.43 to 0.98 for Killarney, from 1.38 to 1.00 for Enniscorthy and from 1.07 to 1.00 for Birr. The divergence from a slope of 1 in Killarney indicates that the recalculated MAC value is still not fully optimized for this location and further refinement is possible. Other parameters used in the aethalometer calculations, for example the multiple scattering parameter and the leakage factor, could be varied in order to bring the relationship between the two measurements to parity.

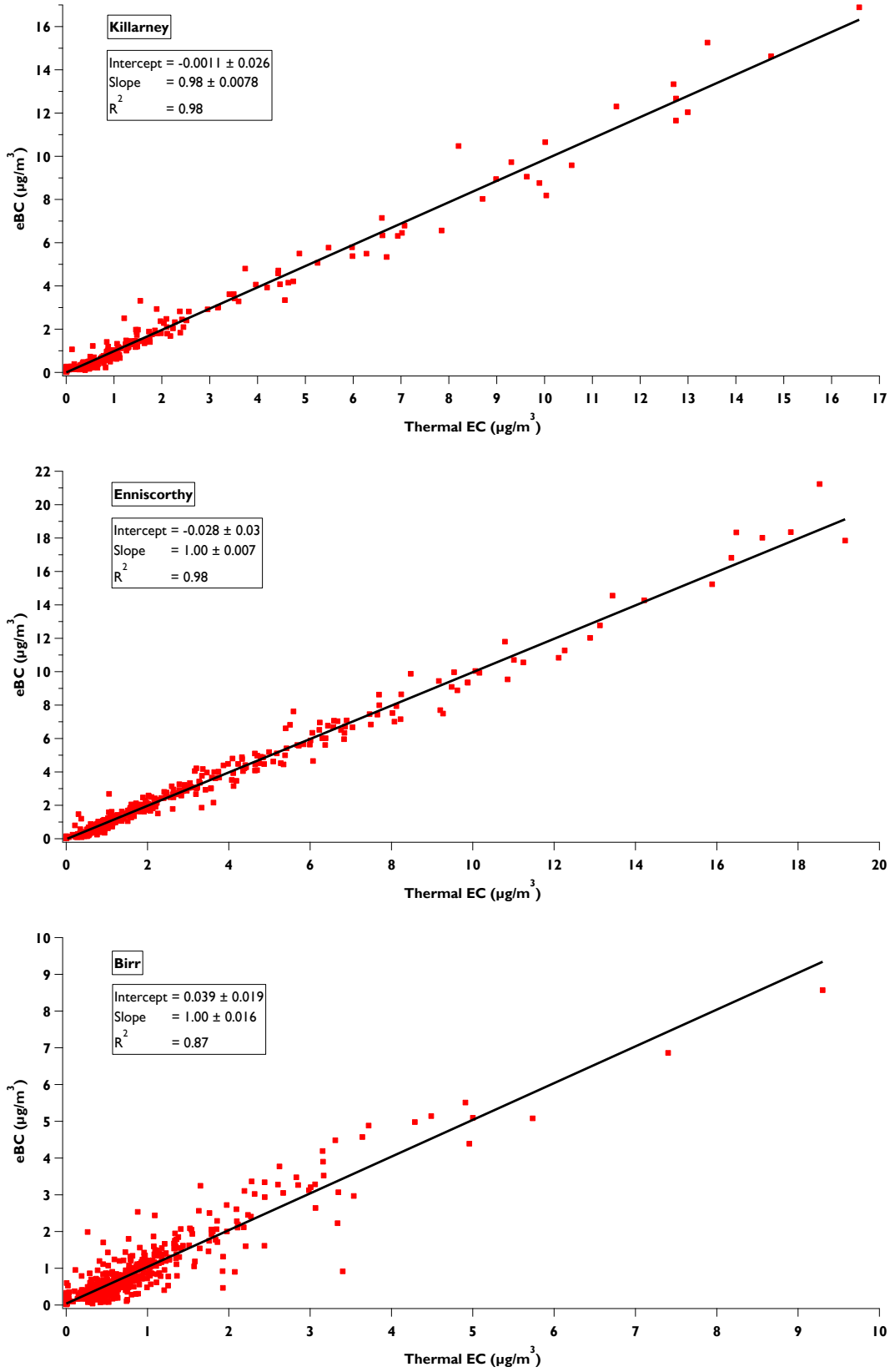

Figure 3.23. Regression of Thermal EC measured by the OCEC instrument and eBC calculated using the site specific MAC values for each location, derived in *Figure 3.18*.

3.3.5. Source Apportionment of eBC

As discussed previously, domestic solid fuel burning has consistently been identified as one of the main contributors to $PM_{2.5}$ in Ireland. This, however, is not reflected by the standard source apportionment model employed by the aethalometer (Sandradewi *et al.*, 2008b), which uses absorption Ångström exponents (Alpha, α) of 1 for fossil fuel related eBC, and 2 for eBC attributed to biomass burning (*Figure 3.24*).

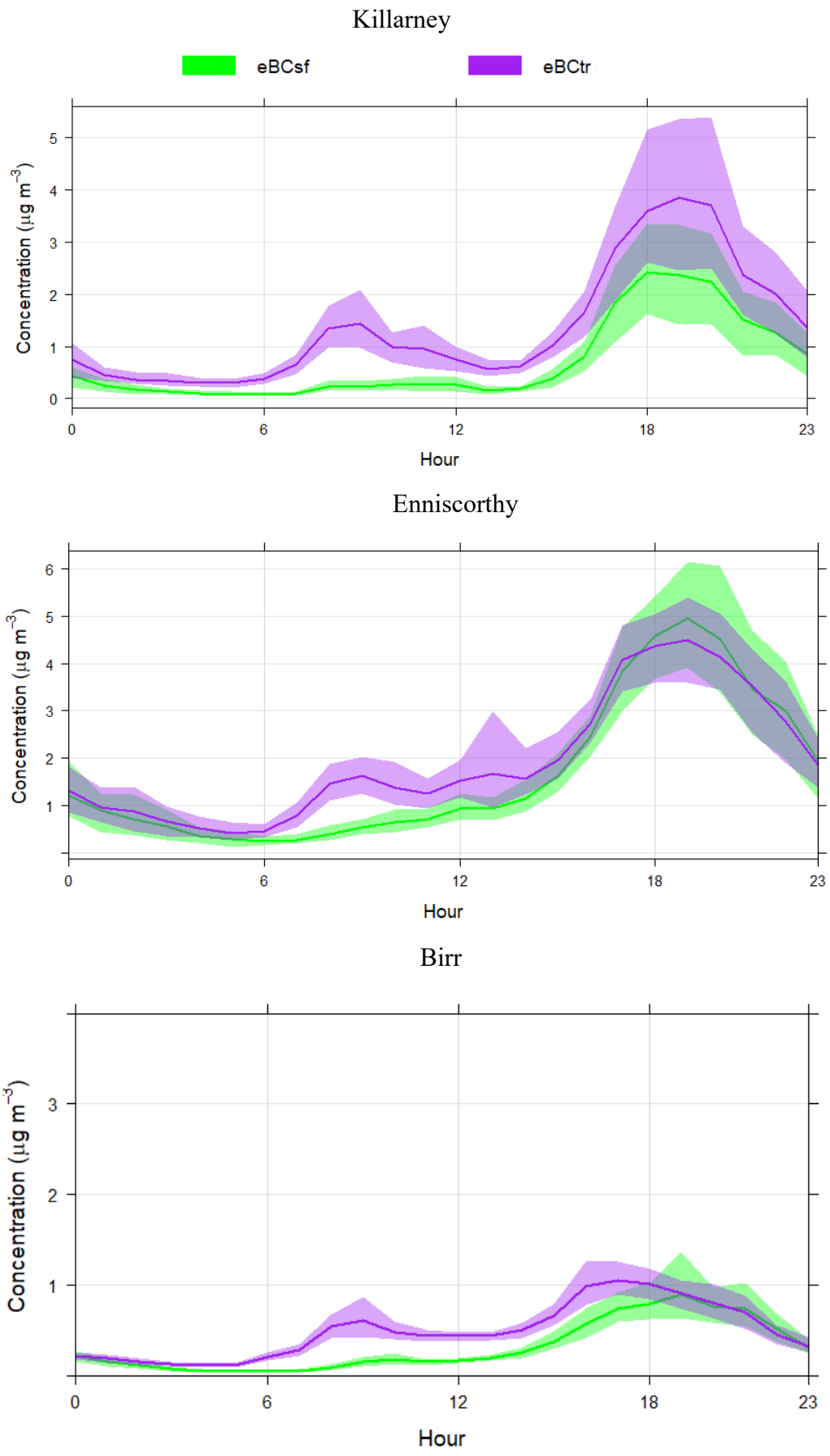

Figure 3.24. Mean diurnal profile for eBC sources, Killarney, Enniscorthy and Birr (calculated using Sandradewi parameters; α_{BB} = 2.0, α_{FF} = 1.0).

Logically, this did not make sense, as data from the OCEC instrument (*Figure 3.15*) point towards a large increase in solid fuel burning in the evening times. In order to investigate this further, the ΔC values (Allen *et al.*, 2004; Wang *et al.*, 2011a, 2011b) were calculated for each location. ΔC is indicative of the presence of solid fuel related particles. In essence, it is the amount of UVPM (BC1 in the raw data), minus the measured eBC (BC6 in the raw data). These profiles (*Figure 3.25*) show that there are significant increases in ΔC values in the evening times.

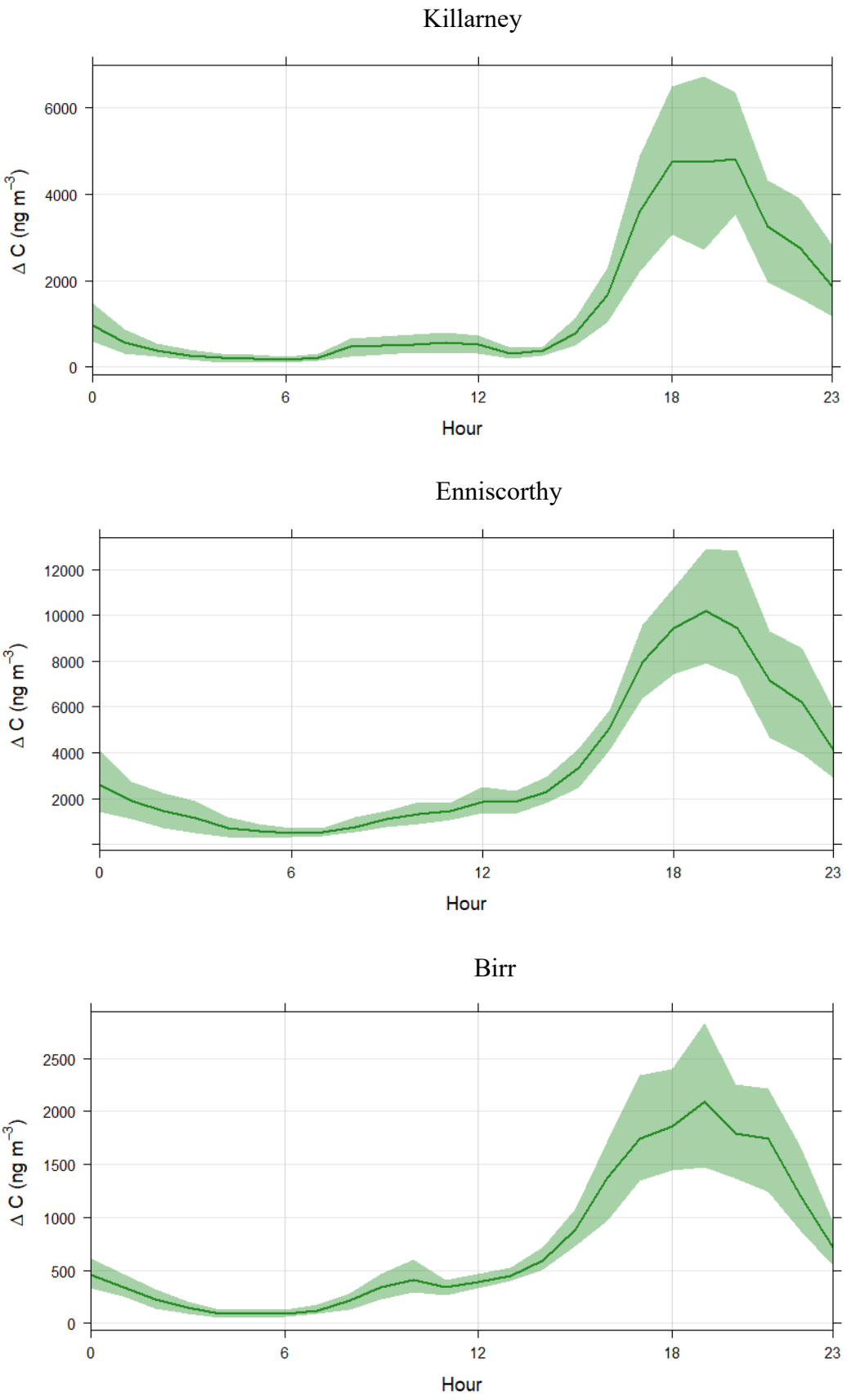

Figure 3.25. Mean diurnal ΔC profiles for Killarney, Enniscorthy and Birr.

Based on these profiles it was concluded that the Sandradewi parameters were not applicable in the Irish environment due to the wide-spread use of other solid fuel types; in addition to wood, coal, bituminous and "low-smoke" varieties, and peat, both freshly cut "sods" and reconstituted briquettes, are utilized for home heating (Lin *et al.*, 2018). It was therefore decided to vary the Alpha values to achieve a result where the majority of eBC was attributed to solid fuel burning. The Alpha values for traffic related eBC (α_{Tr}) were varied between 0.9 and 1.1 at each site, while the alpha values for solid fuel related eBC (α_{SF}) were varied between 1.5 and 2.2. Note that the label for the latter term has been changed from *wb* (wood burning) to *sf* (solid fuel) to reflect the multi-fuel environment of these locations. A wide variety of profiles were generated by varying both α_{Tr} and α_{SF}, with the most appropriate model selected for each site being the one that returned the least amount of negative values in the splits. It has been shown previously that negative values in the profile is indicative of the selection of incorrect Alpha values (Zotter *et al.*, 2017). The final parameters selected for each location are detailed in *Table 3.8*.

Table 3.8. Optimised α values selected for SAPPHIRE locations based on the analysis of frequency distributions of calculated α and temporal profiles of eBC_{SF} and eBC_{Tr}.

Location	**α_{Tr}**	**α_{SF}**
Killarney	0.9	1.59
Enniscorthy	0.9	1.65
Birr	0.9	1.75

The diurnal profiles produced using these "optimised" alpha values (*Figure 3.26*) show an increase in eBC attributed to solid fuel in the evening time, in addition to two peaks attributed to traffic, one during morning traffic hours, and one during evening traffic hours. These parameters attributed 71% of eBC to solid fuel burning in Killarney, 84% in Enniscorthy, and 46% in Birr.

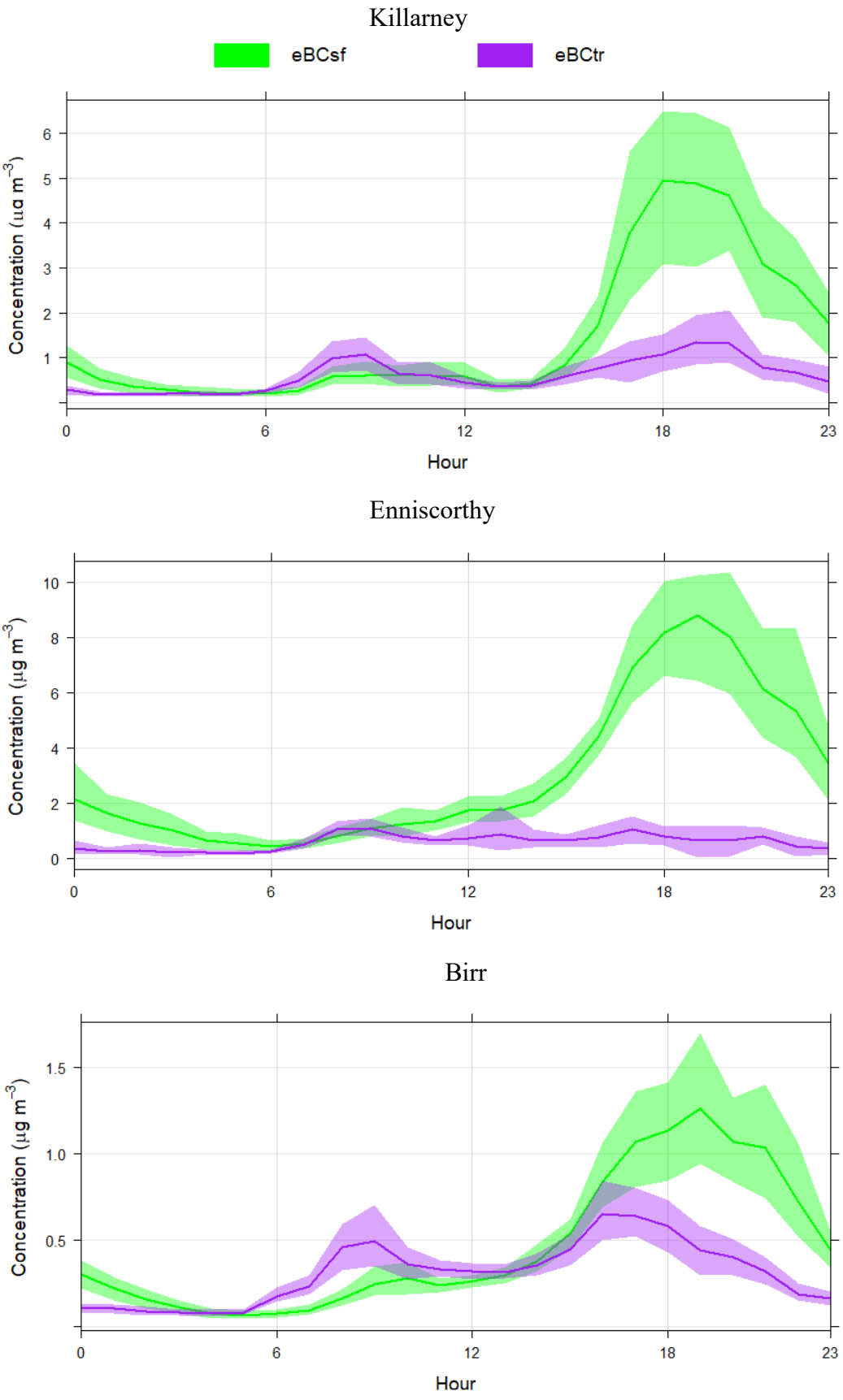

Figure 3.26. Mean diurnal profile for eBC sources, Killarney, Enniscorthy and Birr (calculated using optimized parameters; the α values used at each location are listed in *Table 3.8*).

The lower percentage of eBC attributed to solid fuel burning in Birr is perhaps due to the higher α_{SF} value selected for the campaign. This value was selected to minimize the negative values observed in the temporal profile. The value of α_{Tr} was kept constant for all three locations as the types of fuel used in Ireland do not vary from those used in mainland Europe, α_{Tr} = 0.9 (Zotter *et al.*, 2017). Though the selected values provide logical diurnal profiles for each location, and minimize negative values observed in the temporal profiles, there is no scientific basis for their adoption. Therefore it was decided to utilize the α_{SF} value of 1.68 recommended by Zotter *et al.* (2017). The profiles generated using the Zotter parameters (*Figure 3.27*) retained the larger solid fuel peaks observed in the evening times, but also contained larger traffic peaks in the evening time, with the exception of Birr. The reason for the lower evening eBC_{Tr} peak in Birr is the fact that the Zotter parameters resulted in a greater number of negative values in the traffic-associated eBC. The percentage of eBC attributed to solid fuel burning using the Zotter parameters was 61% for Killarney, 86% for Enniscorthy, and 63% for Birr.

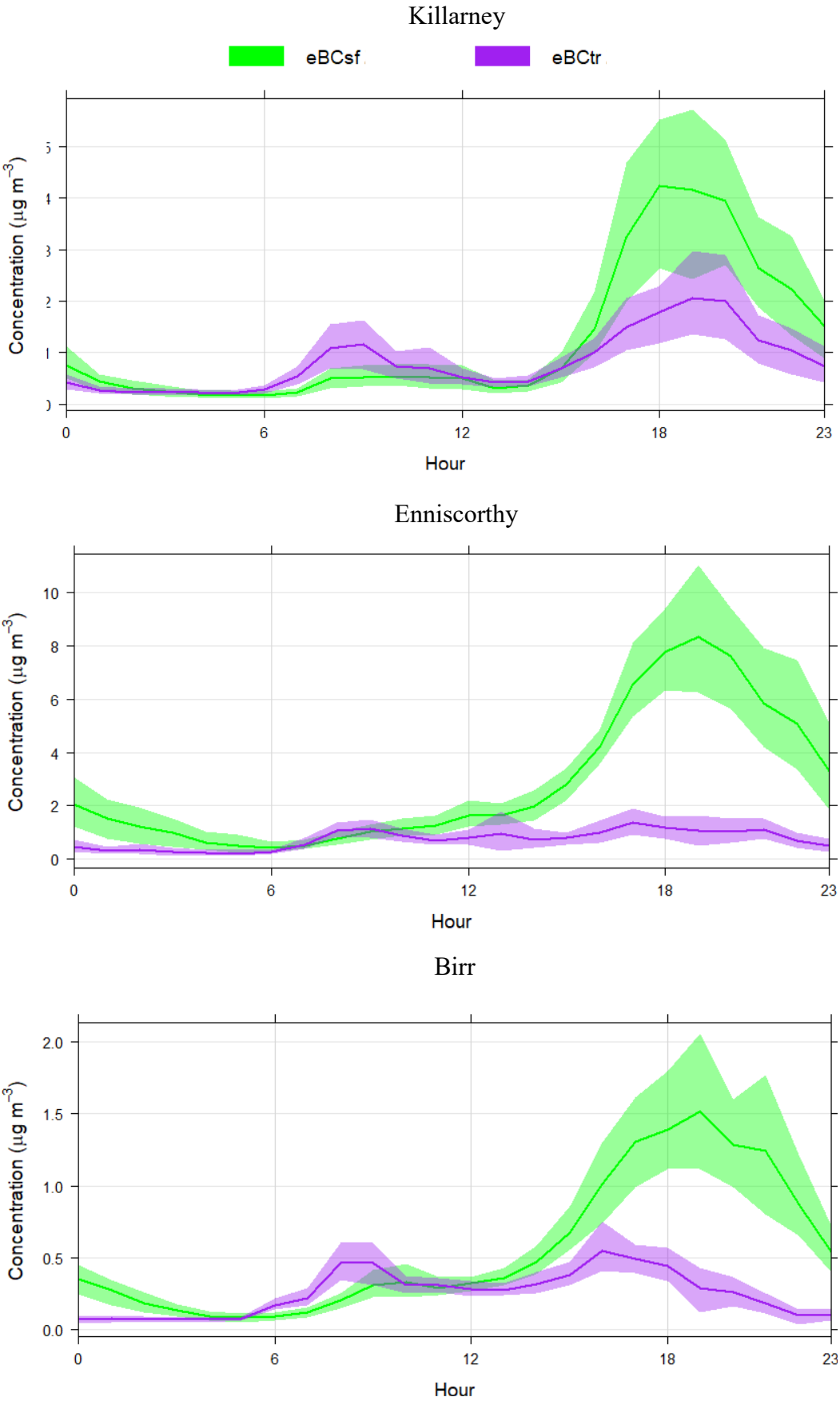

Figure 3.27. Mean diurnal profile for eBC sources, Killarney, Enniscorthy and Birr (calculated using Zotter parameters, $\alpha_{SF} = 1.68$, $\alpha_{Tr} = 0.9$).

The differences in the distributions of alpha and the mean alpha value for each location indicates there was a difference in aerosol composition at each location (*Figure 3.28* and *Figure 3.29*). The higher mean alpha value in Enniscorthy indicates that the aerosol is dominated by emissions from solid fuel burning (Sandradewi *et al.*, 2008a). This is also apparent in Birr and while the mean alpha value is lower, the distribution is shifted more towards the solid fuel value of 1.68 used in this study.

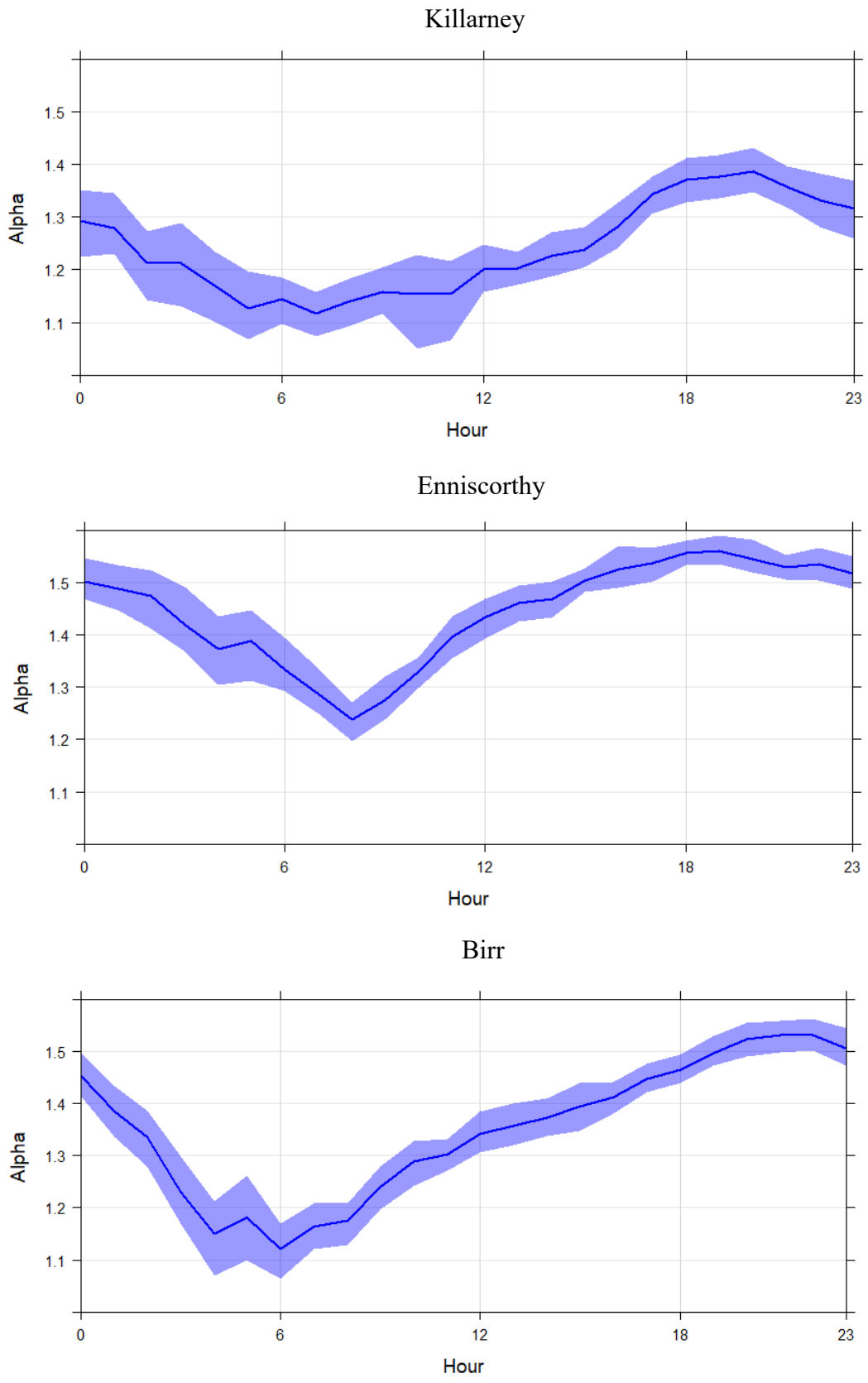

Figure 3.28. Mean diurnal profile of calculated α values in Killarney, Enniscorthy and Birr. Values were calculated using six wavelengths, from 470 to 950 nm.

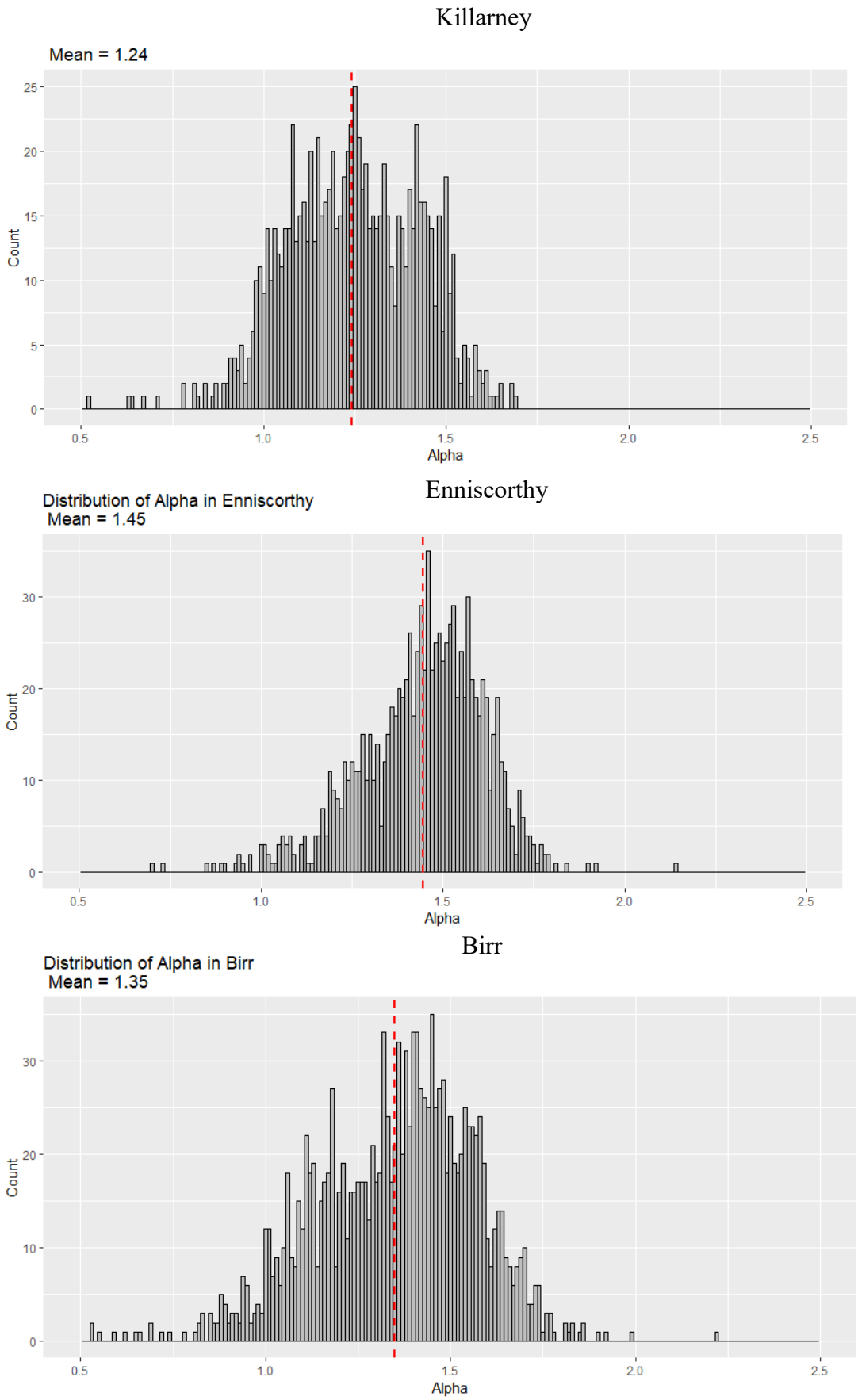

Figure 3.29. Frequency distributions of calculated α values at SAPPHIRE locations, calculated using six wavelengths, from 470 to 950 nm.

The above conclusion that the aerosol composition was dominated by emissions from solid fuel burning (SFB) can be further validated by comparing the results from the aethalometer with those produced using the ATOFMS. Analysis of single particle mass spectra resulted in over 15 particle classes at each location assigned to solid fuel burning, which were grouped into the following categories; coal, peat, wood, indistinguishable coal/peat and unassigned SFB (Arndt *et al.*, in preparation). The mass concentrations of all solid fuel classes were added and compared with the equivalent metric from the aethalometer (eBC_{SF}), *Figure 3.30*. The R^2 value for each location shows that the ATOFMS and AE33 solid fuel profiles correlate very well. In each case, the slope of the regression line is greater than five, but this can easily be explained. The AE33 only measures eBC, while the ATOFMS solid fuel represent the summed mass of all chemical components, i.e. EC, OC, nitrate, sulfate, ammonium, chloride and trace metals such as potassium and sodium (Healy *et al.*, 2010; Arndt *et al.*, in preparation).

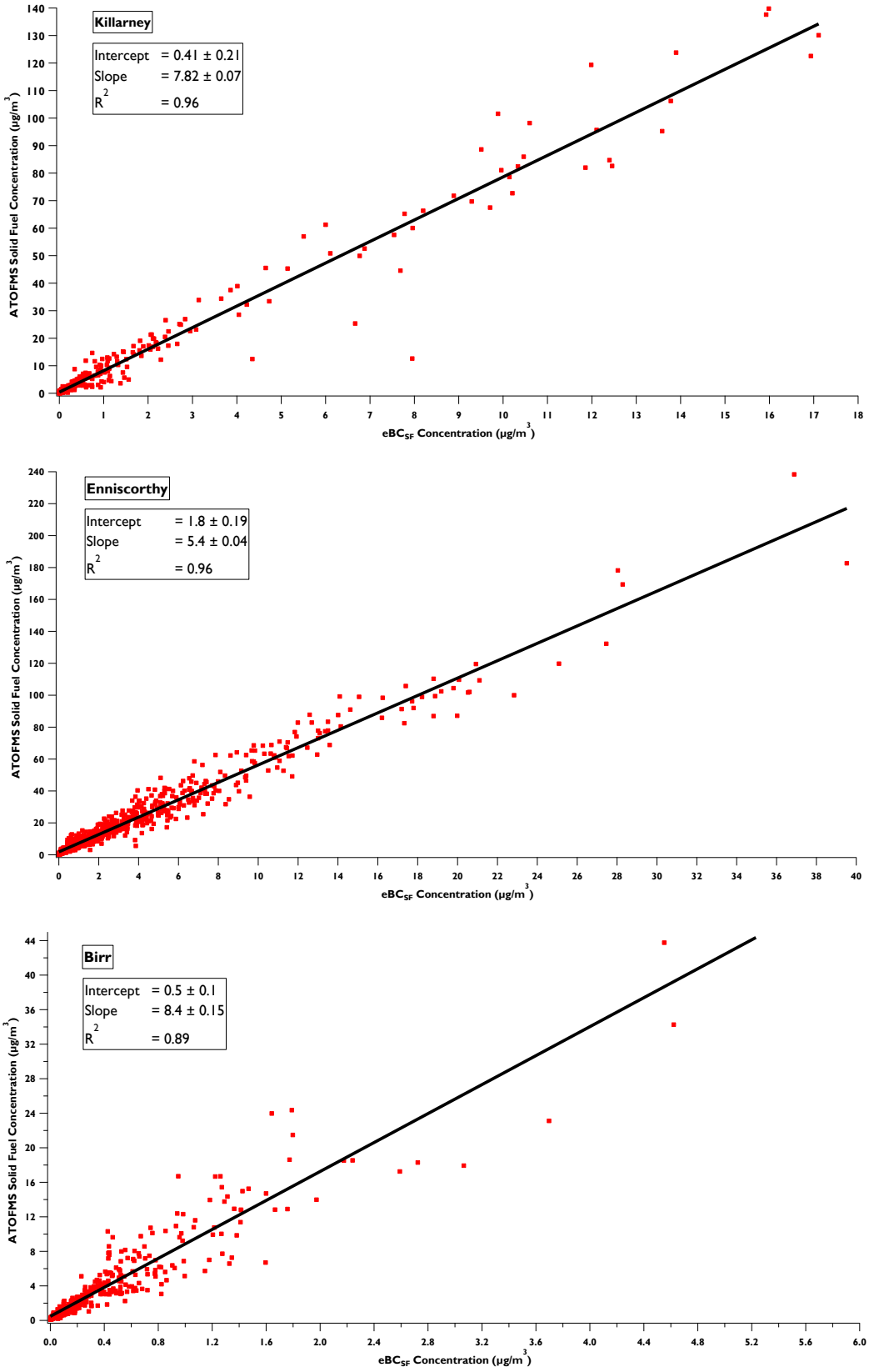

Figure 3.30. Correlations between Solid Fuel related classes from ATOFMS source apportionment and eBC attributed to solid fuel by AE 33. The ATOFMS solid fuel classes encompass all particle types related to peat, coal and wood, not just EC containing classes.

3.4. Conclusions

A suite of instruments including a seven wavelength aethalometer, thermal-optical carbon analyser and ATOFMS, were deployed for the measurement of ambient $PM_{2.5}$ in three small rural towns (Killarney, Enniscorthy and Birr) in Ireland during the winter periods of 2014/15 and 2015/16 as part of the SAPPHIRE project. The measurements from all instruments clearly indicate that domestic solid fuel burning is the major contributor to particulate pollution in all three locations. Meteorological patterns show that the highest concentrations were measured during periods of low wind speeds, when local sources were dominant.

Diurnal profiles for the AE33 and OCEC instruments show strong peaks in the evening for eBC_{SF} and thermal OC. The original source apportionment model of eBC (Sandradewi *et al.*, 2008b), contained peaks in both solid fuel and traffic related eBC in the evening times at all three locations. Based on the OCEC and ΔC profiles, this result was deemed to be erroneous and the absorption Ångström exponents (α) for both solid fuel burning and traffic sources were varied in order to improve the source apportionment. The "optimized" parameters, using α_{SF} values of 1.59, 1.65, and 1.75 for Killarney, Enniscorthy and Birr respectively, along with an α_{Tr} value of 0.9 for each site, resulted in diurnal patterns that showed only solid fuel related eBC peaking in the evening hours. These values were selected in order to minimize the occurrence of negative values, and to generate a profile that had similar traffic peaks in the morning and evening. Since these α values do not have a strong scientific basis, it was decided to proceed with the most recently recommended values of $\alpha_{SF} = 1.68$ and $\alpha_{Tr} = 0.9$ (Zotter *et al.*, 2017). This approach yielded similar profiles that correlated well with results from the OCEC analysis. A comparison between thermal EC and the eBC measurements was used to derive MAC values of 11.1, 9.8, and 8.8 m^2/g for Killarney, Enniscorthy and Birr respectively. Recalculation of eBC concentrations for each location using these site specific MAC values further improved the correlation between eBC and thermal EC.

Comparison of the AE33 data with the results obtained from the ATOFMS also proved to be valuable. Excellent correlations were obtained between the summed ATOFMS solid fuel classes and the eBC mass concentration attributed to solid fuel burning. However, the slope of the linear regression was much greater than unity due

to the fact that the ATOFMS measures all components in the single particles, whereas the aethalometer measures BC only. The aethalometer source apportionment also agreed well with the results obtained using the ATOFMS, as indicated in *Table 3.9.* This demonstrates that the use of appropriate alpha pairs in the aethalometer model could potentially allow for source apportionment that is comparable to that provided by the ATOFMS, a significantly more expensive and complicated instrument. In addition, optimization of the Mass Absorption Cross-Section values increases the agreement between the aethalometer and the OCEC analyser. Deriving MAC values for specific locations could allow for deployment of the aethalometer without the OCEC, an instrument which requires a constant supply of gases and significantly more maintenance than the AE33.

Table 3.9. Contribution (as %) of solid fuel burning emissions to ambient $PM_{2.5}$ calculated using the ATOFMS data and the contribution (as %) of solid fuel burning emissions to ambient eBC calculated using the aethalometer using different α during the SAPPHIRE campaigns.

Location	%SFB by ATOFMS	%SFB by Aethalometer ("optimised" parameters)	%SFB by Aethalometer ("Zotter" parameters)
Killarney	64	71	61
Enniscorthy	70	84	80
Birr	54	46	63

4. Source Apportionment of eBC During the AEROSOURCE Campaign

Contents

4.1. Introduction

4.1.1. Global Long Term Studies of Black Carbon

Long term monitoring of atmospheric pollutants is important for assessing health impacts, climate impacts, and the effectiveness of abatement measures. Such monitoring activities also allow for the characterisation of seasonal trends, determination of the influence of meteorological conditions and evaluation of the impact of significant pollution events. The European Union has facilitated the collaborative measurement of air pollutants for decades. In 1979, the United Nations Economic Commission for Europe (UNECE) established the Convention on Long-range Transboundary Air Pollution (CLRTAP) as an international collaborative effort to protect the environment (UNECE, 2004). A downward trend has been observed in the concentrations of all pollutants monitored in the European Union since the year 2000 (*Figure 4.1*). The European Monitoring and Evaluation Programme (EMEP) is a co-operative programme for monitoring and evaluating air pollution in Europe established with the aim of providing scientific information and data to the CLRTAP. In 2017, there were 35 organisations participating in the programme, with 171 measurement sites. The measured pollutants include ozone, PM_{10}, $PM_{2.5}$, inorganic ions, depositions of sulfur and nitrogen, as well as meteorological parameters (*EMEP Status Report*, 2019). Typically, the results show that as the annual gross domestic product (GDP) of the member states has increased, the pollution levels have decreased. The notable exception to this trend was in the years after the economic recession of 2008.

Long term monitoring of black carbon (BC) has been conducted at a large number of locations around the world. Monitoring networks have been established in several countries in an effort to track changes in pollution levels, and establish the major sources (Reche *et al.*, 2011). The European Environment Agency report in 2018 showed that BC emissions for the EU member states have decreased by 41% between 1990 and 2016 (EEA, 2018). From 2015 to 2016, the EEA reported a reduction of 2.5% in BC emissions from the member states. All but 6 locations involved in the EMEP monitoring network reported a decrease in total BC emissions between 2000 and 2017 (*Figure 4.2*). According to this report, BC emissions from Ireland decreased

47% from 1990 to 2016, including a 4.4% reduction between 2015 and 2016. The emissions from Ireland accounted for 1.0% of BC emissions from the EU member states in 2016.

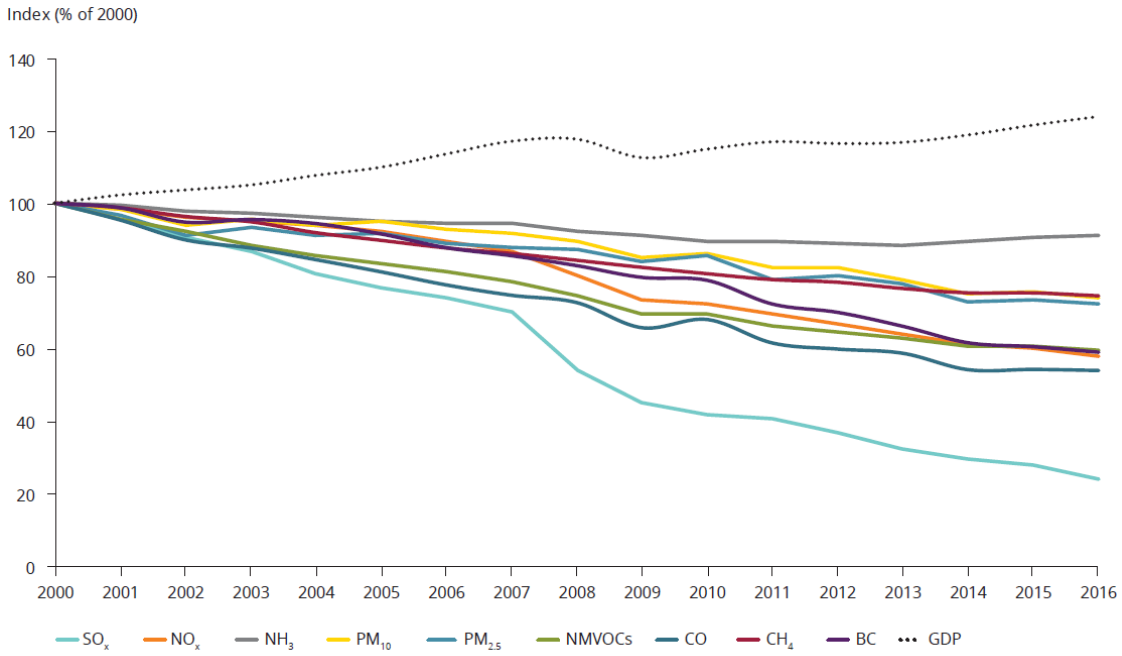

Figure 4.1. Total emissions of pollutants in the EU member states as a percentage of their value in the year 2000 (European Environment Agency, 2018).

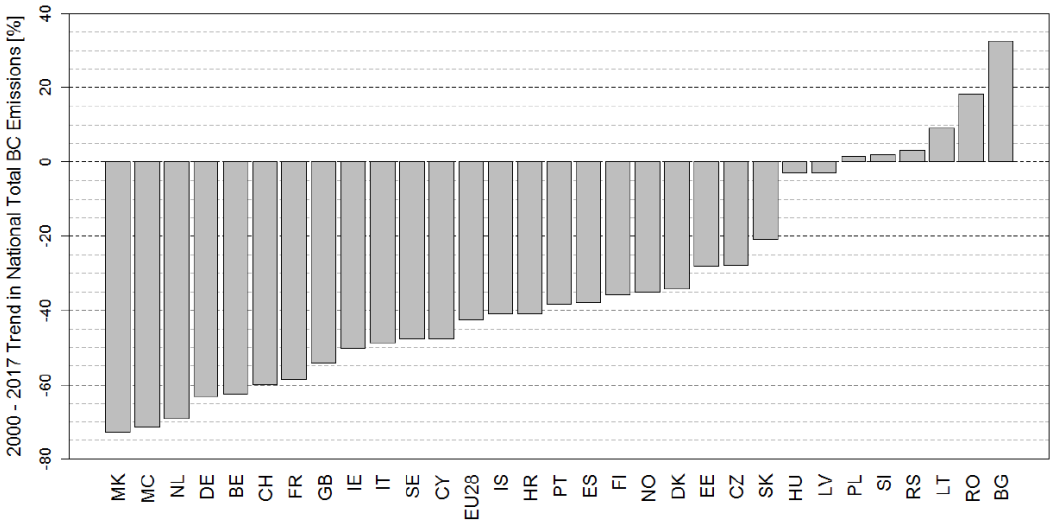

Figure 4.2. Trends in total BC emissions at 30 of 39 EMEP sites across 28 EU member states, 2000 – 2017 (EMEP Status Report, 2019).

In the United Kingdom, the Department for Environment, Food & Rural Affairs (DEFRA) has coordinated a large monitoring network since the 1960s (Fuller and Connolly, 2012; Longhurst *et al.*, 2016). Initially the network of monitoring stations measured black smoke (BS) concentrations, an older metric based on the shade of the area of filter paper where particles had been deposited. The network was upgraded in 2008 to use aethalometer instruments (Bower *et al.*, 2009). At the inception of this upgrade a total of 22 locations monitored black smoke or black carbon. As of 2018, a total of 14 locations were measuring black carbon in the UK (DEFRA, 2019a). Data from seven of these stations were used to analyse the trend in BC concentrations across the UK from 2009 to 2016 by Singh *et al.* (2018). The results show a statistically significant decrease of BC concentrations at five out of the seven locations, with Harwell, a rural location, and Strabane, a suburban location, being the exceptions. This trend was also observed across 65 monitoring stations between 2009 and 2014 by Font and Fuller (2016), who proposed that the decreasing trend in emissions was related to the introduction of legislation aimed at combatting air pollution.

In Germany, a large network of 171 stations, maintained by the federal states and the German Environment Agency dating back to the mid-1990s, shows a decreasing trend in pollution. A total of 12 stations were used in a targeted analysis (Kutzner *et al.*, 2018) on the trends in BC observations between 2005 and 2014. Auto-regressive integrated moving average (ARIMA) modelling showed a downward trend in measured BC concentrations at nearly all locations. Larger reductions were observed at traffic sites. This was attributed to the higher concentrations of BC at these locations compared to urban and rural sites.

In the Czech Republic, a two year measurement campaign in the city of Ostrava was conducted between 2012 and 2014 by Kucbel *et al.* (2017). An average BC concentration of 3.48 $\mu g/m^3$ was obtained, while a slight increase in the annual average of approximately 10% was observed (3.31 ± 3.84 $\mu g/m^3$ in 2012 to 3.65 ± 4.42 $\mu g/m^3$ in 2014). December, January and February had the highest average BC concentrations, while the lowest levels were recorded in May, June, July and August. The highest BC concentrations corresponded to periods with large amounts of coal burning, high levels of organic compounds originating from vehicle exhausts and the presence of the mineral hematite (Fe_2O_3) in the ambient aerosol. The diurnal average

profile shows an increase in BC concentration during morning and evening hours, attributed to increased traffic volumes and domestic biomass burning respectively.

A large number of studies have been conducted into the nature and sources of carbonaceous aerosols in Paris, France, as part of both ongoing monitoring and intensive field campaigns. For example, during the large-scale MEGAPOLI project (Baklanov *et al.*, 2010), approximately 60% of the EC measured during the field measurement campaign was attributed to local sources, i.e. within 50 km of the centre of Paris (Skyllakou *et al.*, 2014). Using the ATOFMS for single particle chemical speciation, Healy *et al.* (2012) identified carbonaceous aerosol classes associated with biomass burning and traffic sources. The source contributions determined by the ATOFMS were in relatively good agreement with those determined using the aethalometer, r^2 = 0.60 for fossil fuel and r^2 = 0.48 for biomass burning particle classes. From the BC data collected during the MEGAPOLI campaign, Beekmann *et al.* (2015) performed a comparison with other megacities around the globe (Delhi, São Paulo, Beijing, Cairo, Hyderabad, Shanghai, Seoul, Mexico City, Bangkok, Rio de Janeiro, Tokyo, London, New York City and Barcelona). The values recorded in Paris were generally lower than most of these cities, but on a par with those in Tokyo, New York City and London, which have similar efficiency in energy use.

In New Zealand, annual reports by the Institute of Geological and Nuclear Sciences Limited (GNS Science) present BC measurements collected from a network of approximately 40 stations across the country. In the latest report, Davy and Trompetter (2018), report that the highest peak concentrations (10–15 μg/m^3 as a 24 hour average) occurred in urban areas during the winter months due to the prevalence of domestic solid fuel burning. The highest annual average concentrations of BC (2–5 μg/m^3) occurred in urban centres with high traffic densities. The long-term trends in BC concentrations were generally decreasing and mainly attributed to the reductions in motor vehicle emissions. However, in the city of Nelson, a local policy implemented to replace old, inefficient wood burning stoves with newer models and to reduce the number of open fires played a significant role in reducing BC emissions. The measurements also show that the concentrations of BC vary throughout the country. A general North-South increase in biomass burning contributions to ambient BC was observed. This is due to a combination of environmental factors that limit the dispersion of emissions and the increased use of solid fuels for domestic heating purposes. The authors noted that BC concentrations in New Zealand urban locations

were generally higher than those observed in Europe and the United States. The authors determined that this was most likely due to a higher prevalence of biomass burning for domestic heating and an inherent time lag in the improvement of motor vehicle emissions technology.

For the United States, Kirchstetter *et al.* (2017) constructed a timeline of BC concentrations from 1965 to 2000. This timeline was constructed using coefficient of haze (COH) data collected by various state bodies, such as the California Air Resources Board (CARB) and the New Jersey Department of Environmental Protection (NJDEP). Following a two year study comparing the COH measurement method to the aethalometer instrument, an equation for converting COH values to BC concentration was determined;

$$BC\ (\mu g/m^3) = 6.7*COH + 0.1$$

Complete timelines for California and New Jersey were generated using this method. In addition, COH data for the years 1965 to 1980 from Illinois, Virginia, Ohio, Pennsylvania, Colorado, Missouri and Washington were also converted to BC concentrations. During that period, annual average BC concentrations in Illinois, Ohio, and Virginia decreased by 500%, concentrations in Missouri decreased by 400%, and concentrations in Pennsylvania decreased by 250%. For the entire study period (1965 – 2000), the annual average BC concentration in New Jersey decreased from 13 to 2 $\mu g/m^3$, and in California the annual average BC concentrations decreased from 4 to 1 $\mu g/m^3$. The higher initial concentrations in New Jersey were attributed to the larger reliance on BC producing fuels in the state compared to California in 1965. For all study areas a decrease in seasonality of emissions was observed from the 1960s onwards, which is attributed to the transition to cleaner fuels for home heating purposes. For example, in the 1970s, distillate fuel oil was replaced by natural gas and electricity as the primary sources of heating in the state of New Jersey. This change in fuel type accounted for the reduction of wintertime BC emissions and the disappearance of seasonal patterns.

Long-term measurements of carbonaceous aerosols on the island of Crete, in the Eastern Mediterranean, showed evidence of long-range transport of biomass burning and related particles from agricultural burning (Sciare *et al.*, 2008). The five year monitoring campaign, performed using a variety of measurement techniques (thermo-optical, optical, and thermal), showed two peaks in concentrations during the early spring and summer months. These periods correspond to post-harvest times in

the surrounding countries where agricultural waste (wheat residuals) are routinely burnt. The authors also noted that light absorbing dust particles contributed to light scattering measurements performed using the aethalometer, causing an increase of ~ 12% to the annual average.

For South Africa, Chiloane *et al.* (2017) presented 3 years of aethalometer data from 3 sites in the middle of the country. In general, the concentrations observed were higher than those observed in the developed world, for example in Western Europe. The highest concentrations were related to household combustion emissions originating from informal and semiformal settlements in the region. Strong seasonal patterns were observed at all locations, with the highest concentrations occurring between June and October, i.e. winter in the Southern Hemisphere. High concentrations were also observed during the dry season, between May and mid-October, and attributed to savannah and grassland fires. Other contributors to BC concentrations in the region included industrial emissions, traffic emissions, and pyrometallurgical processes.

In China, several monitoring campaigns have measured the concentrations of BC at different locations (Zhou *et al.* 2009; Wu *et al.* 2013; Ran *et al.* 2016). In 2005, average BC concentrations of 2.37 $\mu g/m^3$ and 5.47 $\mu g/m^3$ were obtained for Beijing and Shanghai respectively (Zhou *et al.* 2009). These values were higher than most locations in Europe and North America, while concentrations in other Asian locations, such as Sapporo, Japan, and Seoul, South Korea, were between those measured in the two Chinese cities. Wu *et al.* (2013) reported average BC concentrations at a South China Sea background location of 0.54 $\mu g/m^3$ in the wet season and 0.67 $\mu g/m^3$ during the dry season. Measurements at a Pearl River Delta (PRD) background site showed slight differences between the wet and dry seasons, 2.62 $\mu g/m^3$ and 2.88 $\mu g/m^3$ respectively, similar to levels measured at North China Plain background locations. In the PRD urban area the average BC concentration was 12.31 $\mu g/m^3$ in the dry season and 6.17 $\mu g/m^3$ during the wet season. Ran *et al.* (2016) conducted a two year long measurement campaign in Xianghe County, in the North China Plain. The yearly average BC mass concentration was estimated to be 5 $\mu g/m^3$, which is comparable to levels previously measured in similar locations around China.

In India, long term observations of BC at a rural location in the southern Indian peninsular area showed annual average concentrations of 2.2 $\mu g/m^3$ between 2008 and 2017 (Kiran *et al.*, 2018). The annual maximum concentrations occurred in March,

while the annual minimum concentrations occurred in July. Similar seasonal variations were observed in the Bay of Bengal (Kompalli *et al.*, 2013). Over the ten year period the maximum, minimum and annual average values decreased in response to reductions in agricultural biomass burning, a potential indicator of changing agricultural practices in the area (Kiran *et al.*, 2018).

In Pakistan, BC concentrations measured in Karachi from March 2006 to December 2008 showed a distinct seasonal pattern similar to that observed in India (Bibi *et al.*, 2017a, 2017b). The maximum value (12.7 $\mu g/m^3$) occurred during January 2007, and the minimum value (2.2 $\mu g/m^3$) occurred in June 2006.

In Ireland, long-term measurements of BC have been conducted at the Mace Head research station, located on the west coast in Carna, Co. Galway (Jennings *et al*., 2003). Various generations of aethalometer instruments have been installed at the Atlantic coastal site since February 1989. Initial measurements were carried out using the model AE8 aethalometer, which was subsequently upgraded in 1994 to the AE9 instrument. At present, an AE31 instrument is located at Mace Head.

Using the model AE8 aethalometer, Jennings *et al.* (1993) reported BC mass concentrations between February 1990 and April 1991. Concentrations of 38 ± 11 ng/m^3 were recorded during periods of clean air originating from the North Atlantic. Air masses originating from the continent contained several hundred ng/m^3 of BC. A strong correlation was observed between BC mass and the number concentration of smaller sized particles.

BC mass concentrations from the aethalometers were used in conjunction with accumulation mode particle number concentrations to differentiate between marine and continental air masses (Jennings *et al.*, 1997). BC concentrations for marine air masses were found to generally be in the range of 5–40 ng/m^3 over the course of the whole monitoring campaign. Mean concentrations measured during the winter period were 14.7 ng/m^3, accounting for 0.6% of the aerosol mass. During the summer period, the mean BC concentration was 25.6 ng/m^3, accounting for 1.2% of the aerosol mass. Analysis of the BC concentrations arriving from the continent showed that BC contributed 4–6% of the mass loading during those periods.

Seven years of continuous BC measurements, using the model AE8 and AE9 aethalometers from February 1989 to June 1996, was reported by Cooke *et al*. (1997). A geometric mean BC concentration of 14.2 ng/m^3 was found for clean marine North Atlantic air masses during this period. The concentrations measured in air masses

originating from the continental sector were approximately 15 times greater than the concentrations observed in the clean air masses. A seasonal cycle was observed, with peaks in February and May. The peak in February was attributed to increased emissions during the northern hemisphere winter, and the peak in May, the maximum concentration, was attributed to the reduced precipitation levels during late spring/early summer.

A study into regionally polluted air masses arriving from the European continent was conducted between 1 January 1995 and 31 December 1998 (Derwent *et al.*, 2001). Using the model AE9 aethalometer, hourly BC measurements were used, in conjunction with carbon monoxide, and a wide range of other trace gases, to estimate the European emission source strength of BC emissions. In general, BC concentrations < 1000 ng/m^3 were associated with clean, unpolluted air masses originating from the North Atlantic. Periods where the concentrations were > 1000 ng/m^3 were indicative of polluted air, either from the immediate vicinity or transported from Europe, containing emissions from traffic, industrial, and biomass burning related sources. The authors noted that during periods of increased BC emissions from local sources no corresponding increase in any of the trace gases was observed. In contrast, periods of elevated BC occurring over several days were closely related to elevated levels of CO_2, methane and other trace gases, indicative of regionally polluted air masses.

Total Carbon (TC) was also measured at Mace Head between July 1998 and September 1999 using a catalytic combustion method (Kleefeld *et al.*, 2002). The measurement period was subdivided into three sections; April – September 1998 (Period I) representing the summer period of 1998, October 1998 – March 1999 (Period II) representing the winter period of 1998/1999, and April – September 1999 (Period III) representing the summer period of 1999. On average, measured TC mass concentrations were 591 ± 75 ng/m^3, accounting for 5.61 ± 0.70% of the total aerosol mass. Two distinct air mass types were identified, “clean marine air samples”, and “modified marine air samples”. For clean marine air samples during summer, BC accounted for 4 ± 0.2% of the TC mass concentration. For the modified marine air samples during the winter and summer periods, BC accounted for 28 ± 3% and 22 ± 2% of TC mass concentrations respectively.

Long term, continuous monitoring of BC on the island of Ireland has also been carried out in Belfast, Northern Ireland, since 2008 as part of the UK Black Carbon

network (Bower *et al.*, 2009). The trend of annual averaged BC concentrations, shown in *Figure 4.3*, is generally decreasing, in line with the downward trend observed at EMEP locations. From 2009 to 2018, the annual average BC concentration decreased by 40.5%.

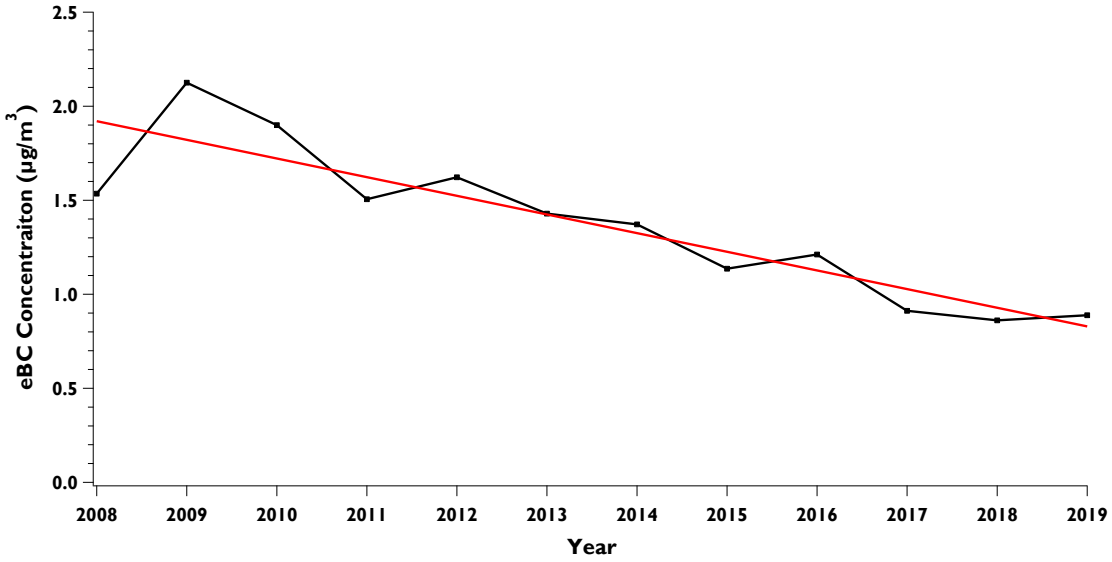

Figure 4.3. Annual average BC concentrations (µg/m^3) from a monitoring location in Belfast city, 2008 – 2019 (DEFRA, 2019b).

4.1.2. Source Apportionment of Black Carbon Measurements

The first campaigns to include source apportionment of BC took place in Switzerland (Sandradewi *et al.*, 2008a, 2008b; Herich, Hueglin and Buchmann, 2011). In a series of short term studies, Sandradewi *et al.* developed a method for separating the contributions of fossil fuel burning and biomass burning to total BC mass. This method was based on different α values for the two sources and showed good agreement with other source apportionment methods such as OCEC analysis. Following the pioneering work of Sandradewi *et al*. in 2008, source apportionment of BC using the aethalometer model was used by Favez *et al.* (2009) during a short-term study in Paris and by Herich *et al.* (2011) during a two and a half year study in Switzerland. It was found that wood burning contributed up to 20% of $PM_{2.5}$ mass in Paris in January and February, while during the winter in Switzerland, BC from wood burning contributed 33% and 30% of the total BC mass in rural locations, and 24% of the total BC mass in Zurich. Since its development, the use of the aethalometer source apportionment model has become increasingly prevalent for the quantification of the contributions from fossil fuels and wood burning. A selection of studies performed over the last decade, and the α pairings used in each study, are summarized in *Table 4.1*.

As part of the MEGAPOLI winter field measurement campaign, Healy *et al.* (2012) showed that the two-source aethalometer model agreed extremely well with the source apportionment of EC particles by the ATOFMS. The aethalometer model estimated that fossil fuel and biomass burning contributed 85% and 15% of BC mass concentration, respectively, while the ATOFMS attributed 88% and 12% of EC mass to fossil fuel combustion and biomass burning. Petit *et al.* (2015) also deployed an aethalometer in Paris along with an Aerosol Chemical Speciation Monitor (ACSM) and performed source apportionment on approximately 280,000 BC data points collected between June 2011 and June 2013. BC from biomass burning displayed a highly seasonal pattern with the highest concentrations occurring during the cold seasons and at low wind speeds. This finding provided evidence for the stronger influence of local sources on pollution levels in winter. A series of pollution events during the two year monitoring campaign were also investigated in detail (Petit *et al.*,

2014), while a specific pollution event that occurred in March 2015 was analysed using a different, multi-site approach (Petit *et al.*, 2017).

Fuller *et al.* (2014) performed source apportionment analysis on a three year aethalometer data set collected in the London area. The dominant contribution to BC mass was determined to be fossil fuel combustion. Diurnal profiles exhibited a significant morning peak due to traffic emissions and a smaller peak during the evening, attributed to wood burning. Evidence for additional wood-burning was found during weekends. The highest monthly contribution from wood burning occurred during January and December (23%), with the lowest contribution occurring during May and June (11%). Crilley *et al.* (2015) conducted a short winter campaign at three different locations in and around London during 2012. The highest average BC concentrations were observed at the North Kensington monitoring site, 1.4 ± 1.3 $\mu g/m^3$. The concentrations at the rural locations in Harwell and Detling were 0.7 ± 0.6 $\mu g/m^3$ and 0.9 ± 0.8 $\mu g/m^3$ respectively. The traffic contribution to BC mass concentration at North Kensington was determined to be 85 ± 12%, with the contribution from wood burning determined to be 15 ± 12%. In Detling, the traffic contribution to BC mass concentration was determined to be 70 ± 13%, with wood burning contributing 30 ± 13%.

Source apportionment of BC data collected in Canada has been performed on long-term datasets and also to characterise short-term pollution events (e.g., Healy *et al.*, 2017, 2019). A year-long study, conducted between June 2015 and May 2016, encompassed nine monitoring locations, seven of which were classified as near-road sites, one residential location, and one background location. The highest biomass burning contribution occurred at the residential monitoring location (26%) during the winter months (Healy *et al.*, 2017). High biomass burning contributions, up to 63–69%, were also observed in British Columbia during periods when wildfires were prevalent in the area. The standard α values (0.9 and 2.09 for fossil fuel and biomass burning respectively) underestimated the contributions from wildfires to BC mass concentrations and, using a background extraction technique, the authors derived a wildfire specific α value range, 1.23 to 1.49 (Healy *et al.*, 2019). These different α values suggest that atmospheric processing occurred during transport of the aerosol.

Data collected at two locations in Athens, Greece, from 6 December 2014 – 10 March 2015 highlighted the important contribution of biomass burning to BC mass concentrations during the winter months (Kalogridis *et al.*, 2018). BC_{wb} contributed

up to 30% of BC mass concentrations during the winter months, with the diurnal profile clearly showing that the majority of BC_{wb} was emitted during the evening hours.

Several BC source apportionment studies have been conducted on the subcontinent of India. BC concentrations at an urban location in Delhi between December 2015 and February 2016 averaged 24.4 ± 12.2 μg/m^3 (Dumka *et al.*, 2018). Peaks in fossil fuel related BC were observed in the morning and evening hours, corresponding to rush hour traffic times. A large peak in wood burning associated BC was also observed during the evening and attributed to biofuel burning for heating and cooking purposes. Overall, approximately 72% of the measured BC mass was attributed to fossil fuel combustion.

Over 1.5 years of data was collected using the AE33 aethalometer at Mt. Mugogo, Rwanda (DeWitt *et al.*, 2019). Strong seasonal and diurnal variations were observed in BC mass concentrations and the calculated α values. Rwanda has two rainy seasons (March to May and September to November) and two dry seasons (December to February and June to August). The peak concentrations of BC (ca. 20 μg/m^3) were observed during the dry seasons. The diurnal profile for each dry season shows two peaks, one in mid-morning and the other in early evening, corresponding to times when kerosene is burnt or generators are used for home lighting/heating. The average α value for the entire campaign was calculated to be 1.65 (± 0.14). Significant differences in the calculated α values were observed between the seasons. The monthly average value during the dry season was 1.5, while the average value at the end of the rainy season was 1.9. The authors noted that the different fuel types and burning practices used in Africa call in to question the validity of using parameters determined from measurements in Europe and North America.

The variability of potential α pairs has been demonstrated for kerbside and residential locations in Helsinki, Finland (Helin *et al.*, 2018). The authors found that different α_{FF} values yielded the best source apportionment results in the different environments, the α_{FF} value at the kerbside location was set to 1.1, while the α_{FF} value at the residential location was set to 0.95. A wide range of α_{WB} values were tested, between α_{WB} = 1.4 and 2.2, but a value of 1.6 was settled upon after comprehensive analysis. The source apportionment results showed that eBC_{WB} accounted for 9 ± 13% of $PM_{2.5}$ at the residential site during the winter months, and 2 ± 7% at the kerbside

location, while total eBC accounted for 18 ± 20% of $PM_{2.5}$ mass at the residential location and 21 ± 18% at the kerbside.

Table 4.1. Summary of time campaign duration and α pairings used during a sample of monitoring campaigns where source apportionment of BC was carried out.

Study	Time Period	Location	α_{ff}	α_{wb}
Sandradewi *et al.*, 2008	Jan 2005–Dec 2005	Roveredo, Switzerland	1.1	1.9
Favez *et al.*, 2009	Jan 2005–Feb 2005	Paris, France	1.1	2.0
Herich *et al*., 2011	Mar 2008–Oct 2010	Swiss Alps	0.9	1.9
Healy *et al.*, 2012	Jan 2012–Feb 2012	Paris, France	1.0	2.0
Fuller *et al*., 2014	Jan 2009–Dec 2011	London, England	1.0	2.0
Crilley *et al.*, 2015	Jan 2012–Feb2012	London, England	1.0	2.0
Petit *et al.*, 2017	Jun 2011–Jun 2013	Paris, France	1.0	2.1
Healy *et al.*, 2017	Jun 2015–May 2016	Ontario, Canada	0.9	2.09
Kalogridis *et al.*, 2018	Dec 2014–Mar 2015	Athens, Greece	0.9	2.0
Dunka *et al*., 2018	Dec 2015–Feb 2016	Delhi, India	1.0	1.8
Helin *et al.*, 2018	Oct 2015–June 2017	Helsinki, Finland	0.95/ 1.1	1.6
Healy *et al.*, 2019	Sep 2016–Aug 2017	British Columbia, Canada	0.9	2.1
DeWitt *et al*., 2019	May 2015–Jan 2017	Mt. Mugogo, Rwanda	1.0	2.0

4.1.3. The AEROSOURCE Project

The long history of measurements at the Mace Head Atmospheric Research Station has allowed for the detailed characterisation of aerosols contained in air masses originating from the Atlantic Ocean and North America. Until recently, characterisation of aerosols contained in air masses originating from the Arctic or the continent of Europe had received comparatively little attention in Ireland. This deficiency was addressed in the Irish EPA funded project (2016-CCRP-MS.31)

"Source apportionment of airborne pollutants transported to and across Ireland using Aerosol Mass Spectrometry and Positive Matrix Factorization Techniques" (AEROSOURCE). In this project, a network of online monitoring instruments was deployed at three locations; Mace Head, Carnsore Point and University College Dublin, providing coverage of air masses arriving from the west, south and east, *Figure 4.4*. This network, operated by National University of Ireland Galway (NUIG), was the first of its kind in Ireland.

Figure 4.4. Map of Ireland with AEROSOURCE locations marked; UCD (orange), Carnsore Point (magenta), and Mace Head (green).

Each monitoring location in the AEROSOURCE project was equipped with an Aerodyne aerosol mass spectrometer (ACSM or HR-TOFMS) for measuring the

contributions of organic aerosol (Org), sulfate (SO_4), nitrate (NO_3), ammonium (NH_4) and chloride (Chl) to PM_1 mass. Positive Matrix Factorization was performed on the organic fraction for source apportionment purposes. An aethalometer (Model AE31 or AE33) was also installed at each site to determine equivalent black carbon concentrations (eBC).

The ACSM-aethalometer combination has proven to be very effective in providing reconstructed PM_1 mass and detailed information on its sources. To date, two publications have arisen from the project, the first focussing on two extreme pollution events in Dublin during winter 2016-2017, on 19 November 2016 (P1) and 22 January 2017 (P2) (Lin *et al.*, 2018), and the second comparing pollution levels and the chemical composition at four locations around Ireland during December 2016 (Lin *et al.*, 2019b). The analysis of the extreme pollution events showed a significant contribution from solid fuel burning during evening times, with a peak concentration of 302 μg/m^3 during P1 and 273 μg/m^3 during P2, *Figure 4.5*. Organic Aerosol (OA) and eBC accounted for 89% of PM_1 mass during P1 and 88% of PM_1 mass during P2. The diurnal profiles for the individual components of OA during both pollution events show significant contributions from peat burning, *Figure 4.6.*

The second study compared the aerosol composition at four different locations in Ireland (Dublin, Birr, Mace Head and Carnsore Point) and showed that organic aerosol is the largest contributor to winter-time PM_1 mass at all locations (*Figure 4.7*). The highest average OA contributions to PM_1 mass were observed in Dublin, 66%. PMF results indicate that the largest source of OA in Dublin was peat (30%), followed by OOA at 26%. The second highest average OA contribution was observed in Birr (58%), where OOA was the largest contributor to OA mass (35%), followed by peat (27%). The OA contributions observed at Carnsore Point and Mace Head, both classed as regional background locations, were 32% and 33% respectively. The highest contributor to OA mass at both locations was OOA, 71% and 45% at Carnsore Point and Mace Head respectively.

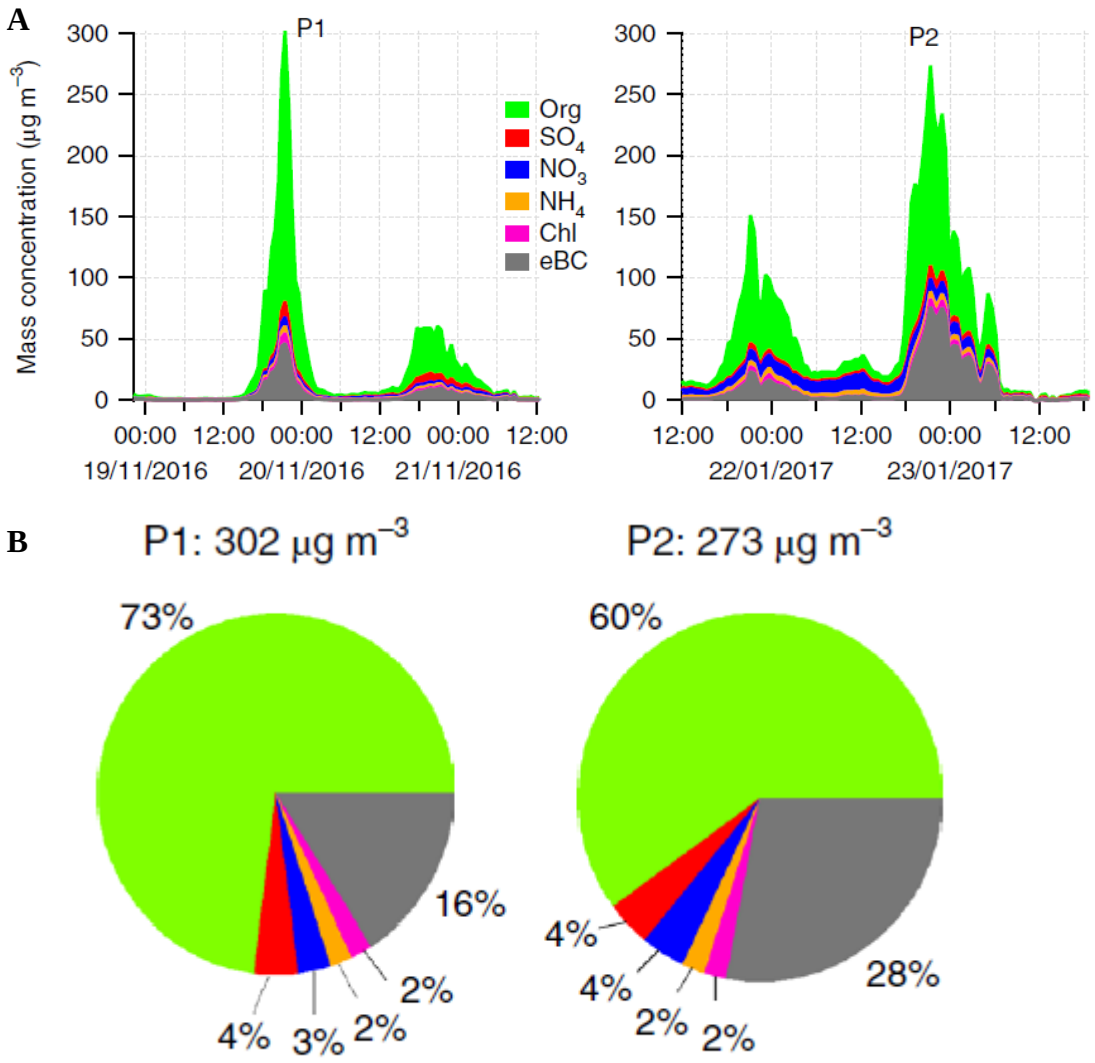

Figure 4.5. **A.** Hourly average concentrations of ACSM fractions and eBC for P1 and P2; and **B.** Percentage contributions from PM_1 sources during P1 and P2 (adapted from Lin *et al.* 2018).

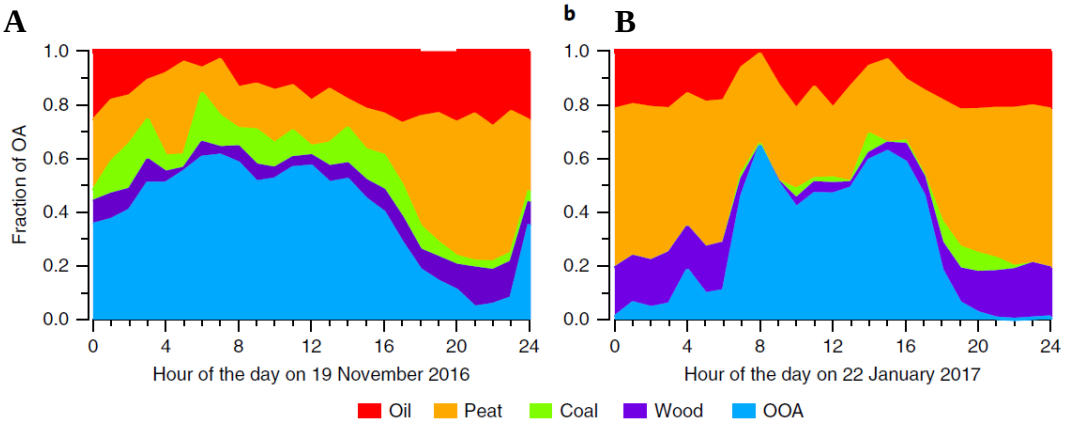

Figure 4.6. **A.** Diurnal profile of OA contributors during P1; and **B.** Diurnal profile of OA contributors during P2 (adapted from Lin *et al.* 2018).

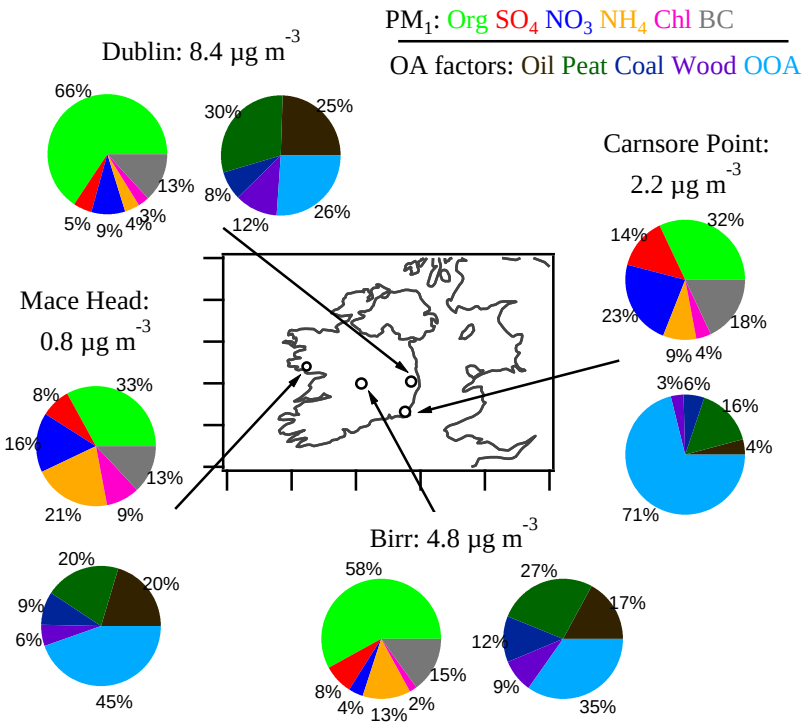

Figure 4.7. Comparison of PM_1 composition and OA source apportionment at monitoring locations in Dublin, Birr, Mace Head and Carnsore Point during December 2016 (Lin *et al.*, 2019b).

4.1.4. Aim of this Work

The aim of the work presented in this chapter is to conduct the first measurements of BC concentrations in Dublin, Ireland, using the AE33 aethalometer instrument (Drinovec *et al.*, 2015). The results are used to assess the diurnal, weekday-weekend, and seasonal variations of BC. Source apportionment is used to determine the contributions of traffic and solid fuel burning to BC concentrations at the monitoring location. Additional parameters obtained from the aethalometer, including the absorption Ångström Exponent (α), and ΔC, are used to investigate changes in optical properties during the different seasons. The results are combined with data from the ACSM co-located at the site to give a chemical breakdown of PM_1 and provide further insight into the properties of BC particles in Dublin.

4.2. Methodology

4.2.1. Sampling Site

Sampling for the AEROSOURCE project in Dublin took place on the campus of University College Dublin (UCD) from 5 August 2016 to 20 August 2018. The instruments were located in an air conditioned room on the top floor of the UCD Science Centre North building (53.30902, -6.224386), approximately 20 m in height. The inlet, located on the roof of the building, was fitted with a $PM_{2.5}$ cyclone head and added a metre to the measurement height. The site, marked in yellow in *Figure 4.8*, is located approximately 4 km south of St. Stephen's Green in Dublin city centre and is representative of an urban background location. Directly east of the site, approximately 400 m away, is a large junction, which is part of the R138 roadway (highlighted in red). To the southeast, this route becomes the N11 road, which is one of the main arteries into Dublin city centre, originating from county Wicklow and passing through the large town of Bray. To the east of the monitoring site are several residential areas and the coastline, which is approximately 2 km away. To the south of the site is the rest of the UCD campus (highlighted in orange), a largely pedestrianised area. To the west, north and east of the site, are residential areas, marked in blue. A significant number of residential areas are also located to the south and west of the monitoring location (not shown on map).

Regional meteorological data was obtained from the weather station located at Casement Aerodrome, approximately 15 km from the monitoring site. The parameters used for the analysis were rainfall (mm), temperature (ºC), wind speed (m/s), and wind direction.

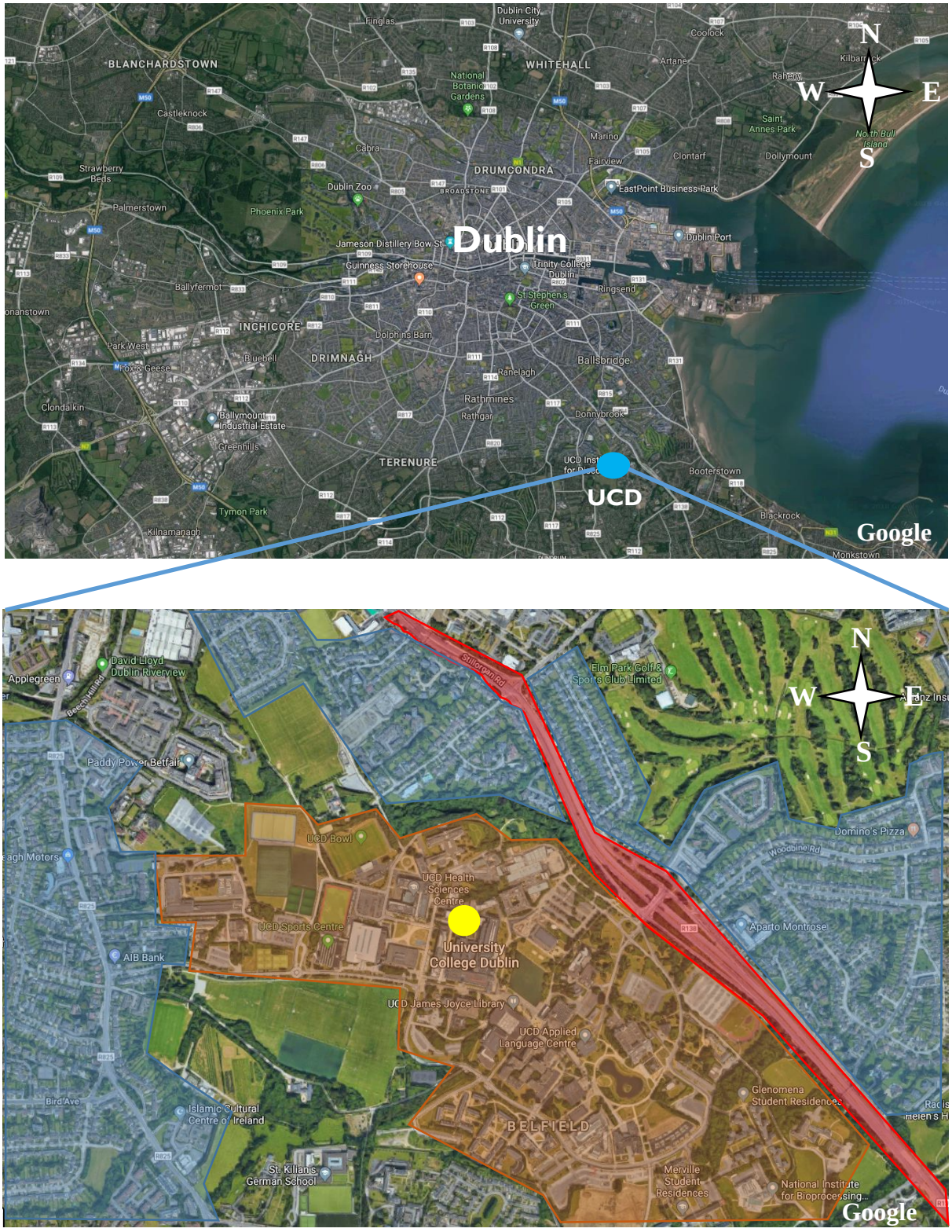

Figure 4.8. Map of Dublin with expanded view of AEROSOURCE monitoring location in UCD, with areas highlighted: Blue – residential; Red – large roadway; Orange – university campus.

4.2.2. Instrumentation and Analysis

The two instruments deployed during this monitoring campaign were the Magee Scientific seven wavelength, dual-spot Aethalometer (Model AE33) (Drinovec *et al.*, 2015), and the Aerodyne Aerosol Chemical Speciation Monitor (ACSM) (Ng *et al.*, 2011). Detailed descriptions of both instruments are provided in Chapter 2.

In brief, the AE33 measures the attenuation of light at seven different wavelengths, ranging from the near-UV to the near-IR. The attenuation of light at the 880 nm wavelength is converted to eBC concentrations using the equations detailed in (Sandradewi *et al.*, 2008b). Source apportionment of the calculated eBC is performed using the methods and parameters described in Zotter *et al.* (2017). The mass concentration is split into two categories, eBC from solid fuel sources (eBC_{SF}), and eBC from traffic sources (eBC_{Tr}). The solid fuel class is comprised of the contribution from wood, peat and coal burning. The absorption Ångström exponent (α) values employed for this study were 1.68 for solid fuel, and 0.9 for traffic (α_{SF} and α_{Tr}).

In addition to the calculated eBC and the source contributions, the AE33 instrument measures the concentration of UV absorbing particulate matter (UVPM). This is calculated from the attenuation of light at 370 nm and is used to determine the ΔC value (UVPM – eBC), which is indicative of the contribution of solid fuel burning to the ambient aerosol and can be used to validate the source apportionment model. The internal calculations performed by the instrument account for potential errors that occur in filter based measurements. One parameter that was investigated was the filter loading correction parameter (k) at the 880 nm wavelength. The filter loading effect is essentially a reduction in the sensitivity of the instrument as the amount of material deposited on the tape increases (Drinovec *et al.*, 2015). The relationship between attenuation and BC loading is linear at lower attenuation values. However, when the attenuation values are high, this relationship becomes non-linear (Gundel *et al.*, 1984). The magnitude of the filter loading effect is indicative of the particle properties and can provide information on the dominant source of particles (Weingartner *et al.*, 2003; Virkkula *et al.*, 2015). It has also been shown that the filter loading effect varies by season, depending on the aerosol properties (Virkkula *et al.*, 2007).

The flow rate for the aethalometer instrument was set at 2.0 litres per minute for the monitoring campaign. The time base for measurements was set to 60 seconds, and the collected data was processed to produce hourly average values. The tape advance was set to occur once every 24 hours, as opposed to the standard practice of advancing the tape after the maximum attenuation has been reached. This was done in order to allow for reflectometry analysis of the tape upon completion of the campaign. An automatic clean air test was also scheduled to ensure satisfactory performance of the instrument throughout the campaign. This 30 minute test was set to occur at midday every Saturday, in accordance with the manufacturer's recommendations. The data for this period was removed prior to analysis, which was conducted using the *Openair* package developed for the *R* programming language (Carslaw and Ropkins, 2012), as described in *Chapter 2*.

The ACSM was deployed in conjunction with the AE33 to measure the non-refractory fraction of PM_1 and was operational from 5 August 2016 to 15 May 2018. The ACSM and AE33 were attached to the same $PM_{2.5}$ inlet. The instrument was operated and calibrated according to the manufacturer's specifications and was maintained by colleagues from NUIG. Ambient aerosol was drawn through a cyclone with a size cut-off of 2.5 μm at a flow rate of 3 L/min. Prior to passing through the aerodynamic lens, the aerosol was dried using a Nafion dryer.

Analysis of the data from the ACSM was performed by Dr Chunshui Lin of NUIG (Lin, 2019). In brief, source apportionment was performed using positive matrix factorisation (PMF) analysis, specifically the multilinear engine (ME-2) in the Source Finder (SoFi) software package. The ME-2 model was constrained using *a priori* ACSM-derived "fingerprint" spectra gathered from combustion experiments (Lin *et al.*, 2017), and temporal profiles of hourly average concentrations for the different source categories were generated.

In addition to the analysis procedures detailed in Chapter 2, data from both instruments was used to analyse parameters relating to the physical properties and sources of BC particles in the ambient aerosol. The BC-to-OA ratio was calculated using the temporal profiles generated from the instruments and provides an indication of the source of BC particles throughout the day. A higher ratio indicates that BC rich sources, such as traffic, are dominant, while a lower ratio indicates OA rich sources, such as solid fuel burning, are dominant (Saleh *et al.*, 2015). A coating factor (CF) for the ambient BC particles was also calculated based on the method developed by

Drinovec *et al.* (2017). The CF is calculated using the sum of the masses of the available coating materials, namely sulfate, ammonium, nitrate and organic aerosol, normalised by the black carbon mass concentration using the equation

$$CF = \frac{(SO_4^{2-} + NO_3^- + NH_4^+ + ORG)}{BC}$$

and can be related to the loading correction parameter derived from the aethalometer measurements as the composition of the particles will alter the optical properties.

In addition to the aethalometer and ACSM instruments, a Partisol filter sampler (Thermo Fisher, Model 2025i) was deployed on site as part of the EMEP Intensive Monitoring Period 2017/18. This study ran from 21/12/17 to 31/03/18. The Partisol was fitted with a $PM_{2.5}$ size selective inlet, and ambient aerosol was sampled for a period of 24 hours on each filter, running from 08:00 to 07:59 the following day. Analysis of these filters was conducted by Eimear Heffernan of UCC at the National Physical Laboratory, UK. In brief, a punch was taken from each filter and placed in a laboratory-based OCEC aerosol analyser (Sunset Laboratory Inc.) and daily average OC and EC concentrations were calculated. The EC concentration was used to calculate a site-specific mass absorption cross-section (MAC) value for the UCD site.

4.3. Results and Discussion

4.3.1. eBC Mass Concentrations

The full temporal trend of calculated eBC is shown in *Figure 4.9*. The data capture for instrument from 5 August 2016 to 20 August 2018 was 95.8%. The missing periods in the dataset were due to the instrument running out of tape, or stoppages for routine maintenance. The highest concentrations of eBC were recorded during the winter months, December, January and February. Lowest concentrations were measured during the summer months, June, July and August. A full breakdown of the monthly and seasonal variations in eBC over the two year period is provided in section 4.3.3.

The average diurnal profiles or each day of the week (*Figure 4.10*) show increased concentrations of eBC in the morning and evening hours. The morning peak, from approximately 06:00 to 11:00, is exclusively related to rush hour traffic emissions, and reaches a maximum around 09:00. The evening peak, from 16:00 to 23:00, peaking at approximately 20:00, is initially related to rush hour traffic but reaches a maximum when a solid fuel burning contribution is present. This is particularly evident during the colder months.

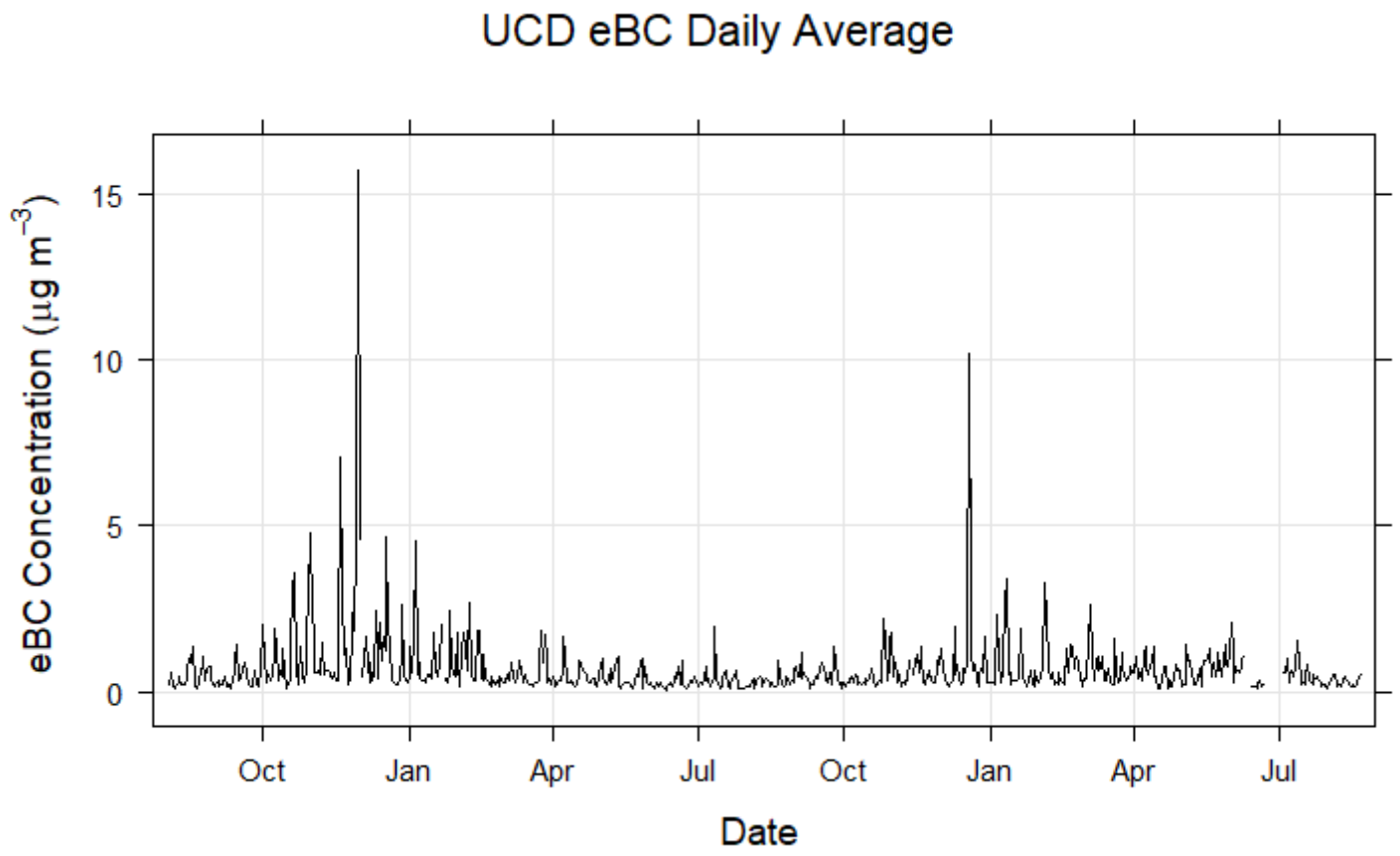

Figure 4.9. Temporal profile of daily averaged eBC concentrations (µg/m^3) at the UCD monitoring site, 5 August 2016 – 20 August 2018.

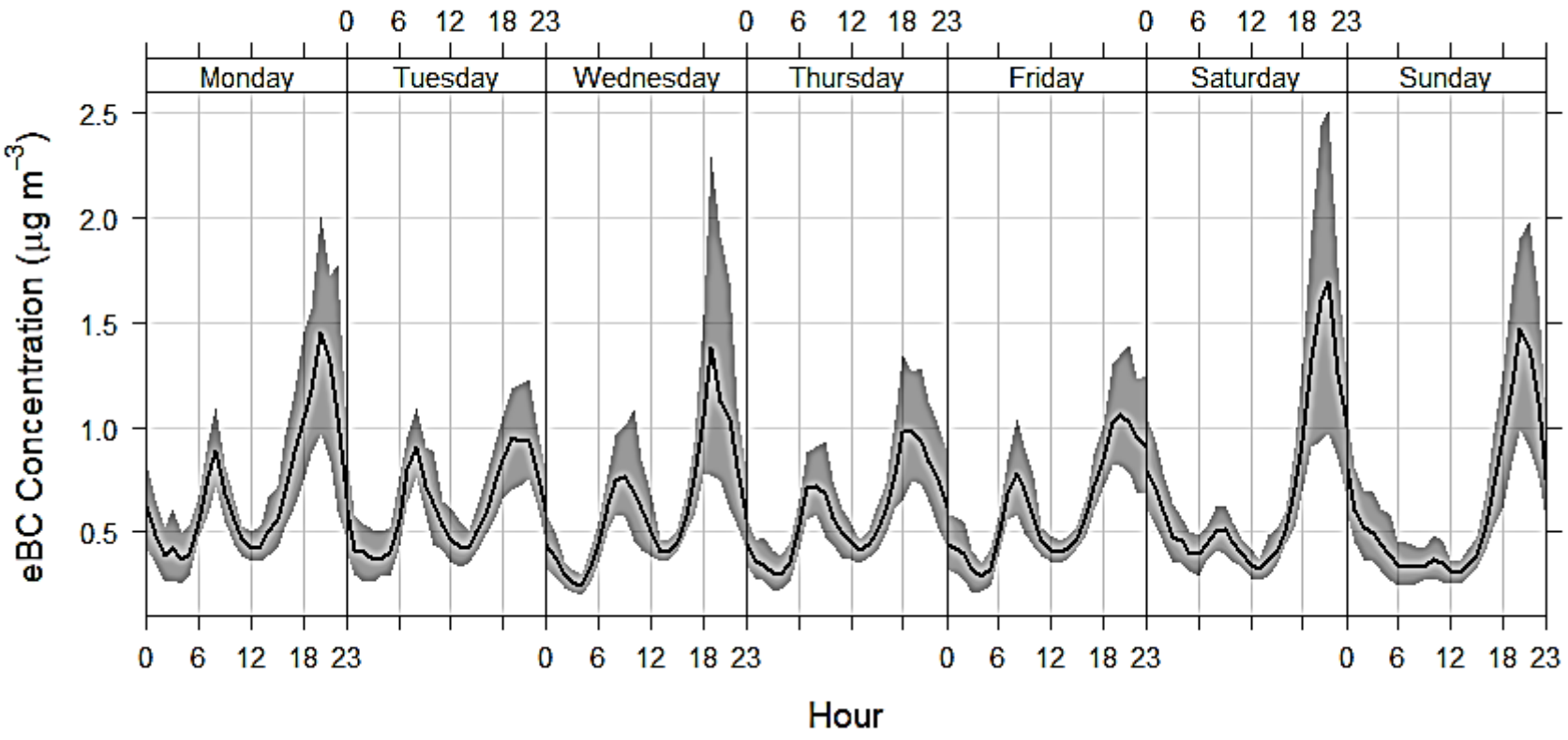

Figure 4.10. Average diurnal profile of eBC concentrations (µg/m^3) for each week day, 5 August 2016 – 20 August 2018, the shaded regions represent the 95% confidence intervals in the calculated mean values.

4.3.2. Meteorological Parameters

The main meteorological parameters investigated during this study were rainfall (mm), temperature (ºC), wind speed (m/s), and wind direction. The full two year profiles for rainfall, temperature and wind speed are presented in *Figure 4.11*. A clear seasonal pattern is observed for the temperature measurements, with higher averages during summer and lower averages during winter. A summary of the seasonal average values is shown in *Table 4.2*. The seasons were divided according to the meteorological calendar; summer is defined as June to August, autumn is September to November, winter is December to February, and spring is March to May.

Table 4.2. Summary of meteorological parameters 5 August 2016 – 20 August 2018; total hourly rainfall, average hourly temperature, average hourly wind speed, seasonally averaged wind direction.

Month(s)	**Rainfall (mm)**	**Temperature (ºC)**		**Wind speed (m/s)**	
	Max	Mean	Range	Mean	Range
Aug 2016	4.6	15.5	7.2–23.5	4.8	0.5–12.9
Sept–Nov 2016	7.0	10.3	-3.4–24.9	4.5	0.0–13.9
Dec 2016–Feb 2017	4.7	6.7	-4.6–14.5	5.4	0.5–20.1
Mar–May 2017	13.5	9.8	-1.9–24.2	4.7	0.5–13.4
Jun–Aug 2017	12.2	14.7	5.6–26.6	4.7	0.0–12.9
Sept–Nov 2017	0.5	10.4	-1.7–19.8	5.4	0.5–20.6
Dec 2017–Feb 2018	5.7	4.8	-6.2–13.1	6.1	0.5–18.0
Mar–May 2018	3.3	8.4	-4.9–21.6	4.8	0.0–16.5
Jun–Aug 2018	7.8	16.3	6.4–26.9	4.1	0.0–10.8

The predominant wind direction observed during each season was southerly to south westerly. It should be noted that both spring seasons were heavily influenced by easterly air masses, shown in *Figure 4.13*. This is also reflected by the frequency distribution of wind directions for each season (*Appendix III*).

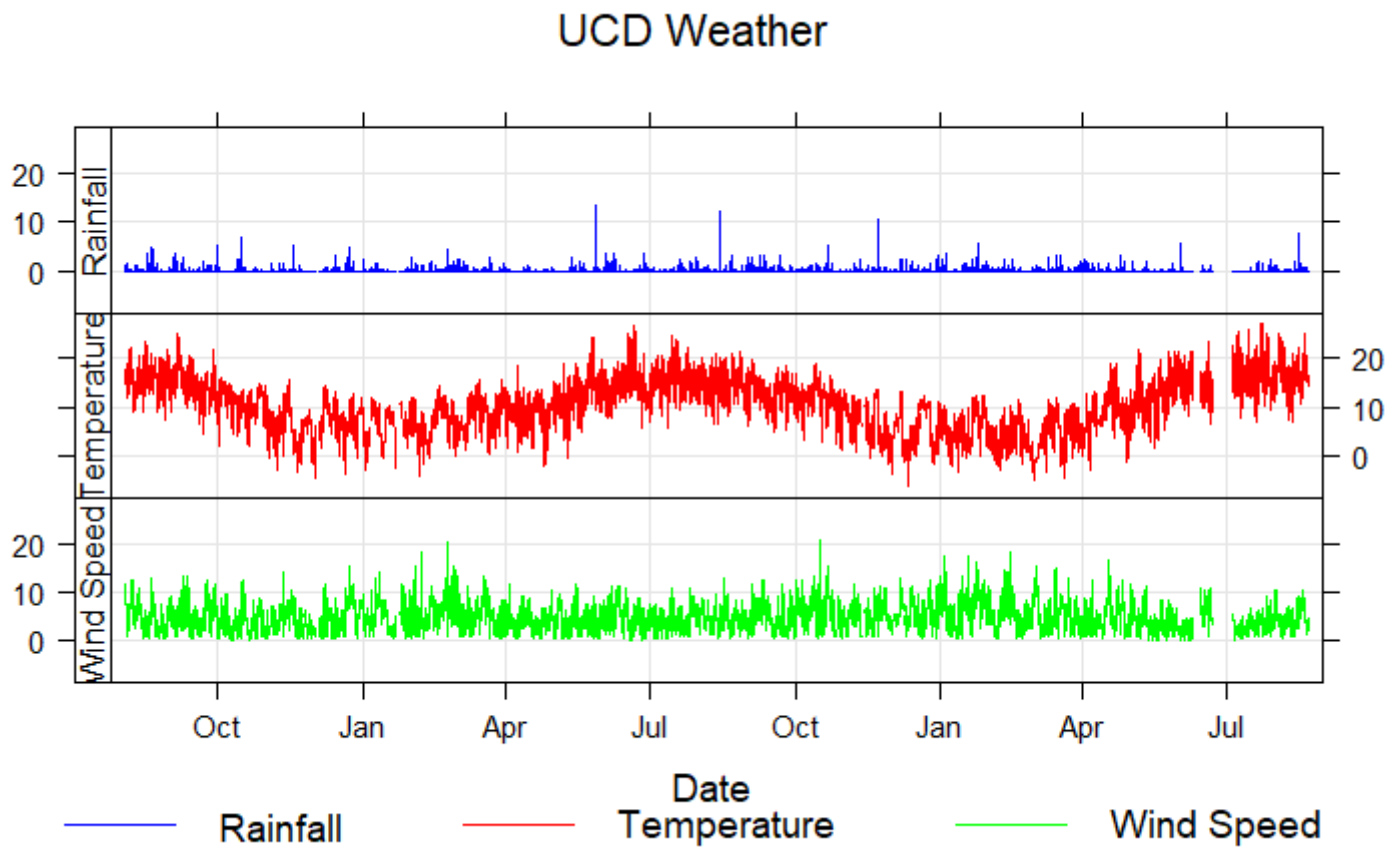

Figure 4.11. Rainfall (mm), temperature (ºC), and wind speed (m/s) from Casement Aerodrome, Dublin.

Over the course of the two year monitoring campaign, the monitoring site was influenced by a number of different air masses and weather conditions. This can be visualised by investigating the relationship between eBC mass concentration and wind direction (*Figure 4.12*).

The highest concentrations, highlighted in red below, were measured in the colder periods of the year, November 2016 and December 2017. These concentrations were observed during periods of south westerly winds, albeit at lower wind speeds (shown in *Figure 4.13*). High concentrations were also measured during periods when the predominant wind direction was easterly. This could potentially be due to high levels of pollution originating from residential areas on the east coast. This was especially evident during late February and early March 2018.

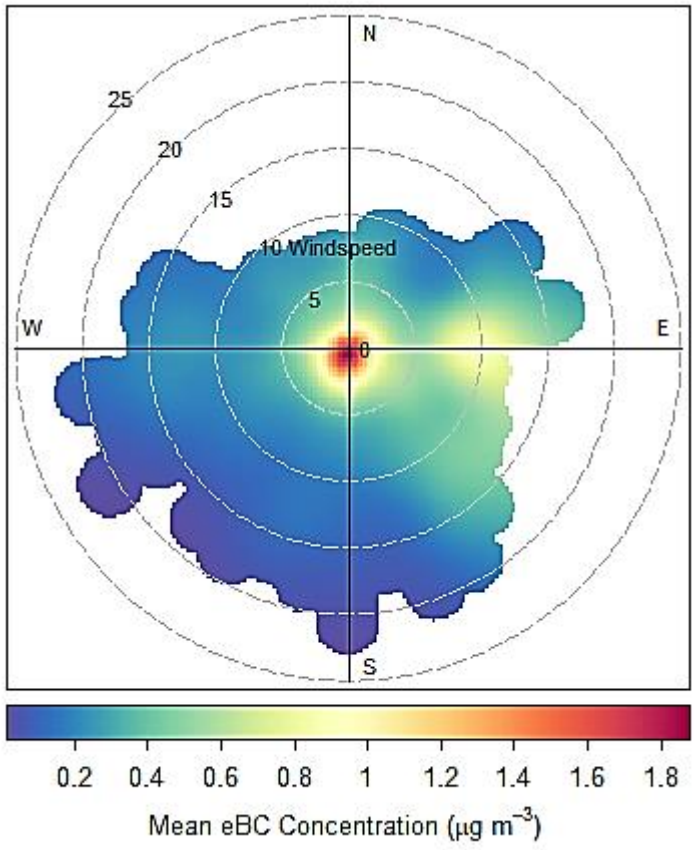

Figure 4.12. eBC mass concentration as a function of wind speed and direction at the UCD monitoring site, 5 August 2016 to 20 August 2018.

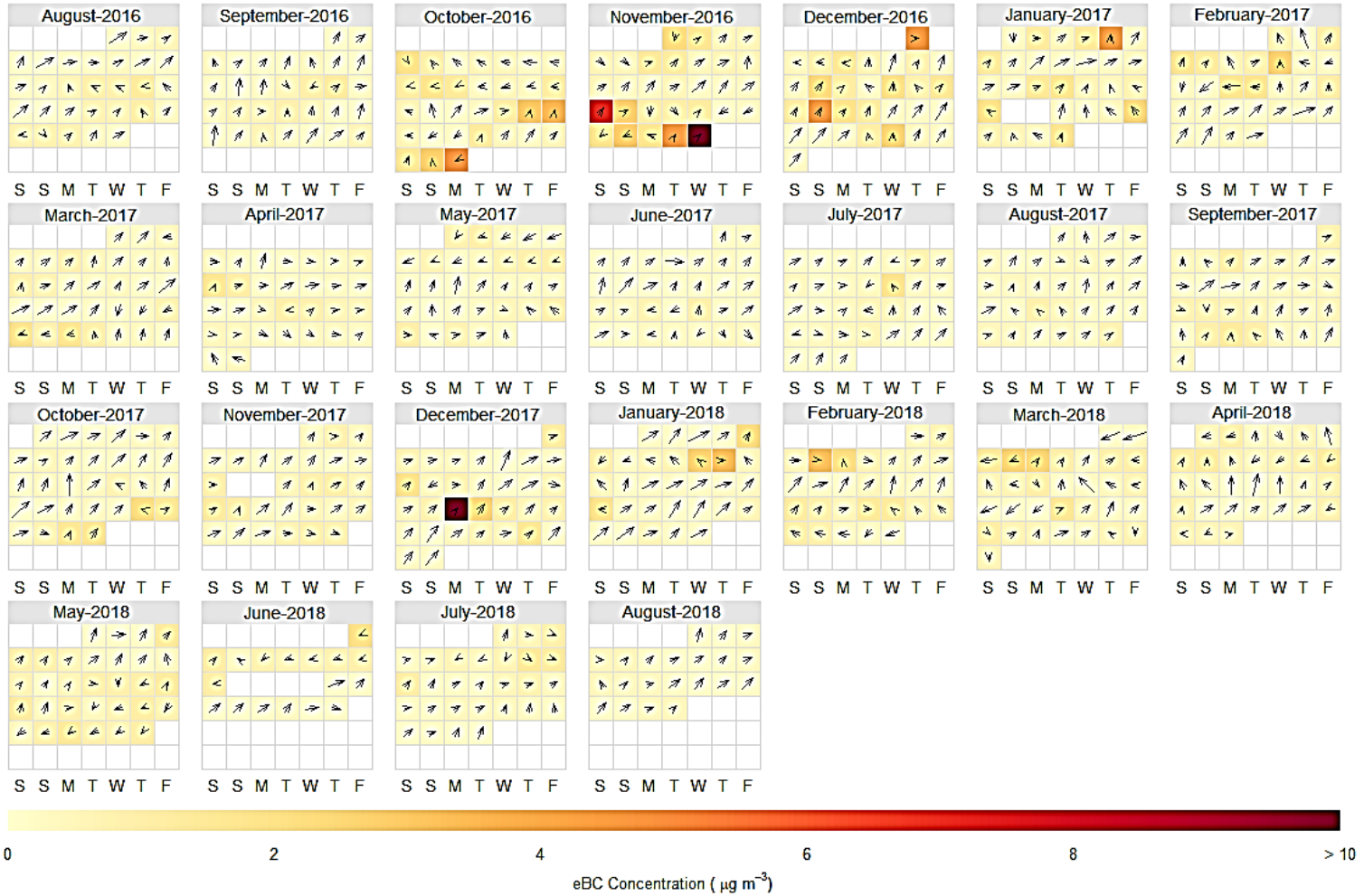

Figure 4.13. eBC mass concentration (µg/m^3) as a function of wind direction and speed for the full AEROSOURCE monitoring period, 5 August 2016 to 20 August 2018. The wind direction is denoted by the direction of the arrows contained in the squares, the magnitude of the average wind speed is related to the length of the arrow, and the daily average eBC concentration is related to the colour of the box as shown in the scale.

4.3.3. Seasonality of BC Concentrations

The diurnal pattern of eBC mass concentrations was highly dependent on season, *Figure 4.17*. The summer diurnal profile shows a large peak in the morning corresponding to rush hour traffic. The magnitude of this morning peak is approximately the same during all seasons, ranging from approximately 0.5 to 0.8 $\mu g/m^3$. The winter diurnal profile also shows a peak in the morning hours. In addition to this, there is a significant peak in the evening time, corresponding to solid fuel burning hours. This evening peak is much larger than the observed peak in the morning, indicating that traffic is not the only source.

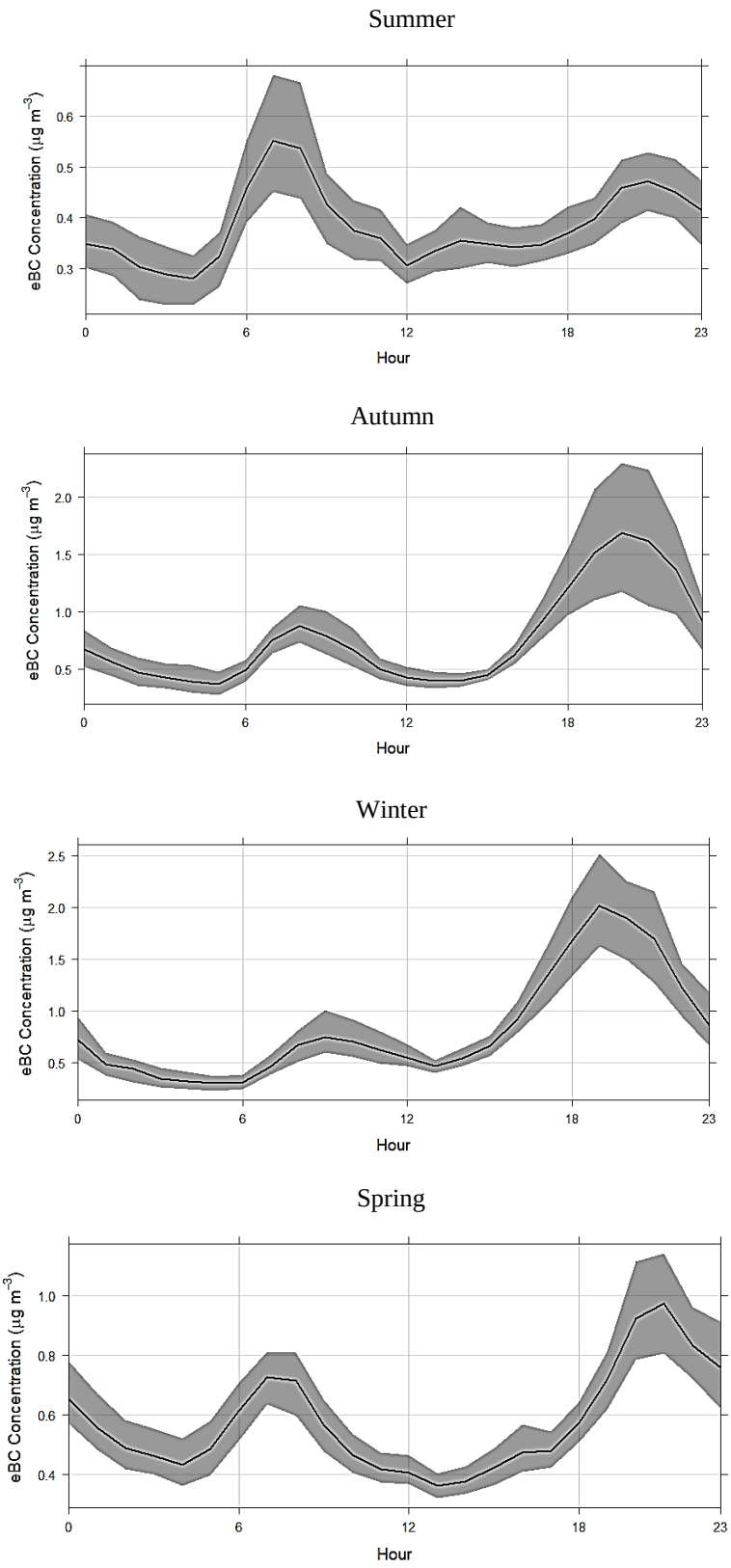

Figure 4.14. Diurnal variations of eBC concentration for summer (June, July and August), autumn (September, October and November), winter (December, January and February), and spring (March, April and May), the shaded regions represent the 95% confidence intervals in the calculated mean values.

The relationship between eBC and wind direction potentially highlights the sources of pollution during the different seasons. Visualising the eBC mass concentration as a function of wind speed and direction, it is clear that the highest concentrations were measured during periods of lower wind speed, *Figure 4.15 (a), (b) and (c).*

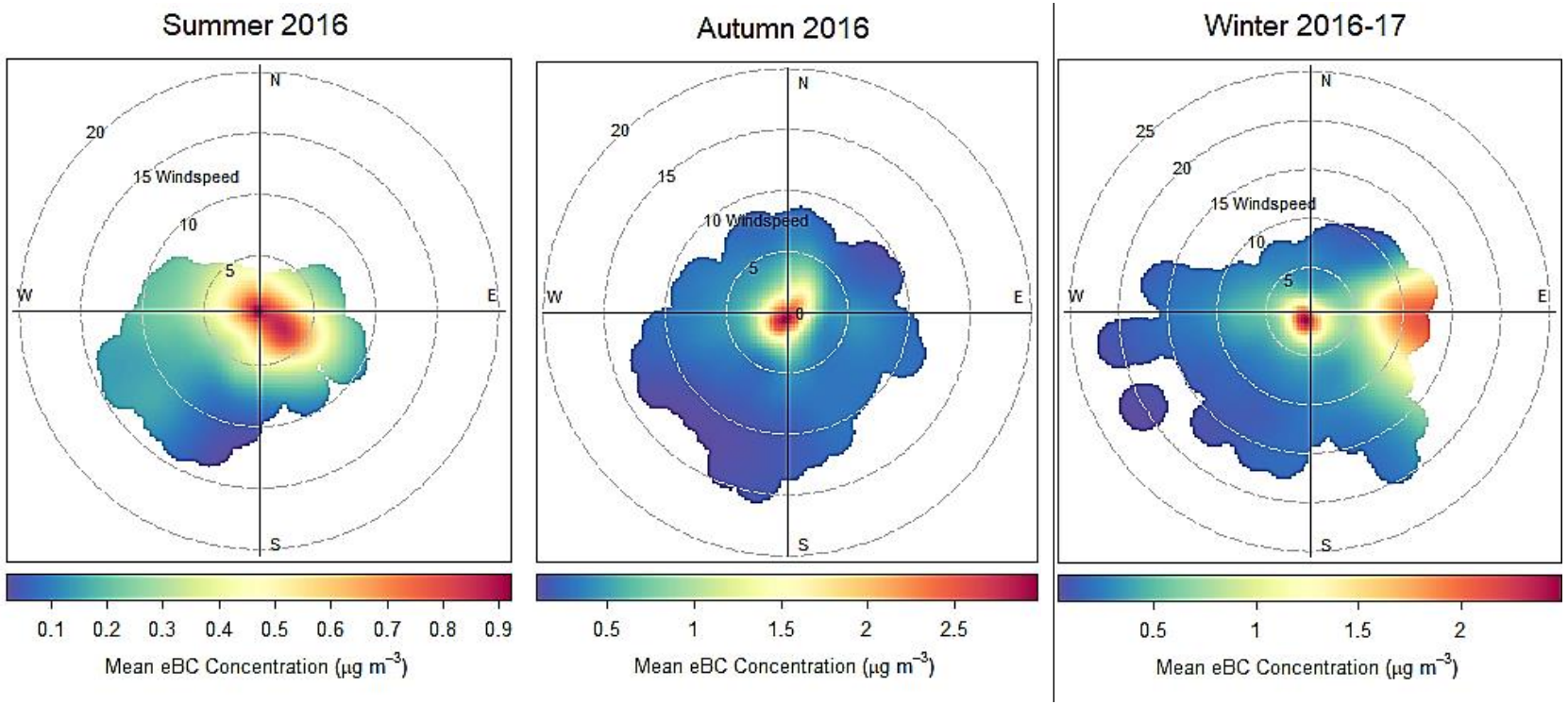

Figure 4.15 (a). eBC mass concentration as a function of wind direction and speed during Summer 2016, Autumn 2016, and Winter 2016-17.

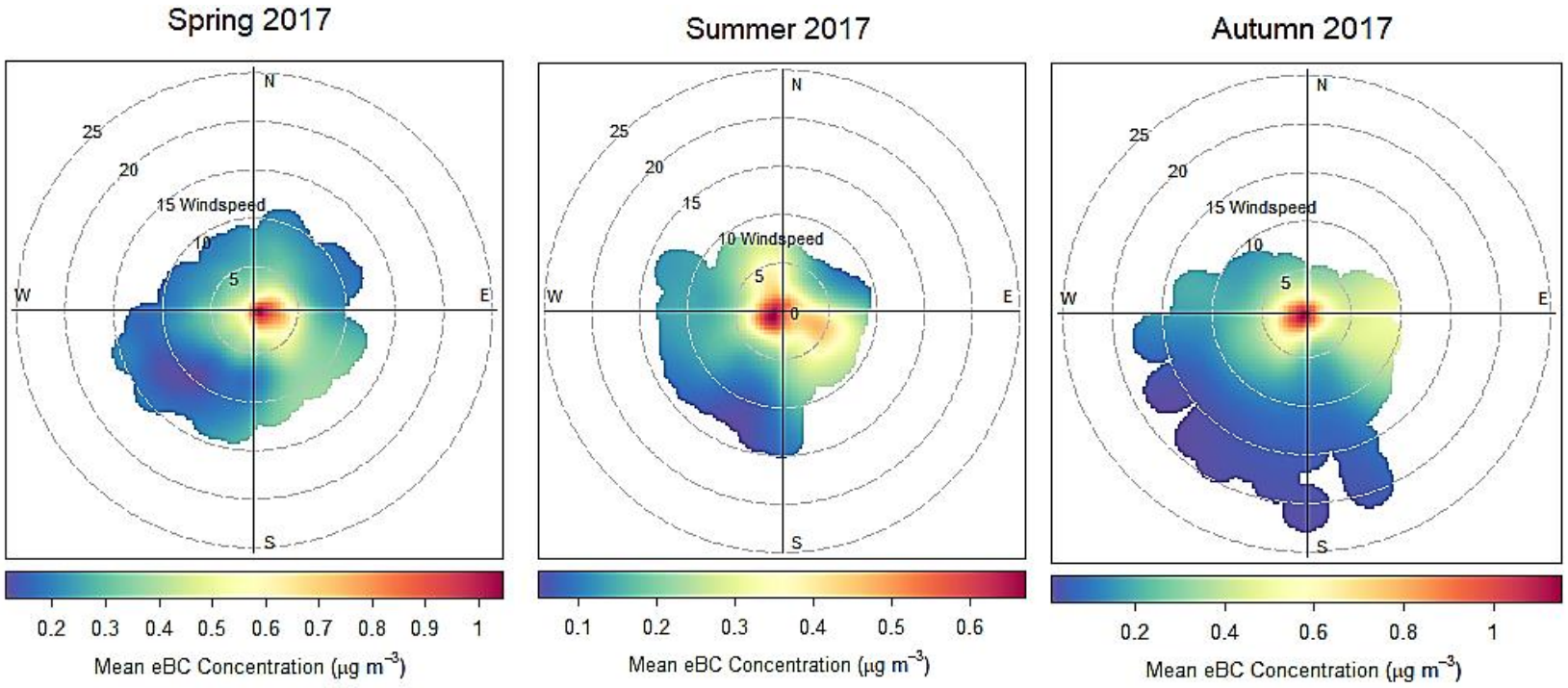

Figure 4.15 (b). eBC mass concentration as a function of wind direction and speed during Spring 2017, Summer 2017, and Autumn 2017.

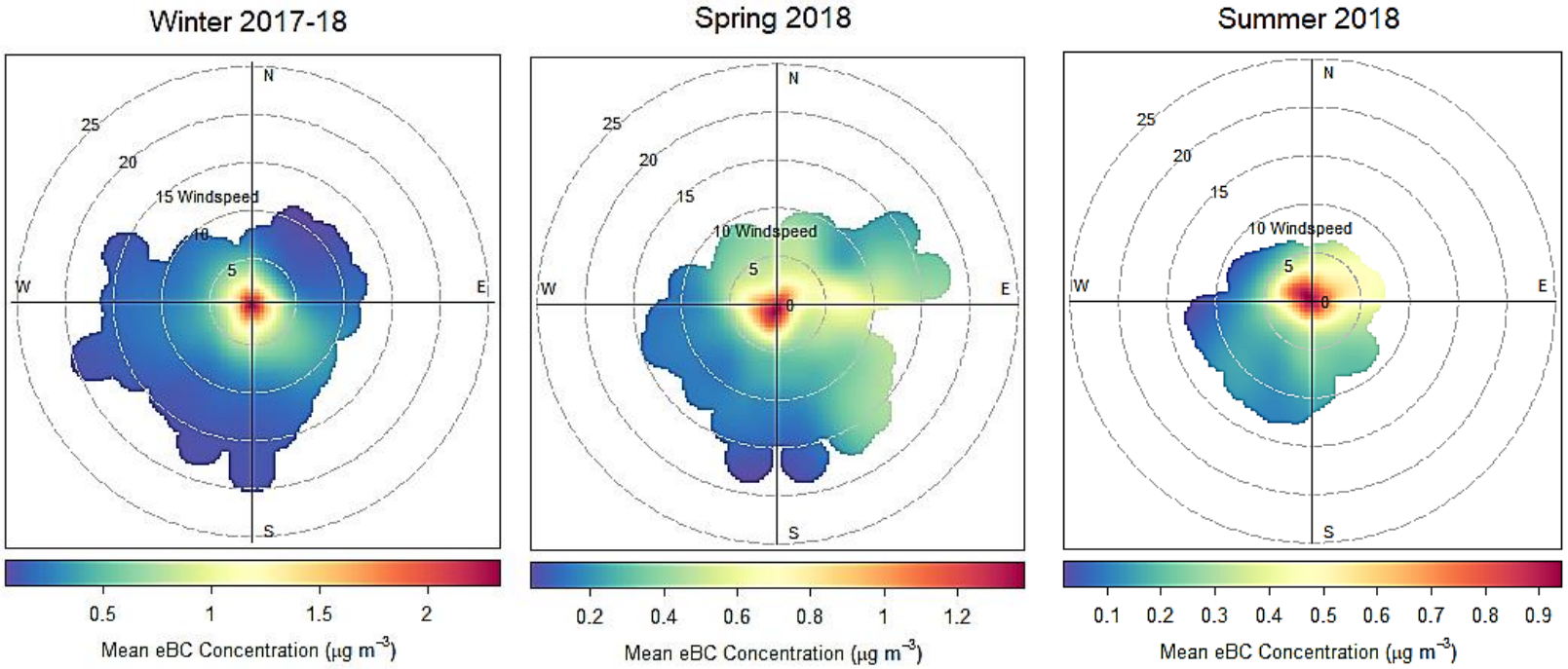

Figure 4.15 (c). eBC mass concentration as a function of wind direction and speed during Winter 2017-18, Spring 2018, and Summer 2018.

4.3.4. Source Apportionment of eBC

Source apportionment of the measured eBC mass concentration was performed using the model described by Zotter *et al.* (2017), which uses α values of 1.68 for solid fuel burning (α_{SF}), and 0.9 for traffic (α_{Tr}). The average diurnal profile for each day of the week is shown in *Figure 4.16*. A sizeable peak in traffic related eBC (eBC_{Tr}) is observed every morning during the weekdays. As expected from traffic patterns, this morning peak is smaller on Saturday and is not present on Sunday. There is also an evening peak in eBC_{Tr} on every day. As expected, solid fuel burning related eBC (eBC_{SF}) peaks strongly during evening hours and is noticeably higher during the weekend. The extended eBC_{SF} range in the Wednesday diurnal profile is related to a significant pollution event that was recorded by the aethalometer on November 30 2016, marked in *Figure 4.13*. This pollution event is also detectable in the ACSM factor profiles, *Figure 4.29*.

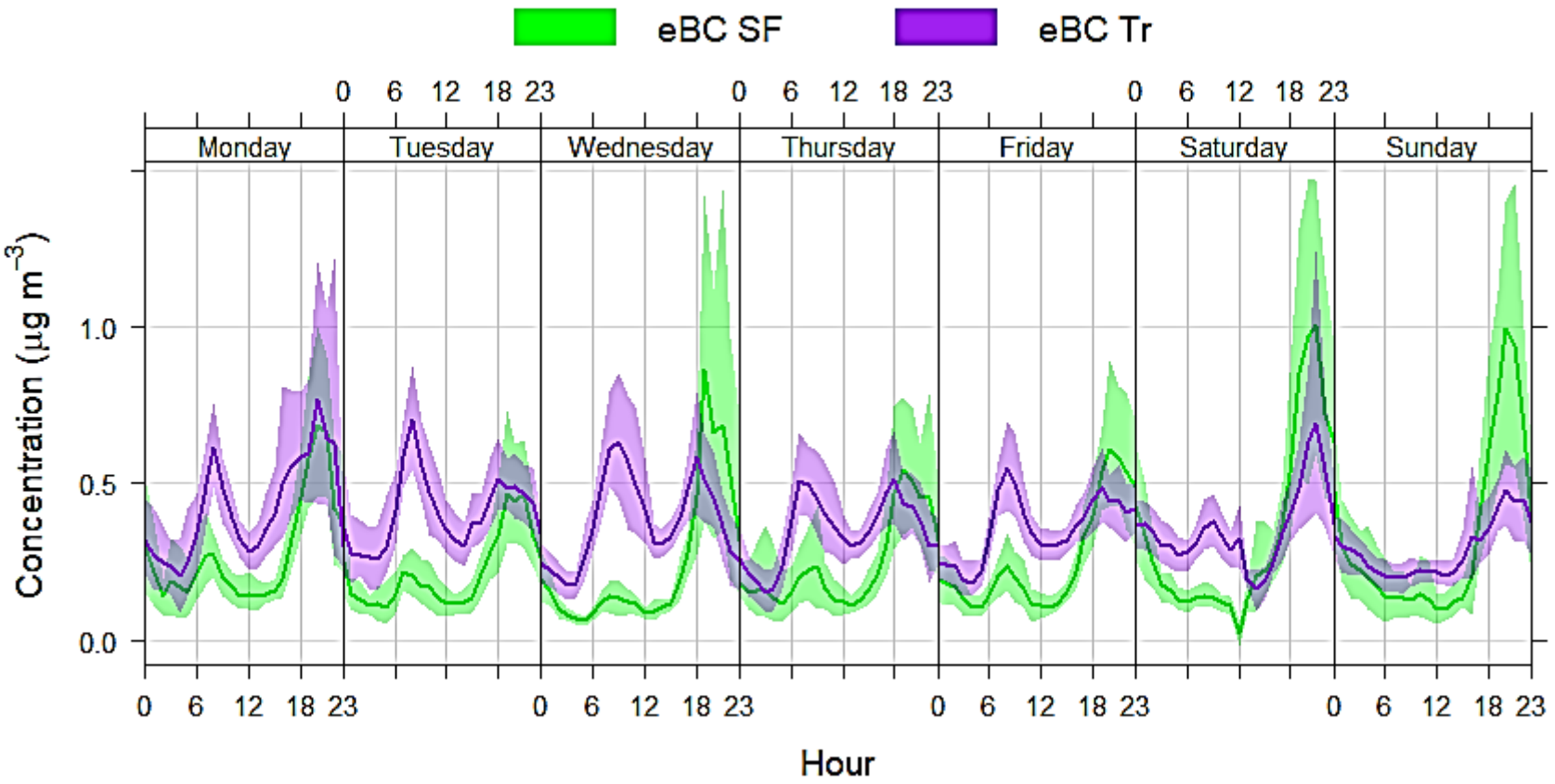

Figure 4.16. Average diurnal profile of eBC_{SF} (green) and eBC_{Tr} (purple) concentrations (μg/m^3) for each week day for the AEROSOURCE campaign, 5 August 2016 to 20 August 2018. The shaded region represents the 95% confidence intervals in the calculated mean values.

There is a distinct seasonal difference in the patterns of eBC, eBC_{Tr} and eBC_{SF}. The highest average eBC concentrations were measured during the colder months, and the lowest concentrations were measured during the warmer months, shown in *Table 4.3*. This is due to significantly higher eBC_{SF} values in the colder months, shown in *Figure 4.17*. There were also higher contributions from traffic sources in October, November, and December, which led to increased eBC concentrations. This increase in eBC_{Tr} could be the result of lower boundary layer heights during these colder months and therefore less dispersion of pollution.

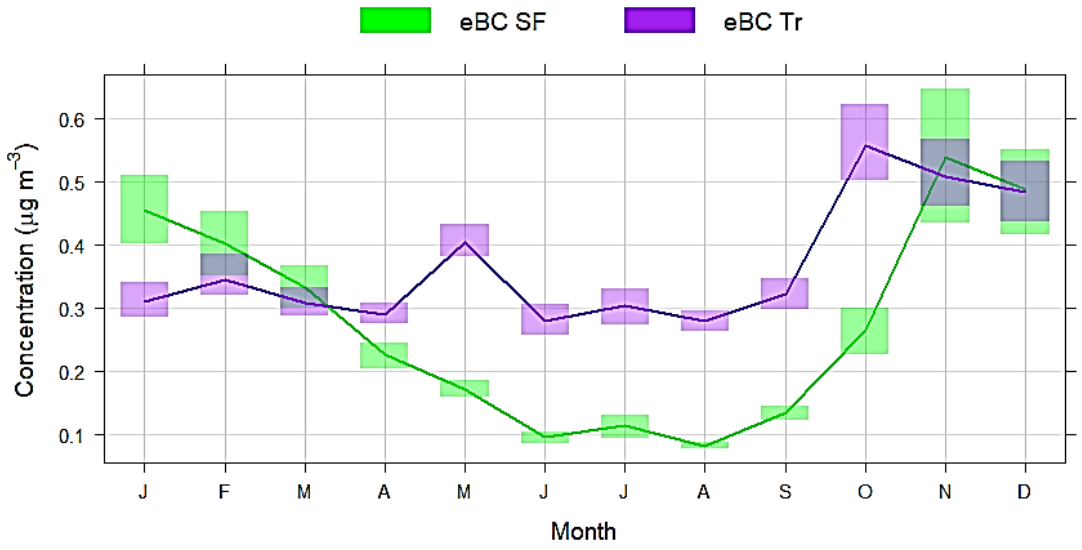

Figure 4.17. Average monthly eBC_{SF} (green) and eBC_{Tr} (purple) concentrations for the AEROSOURCE measurement campaign, 5 August 2016 to 20 August 2018. The shaded regions represent the 95% confidence intervals in the calculated mean values.

The average monthly eBC_{SF} and eBC_{Tr} concentrations, *Table 4.3*, reflect the seasonal variations shown in *Figure 4.17*. The colder months had larger contributions from solid fuel; the highest eBC_{SF} contribution, 63%, occurred in January 2017. The higher solid fuel contribution during the colder months of November 2016 to January 2017 accounts for the higher eBC levels observed in the temporal profile (*Figure 4.9*). The percentage contribution of solid fuel is lower in the corresponding months of 2017 and 2018, accounting for the lower total eBC concentrations during this period. The lowest solid fuel contributions occurred in the warmer months, the lowest eBC_{Tr} contribution, 15%, occurred in July 2017.

Table 4.3. Summary of monthly eBC concentrations (± the standard deviation) and the contributions from solid fuel burning and traffic to eBC concentration, calculated using the source apportionment model parameters derived by Zotter *et al.* (2017) (α_{SF} = 1.68, α_{Tr} = 0.9).

Month	**eBC (μg/m^3) (± SD)**	**% eBC$_{SF}$**	**% eBC$_{Tr}$**
Aug 2016	0.48 (± 0.49)	19	81
Sept 2016	0.40 (± 0.50)	21	79
Oct 2016	1.13 (± 1.98)	37	63
Nov 2016	1.52 (± 3.52)	59	41
Dec 2016	1.16 (± 2.22)	62	38
Jan 2017	0.87 (± 1.36)	63	37
Feb 2017	0.72 (± 1.24)	47	53
Mar 2017	0.51 (± 0.69)	55	45
Apr 2017	0.46 (± 0.52)	46	54
May 2017	0.45 (± 0.42)	29	71
Jun 2017	0.27(± 0.27)	21	79
Jul 2017	0.35 (± 0.47)	15	85
Aug 2017	0.31 (± 0.29)	25	75
Sept 2017	0.52 (± 0.64)	36	64
Oct 2017	0.51 (± 0.82)	21	79
Nov 2017	0.57 (± 0.67)	32	68
Dec 2017	0.79 (± 1.57)	34	66
Jan 2018	0.67 (± 1.45)	56	44
Feb 2018	0.77 (± 1.43)	60	40
Mar 2018	0.77 (± 1.11)	50	50
Apr 2018	0.58 (± 0.64)	42	58
May 2018	0.71 (± 0.79)	30	70
Jun 2018	0.58 (± 0.65)	30	70
Jul 2018	0.50 (± 0.57)	37	63
Aug 2018	0.29 (± 0.24)	28	72

The solid fuel contributions to eBC mass in Dublin during the winter months, 57% in 2016/17 and 49% in 2017/18, were higher than the contributions from wood/biomass burning observed in other locations. In Paris, Petit *et al.* (2015) calculated that biomass burning contributed 15% of eBC mass. In London, Fuller *et al*. (2014) reported that biomass burning contributed 23% of eBC mass during the winter months, while Crilley *et al*. (2015) found that wood burning contributed approximately 30% of eBC mass. In British Columbia, Canada, comparable biomass burning contributions (63%) were measured during periods dominated by emissions from wildfires (Healy *et al.*, 2019), while contributions in residential areas of Ontario reached a maximum of 26% during the winter months (Healy *et al*., 2017). In Athens, Greece, Kalogridis *et al.* (2018) found that wood burning contributed approximately 30% of eBC mass during the winter months.

The diurnal profiles for the four seasons are shown in *Figure 4.18* and reflect the difference in contributions from the different sources. The summer diurnal profile showed a large peak in eBC_{Tr} between approximately 06:00 and 09:00, related to the morning rush hour traffic. A small increase is also observed in the evening hours, from 17:00 onwards, likely related to a more spread out traffic period in the summer. In the autumn diurnal profile, there are similar morning and evening peaks due to rush hour traffic, but a peak in eBC_{SF} is also observed during evening hours, with the maximum concentration appearing at roughly 21:00. In the winter diurnal profile the eBC_{Tr} peaks are similar to those observed in the autumn profile, while the evening peak in eBC_{SF} was the largest among all seasons. The amount of eBC_{SF} peaks at 20:00 in the winter and is approximately double the eBC_{Tr} in the evening hours and extends from roughly 16:00 to 23:00. During the spring months, the diurnal profile is similar to that observed in autumn. The peak concentration of eBC_{Tr} in the morning hours is very similar for all seasons, indicating fairly constant levels of morning traffic all year round

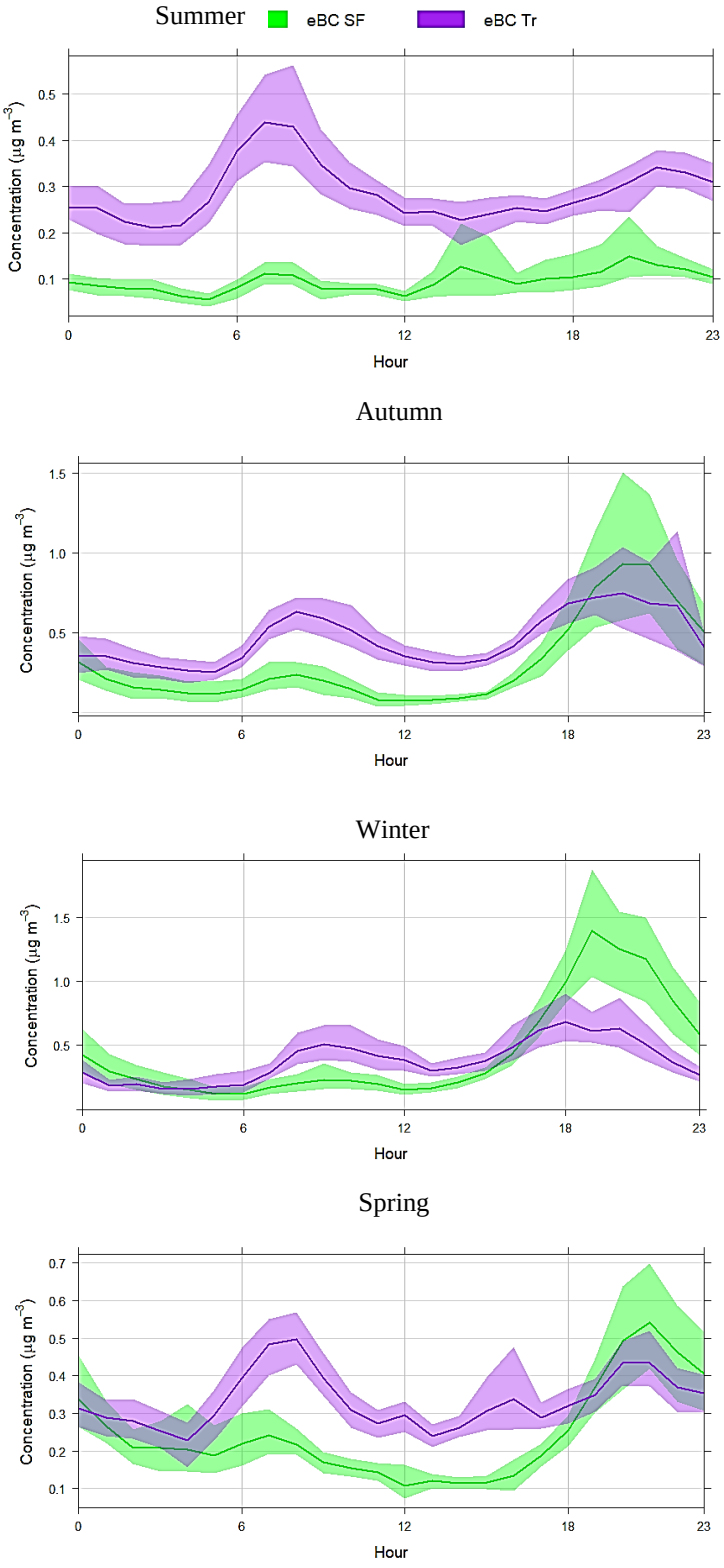

Figure 4.18. Diurnal variations of eBC_{SF} (green) and eBC_{Tr} (purple) concentrations for summer (June, July and August), autumn (September, October and November), winter (December, January and February), and spring (March, April and May). The shaded regions represent the 95% confidence intervals in the calculated mean values.

The eBC_{SF} and eBC_{Tr} concentrations during the four seasons varied depending on wind direction (*Figure 4.19*). The highest concentrations measured during each period occurred when the wind speed was lower than 5 m/s. During the summer months, the highest eBC_{SF} concentrations originated form the south-east, the direction of the college campus and residential areas, while the highest eBC_{Tr} concentrations originated from the north-west, the direction of the city centre. In the autumn, the highest eBC_{SF} concentrations originated from the south-east, while the highest eBC_{Tr} concentrations originated from the north-east, the direction of a large junction on the N11 roadway. The highest eBC_{SF} concentrations during the winter months originated from the south-west, originating from large residential areas. The highest eBC_{Tr} concentrations originated from the north-west. High eBC_{SF} and eBC_{Tr} concentrations also originated from the easterly direction when wind speeds of between 10 – 15 m/s were recorded, potentially originating from European sources. In the spring, the highest eBC_{SF} concentrations were measured during south-westerly wind periods. The highest eBC_{Tr} concentrations originated from the north-east.

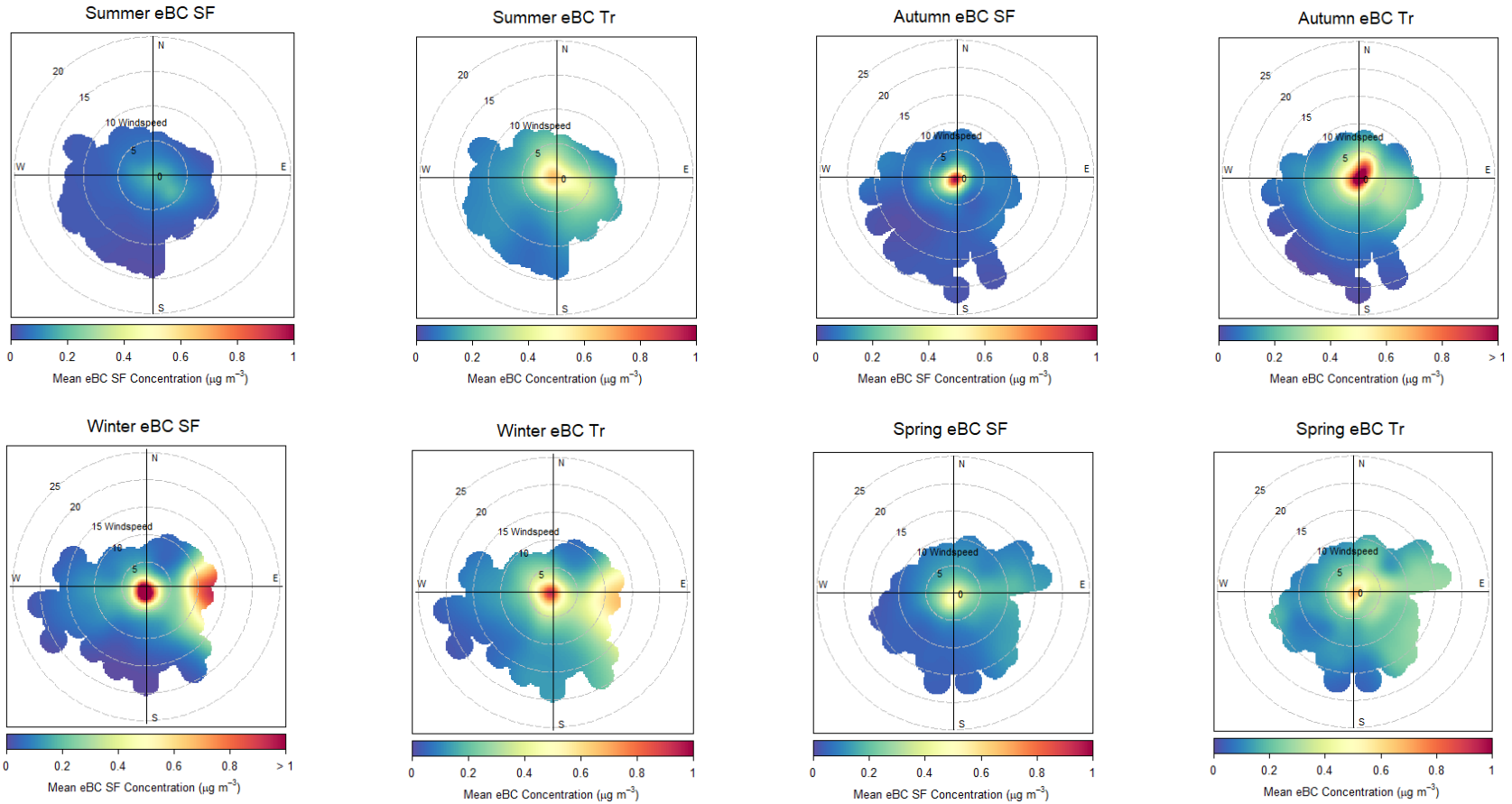

Figure 4.19. eBC_{SF} and eBC_{Tr} mass concentrations as a function of wind direction and wind speed during summer (June, July and August), autumn (September, October and November), winter (December, January and February), and spring (March, April and May).

4.3.5. Additional AE33 Parameters

The source apportionment performed using the Zotter parameters can be validated by analysing the ΔC values for each season. The ΔC value is indicative of the proportion of solid fuel burning related BC particles present in the ambient sample. The diurnal profile of ΔC for the full monitoring campaign, *Figure 4.20*, shows a large peak in the evening hours.

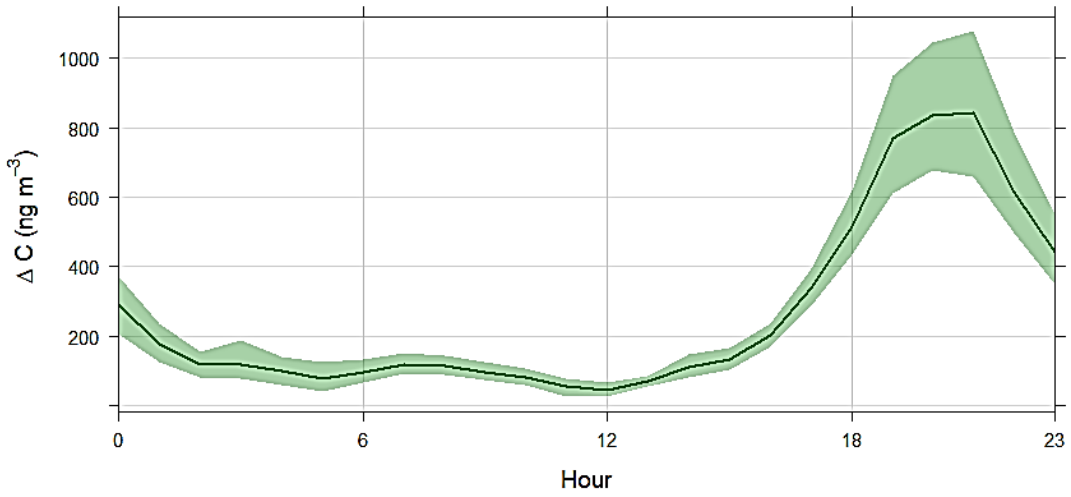

Figure 4.20. Diurnal profile of ΔC (ng/m^3) for the whole AEROSOURCE measurement campaign, 5 August 2016 to 20 August 2018. The shaded region represents the 95% confidence intervals in the calculated mean values.

This profile indicates that the eBC mass concentration measured in the evening is related to solid fuel burning, with larger evening peaks observed at the weekend, *Figure 4.21*, indicating that solid fuel burning is more prevalent on Saturdays and Sundays. Elevated levels of solid fuel burning related pollution at weekends have previously been observed in other cities, for example in London (Fuller *et al.* 2014) and Helsinki (Helin *et al.*, 2018), and are attributed to the so-called "recreational burning" phenomenon.

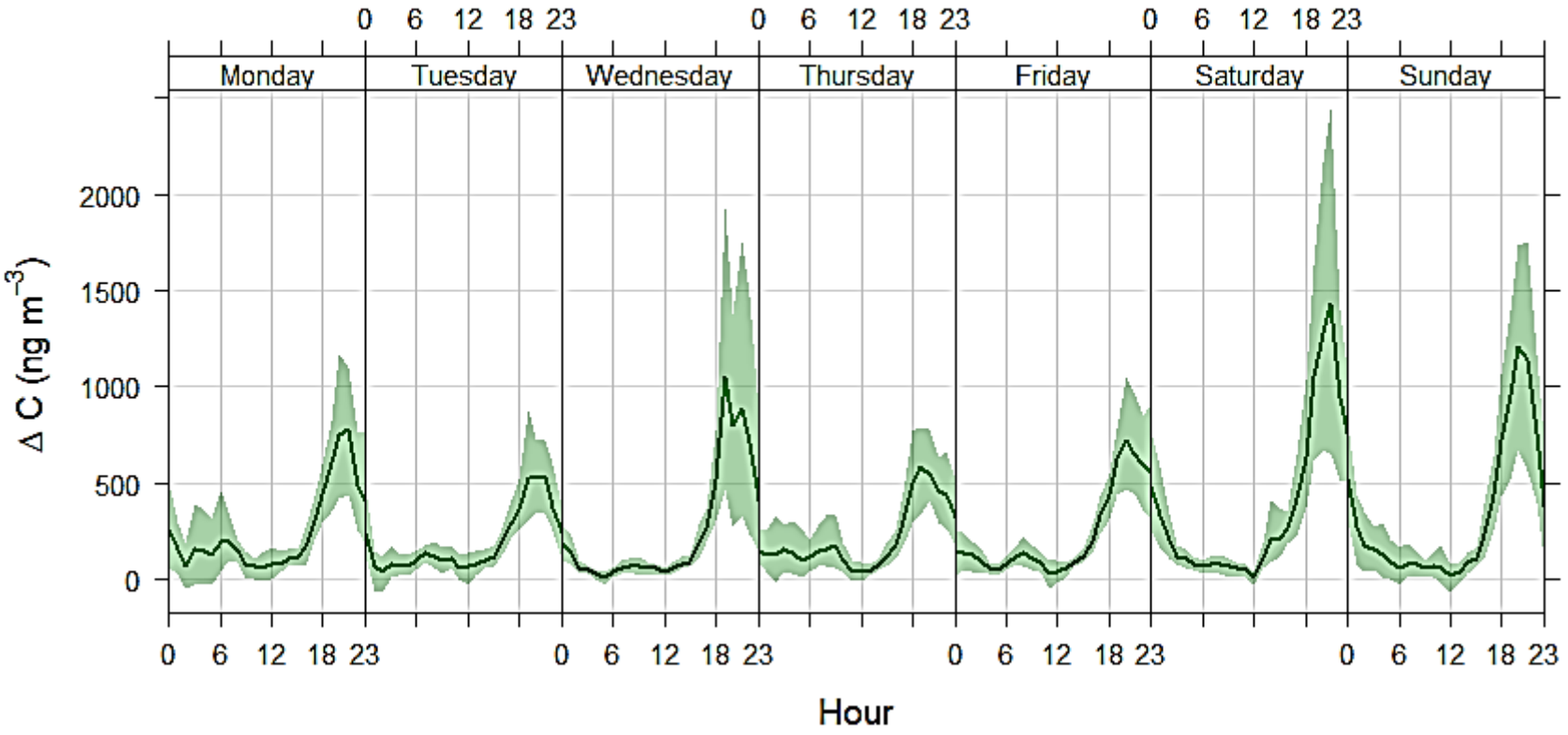

Figure 4.21. Average diurnal profiles of ΔC (ng/m^3) for each weekday during the AEROSOURCE measurement campaign, 5 August 2016 to 20 August 2018. The shaded region represents the 95% confidence intervals in the calculated mean values.

The average ΔC value measured was higher in the winter months than during the rest of the year (*Figure 4.22*). This is another strong indicator of the large contribution of solid fuel burning during these months. The diurnal and monthly average patterns of ΔC are similar to the patterns observed in London by Harrison *et al.* (2012).

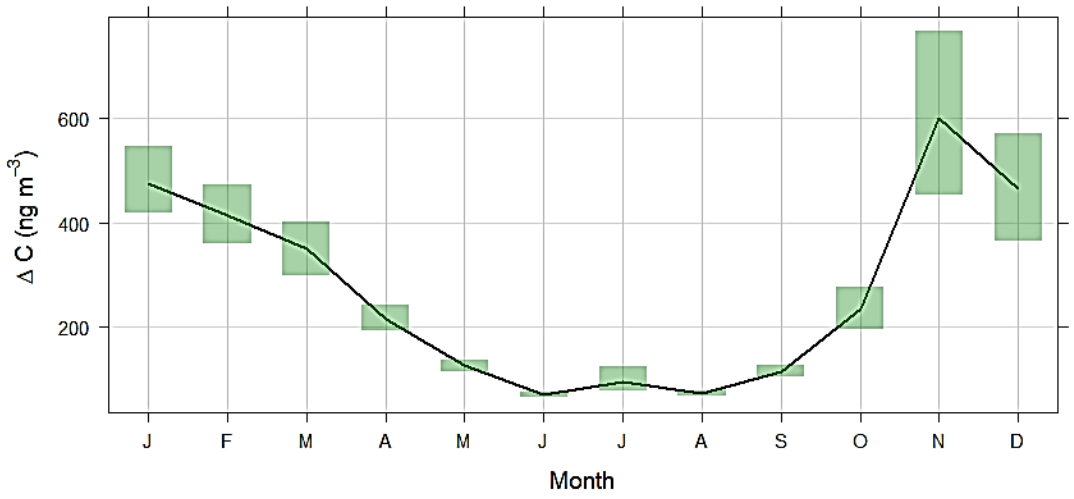

Figure 4.22. Average monthly ΔC values (ng/m^3) for the AEROSOURCE measurement campaign, 5 August 2016 to 20 August 2018. The shaded region represents the 95% confidence intervals in the calculated mean values.

Hourly averaged α values were calculated using six wavelengths. The 370 nm wavelength was omitted because of potential interferences from VOCs and non-BC absorbing species deposited on the filter (Section 2.2.2). The diurnal profiles of α during the different seasons provide an additional indication of the dominant source of eBC (*Figure 4.23*). A value closer to 0.9 indicates that traffic is the dominant source, while a value close to 1.68 indicates that solid fuel burning is the dominant source. During the summer months, the average value remained steady between approximately 1.1 and 1.2. The autumn profile shows a small increase in the evening hours, up to approximately 1.25, which corresponds to the peak observed in the eBC_{SF} mass concentration during this period. The winter diurnal profile shows an increase in α up to 1.4 at 19:00, again reflecting the higher proportion of eBC_{SF} in winter months. Finally, during the spring, the α pattern was similar to that measured during the autumn. The evening peak was slightly higher than that measured during the autumn, with a maximum value of approximately 1.3.

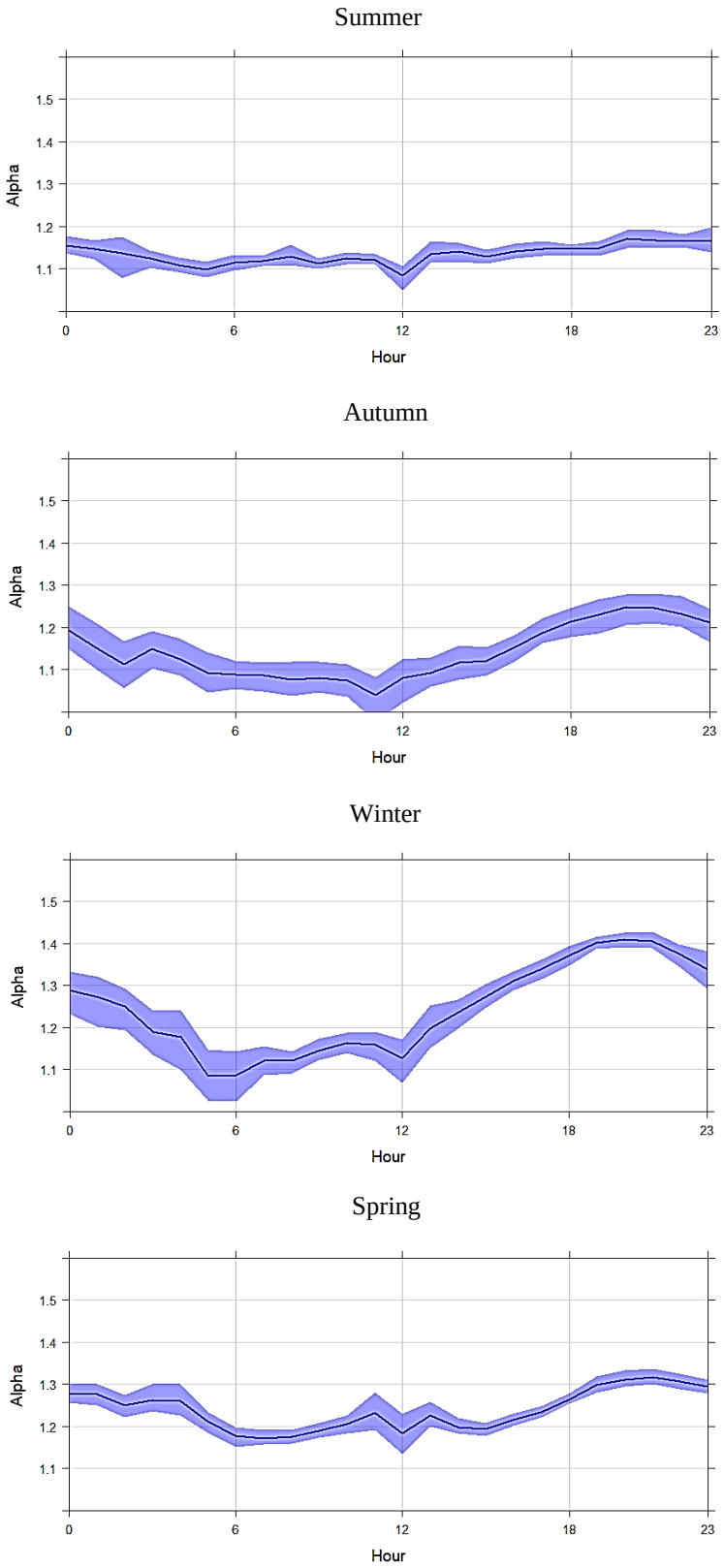

Figure 4.23. Diurnal variations of calculated α during summer (June, July and August), autumn (September, October and November), winter (December, January and February), and spring (March, April and May). The shaded regions represent the 95% confidence intervals in the calculated mean values.

The distribution of calculated α as a function of wind direction and wind speed, shown in *Figure 4.24*, highlights the differences in particle properties originating from different directions. During the summer months, the highest α values, approximately 1.15, originated from westerly directions. In autumn, the highest values, approximately 2, originated from the south-west during periods with wind speeds of between 15 – 20 m/s. The winter distribution was broad, with the highest values, approximately 1.3, observed from the west, north and east. The distribution of α during the spring months was largely similar for all wind directions, ranging from 1.1 to 1.3. Notable exceptions to this were single spots of higher and lower α values, originating from the south west. The average values were lower than those observed in Switzerland during the winter months, which ranged between approximately 1.3 in the morning and 1.8 in the evening, but similar during the summer months, ca. 1.0–1.1 over the course of the day (Sandradewi *et al.*, 2008a). A similar profile was calculated for February and March in Budapest by Ajtai *et al.* (2011, 2019), ranging between approximately 1.0 in the morning and 1.6 in the evening. The pattern of increased average α value during the winter months was also observed in India (α = 1.5 in winter, α = 1.3 in summer, Vaishya *et al.*, 2017), China (α = 1.9 in winter, α = 1.4 in summer, Ran *et al.*, 2016) and London (α = 1.2 in winter, α = 1.1 in summer, Crilley *et al.*, 2015). The lower average α value for winter in Dublin when compared to locations that are dominated by wood burning is likely related to the burning of other solid fuels such as peat and coal in the Irish city, combined with the contribution from evening traffic. The lowest values, calculated for London, are related to the fact that the locations in that study were traffic dominated environments.

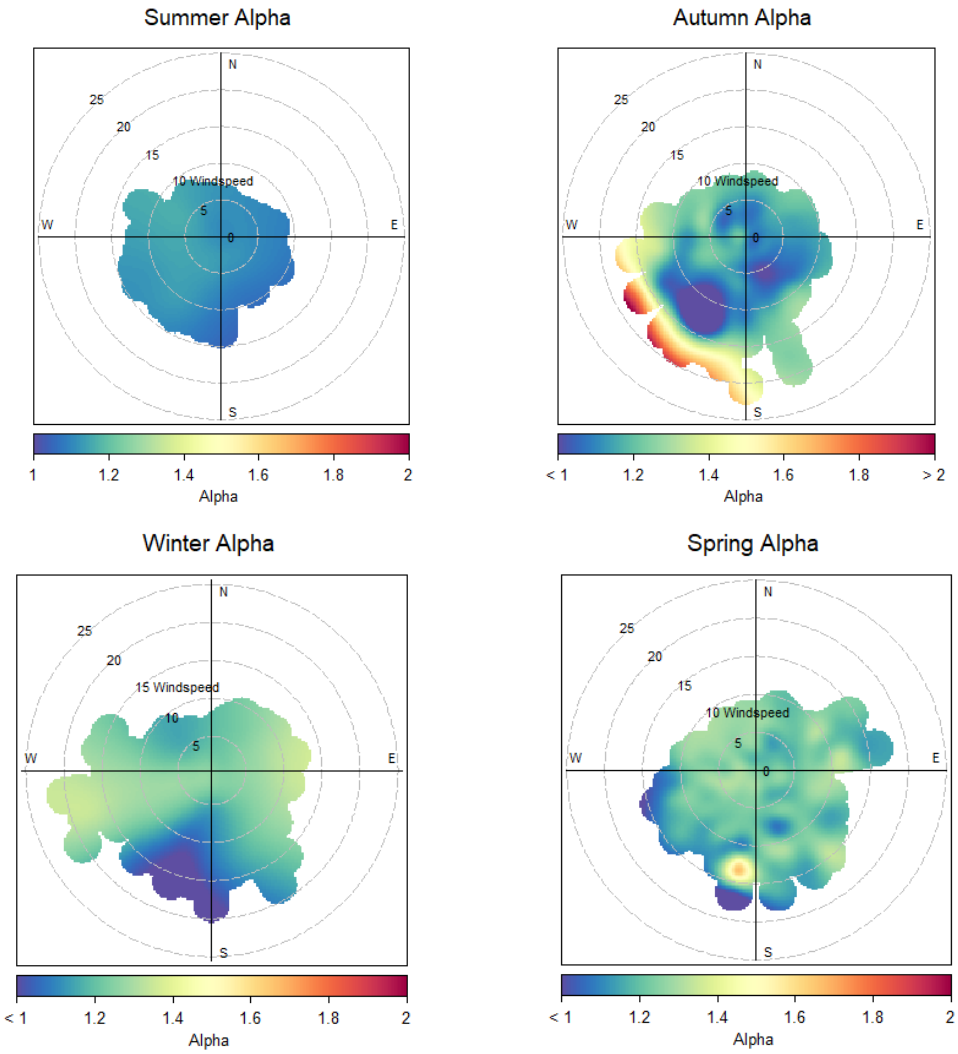

Figure 4.24. Calculated α value as a function of wind direction and speed, during summer (June, July and August), autumn (September, October and November), winter (December, January and February), and spring (March, April and May).

The distribution of the calculated α values shows clear differences during the warmer and colder months (*Figure 4.25*). The distribution for the summer months is quite narrow, implying one dominant source of eBC. With a mean value of α = 1.13, this indicates that the source is traffic. The distributions for spring and autumn are noticeably broader. The mean value for the autumn period was 1.14, indicating that traffic was also the dominant source in this period. The mean value for spring increased to 1.24, indicating that solid fuel burning played a significant role in this season. The winter distribution shows a double peak in the distribution, indicating that both traffic and solid fuel burning are prevalent during the winter period. This is supported by the source apportionment profiles (*Figure 4.23*).

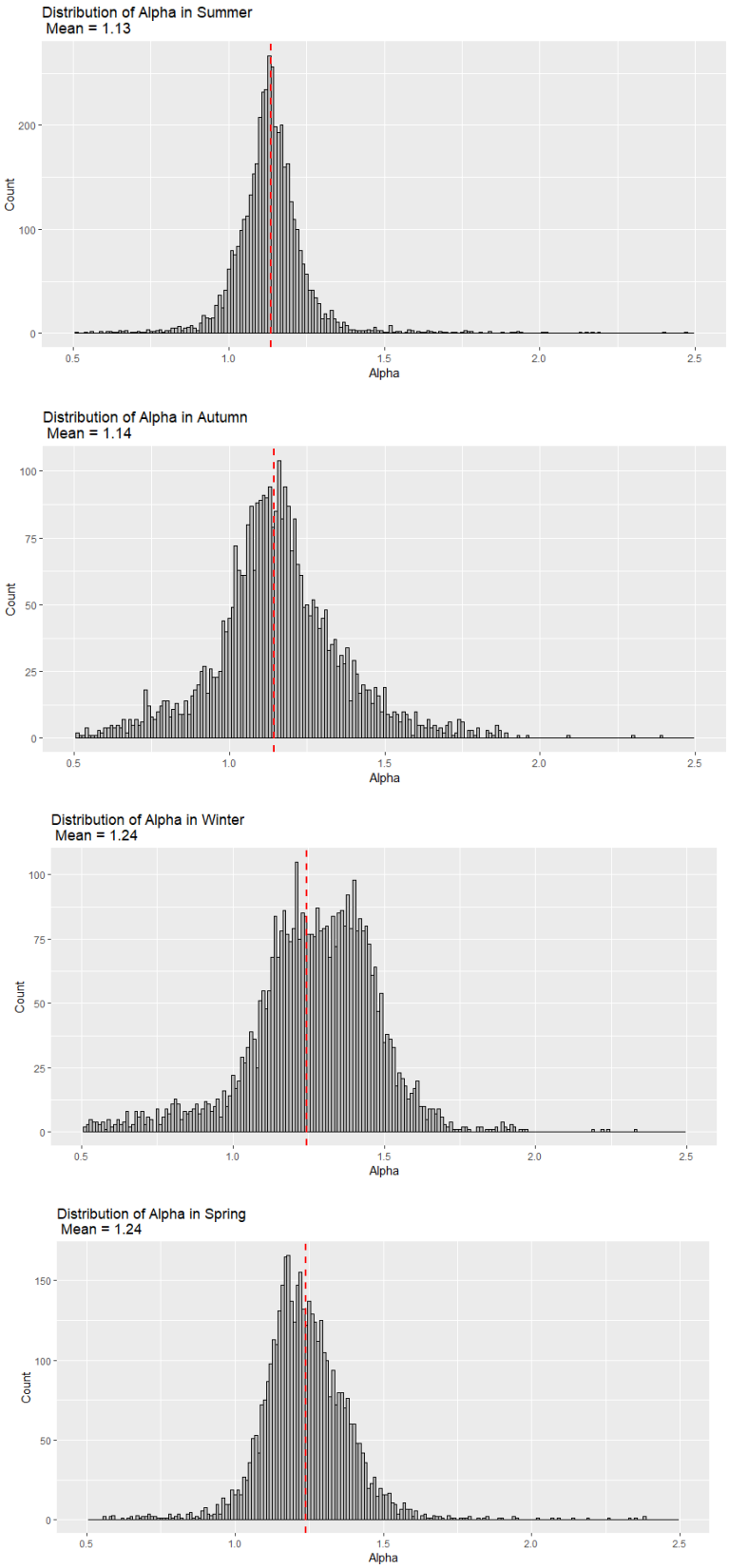

Figure 4.25. Distribution of calculated α values during summer (June, July and August), autumn (September, October and November), winter (December, January and February), and spring (March, April and May). The dashed red line represents the mean calculated α value.

Splitting the winter distribution into two parts, “traffic” hours and “solid fuel burning” hours, provides additional information on the calculated α values related to each source. Traffic related hours were 05:00 - 09:59 and 15:00 - 16:59, while solid fuel burning hours were 17:00 - 04:59. Plotting the frequency distribution for both periods shows a clear distinction in the calculated α values. The distribution during the “traffic” hours, shown in *Figure 4.26*, tends towards the value assigned for traffic, 0.9, while the distribution during the “solid fuel burning” hours tends towards the solid fuel value of 1.68. This divergence between different sources is apparent for both winter periods during the measurement campaign.

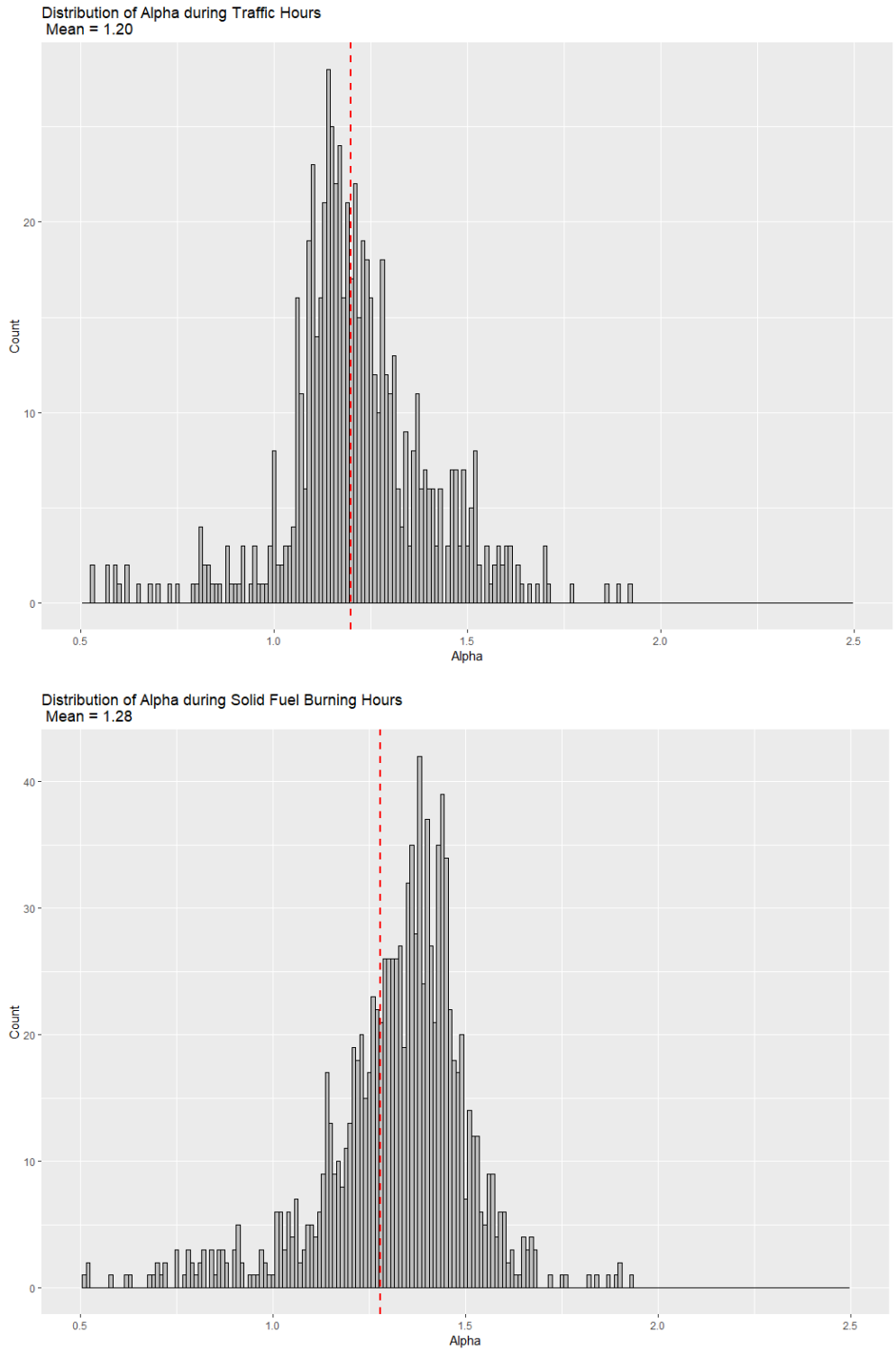

Figure 4.26. Distribution of calculated α values during "traffic" hours (05:00 to 09:59 and 15:00 to 16:59) and "solid fuel burning" hours (17:00 to 04:59) during the winter months (December, January and February) of 2016/2017. The dashed red line represents the mean calculated α value.

The EC concentrations measured during the EMEP campaign, 21/12/17 to 31/03/18, were used to calculate a site-specific mass absorption cross-section (MAC) value for the Dublin city location. This was achieved by comparing the absorption

coefficient (b_{abs}) from the aethalometer to the thermal EC from the OCEC instrument (*Figure 4.27*). The EC concentrations were determined from filter samples collected over a 24 hour period, from 08:00 to 07:59 the following day. The absorption coefficients, initially calculated in hourly values, were matched to the same time period. The slope of that regression is the site specific MAC value for Dublin. The slope of this regression was found to be 15.372 ± 0.56 m^2/g.

This MAC value is higher than the MAC values calculated for the SAPPHIRE measurement locations (11.1, 10.7, and 8.3 m^2/g for Killarney, Enniscorthy and Birr respectively). It should be noted that a different analysis protocol was used to analyse the filters collected in Dublin. The analysis was carried out in National Physical Laboratory (NPL) in London, United Kingdom. In this laboratory, the EUSAAR_2 protocol was used for analysis of the filters (Cavalli *et al.*, 2010). The calculated MAC value for Dublin is in the same range as MAC values previously calculated for a variety of locations in Europe, ranging between 6.2 and 14.4 m^2/g (Herich *et al.*, 2011; Zanatta *et al.*, 2016; Zotter *et al.*, 2017) and in Canada, 11.45 m^2/g for a roadside location and 10.70 m^2/g in a residential area (Healy *et al.*, 2017).

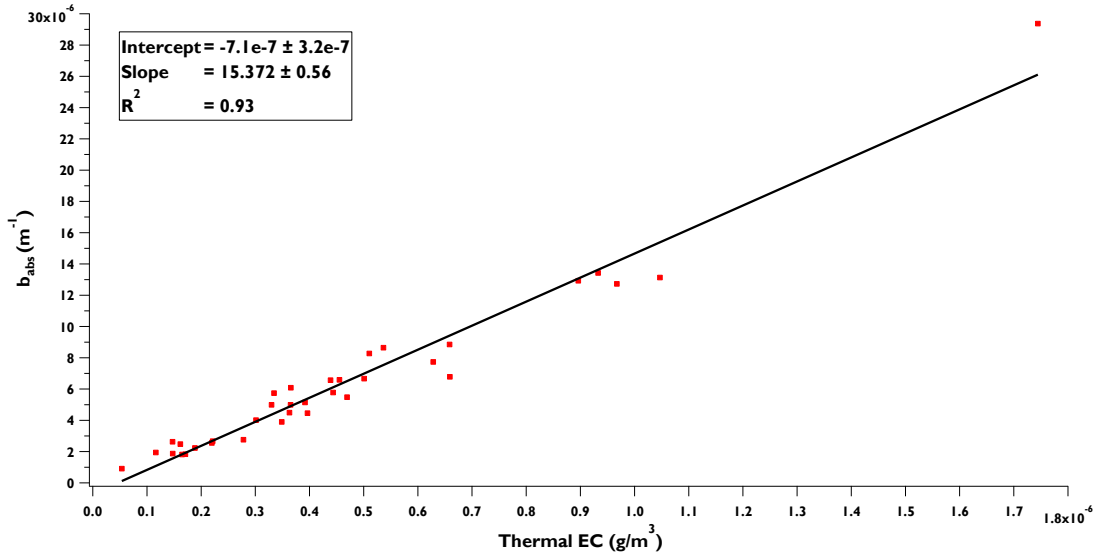

Figure 4.27. Regression of daily average absorption coefficient (b_{abs}), m^{-1}, from the AE33 instrument and daily average Thermal EC, g/m^3, from the Sunset OCEC instrument, for the EMEP campaign, 21/12/17 to 31/03/18.

4.3.6. Aethalometer-ACSM Comparison

The ACSM instrument, operated by colleagues from NUI Galway, measured the mass spectrum of the non-light absorbing organic and inorganic fractions of the sampled aerosol with a time resolution of 30 minutes. Based on previously acquired "fingerprint" spectra for the different fuel types used in Ireland (Lin *et al.*, 2017), Positive Matrix Factorisation (PMF) analysis was performed on the OA fraction to determine source contributions. The PMF analysis produced five factors, which were attributed to hydrocarbon-like OA (HOA), oxygenated OA (OOA), peat, coal, and wood. The full temporal profile of the concentrations of each OA factors and each inorganic fraction are shown in *Figure 4.28*.

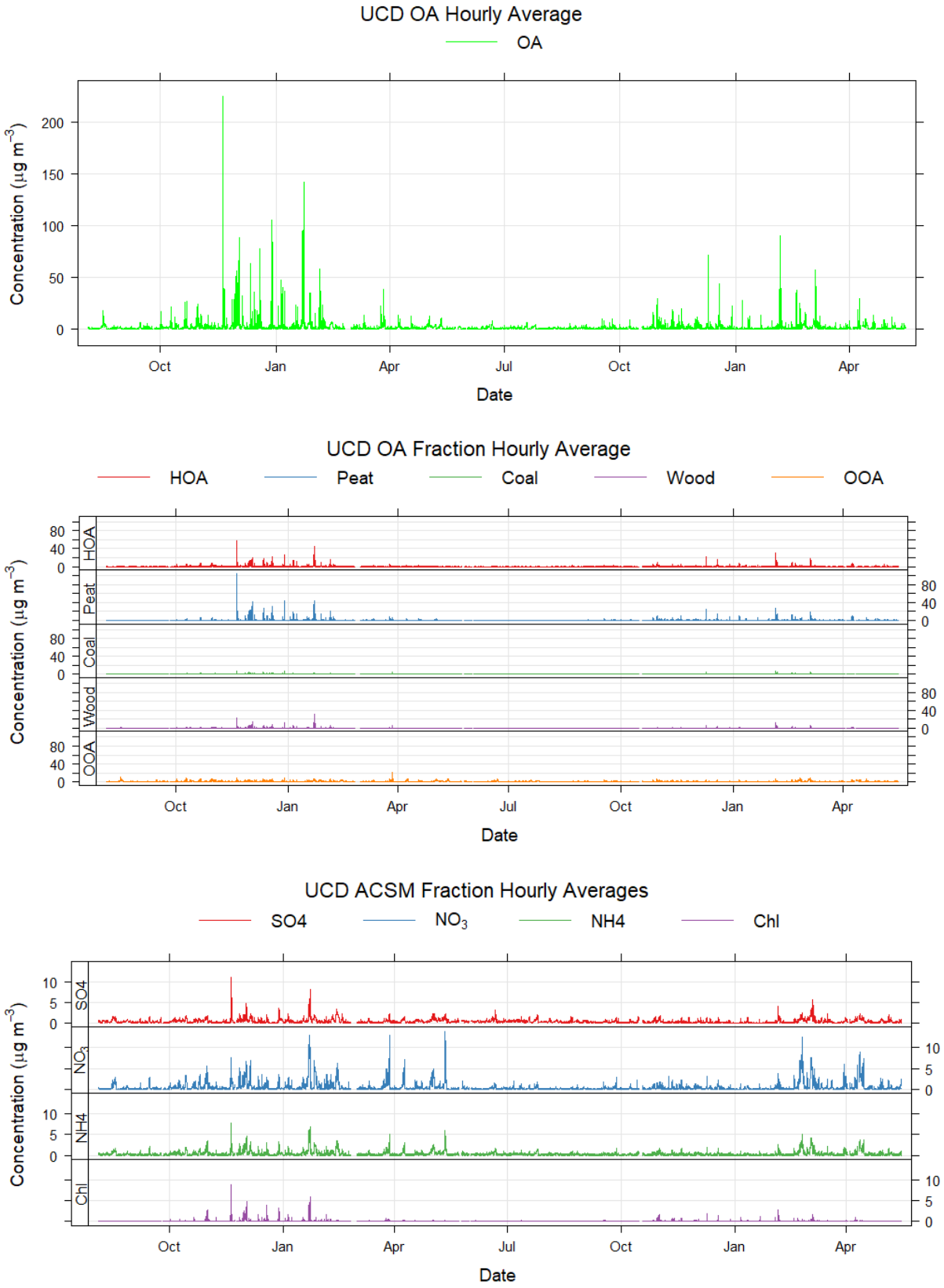

Figure 4.28. Hourly average concentrations of the total OA concentrations (top), factors contributing to OA mass (middle) and other inorganic species (bottom) measured by the ACSM during the AEROSOURCE campaign, August 5 2016 to May 15 2018.

A correlation matrix including all fractions from the ACSM PMF analysis and the AE33 source apportionment model (*Figure 4.29*) shows three clusters. The size of the circles in the matrix represents significance of the correlation, based on the pearson-correlation, *p* value. The larger the circle, the more significant the correlation is. A *p*-value of < 0.01 indicates that the correlation is statistically significant. The null hypothesis in this case is that the individual parameters are all correlated. The colour of the circle is related to the level of correlation between two parameters, i.e. a darker circle indicates a higher R^2. A strong cluster of parameters related to solid fuel burning ("Coal", "Peat", "Wood", "Chl", "OA", "HOA" "eBC" and "eBC_{SF}") is apparent in the top left corner of the matrix. All correlation coefficients in this cluster were greater than 0.6, and all *p* values in the cluster were equal or close to 0.00, indicating statistically significant relationships. A second cluster in the bottom right of the matrix, contains the secondary aerosol components "SO_4", "OOA", "NO_3" and "NH_4". The eBC_{Tr} fraction is not well correlated with any of the other components, indicating that traffic was not a source of any other pollutant considered during this analysis.

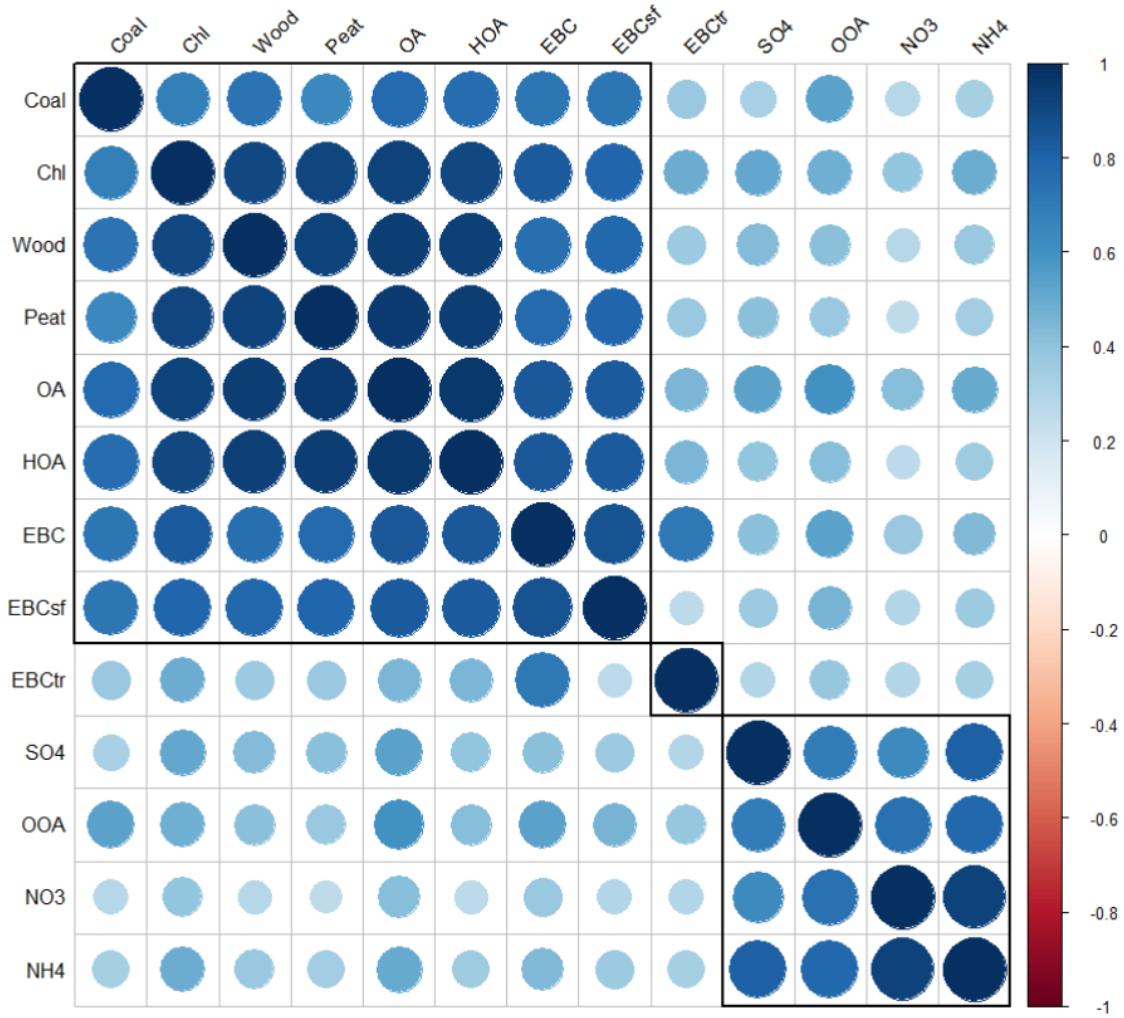

Figure 4.29. Correlation matrix for all ACSM fractions, total eBC and eBC source contributions, featuring hierarchal clustering involving three clusters. The colour of the circles represents the correlation coefficient (R^2) between the parameters, a darker circle represents a larger R^2. The size of the circle represents the significance of the correlation, *p-value*, based on the Pearson-correlation test, a larger circle indicates a significant correlation, i.e. $p < 0.01$.

Investigating the relationship between the OA fraction from the ACSM and the eBC_{SF} from the AE33, *Figure 4.30*, shows a good correlation between the parameters, $R^2 = 0.705$. The slope of the line, 4.15, indicates that on average, eBC_{SF} accounts for approximately 20% of the OA mass concentration. The relationship between eBC_{SF} concentration and some of the individual solid fuel associated OA fractions, peat, coal, and wood, also shows reasonable correlations (*Figure 4.31*). The regression of the wood related OA concentration and eBC_{SF} concentration showed a strong relationship between the parameters ($R^2 = 0.62$) with a slope of 0.38, indicating that wood combustion produced more BC than OA during the monitoring period. The

regression of coal related OA and eBC_{SF} was less well correlated (R^2 = 0.53), and had a slope of 0.22, indicating that coal produced significantly more BC than OA, as expected. Finally, the relationship between peat related OA and eBC_{SF} (R^2 = 0.64) had a slope of 1.53, indicating the peat combustion produced a larger amount of OA than BC.

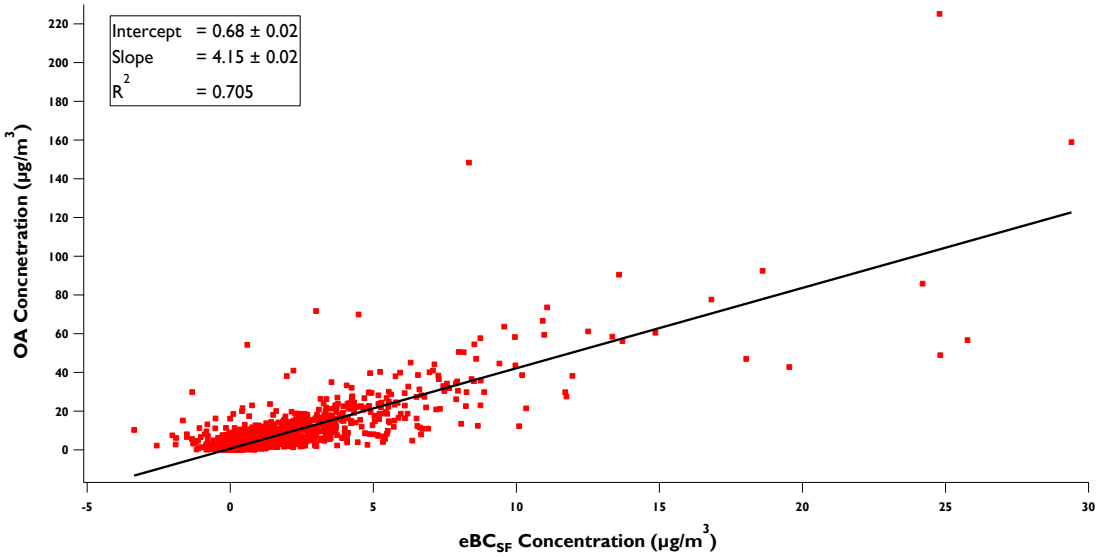

Figure 4.30. Comparison of Organic Aerosol (OA) concentration (µg/m^3) measured by the ACSM and eBC_{SF} concentration (µg/m^3) calculated by the aethalometer source apportionment model using the Zotter *et al*. (2017) parameters, α_{SF} = 1.68, α_{Tr} = 0.9.

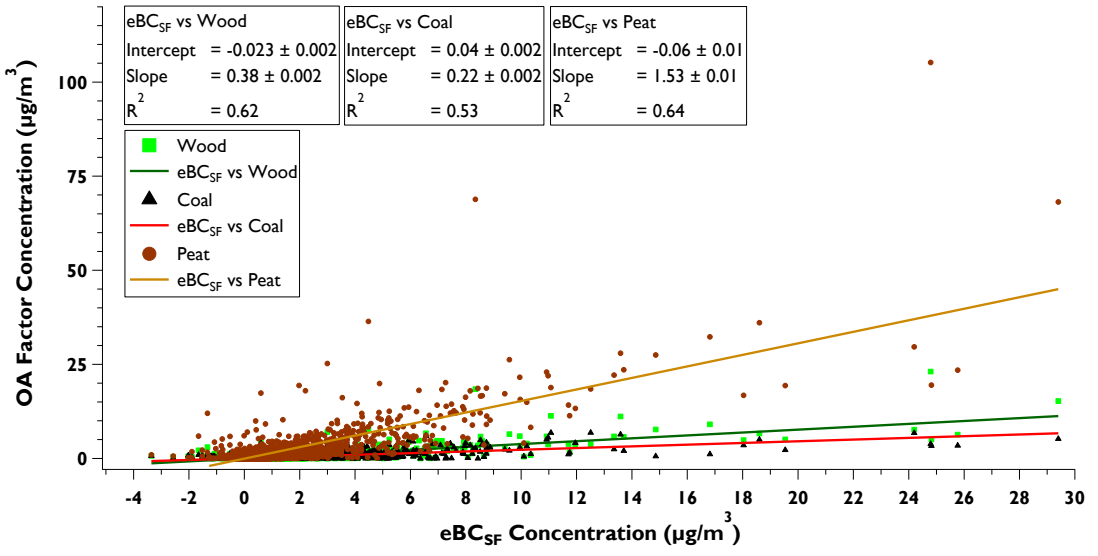

Figure 4.31. Comparison of *Peat*, *Coal*, and *Wood* factor concentrations (µg/m^3) measured by the ACSM and eBC_{SF} concentration (µg/m^3) calculated by the aethalometer source apportionment model using the Zotter *et al*. (2017) parameters, α_{SF} = 1.68, α_{Tr} = 0.9.

The value of eBC:OA provides an indication of the levels of brown carbon (BrC) present in the ambient sample (*Figure 4.32*). Lower eBC:OA values, in the range of 0.1 – 0.5, are indicative of an environment dominated by solid fuel burning emissions (Saleh *et al.*, 2015). This is reflected by the ratios observed during the evening hours. Conversely, a higher eBC:OA ratio is indicative of a traffic dominated environment, as observed during the morning hours.

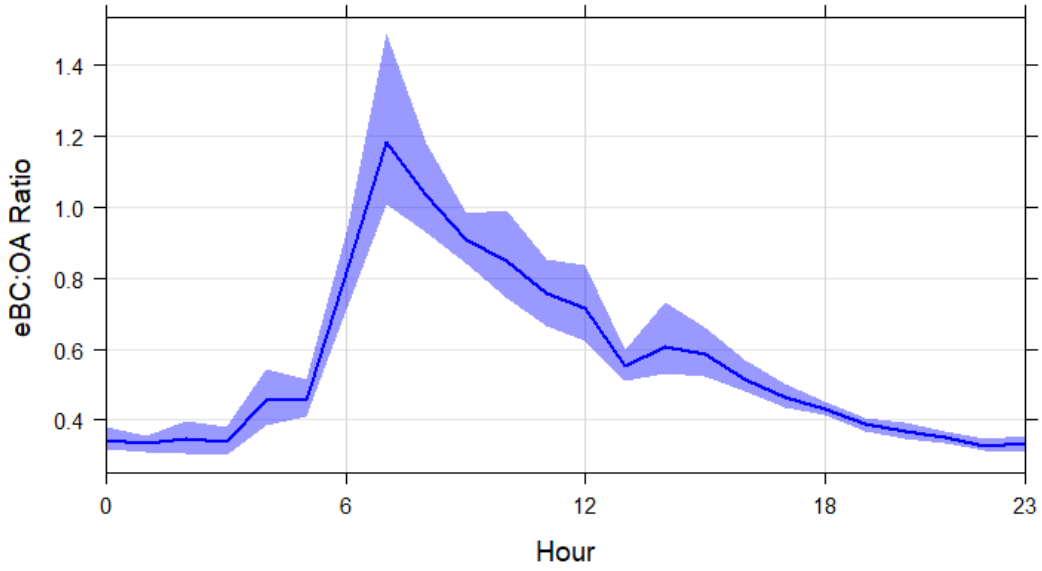

Figure 4.32. Diurnal profile of eBC:OA ratio during AEROSOURCE measurement campaign, August 5 2016 to May 15 2018.

Another parameter that can be determined from the ACSM and AE33 data is the coating factor (CF) for the ambient aerosol. The nature of the coating that is present on BC particles can affect their optical properties and thus the correction factor (k) applied in the aethalometer model. Following the approach employed by Drinovec *et al.* (2017), the correction factor is calculated for the 880 nm wavelength (k_6) for each of the seasons (*Figure 4.33*). In this method, hourly averaged k_6 values are compared to the CF values that are collected in bins that are two units wide. The exception to this is any CF values that are larger than 30, which are collected together in a single bin.

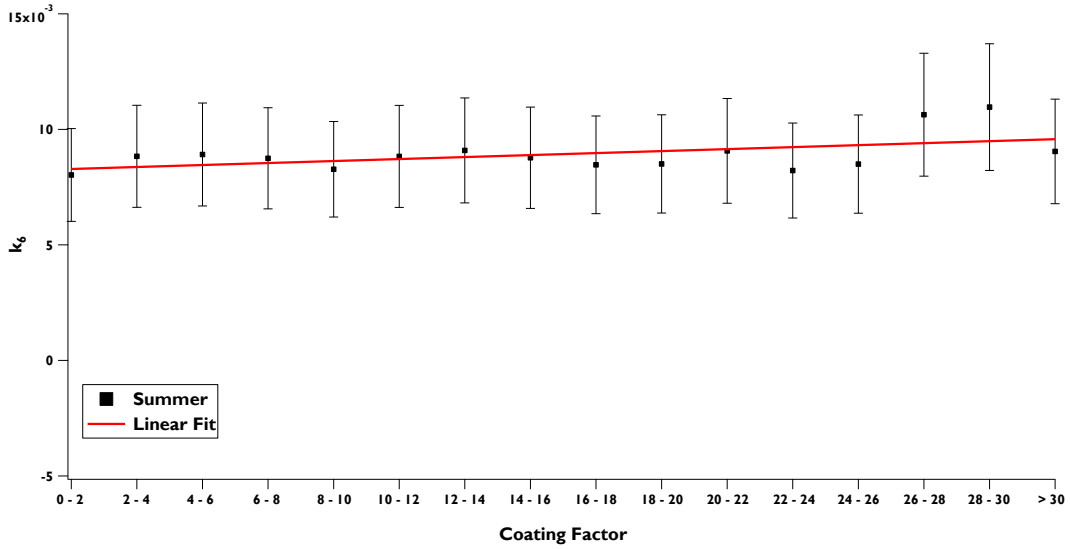
15x10-3
10
5
0
-5
k6
Summer
Linear Fit
0 - 2
2 - 4
4 - 6
6 - 8
8 - 10
10 - 12
12 - 14
14 - 16
16 - 18
18 - 20
20 - 22
22 - 24
24 - 26
26 - 28
28 - 30
> 30
Coating Factor

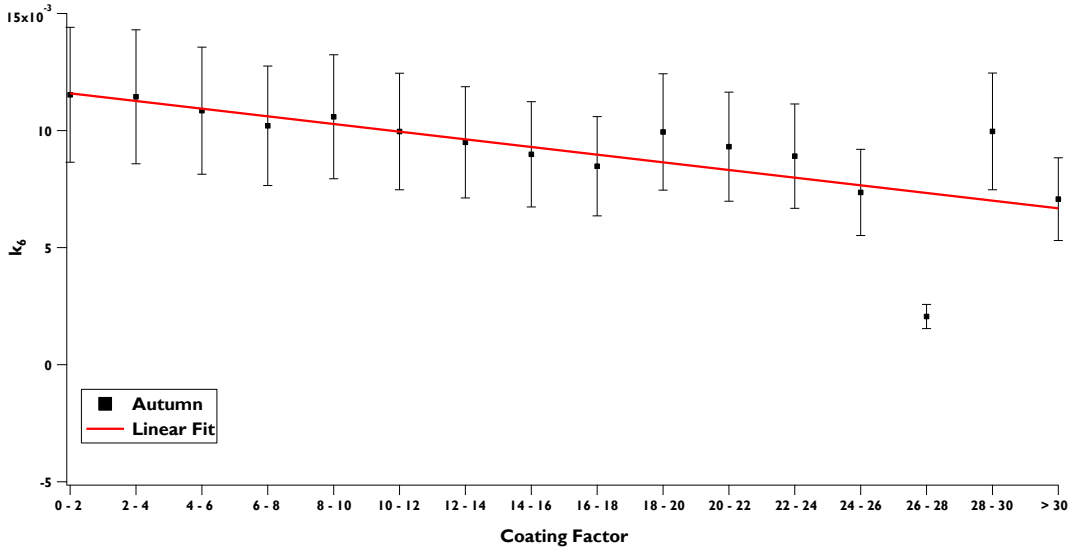
15x10-3
10
5
0
-5
k6
Autumn
Linear Fit
0 - 2
2 - 4
4 - 6
6 - 8
8 - 10
10 - 12
12 - 14
14 - 16
16 - 18
18 - 20
20 - 22
22 - 24
24 - 26
26 - 28
28 - 30
> 30
Coating Factor

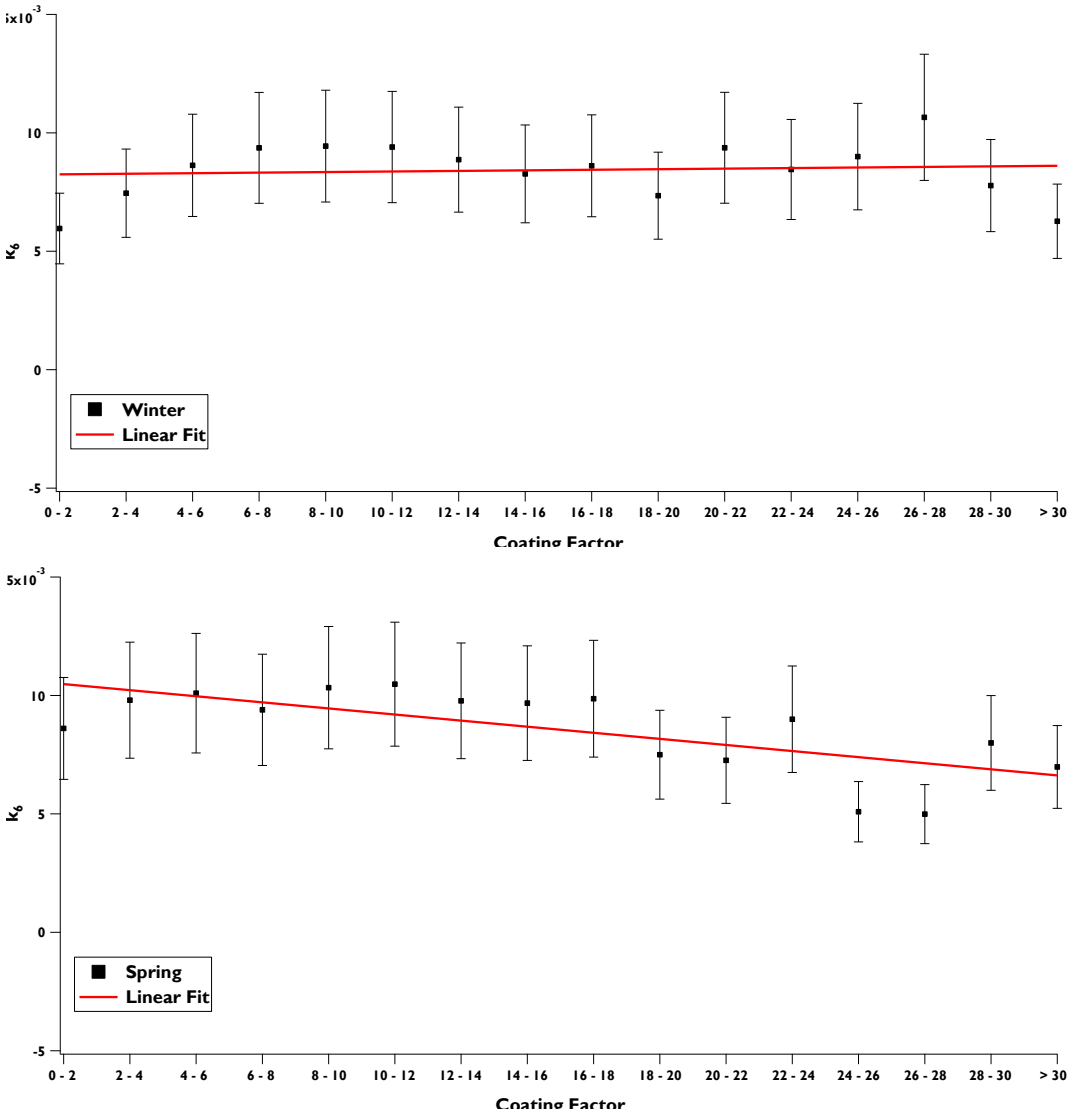

Figure 4.33. Correlation between the filter-loading effect k_6 and the CF during summer (June, July and August), autumn (September, October and November), winter (December, January and February) and spring (March, April and May). Hourly data are averaged in CF bins 2 units wide. The error bars represent the 25th and 75th percentile for each bin.

The results, summarized in *Table 4.4*, show that during the spring and winter months, an increase in coating results in a reduction of the filter-loading effect. The slight increase in k_6 with increasing CF during the winter period is potentially a consequence of the high amount of biomass burning emissions during these months. Previous monitoring campaigns have shown that biomass burning emissions are dominated by organics that are externally mixed with BC (Healy *et al.*, 2013).

Table 4.4. Slope of the regression of the filter-loading parameter k_6 versus the coating factor and AAE during the four seasons in Dublin.

Season	**slope (10^{-4})**	**A**
Summer	0.9 ± 0.4	1.134
Autumn	-3.0 ± 0.9	1.144
Winter	0.2 ± 0.7	1.244
Spring	-3.0 ± 0.7	1.238

4.4. Conclusions

A seven wavelength aethalometer was deployed for a period of two years (Aug 2016 – Aug 2018) on the campus of University College Dublin (UCD) as part of the AEROSOURCE project. An Aerosol Chemical Speciation Monitor (ACSM) was also deployed on site and managed by colleagues from National University of Ireland Galway (NUIG). The measurements from both instruments clearly show a highly seasonal source profile at this urban background location. During the colder months, late autumn and winter, solid fuel burning is the major contributor to particulate pollution. During the summer months, traffic is the dominant source of pollution at the site. Meteorological patterns show that the highest concentrations were measured during periods of low wind speeds, when local sources were dominant.

The equivalent black carbon (eBC) measured by the aethalometer was split into two source contributions, solid fuel burning (eBC_{SF}), and traffic (eBC_{Tr}), using the aethalometer model developed by Zotter *et al*. (2017). During the winter months, morning peaks in eBC were observed due to traffic and evening peaks were attributed to solid fuel burning. The diurnal profile for the winter months is similar to those observed during the SAPPHIRE monitoring campaigns, but with relatively lower amounts of eBC. For the summer months, the diurnal profile shows a peak in the morning related to traffic, and a smaller peak related to traffic in the late afternoon and evening. The magnitude of the morning traffic peak is similar in all seasons, indicating that traffic levels remain consistent throughout the year. The profiles for both autumn and spring are a mixture of the winter and summer profiles. There is a morning peak associated with traffic, as well as an evening peak due to solid fuel burning. The evening peak observed during autumn and spring is smaller than in winter. These seasonal observations are generally in line with expected changes in solid fuel usage in response to the prevailing meteorological conditions.

PMF analysis of the OA mass fraction measured by the ACSM allowed five different source contributions to be identified; coal, peat, wood, hydrocarbon-like OA (HOA), and oxygenated OA (OOA). The ACSM data shows a similar seasonal pattern to the aethalometer source profiles, with high solid fuel burning related contributions to OA mass during winter. Hierarchal clustering of the aethalometer fractions and the ACSM fractions produced two groups; the first one containing eBC_{SF} and all of the

solid fuel related factors from the ACSM and the second one containing secondary aerosol components including sulfate, nitrate, ammonium and OOA fractions. Regression analysis indicates that the total OA concentration is highly correlated to eBC_{SF} and that eBC_{SF} accounts for approximately 20% of the OA concentration over the whole two-year period. The eBC_{Tr} fraction from the aethalometer was not correlated to any other parameter.

A range of additional parameters determined from the aethalometer and ACSM measurements also highlight the seasonal nature of particulate pollution at the monitoring location. The parameters investigated include the ΔC value, absorption Ångström exponent (α), the eBC:OA ratio, the coating factor (CF) and the filter-loading correction parameter (k_6). As expected, the ΔC value increases sharply during evening hours due to domestic solid fuel burning emissions during the colder periods. This effect is further enhanced on Saturdays and Sundays, when "recreational burning" is more prevalent. The average monthly ΔC value is also higher for the colder months, again consistent with the increase in solid fuel burning. The diurnal average of the α values is different for the four seasons. The summer profile is relatively stable at approximately 1.1, while the winter profile exhibits a large increase in α during the evening hours, again, consistent with the increased emissions from solid fuel combustion. The autumn and spring profiles are a mixture of the warmer summer months and the colder winter months. The frequency distributions of α values during the different seasons also highlights the dual source contribution during the winter months. During the summer months, a very narrow distribution was observed, centred on a value of approximately 1.1. During the autumn and spring seasons a much broader distribution was observed, with single peaks centred on approximately 1.1 for the autumn, and approximately 1.2 for the spring. The winter frequency distribution exhibits a very broad distribution containing two distinct peaks. Separation of these peaks produces two distinct distributions, one relating to traffic and one relating to solid fuel burning.

The eBC:OA ratio provides an indication of the amount of brown carbon (BrC) present in the ambient sample, which is indicative of the level of solid fuel burning. The average profile for the monitoring campaign shows a peak in the ratio during the morning hours, consistent with rush hour, and significantly lower values during the evening times. The evening time values observed were in-line with previous literature values for solid fuel emissions.

Comparing the hourly averaged filter-loading correction parameter (k_6) from the aethalometer to the hourly averaged coating factor (CF) highlights the differences in the source contributions for the four seasons. The slight increase in k_6 with higher CF during the winter period is a result of the increased amount of solid fuel burning, and is consistent with previous studies.

Finally, the site specific mass absorption cross-section (MAC) value calculated for December 2017 to March 2018 was 15.372 ± 0.56 m^2/g. This value was higher than previous studies conducted at urban background locations, and was greater than the values calculated for the SAPPHIRE locations. This is potentially due to the BC particles being externally mixed as they are transported to the monitoring location.

In conclusion, the pollution measured at the monitoring site is highly seasonal. High levels of solid fuel related pollution was measured at the site, particularly during the winter months. This indicates that solid fuel combustion is still a major issue in the Dublin city area, despite the introduction of legislation to combat the combustion of bituminous or "smoky" coal. It is clear that additional legislation is required to reduce emissions from domestic solid fuel burning and improve air quality in Dublin.

5. Analysis of Historical Air Pollution and Legislative Changes in Four European Cities

Contents

5.1. Introduction

5.1.1. Long-term Air Pollution Studies

There is a long history of issues and complaints regarding air pollution since the advent of the use of coal for heating and industrial processes (Heidorn, 1979; Brimblecombe, 1987; Fuller, 2018). A significant number of studies have been conducted into the association between particulate matter and mortality in the 20th century. The first major studies detailing the relationship between fog and increased mortality were focused on the fog events that occurred in London during the winter months of 1948, 1952, and 1956 (Logan, 1949, 1952, 1956). Similar fog events previously occurred in the winter months of the years 1873, 1880, 1882, 1891, and 1892. It was initially estimated that the fog episodes in London in 1952 and 1956 led to an additional 4000 and 1000 deaths respectively. However, reanalysis of hospital admission and mortality data has estimated that up to 12,000 people died as a result of the pollution episode in 1952 (Bell *et al*., 2004). The potential link between the pollution episode and a concurrent influenza outbreak was also investigated. It has been suggested that a significant number of deaths initially attributed to the virus may have actually been due to a latent effect of the pollution episode (Bell *et al*., 2004). It was also hypothesised that people may have been more susceptible to the influenza virus after exposure to the high levels of pollution.

Black smoke (BS) was used as a proxy for particulate matter (PM) or total suspended particles (TSP) in previous decades (Ball and Hume, 1977; Heal and Beverland, 2017; Heal *et al*., 2005; Muir and Laxen, 1995). BS is a measure of the reflectance from a sample of particles collected on a filter paper. This reflectance can be converted to a PM concentration using standard equations (Heal and Quincey, 2012). The toxic effects of exposure to BS were investigated using rats, mice and guinea pigs by Pattle *et al*. (1959). The main causes of death in the test subjects were blockages of the air passages by particles and capillary haemorrhage resulting from bronchial spasm. More recent studies in the UK have also demonstrated the links between BS and SO_2 emissions and mortality, e.g., Elliot *et al*. (2007) found that even at low concentrations of BS and SO_2, there is a continuing risk to public health. High

BS concentrations can also lead to other health problems, for example dry eye disease (Stankovic *et al.*, 2019).

Long term studies in Great Britain, Europe, and the United States have highlighted the links between particulate pollution and premature deaths. Hansell *et al*. (2016) conducted a long term study in England and Wales investigating the long term effects of exposure to pollution from 1971 to 2009. The authors analysed the trends of BS and SO_2, with PM_{10} replacing BS for the last decade of the study. A total of 367,658 individuals were followed for the duration of the study. Statistically significant associations between BS and SO_2 exposure in 1971 and all-cause mortality were established. Analysis of different subgroups showed chronic obstructive pulmonary disorder (COPD) and lung cancer were the highest mortality risks. A study in Scotland from 1972 – 1976 found a similar relationship between air pollution and mortality (Yap *et al.*, 2012).

The APHEA and PEACE studies analysed the health effects of air pollution in Europe (Katsouyanni *et al*., 1996; Roemer *et al.*, 2000). The APHEA study took place in two separate phases; APHEA and APHEA2. Phase 1, which began in 1991, focused on measuring sulfur dioxide and particulate matter in 15 different cities. This study found that an increase of 50 $\mu g/m^3$ in either SO_2 or black smoke corresponded to a 3% increase in daily mortality (Katsouyanni *et al.*, 1997). The APHEA2 project, initiated in 1998, focused on analysing the association between PM_{10} and BS concentrations and the number of hospital admissions for respiratory diseases, COPD, and asthma (Atkinson *et al.*, 2001). This study focused on data from 8 European cities and found that, on average, a 10% increase in PM_{10} concentrations lead to a 1% increase in hospital admissions. The PEACE study was a collaboration between 14 different European centres in the winter of 1993/1994. The study focused on two cohorts of children between the ages of 6 and 12, who had displayed symptoms of asthma in the previous 12 months. One group of children resided in suburban or rural areas, the other group resided in urban areas. This study found no clear correlation between pollution levels and respiratory illness but the authors acknowledged that the short period of the study was a major limitation.

In the United States, a study by Schwartz and Dockery (1992) reaffirmed the links between total suspended particles and mortality based on analysis of pollution data and mortality figures between 1974 and 1984. This work was part of the larger "six cities" study by Dockery *et al*. (1993) where it was concluded that fine PM was

implicated in the excess mortality rates in certain cities in the United States. The adverse health effects of PM are wide-ranging and extend from mild exacerbation of pre-existing respiratory conditions such as asthma, to more serious consequences such as decreased lung function, chronic respiratory and cardiovascular disease, and premature death (Kim *et al.*, 2015). Links have also been established between air pollution and diabetes (Pearson *et al.*, 2010). In recent years studies by the World Health Organisation (WHO) have estimated that, at the global level, air pollution was responsible for 3.1 million deaths in 2010, and reduced the average life expectancy by roughly 8.6 months (Lim *et al.*, 2012; World Health Organization, 2013).

Several studies have highlighted the positive impacts of new legislation and advancing technologies on air quality. A traffic related study in London, (Font and Fuller, 2016) examined the relationship between pollution emissions, legislative changes and advances in engine technology between 2004 and 2015. This study involved analysis of trends in roadside pollution, including nitrogen oxides (NO_x) and $PM_{2.5}$, from 65 different monitoring locations in London. It was found that over the course of the study, the majority of the sites experienced a significant decrease in NO_2 and $PM_{2.5}$ concentrations, with reductions in the ranges of 8 – 13% and 15 – 45% respectively. It was concluded that the drop in NO_x emissions was related to the introduction of the Low Emission Zone in the London City Area, as well as the introduction of "cleaner" vehicles. The $PM_{2.5}$ reduction was attributed to improvements in the particulate filters attached to diesel engines.

Cusack *et al.* (2012) conducted a study of $PM_{2.5}$ concentrations at 28 monitoring sites across nine countries in Europe between 2002 and 2010. A slow downward trend in concentrations was observed at all locations, providing good evidence that the introduction of new pollution abatement strategies by the EU have a positive effect on $PM_{2.5}$ concentrations. Chemical composition studies showed the majority of $PM_{2.5}$ components were reduced in the study period. Two exceptions to this trend were marine aerosol and EC, where no significant decrease was observed, and, in fact, EC concentrations showed a slight increase from 2008, particularly in the autumn and winter seasons. The authors also noted that the economic crisis of 2008 had a significant impact on $PM_{2.5}$ concentrations in Spain, Portugal and Italy. A significant decrease in BC concentrations was observed in Spain as a result of the economic crisis, relating to a decrease in both industrial activity and heavy goods vehicle traffic (Lyamani *et al.*, 2011). The decrease during the winter months was less

apparent as there was an increase in the use of solid fuels for home heating purposes after the economic crisis. Similarly, an increase in wintertime PM concentrations due to wood burning was observed in Thessaloniki, Greece following the economic crisis (Saffari *et al.*, 2013). Long-term studies from the Po Valley, Italy, showed a decrease in annual average $PM_{2.5}$ concentrations between 2002 and 2015, although the concentrations often exceeded EU limit values (Pozzer *et al*., 2019). It is proposed that the observed decreases were the result of improved vehicle technologies and a reduction of the number of older vehicles in the fleet, rather than the introduction of new legislation combating air pollution (Bigi and Ghermandi, 2016). A study from Japan showed that regulation of automobile emissions led to a decrease in respiratory illnesses and allergic reactions in children in urban areas (Hasunuma *et al.*, 2014). It was shown that the introduction of "The Law Concerning Special Measures for Total Emission Reduction of Nitrogen Oxides (Automobile NO_x Law)", and the 2001 amendment to "The Automobile NO_x/PM Law" greatly improved air quality in the enforcement zones during a 12 year study period (1997 – 2009). Suspended particulate matter concentrations decreased twice as fast in the law enforcement zones and resulted in a significant reduction in the reported rates of asthma and wheezing.

5.1.2. Historical Air Pollution Studies in Ireland

In Ireland, the effects of particulate pollution were first discussed in 1664 in Nathaniel Henshaw's *Aero-chanilos.* In his writings, Henshaw detailed his observations regarding the negative effects of poor air quality on human health and proposed that a change in the air could be "the cure for any infirmary" (Henshaw, 1664). Particulate measurements have been made in Ireland sporadically since 1925 (Boylan, 1926). Boylan reported the average numbers of dust particles and the number of condensation nuclei per cubic centimetre, noting that the highest concentrations occurred during episodes of "fog". Additional measurements of particle number in Dublin were conducted over the years 1938 – 1950 (Leonard *et al.*, 1940, 1941, 1942, 1943, 1950; Leonard and McVerry, 1939). Leonard and McVerry (1939) estimated that winter time concentrations in Dublin were 2.4 times greater than summer time concentrations, and that domestic sources contributed 3.3 times more pollution than

industrial sources, due to a high level of domestic coal combustion. Interestingly, Leonard *et al.* (1943) noticed a marked reduction in pollution levels in 1941 and 1942, which was attributed to a decrease in coal combustion due to a supply shortage during the Second World War. It was noted that in those years, samples of particulate matter appeared browner than in previous years, potentially due to the increased use of peat in domestic fires. Leonard *et al*. (1950) recorded increases in pollution levels in 1948 and 1949 as coal became more available after the conclusion of the war. Systematic air pollution monitoring was finally established in Ireland in 1963, with the introduction of a network in Dublin for measuring black smoke and sulfur dioxide in response to the *Local Government (Sanitary Services) Act*. Reports from Dublin City Council show that four stations were opened in the Dublin city area during 1963, namely the City Laboratory station at Cornmarket, the Baggot Street Hospital station, the Custom House station, and the St James' station. Additional stations were opened in Dublin in 1964 at the East Wall Road, and in 1965 at the power station at Ringsend. Around the same time, monitoring stations was also opened in Cork (at the Regional Laboratory in Cornmarket, (1964) and at the power station in Marino (1965)), and Galway (at the regional laboratory in Newcastle (1964)). Over the next few decades, a number of monitoring stations were opened and closed in several cities across Ireland, before widespread BS measurements finally ceased in 2009 and PM_{10} became the key parameter for particulate pollution (O'Leary, 2010).

A report by McGettigan and O'Donnell (1995) analysing the emissions, depositions and concentrations of pollutants in Ireland between 1984 and 1994 showed a decreasing trend in BS and SO_2 concentrations in Dublin. A total of 65 monitoring sites were in operation during the study period, maintained by 17 different local authorities and the Electricity Supply Board (ESB). Almost half (30) of the 65 sites were located in the Dublin city area. Data from Dublin city centre in 1996 showed that the majority of PM_{10} and BS originated from traffic related sources (Keary *et al.*, 1998). Average PM_{10} concentrations at locations outside of the city centre were substantially lower than those observed at College Green. The average concentration measured at College Green was 49 $\mu g/m^3$, while the average concentrations measured in Rathmines and Ashtown Grove were 31 $\mu g/m^3$ and 28 $\mu g/m^3$ respectively. These concentrations were consistent with those measured at similar locations in the UK (QUARG, 1996). Additional measurements at urban background locations in Clontarf and Phoenix Park showed even lower average concentrations, as expected, 14 $\mu g/m^3$

and 17 μg/m^3 respectively. A comparison between PM_{10} and BS at the College Green, Rathmines and Ashtown Grove sites showed strong correlations between the two parameters, with an R^2 value of 0.75 for College Green, 0.69 for Rathmines and 0.65 for Ashtown Grove.

The positive impact of air quality legislation in Ireland has been previously demonstrated by Clancy *et al*. (2002) who focused on the years surrounding the introduction of the ban on the sale of bituminous coal in Dublin city in September 1990. The authors demonstrated that this one piece of legislation was responsible for a 70% reduction in black smoke concentrations. This decrease in black smoke coincided with an annual reduction of 15.5% in respiratory related deaths, and a 10.3% decrease in annual cardiovascular deaths. In total, approximately 360 fewer deaths occurred annually in the Dublin area after the introduction of the ban.

5.1.3. Aim of this Work

The original objective of the study was to compare the present day concentrations of black carbon in Dublin with the historical black smoke measurements in order to assess changes and trends in carbonaceous aerosols over the last few decades. During the course of this work, a rich database of BS and SO_2 measurements was discovered and it was subsequently decided to 1) compile a time series for historical black smoke and SO_2 measurements for Dublin city; 2) to compare the data collected in Dublin with data from other European cities, in this instance, Belfast, London, and Paris; and 3) analyse the air pollution trends in relation to changes in air quality legislation over the course of the study period.

5.2. Methodology

5.2.1. Measurement Techniques

Black smoke measurements were made in accordance with the methods outlined by the Organization for Economic Cooperation and Development (OECD, 1964). This convention was adopted by Britain in 1969 and is described in the British Standards Institute document BS 1747-2 (1969): Determination of concentration of suspended matter (British Standards Institute, 1969a). In brief, air was passed through a Whatman No. 1 filter paper at a set flow rate. The reflectance of the particulate matter collected on the filter was measured using a reflectometer and converted to $\mu g/cm^2$ using a well-established equation (Christolis *et al.*, 1992). Reflectance measurements were also converted into a Black Smoke Index (BSI) value using a standard table based on ISO 9835 (1993). Irish, British and European measurements were made in accordance with this procedure (Goodman, 1999; Goodman *et al.*, 2009; Quincey *et al.*, 2009).

SO_2 measurements were made in accordance with the International Standards Organisation document 4219:1979, "Air quality – Determination of gaseous sulfur compounds in ambient air – Sampling equipment" (ISO, 1979). This method is summarised by the British Standards Institute document BS 1747-3 (1969): Determination of sulfur dioxide (British Standards Institute, 1969b). In brief, the concentration of sulfur dioxide was determined by passing a sample of filtered air through a bubbler containing an acidified solution of hydrogen peroxide, pH ~4.5. The SO_2 is absorbed into the acidified solution, the solution is then titrated against a standard basic solution to determine how much SO_2 has been absorbed (AFA Technology, 1999).

5.2.2. Data Acquisition for Dublin

BS and SO_2 concentrations for Dublin between 1963 and 2009 were gathered from several different sources. Data for the period April 1994 to June 2009 was downloaded from the "EPA Ireland archive of Black Smoke monitoring data" and the "EPA Ireland archive of SO_2 (Total Acidity Method) monitoring data" databases

(available at www.erc.epa.ie/safer). Most of the data for the period May 1963 to March 1994 was obtained from the archives of Dublin City Council (DCC), which came in the form of printed reports containing monthly average values for BS and SO_2 at the various measurement sites. However, DCC did not have data for the following periods; 1972 – 1974, 1977 – 1978, and 1982 – 1989. These gaps were filled by using data acquired from Prof. Pat Goodman, Dublin Institute of Technology (DIT), who provided monthly average values on a citywide basis. A complete time series for BS and SO_2 from May 1963 to March 2003 was constructed by combining data from all three sources.

In total, 23 measurement sites were operational in the Dublin city area from May 1963 to July 2009. The site locations are shown in *Figure 5.1*, with further details provided in *Table 5.1*. Several sites were opened, closed or moved to a nearby location over the duration of the study period. For the intercomparison with other cities, one representative location was selected for Dublin in an effort to avoid preferential sampling bias due to these changes in the monitoring network (Shaddick and Zidek, 2014). The selection of a suitable site was largely dependent on the availability of data for the entire study period. Although none of the sites fulfilled this criterion, it was decided to combine the measurements taken at the urban background sites on Baggot Street (1963 – 1979) and Herbert Street (1979 – 2003) as these stations are approximately 600 m apart and the data generates an almost complete timeline.

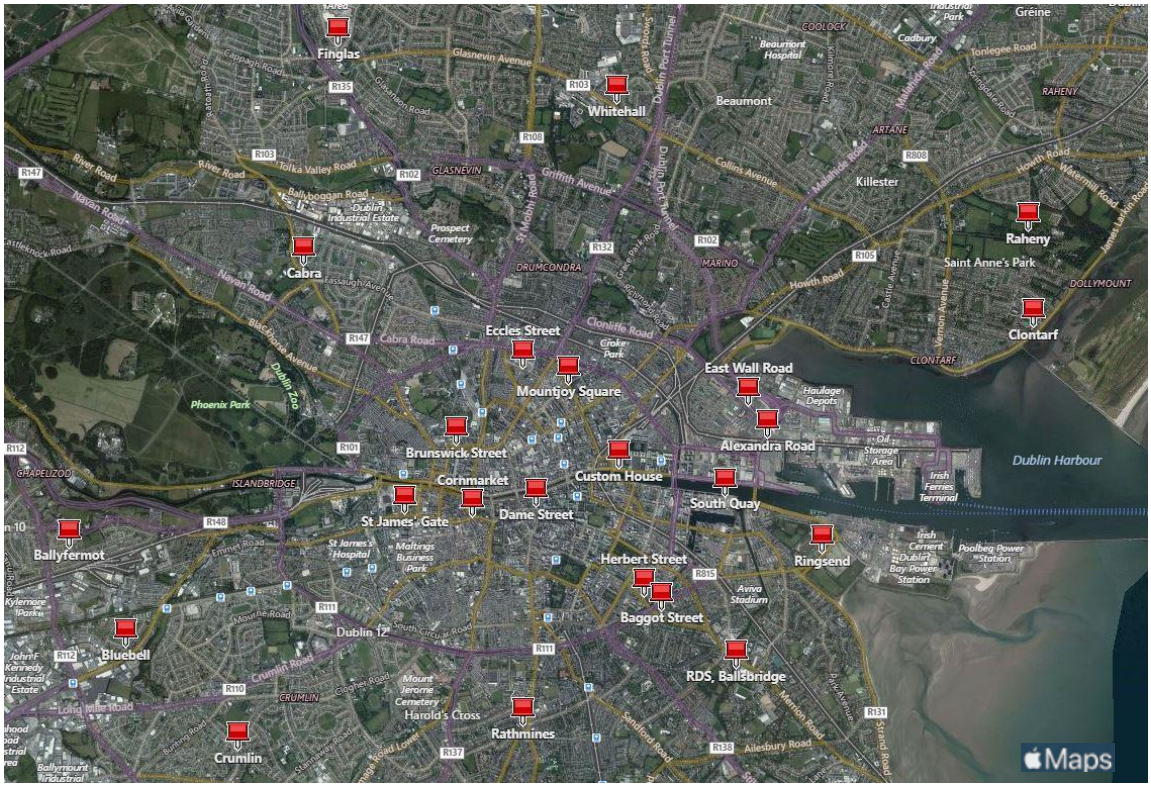

Figure 5.1. Map of Dublin, showing the monitoring sites used in the analysis of historical BS and SO_2 measurements.

Table 5.1. Details of Dublin monitoring sites used in the analysis of historical BS and SO_2 measurements.

Station Name	Active Dates	Latitude	Longitude
Dame Street	Jan 1975 – Mar 1981	53.34427	-6.26456
RDS, Ballsbridge	Jan 1975 – Mar 2000	53.32793	-6.23061
Eccles Street	Jan 1975 – Mar 1981	53.35836	-6.26681
Rathmines	Jan 1975 – Jul 2003	53.32206	-6.26680
Custom House	Jun 1964 – Mar 1981	53.34816	-6.25055
Ballyfermot	Jan 1975 – Jun 2003	53.34015	-6.34389
South Quay	Jan 1964 – Mar 1981	Exact Location Unknown	
Ringsend	Jun 1965 – Jul 2009	53.339614	-6.2159495
Clontarf	Jan 1975 – Aug 2008	Exact Location Unknown	
East Wall Road	Jan 1964 – Jun 1966	Exact Location Unknown	
Alexandra Road	Jan 1975 – Mar 1981	Exact Location Unknown	
Finglas	Jan 1975 – Jun 2009	Exact Location Unknown	
Cornmarket	Feb 1963 – Mar 1981	53.343253	-6.2753352
Baggot Street*	May 1963 – Feb 1979	53.333803	-6.2432048
Herbert Street*	May 1979 – Mar 2003	53.335233	-6.2462708
Bluebell	Apr 1980 – Mar 2003	Exact Location Unknown	
St James' Gate	Jan 1964 – Dec 1971	Exact Location Unknown	
Brunswick Street	Apr 1994 – Mar 2002	53.35054	-6.278125
Mountjoy Square	Apr 1994 – Mar 2000	53.35676	-6.259064
Cabra	Apr 1994 – Jun 2009	Exact Location Unknown	
Crumlin	Apr 1994 – Jun 2009	53.319584	-6.315179
Whitehall	Apr 1994 – Feb 2000	Exact Location Unknown	
Raheny	Apr 1994 – Apr 2000	Exact Location Unknown	

*Sites used for further detailed analysis

5.2.3. Data Acquisition for London, Belfast and Paris

The BS and SO_2 data for Belfast and London were both acquired from the Department for Environment, Food and Rural Affairs (DEFRA) archive, www.uk-air.defra.gov.uk. This database provides information on air quality, both current and historical, as well as all data previously gathered by stations in the UK monitoring networks. BS data for Paris were obtained from L'Obseratoire de l'air en Ile-de-France. The measurements were made at Laboratoire d'Hygiène de la Ville de Paris, located in the 13th Arrondissement (shown in *Figure 5.4.*). The data was provided as a "winter-time" average from 1956/1957 to 2017/2018. The "winter-time" period in this instance ran from October 1st to March 31st of the following year. The European BS measurement standard is different to that employed in the United Kingdom (OECD in Europe and BSI in the United Kingdom). In order to compare the two measurements, a conversion was required (Quincey, 2007) The equation used is detailed below;

$$BS_{British} = BS_{OECD} * 0.8667$$

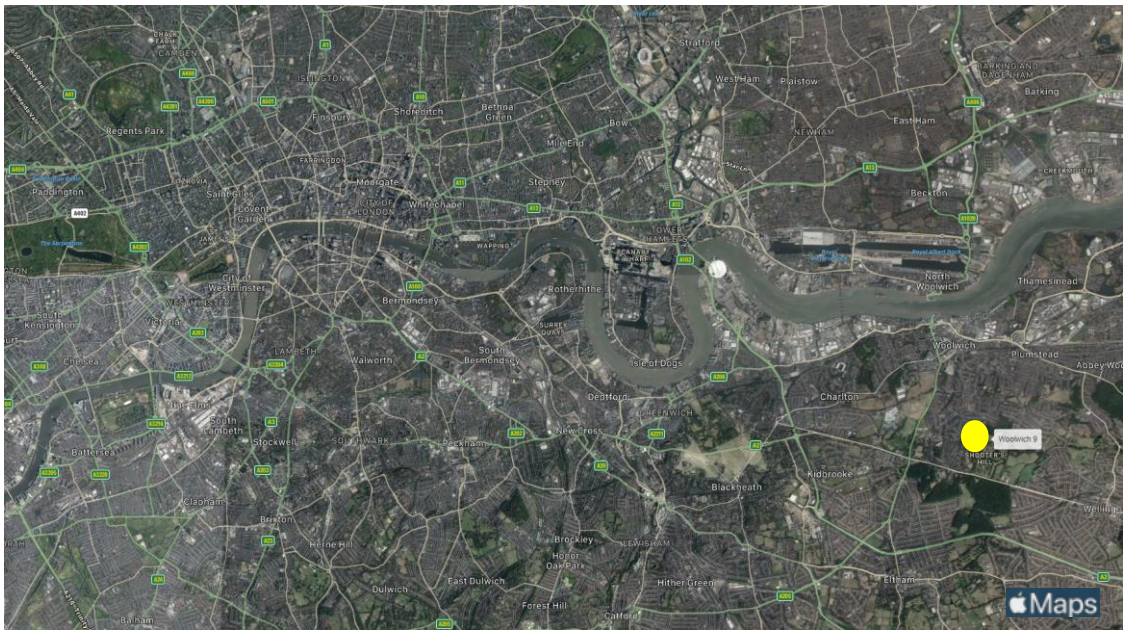

Figure 5.2. Map of London with the location of the Woolwich 9 measurement site marked (yellow).

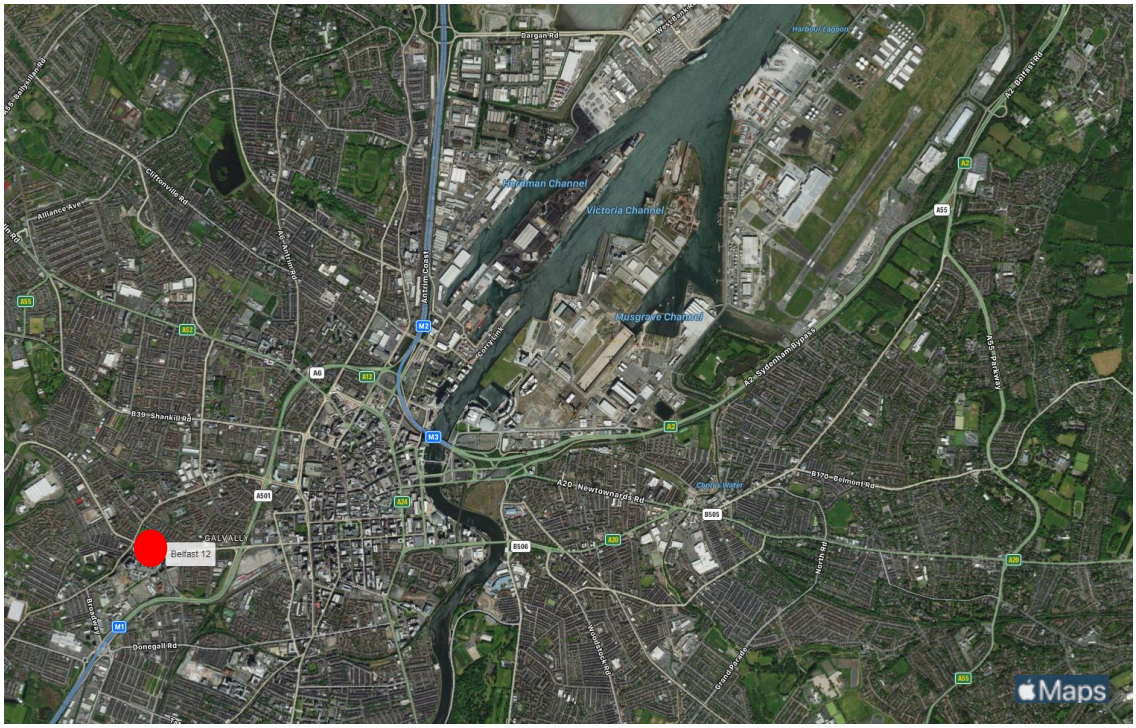

Figure 5.3. Map of Belfast with the location of the Belfast 12 measurement site marked (red).

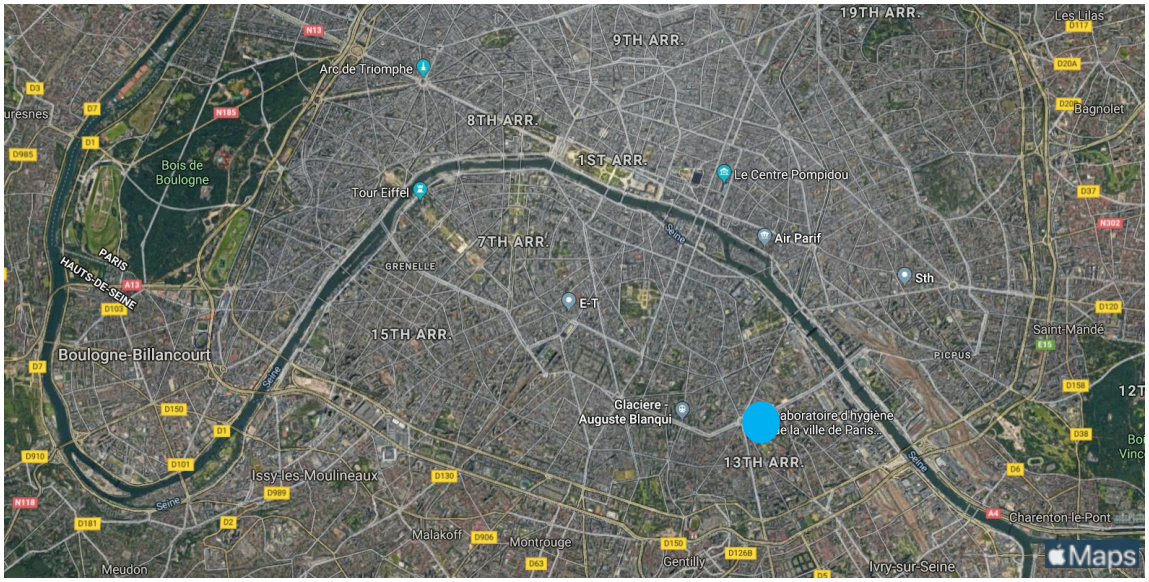

Figure 5.4. Map of Paris with the location of the measurement site marked (blue).

In order to compare the different locations, a single site was selected in each city. Details of the selected locations are provided below in *Table 5.2.* For Belfast, London, and Paris, a single measurement site was in operation for the entire study period. As stated previously, this was not the case in Dublin, and a combination of Baggot Street and Herbert Street was selected. These sites were selected as a full

timeline of BS measurements were available at these locations, while other sites had large interruptions or closures during the study period.

Table 5.2. Monitoring location details of the sites selected for the comparison of historical pollution trends.

City	Site Location	Latitude	Longitude
Dublin	Baggot Street and Herbert Street	53.343253 and 53.335233	-6.2432048 and -6.259064
Belfast	Royal Victoria Hospital, Grosvenor Road	54.594256	0.073398312
London	Shrewsbury Park, Woolwich	51.472720	0.073398312
Paris	Paris Hygiene Laboratory, 13th Arrondissement	48.828900	2.359240

The temporal trends for these representative sites in each city were compared and related to the various legislative changes introduced during the study period. Legislative acts introduced by the Government of Ireland were found using the Irish Statute book (Government of Ireland, 2019). The legislative changes introduced in Belfast and London are available from the National Archives of the UK (The National Archives, 2019). Finally, the legislative changes enacted by the European Union were found using the European Union law library (European Union, 2019).

5.3. Results and Discussion

5.3.1. Pollution Trends and Legislative Changes in Dublin

Monthly average concentrations of BS and SO_2 at all monitoring sites in Dublin from 1963 to 2003 are shown in *Figure 5.5* and *Figure 5.6*, respectively. A clear seasonal pattern is apparent, with much higher concentrations observed in the colder months, and lower concentrations in the warmer months. Monitoring sites located in the city centre were more polluted initially, e.g. Baggot Street and East Wall Road, while concentrations at monitoring locations in the suburban areas were among the lowest, with significant concentrations still observed during the colder months, e.g. Clontarf. A gradual decrease in winter-time peaks was observed during early 1970s, followed by a plateau. Further increases were recorded in the 1980s before a significant reduction after 1990. Outliers in this trend were observed during 1979 and the winter of 1981/1982. The highest concentrations in 1979 were measured in Ballyfermot, a residential area outside the city centre.

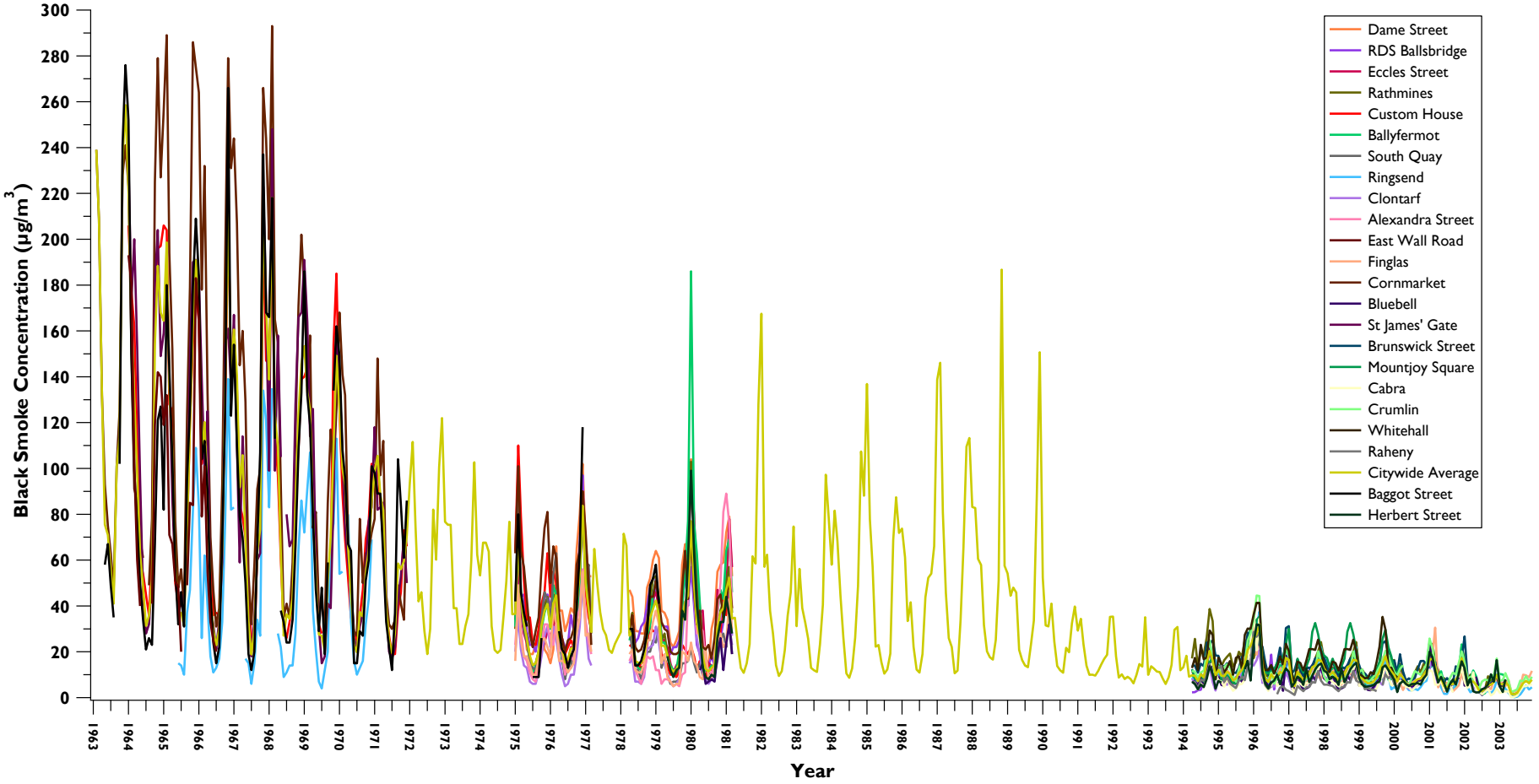

Figure 5.5. Monthly average BS concentrations (µg/m^3) at all monitoring sites in the Dublin city area 1963 – 2009. Citywide average value (µg/m^3) is also shown.

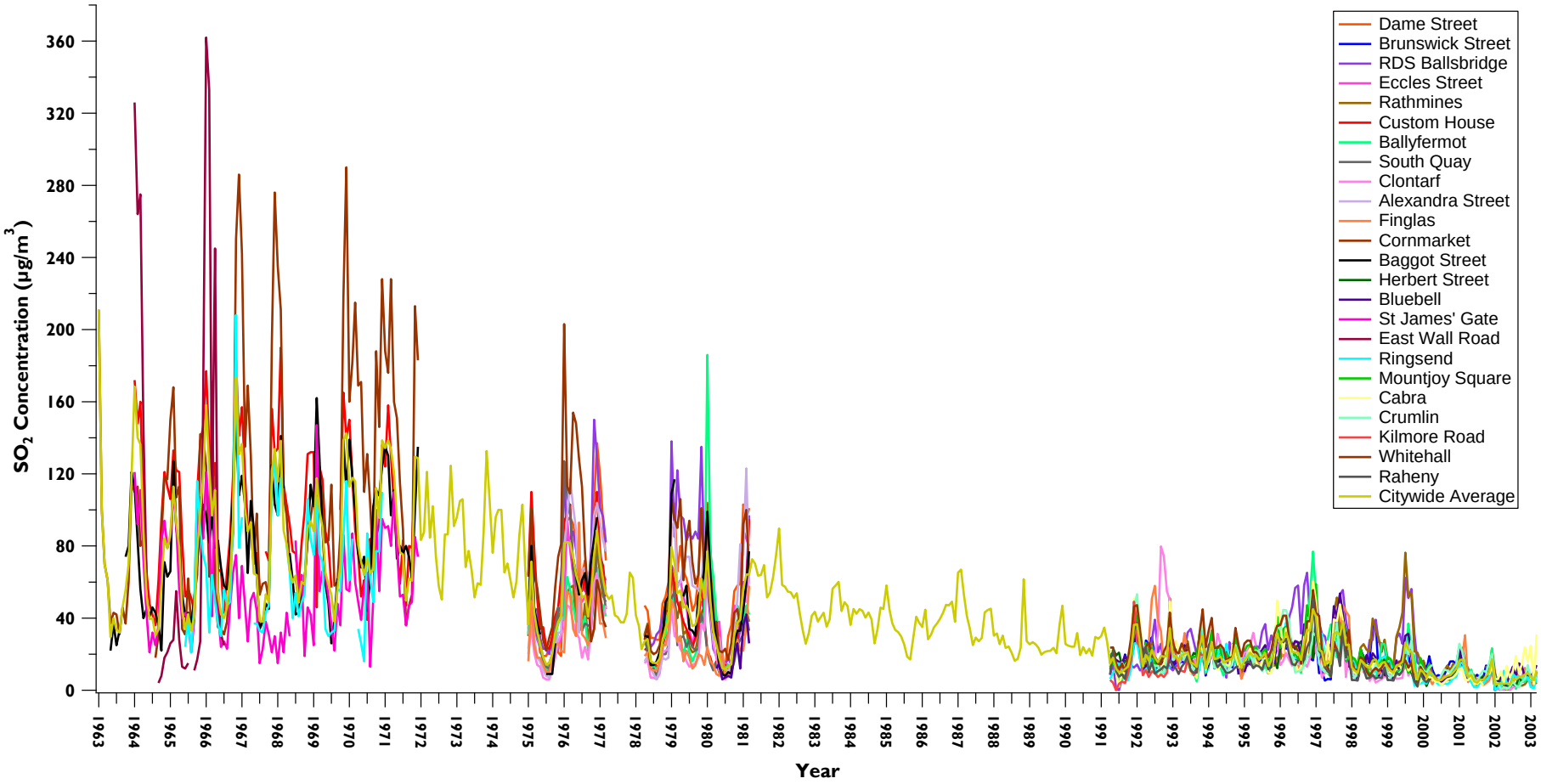

Figure 5.6. Monthly average SO_2 concentrations (µg/m^3) at all monitoring sites in the Dublin city area 1963 – 2003. Citywide average value (µg/m^3) is also shown.

The temporal trends of BS and SO_2 in Dublin can be more easily assessed by considering measurements made at one urban background location that is deemed representative of the city. As outlined above, the combination of the Baggot Street and Herbert Street sites was selected for this purpose and the representativeness of this location was investigated by examining the relationship between the monthly average concentrations of BS and SO_2 with the citywide average values. As shown in *Figure 5.7*, excellent correlations are obtained, thus confirming that the site is representative for the Dublin city area.

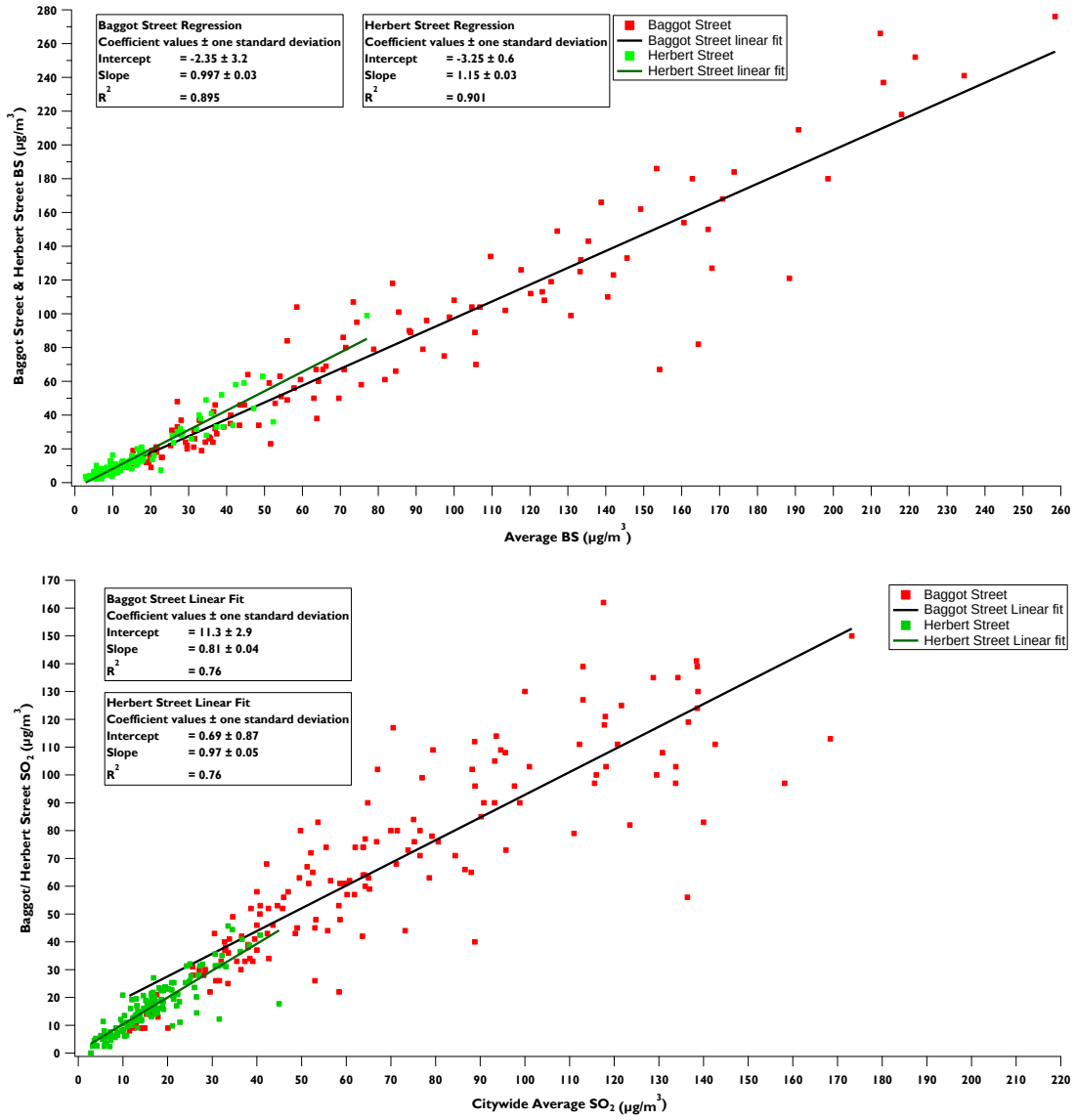

Figure 5.7. Correlation between monthly average pollutant levels at the Baggot Street/Herbert Street sites and the Dublin citywide average (n = 254).

Figure 5.8 shows the monthly average concentrations for BS and SO_2 at the combined Baggot Street and Herbert Street sites from May 1963 to March 2003. A clear seasonal pattern is apparent, with much higher concentrations of both pollutants measured during the winter months. The temporal trend follows the other sites very closely and is interpreted in relation to the changes in legislation below.

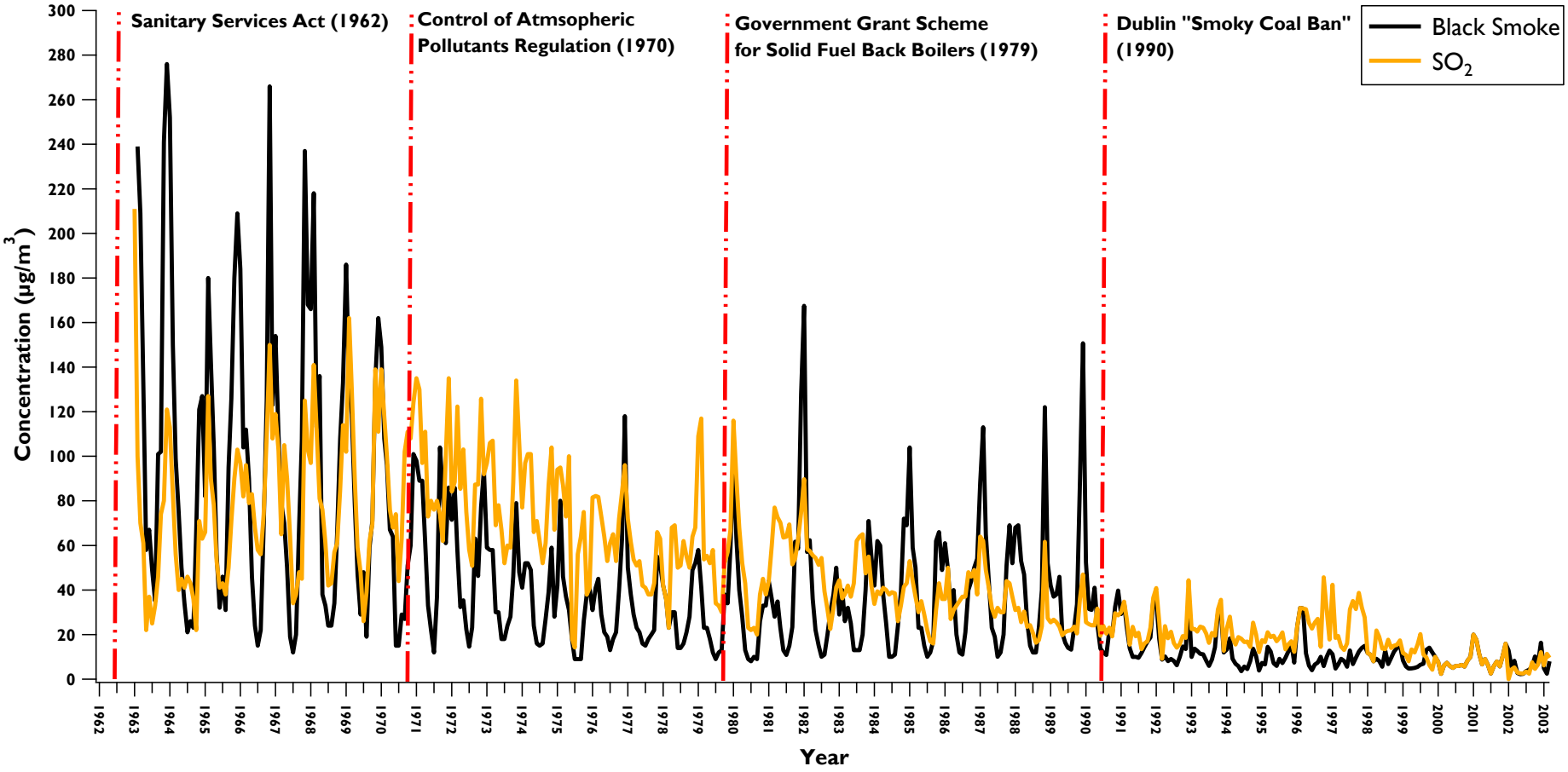

Figure 5.8. Monthly average concentrations of black smoke (black) and SO_2 (yellow) in Dublin city from Baggot Street and Herbert Street (1963 – 2003), supplemented by citywide average values (1972 – 1974, 1977 – 1978, and 1981 - 1994). Some key legislative changes are marked in red.

The first piece of legislation that dealt with air pollution in Ireland was the *Local Government (Sanitary Services) Act* (No. 26 of 1962). Section 10 of this Act, *Control of Pollution in the Atmosphere*, enabled local authorities to regulate sources of "smoke, dust, grit or gas". As indicated in *Figure 5.8*, this did not have a significant impact on BS or SO_2 concentrations and in 1970, the act was supplemented by the *Control of Atmospheric Pollution Regulations* (1970), which outlined the definitions of "dark smoke" and "black smoke", according to the Ringlemann chart (1967), and set limits for emissions of these pollutants. The introduction of this act coincided with a clear decrease in monthly average BS values between 1970 and 1975 (*Figure 5.8*). In 1973, Ireland became a member of the European Economic Community (EEC), and was subject to new regulations and further legislative changes, which are discussed in Section 5.3.4.

In response to the global oil crisis of 1973/74, the Government of Ireland made efforts to reduce its dependence on imported oil by setting the value-added tax (VAT) on solid fuels to 0% (Finance (No. 2) Act, 1975). Following this reduction in the price of solid fuels, the concentrations of BS and SO_2 increased significantly from 1976 to 1989. A noteworthy spike in concentrations during the winter of 1981/1982 can be attributed to an unusually cold period, while the general rise in pollution levels up to 1989 can be related to the increased use of coal, peat and wood for home heating. There were two key factors behind this increase. The first was the introduction of "House Improvement Grants to Reduce Dependence on Oil" brought in by the Department of the Environment in 1979 (DCC, 2009), which led to a large number of house owners installing coal-fired back boiler systems. The second factor was the introduction of the Turf Development Scheme by the Irish Government (Government of Ireland, 1981), which provided grants for private turf producers to increase production. It is estimated that the production of peat based products by private producers rose from 350,000 tonnes of peat in 1983 to 1.4 million tonnes in 1990 (Bord na Móna, 2006).

The high levels of air pollution resulting from the widespread combustion of solid fuels prompted the Irish government to introduce the *Air Pollution Act* (1987). This act defined air pollution as "a condition of the atmosphere in which a pollutant is present in such a quantity as to be liable to i) be injurious to public health, or ii) have a deleterious effect on flora or fauna or damage property, or iii) impair or interfere with amenities or with the environment". The act provided a framework for

establishing air quality management plans and for setting air quality standards, initially at the discretion of individual local authorities, and also introduced regulations concerning acceptable fire place designs. Under this act, a wide variety of additional legislation was introduced, including the national air quality standards (1987b). This act adopted the existing standards set down by the EEC in relation to SO_2, suspended particles, lead and NO_2 (see Section 5.3.4). Also under this act, regulations were introduced limiting fuel use in certain areas of Dublin city, and establishing special control areas (Government of Ireland, 1988a, 1988b).

The Air Pollution Act was followed by the *Retail Sale of Solid Fuel Regulations* (1989) that required retailers to stock "smokeless" or "low-smoke" alternatives to existing fuel types, namely Bord na Móna peat briquettes and Rheinbraun union nuggets/briquettes. This resulted in a reduction of BS concentrations from 1988/1989 to 1989/1990. The largest reduction, however, came with the implementation of the *Marketing, Sale, and Distribution of Fuels Regulations* (1990). This regulation prohibited the sale and distribution of bituminous coals in a pre-defined area of Dublin, and is more commonly referred to as "the Smoky Coal Ban". The introduction of the ban resulted in a 65% reduction in BS concentrations from the winter (November, December and January) of 1989/1990 to the winter of 1990/1991. This has been linked to significant improvements in the health of the population and a reduction in premature deaths resulting from air pollution (Clancy *et al.*, 2002; Goodman *et al.*, 2009). It is estimated that 58% of the observed reduction in BS concentrations was related to residents switching to non-solid fuels, while 42% was due to residents switching to low smoke alternatives. For SO_2, those figures were estimated to be 88% and 12% respectively (Jones *et al.*, 2005; McLoughlin, 2001). This ban has subsequently been extended to cover other large population centres around Ireland (Government of Ireland, 1994, 2000, 2003, 2004). Following the "Smoky Coal Ban", the Irish Environmental Protection Agency was established in 1992 with the *Environmental Protection Agency Act* (1992). This created a centralised entity that controlled measurement and enforcement of environmental parameters. In the remaining years of the study period and beyond, the legislation introduced by the Irish government was related to enforcing EU regulations on air pollution which addressed a range of pollutants, including SO_2, PM, O_3, and NO_x.

In a 2016 report, the North South Ministerial Council (NSMC) of Ireland highlighted the downward trend in solid fuel combustion in the Republic of Ireland

(Abbott *et al.*, 2016). The council noted that solid fuel use fell by 23% between the years 2000 and 2012. It was also noted that the use of manufactured fuels (anthracite and ovoids) increased by approximately 10% in the same period. This decrease in solid fuel use corresponds to a generally decreasing trend in BS and SO_2 emissions at the end of the study period from 2000 to 2003.

5.3.2. Pollution Trends and Legislative Changes in London

Figure 5.9 shows the monthly average concentrations for BS and SO_2 in London from October 1961 to December 2005. As for Dublin, a clear seasonal pattern is observed, with higher concentrations in the colder months and lower concentrations in the warmer months.

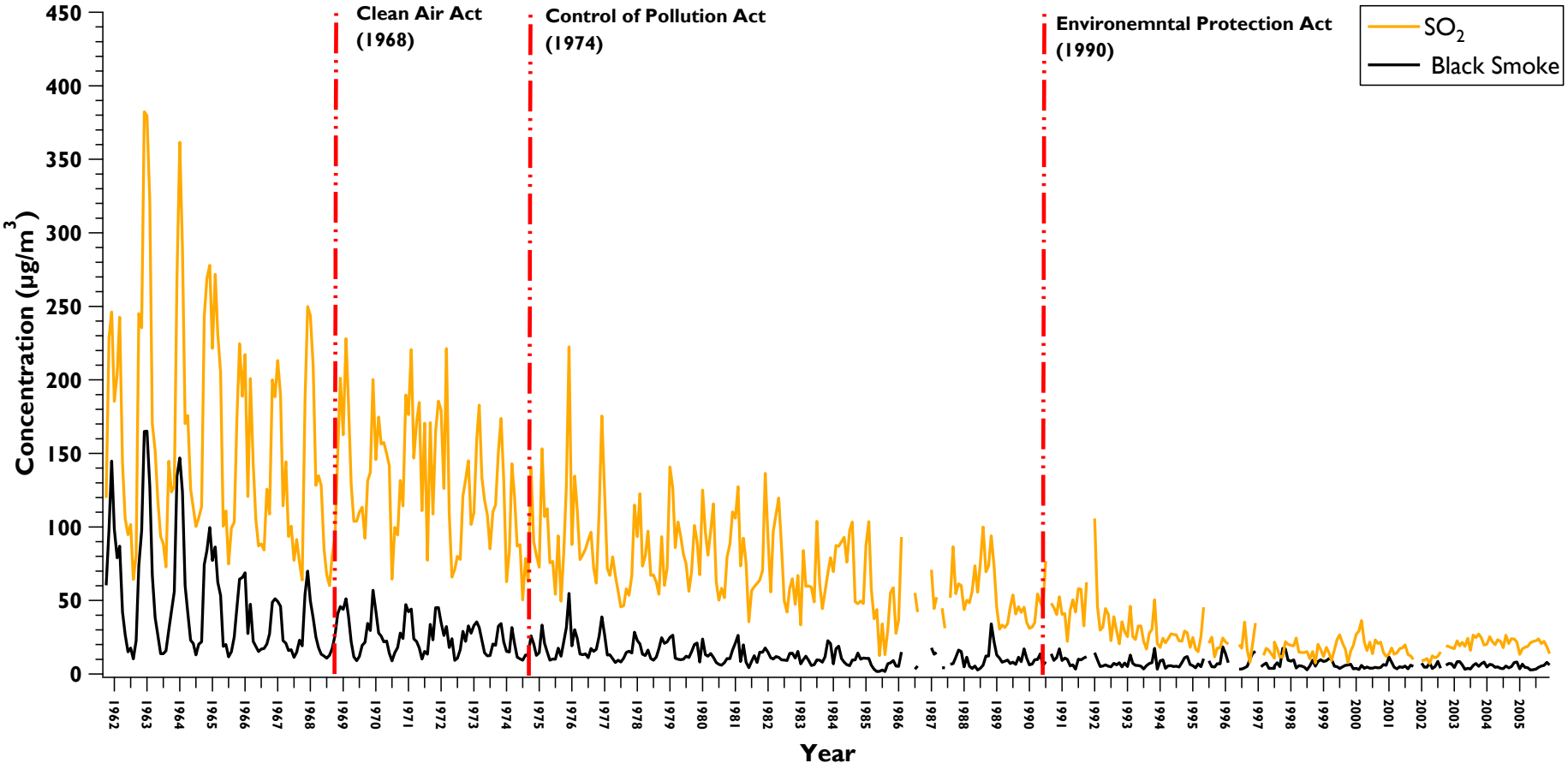

Figure 5.9. Monthly average black smoke (black) and SO_2 (yellow) concentration in London from "Woolwich 9" station (1961 – 2005). Some key legislative changes are marked in red.

Peter Brimblecombe provides a detailed description of air pollution in the United Kingdom, dating back as far as the bronze age, in his book "The Big Smoke" (1987). The first piece of legislation is the *Clean Air Act* of 1956 (Government of United Kingdom, 1956) which prohibited the emission of "Dark Smoke" from chimneys, introduced smoke control areas, and provided powers of enforcement to local councils (Longhurst *et al.*, 2016). The *Clean Air Act* was updated in 1968 (Government of United Kingdom, 1968) and prompted a decrease in BS concentrations in subsequent years. The concentrations of SO_2 remained relatively consistent until the introduction of the *Control of Pollution Act* (Government of United Kingdom, 1974). After the introduction of this Act, the concentrations of SO_2 began to decrease. The progress in reducing SO_2 concentrations was accelerated by the introduction of *The Oil Fuel (Sulfur Content of Gas Oil) Regulations* and *The Motor Fuel (Sulfur Content of Gas Oil)* (Government of United Kingdom, 1976b, 1976a). From 1976 to 1991, twenty commencement orders were introduced, consolidating the progress made by the previous legislative instruments. 1989 saw the introduction of three separate acts relating to air quality standards, smoke control, and industrial emissions (Government of United Kingdom, 1989a, 1989b, 1989c). These were followed in 1990 by the *Environmental Protection Act* that made provisions for improving the control of pollution originating from various industrial and domestic processes, and the *Oil Fuel (Sulfur Content of Gas Oil) Regulations* and *Motor Fuel (Sulfur Content of Gas Oil)* Regulations (No. 1096 and 1097 respectively) (Government of United Kingdom, 1990a, 1990c, 1990d). The Act from 1990 was reinforced by updates to the *Clean Air Act in 1993* (Government of United Kingdom, 1993) and the introduction of the *Environment Act* in 1995, specifically Section IV "*Air Quality*" (Government of United Kingdom, 1995). This section of the Act legislated for the establishment of a new Environmental Protection Agency, the unveiling of a new national air quality strategy, defined the responsibilities of different local authorities and specifically detailed the powers of the Mayor of London. These powers were further extended in 1999 with the *Greater London Authority Act*, which provided decision making abilities to the Mayor of London and the London Assembly (Government of United Kingdom, 1999). In particular, Part IX, "*Environmental functions"* provided details on the Mayor's air quality action plan, as well as the responsibilities of the Assembly. This Act was added to in 2007 with a second *Greater*

London Authority Act that provided details on climate change and energy strategies (Government of United Kingdom, 2007).

5.3.3. Pollution Trends and Legislative Changes in Belfast

Figure 5.10 shows the monthly average concentrations for BS and SO_2 in Belfast from January 1963 to December 2005. The seasonal pattern is once again present and the observed trend is similar to that of Dublin. As Northern Ireland is part of the United Kingdom, Belfast was governed by the same legislation as London, but with some differences over the decades.

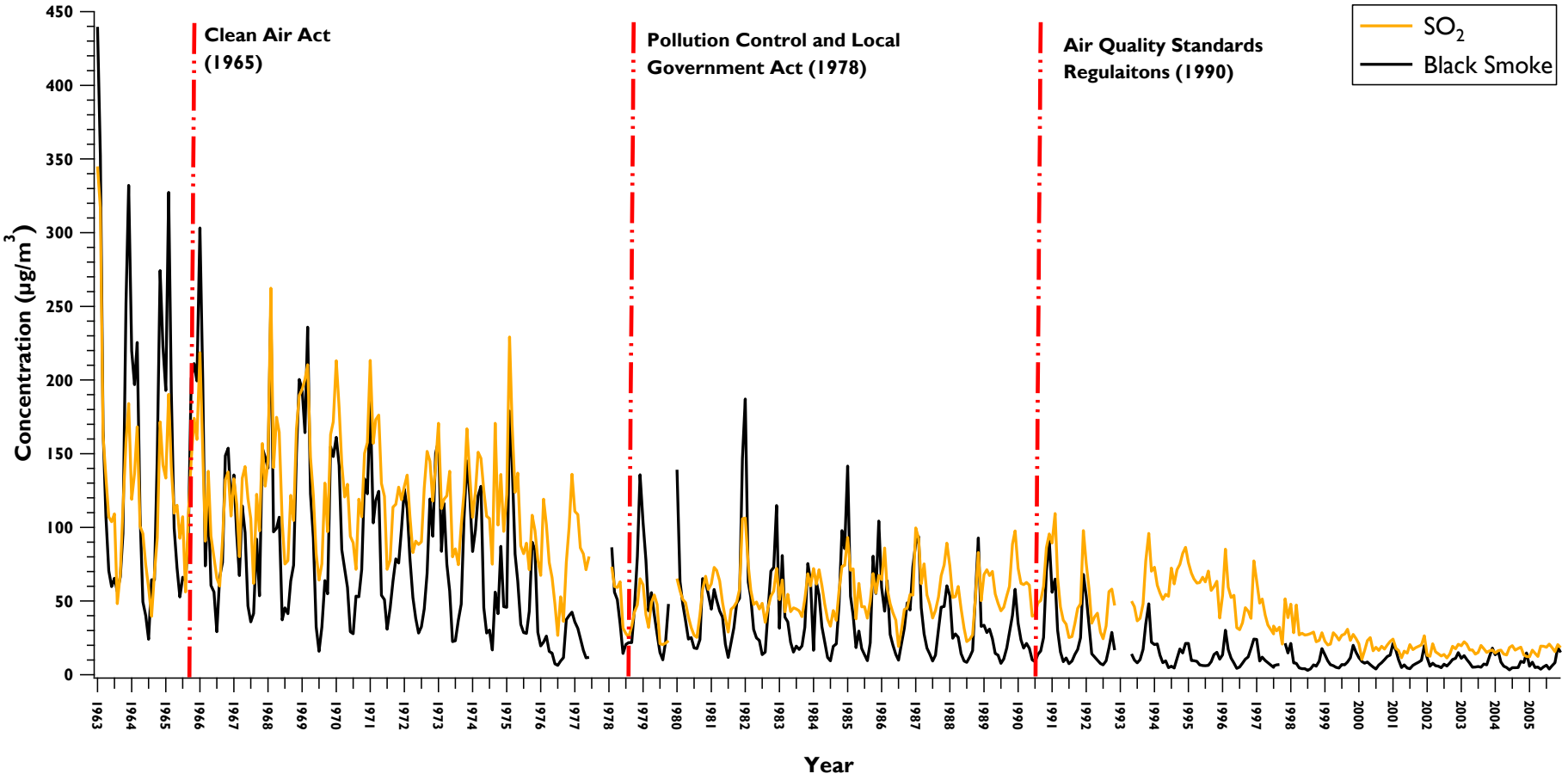

Figure 5.10. Average monthly black smoke (black) and SO_2 (yellow) concentrations in Belfast from "Belfast 12" station (1961 – 2005). Some key legislative changes are marked in red.

The first legislative change introduced in NI was the *Clean Air Act* of 1965, which came into effect under the name "*Dark Smoke (Permitted Periods) Regulations*" (1965). The introduction of the *Clean Air Act* in NI significantly reduced the measured concentrations from the winter of 1965/1966 to the winter of 1966/1967, where a 43% decrease in BS concentrations, and a 31% reduction in SO_2 concentrations were observed. In 1969, a grant was announced for the purpose of reimbursing the "owners or occupiers of private dwellings who have to incur expenditure on adaptions to their heating and cooking arrangements to comply with a Smoke Control Order" (Government of United Kingdom, 1969). The "Smoke Control Order" refers to *Smoke Control Areas Regulations* introduced between 1965 and 1969. A slight increase in concentrations occurred in the winter of 1974/1975 in the aftermath of the oil crisis. In 1976, two acts were introduced in an effort to reduce sulfur emissions, namely The Oil Fuel (Sulfur Content of Gas Oil) Regulations and The Motor Fuel (Sulfur Content of Gas Oil) Regulations. Following on from these acts, the *Pollution Control and Local Government (Northern Ireland) Order* was introduced in 1978. Part IV of this bill focused on air pollution, in particular the sulfur content of oil for use in engines or furnaces. This act resulted in a reduction in sulfur emissions in the following years. The next major act introduced in NI was the *Clean Air (Northern Ireland) Order* (1981) which defined the authorized fuels for the region, set the permissible levels of "dark smoke", also based on the Ringlemann chart, and defined the levels of smoke that are "prejudicial to health". The introduction of the *Clean Air Order* did not immediately result in a reduction in pollution levels. In fact, during the winter months of 1981/1982, an increase in concentration occurred, similar to the peak observed in the Dublin trend, due to the unusually cold period. In 1990, the *Air Quality Standards Regulations*, introduced in 1989 in the UK, were enforced in NI, and set out the air quality emission standards (Government of United Kingdom, 1990b). These standards were amended in 1994 and 1996 to reflect changing standards in Europe (Government of United Kingdom, 1994, 1996). Both BS and SO_2 concentrations decreased continuously after the introduction of these acts. That progress was consolidated in 2002 with the introduction of *The Environment (Northern Ireland) Order*, with Part III focusing specifically on air quality (Government of United Kingdom, 2002). This act detailed an air quality strategy for the region, designated air quality management areas, established powers for enforcing authorities, provided details on what constitutes an offence and provided information

on the financial assistance available for bodies attempting to perform air quality checks and/or develop new action plans. The *Environment Act* was enforced gradually between 2003 and 2018, corresponding to gradual decreases in SO_2 and BS concentrations. The final piece of legislation introduced during the study period, with the exception of updates and amendments to existing and regulations was *The Pollution Prevention and Control Regulations* (Government of United Kingdom, 2003). This established the "best available methods" for measurement of pollutants, defined the scope of the functions of those in charge of monitoring and enforcement, reviewed the existing permit process and updated the powers of inspectors. In the years following the study period, various updates and amendments were introduced in order to keep pace with EU legislative changes and reductions in recommended pollution levels.

5.3.4. Comparison of BS and SO_2 Trends in Dublin, Belfast and London

The trends in annual average BS concentrations for each location are presented in *Figure 5.11*. The concentrations measured in London were lower than both Dublin and Belfast for the entire study period. Belfast was the most polluted location for the majority of the period. The only exception to this is the period between 1987 and 1989 when Dublin became the most polluted location due to increased solid fuel burning in the city.

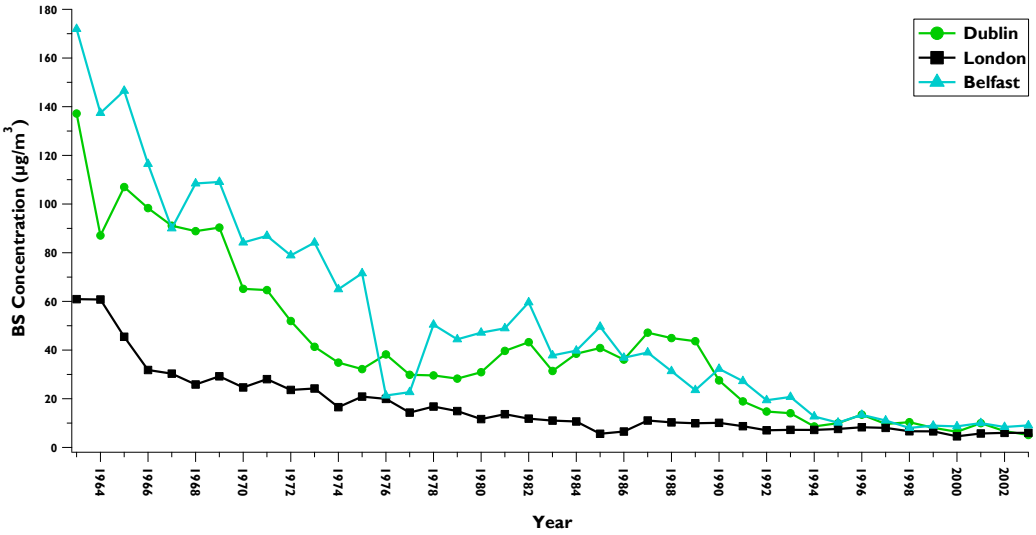

Figure 5.11. Annual average BS concentrations (µg/m^3) in Dublin (green), London (black) and Belfast (blue), 1963 to 2003.

The trends in annual average SO_2 concentrations for each location are presented in *Figure 5.12*. The concentrations measured in London were initially higher than in Belfast and Dublin, potentially due to the greater number of vehicles moving through the city. The SO_2 levels in London decline steadily throughout the study period as legislation regulating the sulfur content of fuels was introduced. From 1989 to 1999, the concentrations were highest in Belfast, while the annual average concentration at the conclusion of the study, in 2003, was once again highest in London.

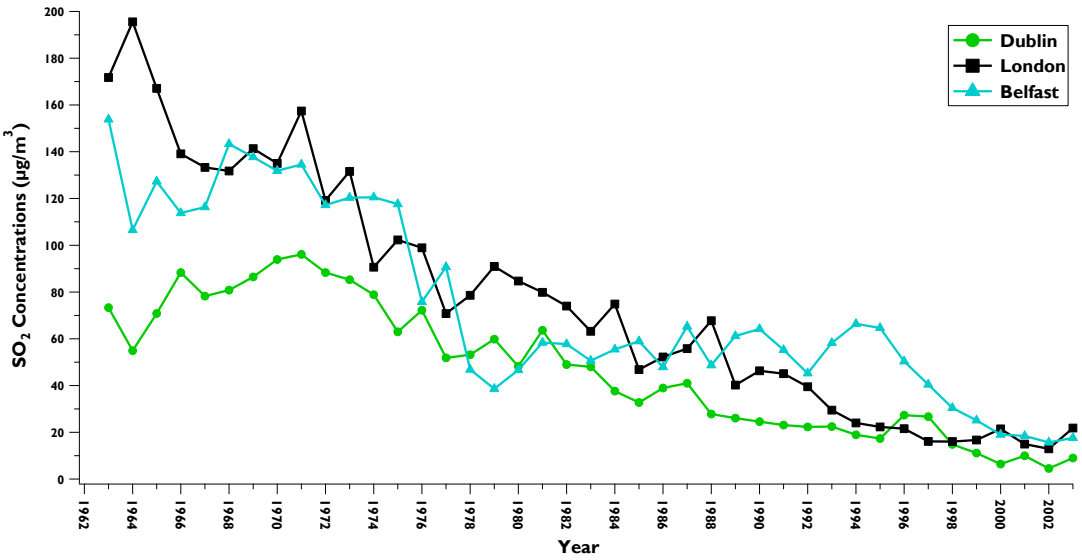

Figure 5.12. Annual average SO_2 concentrations (µg/m^3) in Dublin (green), London (black) and Belfast (blue), 1963 to 2003.

In order to compare the pollution trends in each city, the average monthly BS concentrations for each location were plotted against each other (*Figure 5.13*). The most closely related locations were Dublin and Belfast (slope = 1.03), in spite of the differences in legislation introduced over the study period. The relationships between London and Belfast and London and Dublin were largely the same. The slope of the regression for London and Dublin was 0.32, and the slope of the regression for London and Belfast was 0.27, indicating that the concentrations in Dublin and Belfast were much greater than those measured at the London location.

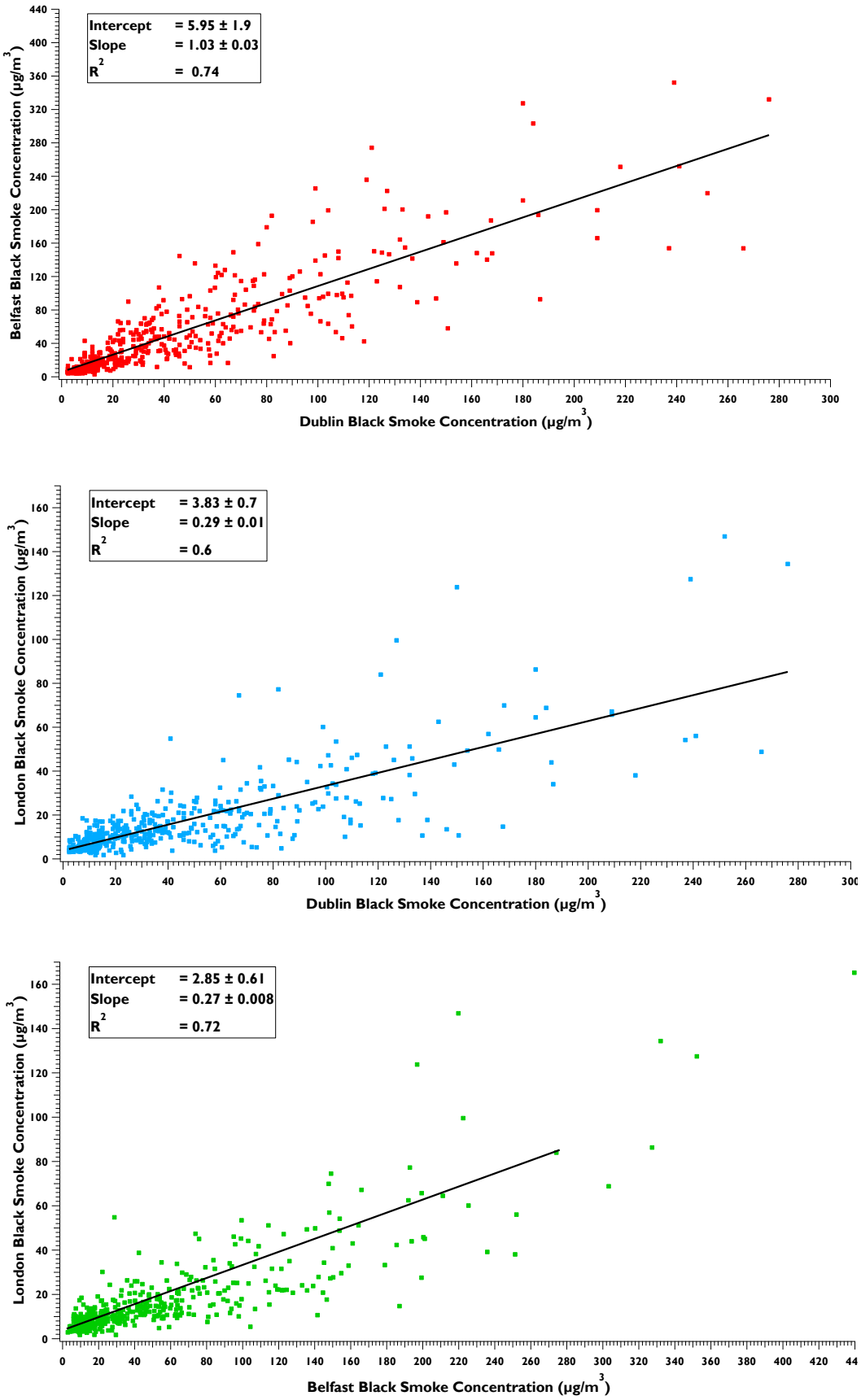

Figure 5.13. Comparison between Dublin and Belfast (top), Dublin and London (middle), and Belfast and London (bottom).

The relationship between BS and SO_2 emissions at each location was investigated using the ratio of BS to SO_2 (*Figure 5.14.*). This metric provides an indication of the type of fuel used. A lower BS:SO_2 ratio indicates the use of bituminous coal or other sulfur rich fuels. This parameter has been previously used by Penner *et al*. (1993) to investigate distinct regional differences in BC and sulphur emissions. As shown in *Figure 5.14*, a clear seasonal pattern is evident at each location, with the ratio increasing during the winter months, reflecting the higher BS concentrations due to increased solid fuel burning. The lowest ratios were in London, where it was consistently lower than 0.5, until the late 1990s. This is due to the fact that SO_2 was higher than BS concentrations in London for the majority of the study period (*Figure 5.10*). The most dramatic series of ratio increases occurred in Dublin during the late 1980s when elevated BS concentrations were observed due to the increased use of solid fuels for home heating. The trend for Belfast is generally similar to that for Dublin, with the exception of the late 1980s and the winters of 1978/1979 and 1979/1980, when a spike in BS values occurred in Belfast (*Figure 5.14*).

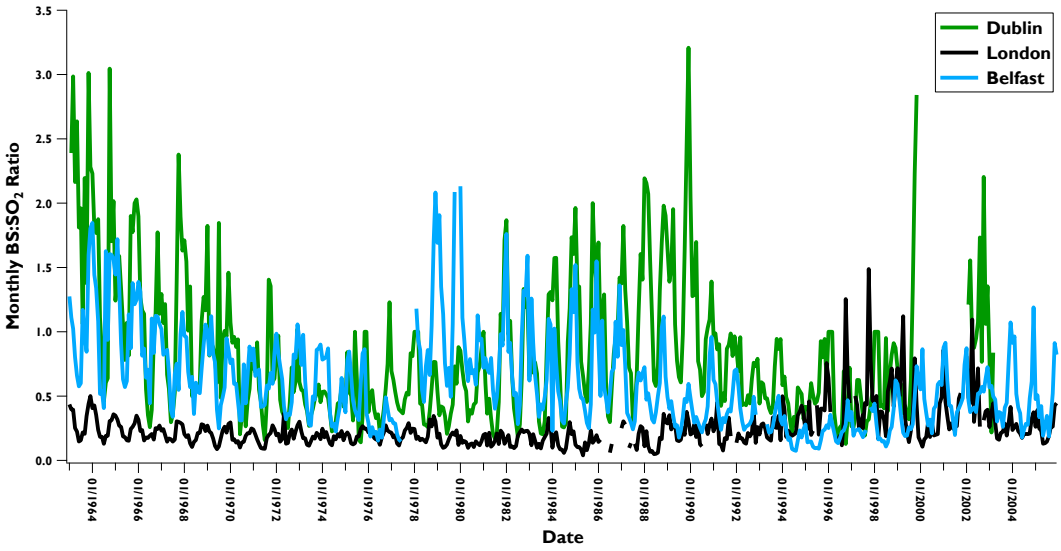

Figure 5.14. Monthly BS:SO_2 ratios 1964 – 2003 for Dublin (green), London (black) and Belfast (blue).

A noticeable demarcation in the trends of SO_2 and BS occurred in Belfast and London after the introduction of *The Oil Fuel (Sulfur Content of Gas Oil) Regulations* and *The Motor Fuel (Sulfur Content of Gas Oil)* acts in 1976. This is illustrated by the regression of SO_2 and BS from 1963 to 1976, and from 1977 to 2005 for Belfast (*Figure 5.15.*) and London (*Figure 5.16.*).

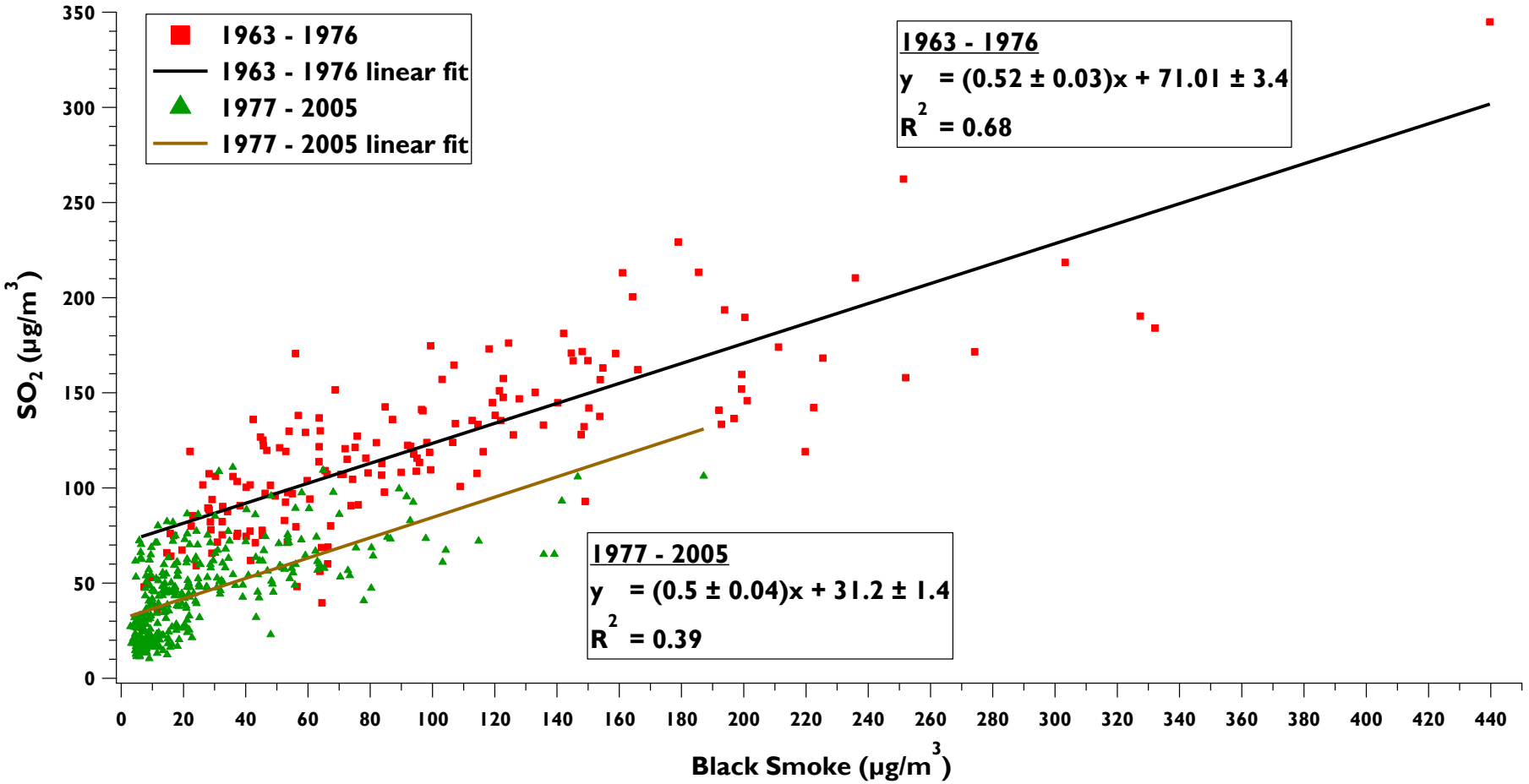

Figure 5.15. Comparison of SO_2 and BS concentrations in Belfast before 1976 (red) and after 1976 (green).

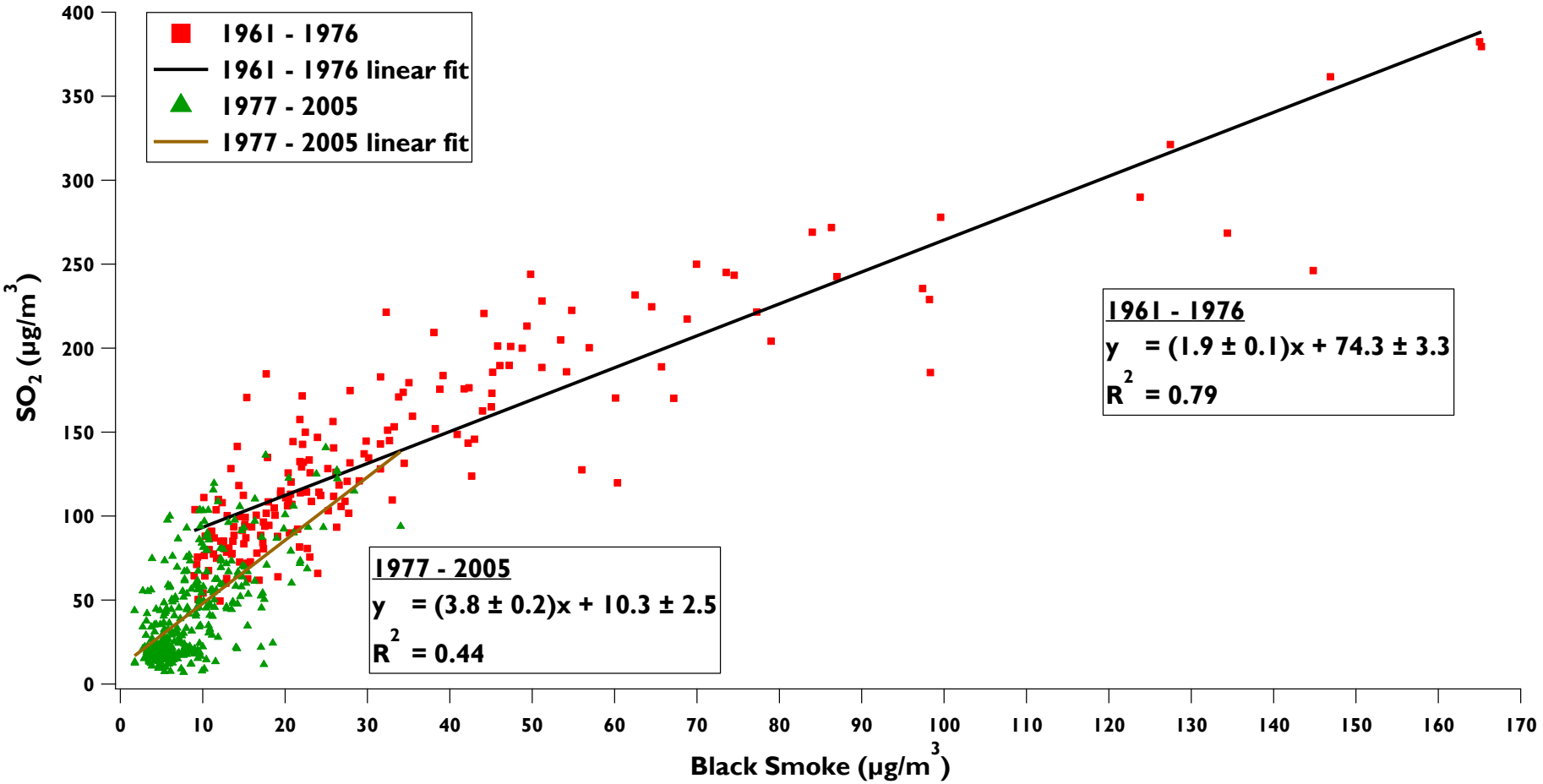

Figure 5.16. Comparison of SO_2 and BS concentrations in London before 1976 (red) and after 1976 (green).

In Belfast, while the ratio is similar for the two periods, the correlation between the two parameters is significantly decreased during the later period, 1977 – 2005. It is also apparent that the concentrations of SO_2 and BS are reduced after 1977. In London, a similar pattern is observed in terms of the correlations (0.79 from 1963 – 1976, and 0.44 from 1977 – 2005). This shows that the sources of SO_2 and BS are not as closely related after the introduction of the acts in 1976.

5.3.5. Pollution Trends in Paris and Legislative Changes in Europe

In addition to the legislative changes enacted in the individual countries, the cities were also subject to the regulations and acts introduced by the European Economic Council, and later, the European Union. The historical trend in BS concentration for Paris, France, is shown in *Figure 5.17*. The winter-time average (October 1st – March 31st) shows a large reduction over the period 1955/1956 to 2005/2006.

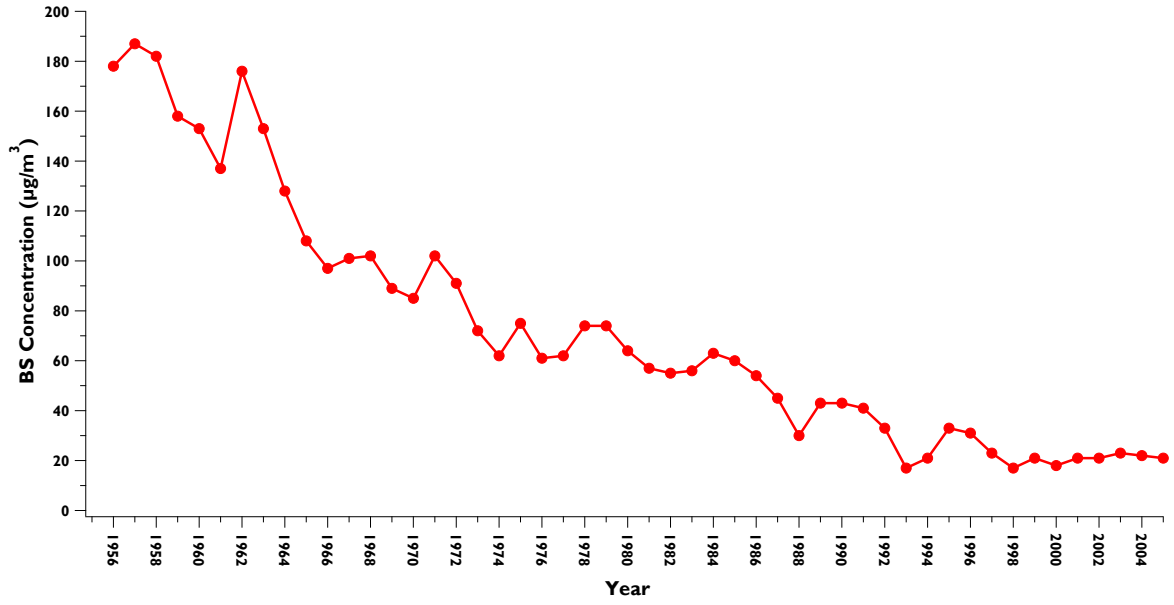

Figure 5.17. Winter-time BS concentrations (µg/m^3) in Paris, France (1955/1956 – 2005/2006).

The first piece of legislation introduced during the study period was Council Directive *70/220/EEC* in 1970 (Council of the European Union, 1970). This directive required all member states to update their laws regarding gaseous air pollution from motor vehicles and was continuously updated to incorporate technological advancements. This was followed in 1972 by Council Directive *72/306/EEC* (Council

of the European Union, 1972), which required member states to align their legislation on controlling emissions from diesel engines. In 1975, Council Directive *75/716/EEC* established a common law for limiting the sulfur content of liquid fuels (Council of the European Union, 1975). The introduction of these acts contributed to the observed decline in winter time concentrations in Paris during the 1970s. In 1980, a directive targeting the SO_2 and suspended particle emissions was passed by the Council (80/779/EEC, 1980). This directive established limits for the two pollutants, and resulted in a further decline in their concentrations. Over the next decade, a series of directives were passed targeting gaseous emissions from engines and setting limits for a number of pollutants, including lead and nitrogen oxides. In 1990, the European Environment Agency and the European Environmental Information Observation Network were established (Council of the European Union, 1990). In 1992, amendments were made to directives related to limiting the pollution from motor vehicles (European Commission, 1992). This was followed by a directive targeting the emissions from diesel engines (96/1/EC) and a directive focused on ambient air quality assessment and management procedures (96/62/EC), both passed in 1996. In 1999, a Council directive was issued further limiting the permissible concentrations of SO_2, NO_2 and other oxides of nitrogen, PM and lead in ambient air (1999/30/EC, 1999). Each of these legislative changes likely contributed to the gradual reduction in BS values throughout the 1990s, with concentrations showing a plateau from 1998 until the end of the timeline in 2005/2006.

Figure 5.18 shows the comparison between winter time (October 1st – March 31st) average BS concentrations for Dublin, London, Belfast and Paris. Initially, the concentrations measured in Belfast and Dublin were higher than those recorded in London and Paris, the two larger cities in the study. During the 1970s and 1980s, London consistently showed the lowest BS concentrations of the four cities, while similar levels and trends were observed in the other three cities. BS concentrations measured in Dublin during the late 1980s were the highest of all the locations for a period of three years, 1987 to 1989. After the introduction of the "Smoky Coal Ban", the winter-time concentrations in Dublin decreased significantly, and by the mid-1990s, Paris was the most polluted city in the study.

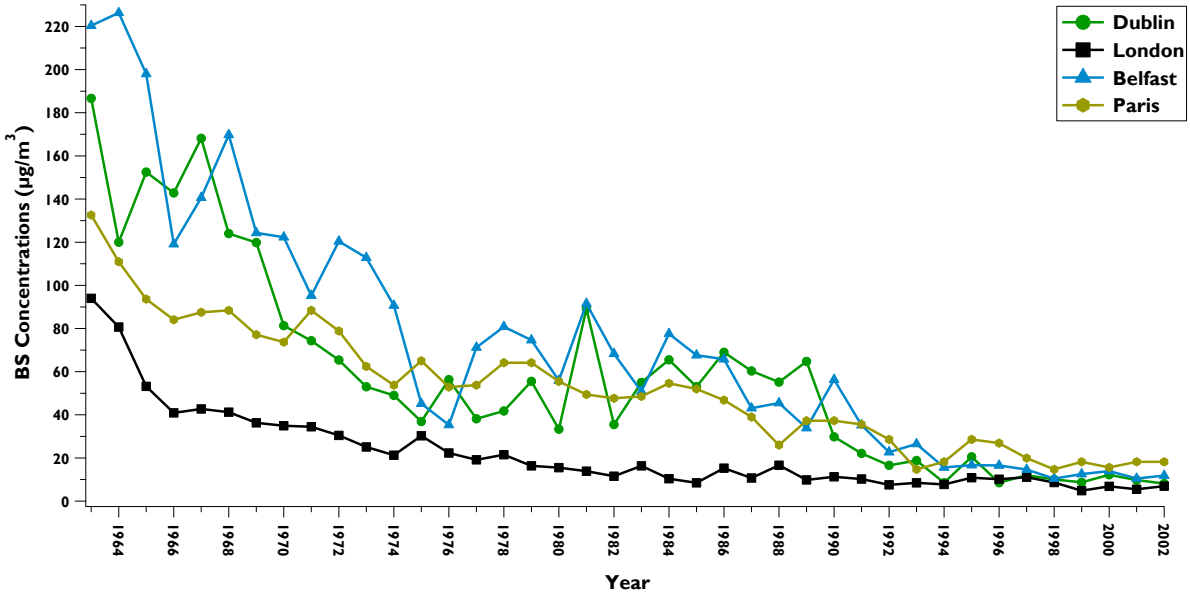

Figure 5.18. Winter-time average BS concentrations in Dublin (green), London (black), Belfast (blue) and Paris (yellow) from the winter period (October 1st to March 31st) of 1963/1964 to the winter period of 2002/2003.

5.3.6. Comparison with Modern Measurements

As part of the AEROSOURCE project, measurements of equivalent Black Carbon (eBC), have been made on the campus of University College Dublin (Lin *et al.*, 2018). In order to compare the eBC data with the historical BS measurements, the equation developed by Heal and Quincey (2012) was used to convert BS values to BC values. It should be noted that there is a distance of approximately 4 km between the locations of the historical measurements and modern day measurements. The average annual BC concentrations between 1963 and 2017 are presented in *Figure 5.19*. The average eBC for the final full year of measurements (where 12 months of measurements were available) with the old black smoke network, 2002, was 1.79 µg/m^3. The annual average eBC concentration for the year 2017, the only full calendar year covered during the AEROSOURCE project, was 0.51 µg/m^3.

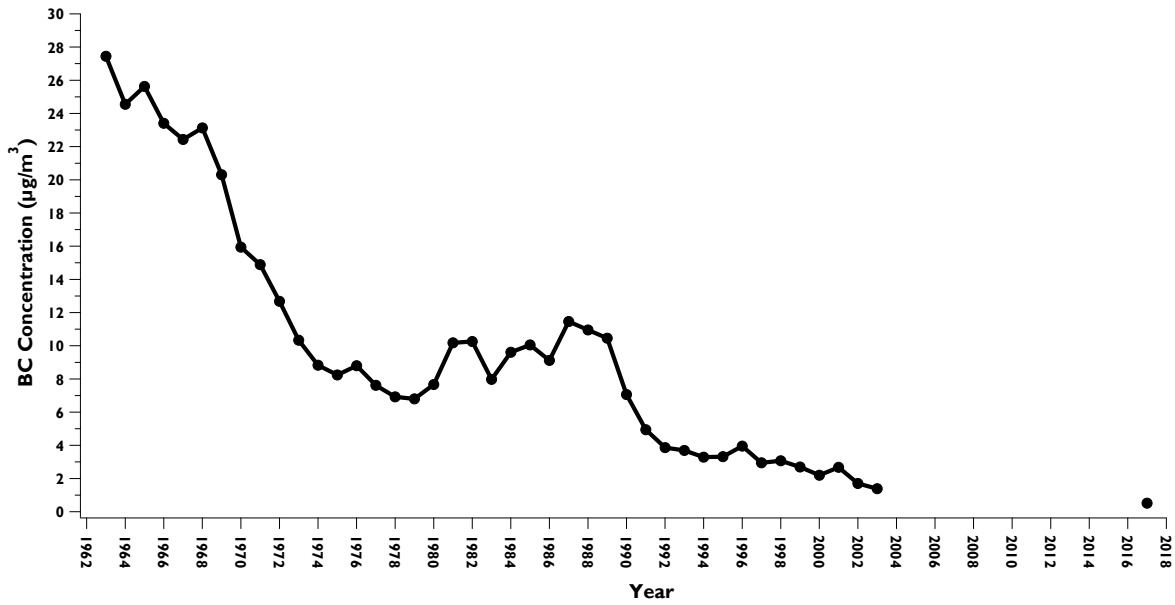

Figure 5.19. Annual average calculated BC concentrations (µg/m^3) in Dublin, 1963 – 2017.

Daily average eBC concentrations from the UCD monitoring location were compared to eBC concentrations measured in London and Belfast during 2017 (*Figure 5.20*). The London site is in North Kensington, while the Belfast site is located in the city centre. Over the course of the year the average eBC concentrations in Dublin were generally the lowest of the three locations, with an annual average of 0.55 ± 0.71 µg/m^3. However, there were a number of spikes in pollution, especially during the winter months, e.g., the highest daily average concentration at all three sites, 10.2 µg/m^3, was observed in Dublin on 18 December 2017. The monthly average eBC concentrations show similar seasonal patterns in all three cities (*Figure 5.21*). Higher concentrations were measured in the colder months, particularly in Belfast. This is most likely due to domestic solid fuel burning. The highest concentrations measured during the summer months were recorded at the London site, which experiences higher traffic volumes.

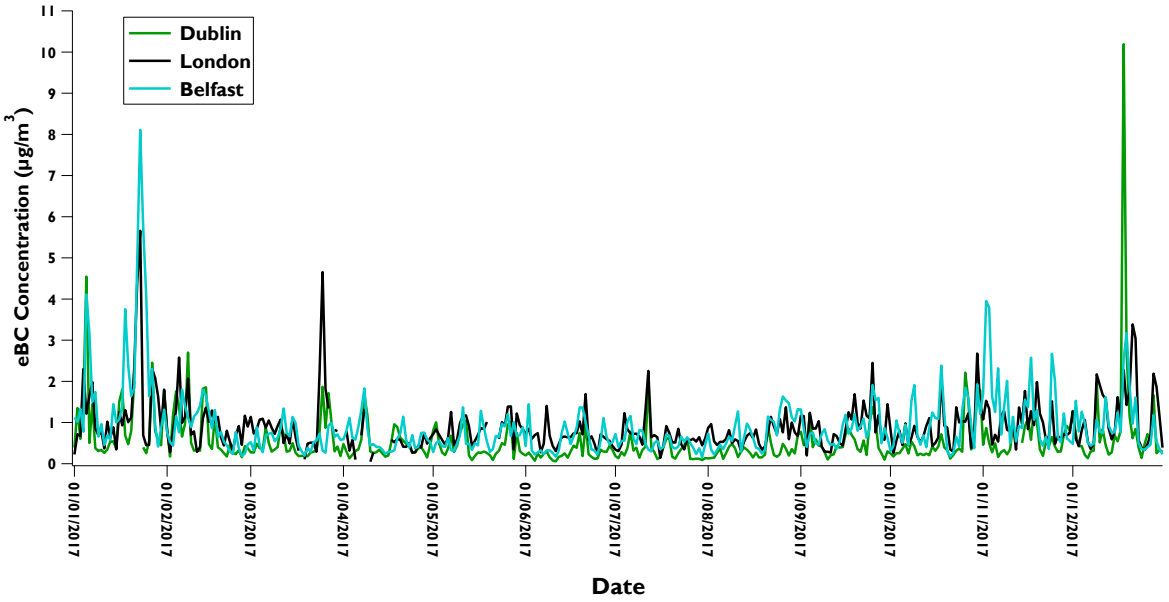

Figure 5.20. Daily average eBC concentrations (µg/m^3) for 2017 at sites in Dublin (green), London (black) and Belfast (blue).

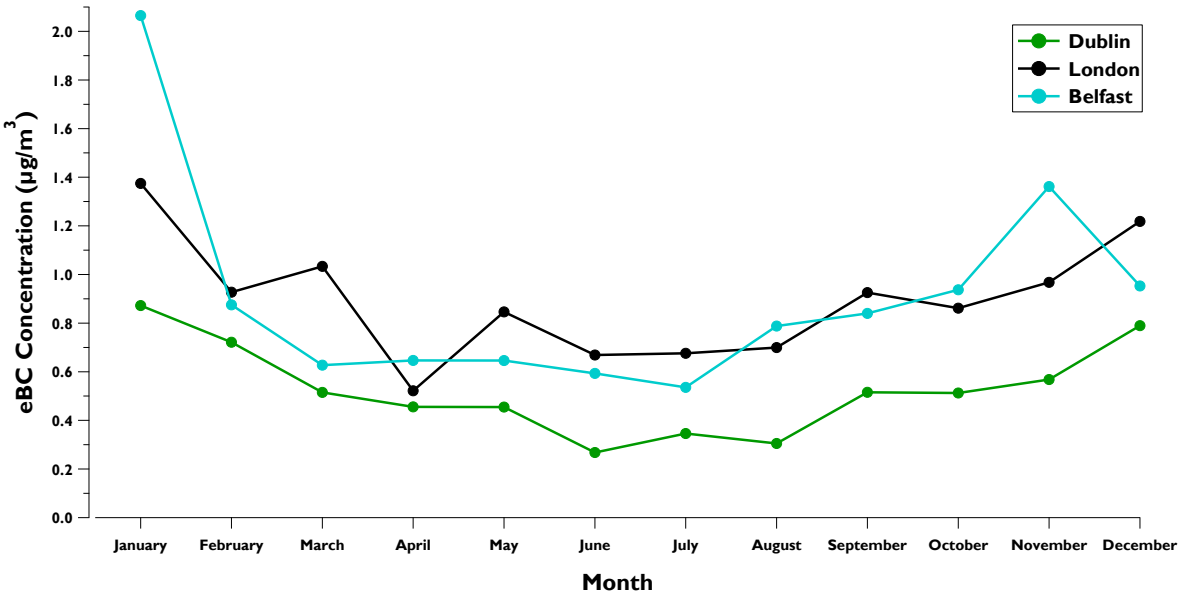

Figure 5.21. Monthly average eBC concentrations (µg/m^3) for 2017 at sites in Dublin (green), London (black) and Belfast (blue).

5.4. Conclusions

It is clear that the introduction of new legislation has led to reductions in BS and SO_2 concentrations in all of the cities included in this study. For Dublin, the annual average Black Smoke concentration was 137.18 μg/m^3 in 1963, while the annual average for 2002 was 6.74 μg/m^3. This represents a decrease of 96.27% over the 39 year period in Dublin city. For London, a decrease in BS concentration of approximately 92.1% was observed between the years of 1963 and 2005, and for the same time period in Belfast, a 96.6% decrease was measured. As the legislative action introduced in London and Belfast were largely similar, it would be reasonable to assume the trends in pollution would be similar. This however was not the case, as illustrated by *Figure 5.13*. In fact, the BS concentrations in Belfast were strongly correlated with those measured in Dublin (R^2 = 0.74, slope = 1.03), potentially due to the similar fuel burning habits in both locations. The relationship between Belfast and London was not as strong in terms of measured concentrations (R^2 = 0.72, slope = 0.27). This could be due to slight differences in the dates that the new acts were introduced as there were often delays of up to a year between the commencement of new laws in Great Britain and in Northern Ireland. The lower concentrations measured in London from the beginning of the study period were due to the conscious efforts made to reduce air pollution in the city following the smog episodes of 1952 and 1956. Comparing the winter-time (October 1st to March 31st) average BS values from Dublin, Belfast, London and Paris, *Figure 5.18*, shows that the concentrations in London and Paris were far lower than those measured in Dublin and Belfast, despite the large difference in population sizes. This can be related to the prevalent use of solid fuels for domestic heating in Dublin and Belfast.

The most effective piece of legislation introduced during the study period was the so called "Smoky Coal Ban" that came into effect in Dublin in 1990. This ban, which prohibited the sale and distribution of bituminous coal in the Dublin area, accounted for a 65% decrease in BS concentrations in a single year. In contrast, pollution levels in Dublin increased after the introduction of the Finance No. 2 Act in 1975, which reduced the VAT on solid fuels to 0%, and the "House Improvement Grants to Reduce Dependence on Oil" scheme. These acts were introduced to ease the financial burden on families in Ireland but resulted in very high levels of BS in the

Dublin city area. This type of legislation is a prime example of how government action can have serious unintended consequences.

The conversion of historical BS measurements to BC allowed for a comparison between historical and modern measurements. The annual average concentration of BC in Dublin was calculated to be 1.79 $\mu g/m^3$ in 2002 and 0.51 $\mu g/m^3$ in 2017. This represents a reduction of 72% over the 15 year period. The BC concentrations measured in Belfast and London in 2017 were generally higher than the concentrations measured in Dublin, however the highest daily average concentration was measured in Dublin during the winter months.

A potential limitation of this study is the use of a single location in each city in an effort to avoid preferential sampling biases. When using a city wide average, biases can be created by the movement or closures of stations over a long period of time. The use of single stations can, however, result in biased concentrations depending on local sources in the area of the monitoring site.

6. Conclusions

Contents

6.1. Summary

A seven wavelength dual spot aethalometer (Magee Scientific, Model AE3) was deployed at residential locations in small towns around Ireland and at an urban background location in Dublin during the SAPPHIRE and AEROSOURCE field measurement campaigns respectively. The aethalometer provided real-time information on the optical properties of ambient aerosol deposited on the filter tape and enabled equivalent black carbon concentrations to be determined. Source apportionment modelling was also carried out using pre-selected parameters, such as the absorption Ångström exponent (α). The results of the source apportionment model were used to determine the origins of the black carbon aerosols in three small towns in Ireland, as well as in Dublin.

During the SAPPHIRE monitoring campaign, measurements were made in Killarney, Enniscorthy, and Birr, during the winter months of 2014 and 2015. The eBC concentrations measured by the aethalometer correlated well with measurements from all other instruments. Maximum eBC concentrations were observed during periods of high $PM_{2.5}$ mass and number concentrations, and all occurred during the evening hours. eBC accounted for an average of 9.9% of $PM_{2.5}$ mass in Killarney, 13.2% in Enniscorthy, and 11.4% in Birr. The source apportionment of eBC mass into solid fuel related BC (eBC_{SF}) and traffic related BC (eBC_{Tr}) was performed using two approaches. The first approach involved determination of the best α pair for each location by fixing the α_{Tr} value at 0.9 (Zotter *et al.*, 2017) and varying the α_{SF} value until the fewest negative values were produced. This resulted in α_{SF} values of 1.59,

1.65 and 1.79 for Killarney, Enniscorthy and Birr, respectively and eBC_{SF} contributions of 71% (Killarney), 84% (Enniscorthy) and 46% (Birr). The second approach utilised the latest recommended α values in the literature, $\alpha_{SF} = 1.68$ and $\alpha_{Tr} = 0.9$ (Zotter *et al.*, 2017), and resulted in contributions of 61%, 86% and 63% for Killarney, Enniscorthy, and Birr respectively. These results are in very good agreement with those obtained using the ATOFMS. The EC mass concentration also correlated well with the measured eBC and was used to determine the unique mass absorption cross-section (MAC) values for each location; 11.1 ± 0.09 m^2/g, 10.7 ± 0.07 m^2/g, and 8.34 ± 0.14 m^2/g for Killarney, Enniscorthy and Birr, respectively. Recalculation of the eBC concentrations at each site with these site specific MAC values improved the relationship between eBC and thermal EC.

In the AEROSOURCE project, BC was measured on the campus of University College Dublin (UCD) from 5 August 2016 to 20 August 20 2018. The eBC concentrations showed a strong diurnal pattern with two peaks, one in the morning and the other in the evening. Using the source apportionment model parameters developed by Zotter *et al.* (2017), the eBC was divided into two source contributions; solid fuel burning (eBC_{SF}), and traffic (eBC_{Tr}), which showed a strong seasonal variation. During the summer months, traffic was easily the most dominant source of eBC. The autumn and spring diurnal profiles were similar in nature, showing a traffic related peak in the morning and a strong evening peak with contributions from both sources. The winter months had the largest contribution to eBC from solid fuel burning; 57% in the winter of 2016/2017 and 50% in the winter of 2017/2018. The magnitude of the morning traffic peaks was similar during the four seasons, indicating that traffic volumes passing the site did not vary greatly. However, the morning peak was less apparent during the weekend due to the reduced number of road vehicles.

A site specific MAC value of 15.4 m^2/g was calculated for the UCD site during the EMEP intensive monitoring period, 21 December 2017 to 31 March 2018, which is noticeably higher than those calculated during the SAPPHIRE campaigns, but similar to values calculated at other locations in Europe. The eBC_{SF} values showed a strong correlation with the solid fuel related fractions of organic aerosol (OA) measured by the ACSM, while eBC_{Tr} did not correlate significantly with any fraction. The average eBC:OA ratio also showed a diurnal pattern with values consistent with BC sources dominated by traffic during morning and solid fuel burning in the evening.

Finally, historical black smoke (BS) and sulfur dioxide (SO_2) data collected in Dublin was analysed and compared to similar datasets for Belfast, London and Paris. The pollution trends from 1963 onwards are interpreted in relation to legislative changes on emissions and air quality. The annual average BS concentration in Dublin in 1963 was 137 $\mu g/m^3$, but by 2002 this had decreased by over 96% to 6.7 $\mu g/m^3$. While it is clear that the introduction of legislation to improve air quality has had a profound impact, some government actions actually led to an increase in levels of BS. These include the reduction of VAT on the sale of solid fuels and incentives created to increase the production of peat based products. Both of these acts were introduced in response to the oil crisis of 1973/1974 in an effort to reduce Ireland's dependence on imported oil. The act that had the largest negative impact on air quality was the "House Improvement Grants to Reduce Dependence on Oil", introduced in 1979 (DCC, 2009). This action led to a large number of house owners installing coal-fired back boiler systems, higher particulate emissions, increased BS levels and a number of winter smog events during the 1980s. The Irish government responded by introducing the *Air Pollution Act* (1987), which established monitoring networks and set the standards for air quality. The largest single reduction of BS and SO_2 emissions occurred after the introduction of the *Retail Sale of Solid Fuel Regulations* (1989) and the *Marketing, Sale and Distribution of Fuels Regulations* (1990), commonly referred to as the "smoky coal ban", which prohibited the sale of bituminous coal in Dublin city and mandated that all retailers stocked low smoke alternatives. This resulted in a 65% reduction in BS concentrations and significant decreases in the number of deaths caused by respiratory and cardiovascular failure. Concentrations continued to fall throughout the 1990s until the monitoring of BS concentrations ceased in 2003. Converting the BS to BC concentrations, shows that pollution levels decreased by 71.5% between 2003 and 2017.

Comparing BS concentrations in Dublin to the concentrations measured in London and Belfast shows how the different legislative changes introduced by the governing bodies affected air pollution. Comparing the winter-time (October 1st to March 31st) average concentrations in Dublin, London, Belfast, and Paris, between 1963 and 2002, Dublin and Belfast exhibited the highest concentrations at the beginning of the study period. This trend continued until the end of the monitoring period, when the winter time average concentrations in Paris were the highest. The concentrations of BS measured in Dublin and Belfast were quite well correlated,

despite the differences in legislation at both locations. There was, however, a difference in the monthly average BS:SO_2 ratio at each location indicating that greater amounts of solid fuels were burnt in Dublin, especially prior to the introduction of the Smoky Coal Ban.

6.2. Perspectives

A reduction in BC emitted into the atmosphere would be beneficial for both climate and public health. Since BC is the second largest warming agent in the atmosphere and has an atmospheric lifetime of approximately one week, a reduction in ambient BC concentrations would have a strong and rapid impact on radiative forcing. Indeed, curtailing BC has been identified as a crucial component of many strategies to limit global temperature increases to 1.5 ºC (IPCC, 2018; Takemura and Suzuki, 2019). As BC particles are small in size and are generally co-emitted with toxic materials, a reduction in the concentration of ambient BC particles would also greatly improve air quality and result in fewer deaths due to pulmonary and cardiovascular illnesses.

In order to reduce ambient BC concentrations, detailed information of the nature of its sources are required. Overall, this work demonstrates that the source apportionment of BC into two sources (traffic and solid fuel burning), using the aethalometer model, can replicate the results from other instruments relatively well. While this source apportionment model is not as comprehensive as the analysis performed using instruments such as the ATOFMS or ACSM, it does provide comparable estimates of the sources of BC particles in Ireland. These online mass spectrometry techniques are significantly more expensive and complex and require more time to produce results. The model AE33 aethalometer has the capacity to perform source apportionment in real time, thus providing valuable information to policy makers and enforcement agencies.

The results from the SAPPHIRE monitoring campaigns show that solid fuel burning is the dominant source of wintertime $PM_{2.5}$ in rural towns around Ireland. These measurements were conducted in areas outside of the existing smoke control

zones and are likely to be replicated in other small towns throughout the country. The results from the AEROSOURCE campaign showed that solid fuel burning emission were also dominant in Dublin during winter months. While the average concentrations observed were lower than the concentrations measured in smaller towns around Ireland, the contribution from solid fuel was still significant, greater than 50% on occasions. This indicates that, despite the smoky coal ban currently in place and the availability of natural gas for home heating, the combustion of solid fuels remains a major source of air pollution in Dublin.

A comparison of the eBC concentrations measured in the three small towns and in Dublin is provided in Table 6.1. The results show that mean eBC concentrations in Killarney and Enniscorthy are significantly higher than those in Dublin during winter due to enhanced emissions from solid fuel burning. At the same time, it is worth noting that the wintertime eBC concentrations in Dublin are slightly lower than those observed in Dublin and Belfast.

Table 6.1. Summary of eBC concentrations and percentage contributions from solid fuel burning and traffic, calculated using α_{SF} = 1.68, α_{Tr} = 0.9 (Zotter *et al.*, 2017) parameters, during the SAPPHIRE monitoring campaigns and the winter months (December, January and February) in Dublin, London and Belfast.

Location	**eBC (µg/m^3)**		**% eBC$_{SF}$**	**% eBC$_{Tr}$**
	Mean (± SD)	Range	Mean	Mean
Killarney	2.06 (± 3.76)	0.0–25.2	61	39
Enniscorthy	3.6 (± 4.76)	0.01–35.2	80	20
Birr	0.8 (± 0.9)	0.01–6.35	68	32
Dublin (2016/2017)	0.92 (± 1.68)	0.0–24.2	58	42
Dublin (2017/2018)	0.74 (± 1.48)	0.0–15.5	49	51
London (2017)	1.18 (± 1.46)	0.0–17.0	-	-
Belfast (2017)	1.31 (± 1.59)	0.0–13.5	-	-

The results of this work show that the largest source of BC in Ireland during the colder months is domestic solid fuel burning. While the SAPPHIRE campaigns only covered three towns, similar levels of solid fuel burning and smoke emissions can be observed in most, if not all, small towns around the country. A nationwide ban on the sale of solid fuels would act to curtail emissions from domestic solid fuel

burning, as seen in Dublin after the ban on the sale and marketing of bituminous coal, which dramatically improved air quality in the city and reduced air pollution related deaths in subsequent years (Clancy *et al.*, 2002b; Goodman *et al.*, 2009). This ban on bituminous coal was relatively easy to enforce as coal was only available through commercial entities, and coal imports could be stopped at the points of entry. The threat of legal action against the Government on the grounds of targeting coal retailers should not deter from enforcing this ban, as the health benefits to the population are well established. A nationwide ban on the sale and use of all solid fuels would be the best way to reduce air pollution in small towns and rural areas, however the use of peat and wood in domestic fires is harder to regulate as individual households can cut peat or chop down trees for firewood. Action to limit or eliminate commercial sales would help to reduce consumption of these fuels. Any reductions in solid fuel use, however, also need to be accompanied by investment in renewable energy sources in order to make up for the loss of solid fuel in the market. The historical analysis of air pollution in relation to legislative changes showed that controls on the types of fuels used for home heating in urban areas can greatly reduce pollution levels from domestic solid fuel burning. The Irish government is planning to extend the smoky coal ban to urban areas with a population of more than 10,000 from September 2020. While this would include another 13 towns in the current legislation, there are still over 50 towns that will not be covered by the ban.

Two other observations obtained from the AEROSOURCE project are worth further consideration. The first is related to road traffic, which is the dominant source of pollution during the morning hours. A reduction in traffic volumes would reduce BC levels and clearly improve air quality. This could be achieved by introducing new legislation to restrict traffic, such as in London (Font and Fuller, 2016), or by promoting and incentivising other modes of transport including cycling, walking, the use of public transport, and electric vehicles. The second is related to the air pollution measurement strategy. The combination of ACSM and model AE33 aethalometer has proven to be highly valuable in delivering a comprehensive analysis of the composition and major sources of PM_1 and could be deployed on a wider basis around Ireland and other countries. A final point is that the field measurements in both SAPPHIRE and AEROSOURCE indicate that ultra-fine particles constitute a dominant fraction of the particle population in winter months. There has been a growing interest in atmospheric nanoparticles and their potential health effects in

recent years (Rönkkö and Timonen, 2019) and more measurements of ultra-fine particles are required to understand their sources, as well as physical and chemical properties.

There are also lessons to be learned from the historical air pollution measurements conducted in Dublin, London, Belfast and Paris, and the effects that specific legislative actions can have on air quality. Legislation specifically targeting the major contributors to air quality has been highly successful in previous years, with clear reductions in PM, SO_2, NO_x, and other parameters. In Ireland however, some legislative actions have had a negative impact on air quality, thus highlighting the need for inter-departmental cooperation in order to avoid unintended impacts from introducing new legislation. These historical examples, should also serve as a warning to policy makers who are considering incentivising the use of wood and wood-fired stoves in an effort to reduce Ireland's carbon footprint. While wood is classed as a renewable fuel, this work has highlighted the negative impact that wood burning can have on air quality. Therefore, simply replacing coal, and potentially peat, with wood will not have a positive impact on air quality. It should also be noted that incorrectly operating a wood burning stove decreases the combustion efficiency and increases emissions. As a result, great care should be taken to ensure all stove operators are aware of the optimum operating procedures (McCrillis, *et al.*, 2012; Fachinger *et al.*, 2017).

The future of air pollution monitoring will undoubtedly see more modelling studies with the aim of predicting the concentrations of atmospheric pollutants on a local, regional and global scale. However, these models require significant amounts of accurately measured data at a large number of locations in order to precisely predict future concentrations. Given that BC is predominately anthropogenic, it provides an excellent indicator of the impact of humankind's activities on the environment (Bond *et al.*, 2013). Therefore, it is vitally important to have accurate measurements of ambient BC levels. While global scale measurements may be impractical, long-term measurements in a large number of environments, coupled with source apportionment approaches can be achieved using a relatively cheap instrument such as the aethalometer.

7. References

Abbott, J. *et al.* (2016) *Residential Solid Fuel and Air Pollution Study, North South Ministerial Council (NSMC)*.

Ackerman, A. S. *et al.* (2000) 'Reduction of Tropical Cloudiness by Soot', *Science*, 288, pp. 1042–1047.

AFA Technology (1999) *Instruction Manual: Smoke and Sulphur Dioxide Network*.

Ajtai, T. *et al.* (2011) 'Inter-comparison of optical absorption coefficients of atmospheric aerosols determined by a multi-wavelength photoacoustic spectrometer and an Aethalometer under sub-urban wintry conditions', *Journal of Aerosol Science*, 42(12), pp. 859–866. doi: 10.1016/j.jaerosci.2011.07.008.

Ajtai, T. *et al.* (2019) 'Diurnal variation of aethalometer correction factors and optical absorption assessment of nucleation events using multi-wavelength photoacoustic spectroscopy', *Journal of Environmental Sciences*. Elsevier B.V., 83. doi: 10.1016/j.jes.2019.01.022.

Alfarra, M. *et al.* (2007) 'Identification of the Mass Spectral Signature of Organic Aerosols from Wood Burning Emissions', *Environmental Science & Technology*, 41(16), pp. 5770–5777.

Allen, G. A., Babich, P. and Poirot, R. L. (2004) 'Evaluation of a New Approach for Real Time Assessment of Wood Smoke PM', in *Air & Waste Management Association Visibility Specialty Conference on Regional Global Perspectives on Haze: Causes, Consequences and Controversies*, pp. 1–11.

Ammann, M. *et al.* (1998) 'Heterogeneous production of nitrous acid on soot in polluted air masses', *Nature*, 215(2), pp. 157–160.

Anderson, B. J. *et al.* (2005) 'User-Friendly Clustering for Atmospheric Data Analysis', *Northfield, MN*.

Anderson, J. O., Thundiyil, J. G. and Stolbach, A. (2012) 'Clearing the Air: A Review of the Effects of Particulate Matter Air Pollution on Human Health', *Journal of Medical Toxicology*, 8, pp. 166–175. doi: 10.1007/s13181-011-0203-1.

AQEG (2005) *Particulate Matter in the United Kingdom: Summary*. London.

Arndt, J. (2015) *Characterisation of Atmospheric Single Particles in Industrial and Regional Background Environments using Aerosol Time of Flight Mass Spectrometry*.

Arndt, J. *et al.* (2017) 'Sources and mixing state of summertime background aerosol in the north-western Mediterranean basin', *Atmospheric Chemistry and Physics*, (17), pp. 6975–7001.

Arndt, J. *et al.* (no date) *Contribution of residential peat, wood and coal burning to ambient PM2.5 in small towns in Ireland*.

Arnott, W. P. *et al.* (1999) 'Photoacoustic spectrometer for measuring light absorption by aerosol: instrument description', *Atmospheric Environment*, 33, pp. 2845–2852.

Atkinson, R. W. *et al.* (2001) 'Acute Effects of Particulate Air Pollution on Respiratory Admissions Results from APHEA 2 Project', *American Journal of Respiratory and Critical Care Medicine*, 164, pp. 1860–1866. doi: 10.1164/rccm2010138.

Baccarelli, A. *et al.* (2009) 'Rapid DNA methylation changes after exposure to traffic particles', *American Journal of Respiratory and Critical Care Medicine*, 179(7), pp. 572–578. doi: 10.1164/rccm.200807-1097OC.

Bahadur, R. *et al.* (2012) 'Solar absorption by elemental and brown carbon determined from spectral observations', *Proceedings of the National Academy of Sciences*,

109(43), pp. 17366–17371. doi: 10.1073/pnas.1205910109.
Baklanov, A. *et al.* (2010) 'MEGAPOLI: concept of multi-scale modelling of megacity impact on air quality and climate', *Advances in Scoence & Research*, 4, pp. 115–120. doi: 10.5194/asr-4-115-2010.
Ball, D. J. and Hume, R. (1977) 'The relative importance of vehicular and domestic emissions of dark smoke in Greater London in the mid-1970s, the significance of smoke shade measurements, and an explanation of the relationship of smoke shade to gravimetric measurements of particulate', *Atmospheric Environment*, 11(11), pp. 1065–1073.
Balmes, J. R. (2019) 'Household air pollution from domestic combustion of solid fuels and health', *Journal of Allergy and Clinical Immunology*. Elsevier Inc., 143(6), pp. 1979–1987. doi: 10.1016/j.jaci.2019.04.016.
Barrett, T. E., Rindy, J. E. and Weathers, K. C. (2019) 'Wet deposition of black carbon: A synthesis', *Atmospheric Environment*. Elsevier Ltd. doi: 10.1016/j.atmosenv.2019.06.033.
Beekmann, M. *et al.* (2015) 'In situ, satellite measurement and model evidence on the dominant regional contribution to fine particulate matter levels in the Paris megacity', *Atmospheric Chemistry and Physics*, 15, pp. 9577–9591. doi: 10.5194/acp-15-9577-2015.
Begam, G. R. *et al.* (2016) 'Measurement and analysis of black carbon aerosols over a tropical semi-arid station in Kadapa , India', *Atmospheric Research*. Elsevier B.V., 171, pp. 77–91. doi: 10.1016/j.atmosres.2015.12.014.
Bell, M. L. (2012) *Assessment of the Health Impacts of Particulate Matter Characteristics*.
Bell, M. L., Davis, D. L. and Fletcher, T. (2004) 'A Retrospective Assessment of Mortality from the London Smog Episode of 1952: The Role of Influenza and Pollution', *Environmental Health Perspectives*, 112(1), pp. 6–8. doi: 10.1289/ehp.6539.
Bibi, S. *et al.* (2017a) 'Observations of black carbon aerosols characteristics over an urban environment: Radiative forcing and related implications', *Science of the Total Environment*. Elsevier B.V., 603–604, pp. 319–329. doi: 10.1016/j.scitotenv.2017.06.082.
Bibi, S. *et al.* (2017b) 'Temporal variation of Black Carbon concentration using Aethalometer observations and its relationships with meteorological variables in Karachi, Pakistan', *Journal of Atmospheric and Solar-Terrestrial Physics*. Elsevier Ltd, 157–158(February), pp. 67–77. doi: 10.1016/j.jastp.2017.03.017.
Bigi, A. and Ghermandi, G. (2016) 'Trends and variability of atmospheric PM2.5 and PM10-2.5 concentration in the Po Valley, Italy', *Atmospheric Chemistry and Physics*, 2, pp. 15777–15788. doi: 10.5194/acp-16-15777-2016.
Birch, M. . (2003) *NIOSH Protocol 2003*. Available at: https://www.cdc.gov/niosh/docs/2003-154/pdfs/5040.pdf.
Birch, M. . and Cary, R. . (1996) 'Elemental Carbon-Based Method for Monitoring Occupational Exposures to Particulate Diesel Exhaust', *Aerosol Science and Technology*, (25), pp. 221–241.
Bond, T. C. *et al.* (2004) 'A technology-based global inventory of black and organic carbon emissions from combustion', *Journal of Geophysical Research D: Atmospheres*, 109(14), pp. 1–43. doi: 10.1029/2003JD003697.
Bond, T. C. *et al.* (2007) 'Historical emissions of black and organic carbon aerosol from energy-related combustion, 1850 – 2000', *Global Biogeochemical Cycles*, 21, pp. 1–16. doi: 10.1029/2006GB002840.

Bond, T. C. *et al.* (2013) 'Bounding the role of black carbon in the climate system: A scientific assessment', *Journal of Geophysical Research: Atmospheres*, 118(11), pp. 5380–5552. doi: 10.1002/jgrd.50171.
Bond, T. C., Anderson, T. L. and Campbell, D. (1999) 'Calibration and Intercomparison of Filter-Based Measurements of Visible Light Absorption by Aerosols', *Aerosol Science and Technology*, 600, pp. 582–600.
Bond, T. C. and Bergstrom, R. W. (2006) 'Light Absorption by Carbonaceous Particles : An Investigative Review', *Aerosol Science and Technology*, 40, pp. 47–67. doi: 10.1080/02786820500421521.
Bonjour, S. *et al.* (2013) 'Solid Fuel Use for Household Cooking: Country and Regional Estimates for 1980 – 2010', *Environmental Health Perspectives*, 121(7), pp. 784–790.
Bord na Móna (2006) *Bord na Móna Living History, A Brief Histroy of The Peat Industry in Ireland*.
Bové, H. *et al.* (2019) 'Ambient black carbon particles reach the fetal side of human placenta', *Nature Communications*. Springer US, pp. 1–7. doi: 10.1038/s41467-019-11654-3.
Bower, J. *et al.* (2009) *Air Pollution in the UK: 2008*.
Boylan, R. K. (1926) 'Atmospheric Dust and Condensation Nuclei', *Proceedings of the Royal Irish Academy*, 37, pp. 58–70.
Briggs, N. L. and Long, C. M. (2016) 'Critical review of black carbon and elemental carbon source apportionment in Europe and the United States', *Atmospheric Environment*. Elsevier Ltd, 144, pp. 409–427. doi: 10.1016/j.atmosenv.2016.09.002.
Brimblecombe, P. (1987) *The big smoke: a histroy of air pollution in London since Medieval times*. Methuen & Co.
ten Brink, H. *et al.* (2004) 'INTERCOMP2000: the comparability of methods in use in Europe for measuring the carbon content of aerosol', *Atmospheric Environment*, 38, pp. 6507–6519. doi: 10.1016/j.atmosenv.2004.08.027.
British Standards Institute (1969a) *British Standard 1747: Part 2: Methods for the Measurement of Air Pollution: Detrmination of concentration of suspended matter*.
British Standards Institute (1969b) 'British Standard 1747: Part 3: Methods for Measurement of Air Pollution: Determination of sulphur dioxide'.
Bruce, N. G. *et al.* (2013) 'Control of household air pollution for child survival: estimates for intervention impacts', *BMC Public Health*. BioMed Central Ltd, 13. doi: 10.1186/1471-2458-13-S3-S8.
Butt, E. W. *et al.* (2016) 'The impact of residential combustion emissions on atmospheric aerosol, human health, and climate', *Atmospheric Chemistry and Physics*, (16), pp. 873–905. doi: 10.5194/acp-16-873-2016.
Byrd, T., Stack, M. and Furey, A. (2010) 'The assessment of the presence and main constituents of particulate matter ten microns (PM10) in Irish , rural and urban air', *Atmospheric Environment*. Elsevier Ltd, 44(1), pp. 75–87. doi: 10.1016/j.atmosenv.2009.09.037.
Calvo, A. I. *et al.* (2013) 'Research on aerosol sources and chemical composition: Past, current and emerging issues', *Atmospheric Research*. Elsevier B.V., 120–121, pp. 1–28. doi: 10.1016/j.atmosres.2012.09.021.
Cape, J. N., Coyle, M. and Dumitrean, P. (2012) 'The atmospheric lifetime of black carbon', *Atmospheric Environment*. Elsevier Ltd, 59, pp. 256–263. doi: 10.1016/j.atmosenv.2012.05.030.
Carslaw, D. (2015) 'The openair manual - open-source tools for analysing air pollution data'. King's College London.

Carslaw, D. and Ropkins, K. (2012) 'openair - An R package for air quality data analysis', *Environmental Modelling and Software*. Elsevier Ltd, 27–28, pp. 52–61. doi: 10.1016/j.envsoft.2011.09.008.
Cassee, F. R. *et al.* (2013) 'Particulate matter beyond mass: recent health evidence on the role of fractions, chemical constituents and sources of emission', *Inhalation Toxicology*, 8378(14), pp. 802–812. doi: 10.3109/08958378.2013.850127.
Castro, L. M. *et al.* (1999) 'Carbonaceous aerosol in urban and rural European atmospheres: estimation of secondary organic carbon concentrations', *Atmospheric Environment*, 33, pp. 2771–2781.
Cavalli, F. *et al.* (2010) 'Toward a standardised thermal-optical protocol for measuring atmospheric organic and elemental carbon: the EUSAAR protocol', *Atmospheric Measurement Techniques*, 3, pp. 79–89.
Ceburnis, D. *et al.* (2006) 'Local and regional air pollution in Ireland during an intensive aerosol measurement campaign', *Journal of Environmental Monitoring*, (1), pp. 479–487. doi: 10.1039/b516029d.
Chen, J. *et al.* (2017) 'A review of biomass burning: Emissions and impacts on air quality, health and climate in China', *Science of the Total Environment, The*. Elsevier B.V., 579(November 2016), pp. 1000–1034. doi: 10.1016/j.scitotenv.2016.11.025.
Cherian, R. *et al.* (2017) 'Black carbon indirect radiative effects in a climate model', *Tellus B: Chemical and Physical Meteorology*. Taylor & Francis, 0889, pp. 1–10. doi: 10.1080/16000889.2017.1369342.
Chiloane, K. E. *et al.* (2017) 'Spatial, temporal and source contribution assessments of black carbon over the northern interior of South Africa', *Atmospheric Chemistry and Physics*, (2), pp. 6177–6196. doi: 10.5194/acp-17-6177-2017.
Chow, J. C. *et al.* (1993) 'The dri thermal/optical reflectance carbon analysis system: description, evaluation and applications in U.S. Air quality studies', *Atmospheric Environment. Part A. General Topics*, 27(8), pp. 1185–1201.
Chow, J. C. *et al.* (2010) 'Black and Organic Carbon Emission Inventories: Review and Application to California', *Journal of Air & Waste Management Association*, 60, pp. 497–507. doi: 10.3155/1047-3289.60.4.497.
Chow, J. C. *et al.* (2011) 'PM2.5 source profiles for black and organic carbon emission inventories', *Atmospheric Environment*. Elsevier Ltd, 45(31), pp. 5407–5414. doi: 10.1016/j.atmosenv.2011.07.011.
Christolis, M. *et al.* (1992) *Instruction Manual for air pollution monitoring Vol. II: Black Smoke Monitoring*.
Clancy, L. *et al.* (2002a) 'Effect of air-pollution control on death rates in Dublin, Ireland: An intervention study', *Lancet*, 360(9341), pp. 1210–1214. doi: 10.1016/S0140-6736(02)11281-5.
Clancy, L. *et al.* (2002b) 'Effect of air-pollution control on death rates in Dublin , Ireland : an intervention study', *Lancet*, 360, pp. 1210–1214.
Cooke, W. F., Jennings, S. G. and Spain, T. G. (1997) 'Black carbon measurements at Mace Head, 1989 - 1996', *Journal of Geophysical Research*, 102, pp. 25339–25346.
Council of the European Union (1970) *Council Directive 70/220/EEC of 20 March 1970 on the approximation of the laws of the Member States relating to measures to be taken against air pollution by gases from positive ignition engines of motor vehicles*. Available at: http://data.europa.eu/eli/dir/1970/220/oj.
Council of the European Union (1972) *Council Directive 72/306/EEC of 2 August 1972 on the approximation of the laws of the Member States relating to the measures to be taken against the emission of pollutants from diesel engines for use in vehicles*. Available at: http://data.europa.eu/eli/dir/1972/306/oj.

Council of the European Union (1975) *Council Directive 75/716/EEC of 24 November 1975 on the approximation of the laws of the Member States relating to the sulphur content of certain liquid fuels*. Available at: http://data.europa.eu/eli/dir/1975/716/oj.
Council of the European Union (1980) *Council Directive 80/779/EEC of 15 July 1980 on air quality limit values and guide values for sulphur dioxide and suspended particles*. Available at: http://data.europa.eu/eli/dir/1980/779/oj.
Council of the European Union (1990) *Council Regulation (EEC) No 1210/90 of 7 May 1990 on the establishment of the European Environment Agency and the European Environment Information and Observation Network*. Available at: https://eur-lex.europa.eu/legal-content/EN/TXT/PDF/?uri=CELEX:31990R1210&rid=1.
Council of the European Union (1996) *Council Directive 96/62/EC of 27 September 1996 on ambient air quality assessment and management*. Available at: http://data.europa.eu/eli/dir/1996/62/oj.
Council of the European Union (1999) *Council Directive 1999/30/EC of 22 April 1999 relating to limit values for sulphur dioxide, nitrogen dioxide and oxides of nitrogen, particulate matter and lead in ambient air*. Available at: https://eur-lex.europa.eu/legal-content/EN/TXT/PDF/?uri=CELEX:31999L0030&rid=1.
Crilley, L. R. *et al.* (2015) 'Sources and contributions of wood smoke during winter in London: assessing local and regional influences', *Atmospheric Chemistry and Physics*, 15, pp. 3149–3171. doi: 10.5194/acp-15-3149-2015.
Crippa, M. *et al.* (2014) 'Organic aerosol components derived from 25 AMS data sets across Europe using a consistent ME-2 based source apportionment approach', *Atmospheric Chemistry and Physics*, 14, pp. 6159–6176. doi: 10.5194/acp-14-6159-2014.
Cross, E. S. *et al.* (2010) 'Soot Particle Studies — Instrument Inter- Comparison — Project Overview Soot Particle Studies — Instrument Inter-Comparison — Project Overview', 6826(October 2015). doi: 10.1080/02786826.2010.482113.
CSO (2011) *Census 2011 Small Area Population Statistics*. Available at: http://census.cso.ie/sapmap_2011/.
CSO (2016) *Quarterly National Housing Survey Module on Household Environmental Behaviours*.
Currie, L. A. (2000) 'Evolution and Multidisciplinary Frontiers of 14C Aerosol Science', *Radiocarbon*, 42(1), pp. 115–126.
Currie, L. A. (2004) 'The Remarkable Metrological History of Radiocarbon Dating [II]', *Journal of Research of the National Institute of Standards and Technology*, 109(2), pp. 185–217.
Cusack, M. *et al.* (2012) 'Trends of particulate matter (PM2.5) and chemical composition at a regional background site in the Western Mediterranean over the last nine years (2002 – 2010)', *Atmospheric Chemistry and Physics*, 12, pp. 8341–8357. doi: 10.5194/acp-12-8341-2012.
Dall'Osto, M. *et al.* (2013) 'Characterization of urban aerosol in Cork city (Ireland) using aerosol mass spectrometry', *Atmospheric Chemistry and Physics*, 13, pp. 4997–5015. doi: 10.5194/acp-13-4997-2013.
Dall'Osto, M. *et al.* (2014) 'Apportionment of urban aerosol sources in Cork (Ireland) by synergistic measurement techniques', *Science of the Total Environment*. Elsevier B.V., 493, pp. 197–208. doi: 10.1016/j.scitotenv.2014.05.027.
Davy, P. K. and Trompetter, W. J. (2018) *Black Carbon in New Zealand*.
DCC (2009) *Dublin Regional Air Quality Management Plan. 2009-2012*.
DEFRA (2019a) *Air Pollution in the UK 2018*.

DEFRA (2019b) *UK Air Information Resources*. Available at: https://uk-air.defra.gov.uk/data/data_selector_service#mid (Accessed: 8 November 2019).
Delfino, R. J. *et al.* (2010) 'Traffic-related Air Pollution and Blood Pressure in Elderly Subjects With Coronary Artery Disease', *Epidemiology*, 21(3). doi: 10.1097/EDE.0b013e3181d5e19b.
Denier Van Der Gon, H. A. C. *et al.* (2015) 'Particulate emissions from residential wood combustion in Europe – revised estimates and an evaluation', *Atmospheric Chemistry and Physics*, 15, pp. 6503–6519. doi: 10.5194/acp-15-6503-2015.
Derwent, R. G. *et al.* (2001) 'Black carbon aerosol and carbon monoxide in European regionally polluted air masses at Mace Head, Ireland during 1995 – 1998', *Atmospheric Environment*, 35, pp. 6371–6378.
DeWitt, H. L. *et al.* (2019) 'Seasonal and diurnal variability in O3, black carbon, and CO measured at the Rwanda Climate Observatory', *Atmospheric Chemistry and Physics*, 19, pp. 2063–2078.
Dockery, D. W. *et al.* (1993) 'An Association Between Air Pollution and Mortality in Six U.S. Cities', *The New England Jounral of Medicine*, 329(24), pp. 1753–1759.
Donaldson, K. *et al.* (2005) 'Combustion-derived nanoparticles: A review of their toxicology following inhalation exposure', *Particle and Fibre Toxicology*, 14. doi: 10.1186/1743-8977-2-10.
Donaldson, K., Li, X. Y. and Macnee, W. (1998) 'Ultrafine (Nanometre) Particle Mediated Lung Injury', *Journal of Aerosol Science*, 29(5), pp. 553–560.
Dou, T.-F. and Xiao, C.-D. (2016) 'An overview of black carbon deposition and its radiative forcing over the Arctic', *Advances in Climate Change Research*. Elsevier Ltd, 7(3), pp. 115–122. doi: 10.1016/j.accre.2016.10.003.
Drinovec, L. *et al.* (2015) 'The " dual-spot " Aethalometer : an improved measurement of aerosol black carbon with real-time loading compensation', *Atmospheric Measurement Techniques*, pp. 1965–1979. doi: 10.5194/amt-8-1965-2015.
Drinovec, L. *et al.* (2017) 'The filter-loading effect by ambient aerosols in filter absorption photometers depends on the coating of the sampled particles', *Atmospheric Measurement Techniques*, 10(3), pp. 1043–1059. doi: 10.5194/amt-10-1043-2017.
Dumka, U. C. *et al.* (2018) 'Assessment of biomass burning and fossil fuel contribution to black carbon concentrations in Delhi during winter', *Atmospheric Environment*. Elsevier, 194, pp. 93–109. doi: 10.1016/j.atmosenv.2018.09.033.
EEA (2018) *European Union emission inventory report 1990-2016 under the UNECE Convention on Long-range Transboundary Air Pollution (LRTAP)*.
EEA (2019) *European Union emission inventory report 1990 - 2017 under the UNECE Convention on Long-term Transboundary Air Pollution (LRTAP)*.
Elliott, P. *et al.* (2007) 'Long-term associations of outdoor air pollution with mortality in Great Britain', *Environmental Exposure*, 5301(2560), pp. 1088–1094. doi: 10.1136/thx.2006.076851.
EMEP Status Report 2019 (2019).
EPA (2015) *Air Quality in Ireland 2015*.
EPA (2019a) *Air Quality in Ireland 2018*.
EPA (2019b) *Map of Smoky Coal Ban Areas*. Available at: https://gis.epa.ie/EPAMaps/ (Accessed: 31 October 2019).
European Commission (1992) *Proposal for a Council Directive amending Directive 70/220/EEC on the approximation of the laws of Member States relating to measures to be taken against air pollution by emissions from motor vehicles*. Available at: https://eur-lex.europa.eu/legal-content/EN/TXT/PDF/?uri=CELEX:51992PC0064&rid=1.

European Environment Agency (2013) *Status of black carbon monitoring in ambient air in Europe*.
European Environment Agency (2018) *Air quality in Europe — 2018 report*.
European Parliament and Council of the European Union (1996) *Directive 96/1/EC of the European Parliament and of the Council of 22 January 1996 amending Directive 88/77/EEC on the approximation of the laws of the Member States relating to the measures to be taken against the emission of gaseous and particulate poll*. Available at: https://eur-lex.europa.eu/legal-content/EN/TXT/PDF/?uri=CELEX:31996L0001&rid=1.
European Union (2019) *EUR-Lex - Access to European Union Law*. Available at: https://eur-lex.europa.eu/homepage.html (Accessed: 21 October 2019).
Fachinger, F. *et al.* (2017) 'How the user can influence particulate emissions from residential wood and pellet stoves: Emission factors for different fuels and burning conditions', *Atmospheric Environment*, 158, pp. 216–226. doi: 10.1016/j.atmosenv.2017.03.027.
Favez, O. *et al.* (2009) 'Evidence for a significant contribution of wood burning aerosols to PM 2.5 during the winter season in Paris, France', *Atmospheric Environment*, 43(February 2005), pp. 3640–3644. doi: 10.1016/j.atmosenv.2009.04.035.
Finlayson-Pitts, B. J. and Pitts, J. N. (2000) *Chemistry of the Upper and Lower Atmosphere: Theory, Experiments, and Applications*. San Diego, USA: Academic Press.
Flanner, M. G. *et al.* (2009) 'Springtime warming and reduced snow cover from carbonaceous particles', *Atmospheric Chemistry and Physics*, pp. 2481–2497.
Font, A. and Fuller, G. W. (2016) 'Did policies to abate atmospheric emissions from traf fi c have a positive effect in London ? *', *Environmental Pollution*. Elsevier Ltd, 218, pp. 463–474. doi: 10.1016/j.envpol.2016.07.026.
Fuller, G. W. *et al.* (2014) 'Contribution of wood burning to PM10 in London', *Atmospheric Environment*, 87, pp. 87–94. doi: 10.1016/j.atmosenv.2013.12.037.
Fuller, G. W. (2018) *The Invisible Killer: The rising Global Threat of Air Pollution - and How We Can Fight Back*.
Fuller, G. W. and Connolly, E. (2012) *Reorganisation of the UK Black Carbon Network*.
Gard, E. *et al.* (1997) 'Real-Time Analysis of Individual Atmospheric Aerosol Particles : Design and Performance of a Portable ATOFMS', *Analytical Chemistry*, 69(20), pp. 4083–4091.
Goldberg, E. D. (1985) 'Black Carbon in the Environment - Properties and Distribution', *John WIiley and Sons Inc.*, p. 216.
Gong, T. *et al.* (2019) 'Associations of black carbon and PM2.5 with daily cardiovascular mortality in Beijing, China', *Atmospheric Environment*. Elsevier, 214. doi: 10.1016/j.atmosenv.2019.116876.
Goodman, P. G. (1999) *Particulate Air Pollution and Mortality in Dublin 1980 - 1996*.
Goodman, P. G. *et al.* (2009) 'Effect of air pollution controls on black smoke and sulfur dioxide concentrations across Ireland', *Journal of the Air and Waste Management Association*, 59(2), pp. 207–213. doi: 10.3155/1047-3289.59.2.207.
Government of Ireland (1962) *Local Government (Sanitary Services) Act, 1878 to 1962*. Ireland. Available at: http://www.irishstatutebook.ie/eli/1962/act/26/enacted/en/print.html.
Government of Ireland (1970) *Control of Atmospheric Pollution Regulations, 1970*. Ireland. Available at:

http://www.irishstatutebook.ie/eli/1970/si/156/made/en/print?q=Control+of+Atmospheric+Pollution+Regulations#.
Government of Ireland (1975) *Finance (No. 2) Act, 1975*.
Government of Ireland (1981) *Turf Development Act, 1981*.
Government of Ireland (1987a) *Air Pollution Act, 1987*. Ireland. Available at: http://www.irishstatutebook.ie/eli/1987/act/6/enacted/en/print.html.
Government of Ireland (1987b) *Air Pollution Act, 1987 (Air Quality Standards) Regulations, 1987*. Ireland. Available at: http://www.irishstatutebook.ie/eli/1987/si/244/made/en/print?q=Air+Quality+Standards.
Government of Ireland (1988a) *Air Pollution Act, 1987 (Authorised Fuel) Regulations, 1988*. Ireland. Available at: http://www.irishstatutebook.ie/eli/1988/si/298/made/en/print?q=298.
Government of Ireland (1988b) *Special Control Area (Ballyfermot) Order, 1988 (Confirmation) Order, 1988*. Ireland. Available at: http://www.irishstatutebook.ie/eli/1988/si/282/made/en/print?q=282.
Government of Ireland (1989) *Air Pollution Act, 1987 (Retail Sale of Fuels) Regulations 1989*. Ireland. Available at: http://www.irishstatutebook.ie/eli/1989/si/333/made/en/print?q=333.
Government of Ireland (1990) *Air Pollution Act, 1987 (Marketing, Sale and Distribution of Fuels) Regulations, 1990*. Ireland. Available at: http://www.irishstatutebook.ie/eli/1990/si/123/made/en/print?q=123.
Government of Ireland (1992) *Environmental Protection Agency Act, 1992*. Ireland. Available at: http://www.irishstatutebook.ie/eli/1992/act/7/enacted/en/print.html.
Government of Ireland (1994) *Air Pollution Act, 1987 (Marketing, Sale and Distribution of Fuels) (Cork) Regulations, 1994*. Ireland. Available at: http://www.irishstatutebook.ie/eli/1994/si/403/made/en/print?q=403.
Government of Ireland (2000) *Air Pollution Act, 1987 (Marketing, Sale and Distribution of Fuels) (Amendment) Regulations, 2000*. Ireland. Available at: http://www.irishstatutebook.ie/eli/2000/si/278/made/en/print?q=278+2000.
Government of Ireland (2003) *Air Pollution Act, 1987 (Marketing, Sale and Distribution of Fuels) (Amendment) Regulations, 2003*. Ireland. Available at: http://www.irishstatutebook.ie/eli/2003/si/111/made/en/print?q=111+2003.
Government of Ireland (2004) *Air Pollution Act 1987 (Marketing, Sale and Distribution of Fuels) (Amendment) Regulations 2004*. Ireland. Available at: http://www.irishstatutebook.ie/eli/2004/si/713/made/en/print?q=713+2004.
Government of Ireland (2019) *electronic Irish Statue Book*. Available at: http://www.irishstatutebook.ie/ (Accessed: 21 October 2019).
Government of United Kingdom (1956) *Clean Air Act, 1956*. United Kingdom. Available at: http://www.legislation.gov.uk/ukpga/Eliz2/4-5/52/contents.
Government of United Kingdom (1965) *Clean Air Dark Smoke - Permitted Periods 1965*. Northern Ireland. Available at: http://www.legislation.gov.uk/nisro/1965/73/pdfs/nisro_19650073_en.pdf.
Government of United Kingdom (1968) *Clean Air Act 1968*. United Kingdom. Available at: http://www.legislation.gov.uk/ukpga/1968/62/contents.
Government of United Kingdom (1969) *Clean Air Act (Northern Ireland) 1964 Grant Extension*. United Kingdom.
Government of United Kingdom (1974) *Control of Pollution Act 1974*. United Kingdom. Available at: http://www.legislation.gov.uk/ukpga/1974/40/contents.
Government of United Kingdom (1976a) *The Motor Fuel (Sulphur Content of Gas*

Oil) Regulations 1976. United Kingdom. Available at: http://www.legislation.gov.uk/uksi/1976/1989/contents/made.
Government of United Kingdom (1976b) *The Oil Fuel (Sulphur Content of Gas Oil) Regulations 1976*. United Kingdom. Available at: http://www.legislation.gov.uk/uksi/1976/1988/contents/made.
Government of United Kingdom (1978) *The Pollution Control and Local Government (Northern Ireland) Order 1978*. United Kingdom. Available at: http://www.legislation.gov.uk/nisi/1978/1049/pdfs/uksi_19781049_en.pdf.
Government of United Kingdom (1981) *Clean Air (Northern Ireland) 1981*. United Kingdom. Available at: http://www.legislation.gov.uk/nisi/1981/158/pdfs/uksi_19810158_en.pdf.
Government of United Kingdom (1989a) *Control of Smoke Pollution Act 1989*. United Kingdom. Available at: http://www.legislation.gov.uk/ukpga/1989/17/contents.
Government of United Kingdom (1989b) *The Air Quality Standards Regulations 1989*. United Kingdom. Available at: http://www.legislation.gov.uk/uksi/1989/317/introduction/made.
Government of United Kingdom (1989c) *The Control of Industrial Air Pollution (Registration of Works) Regulations 1989*. United Kingdom. Available at: http://www.legislation.gov.uk/uksi/1989/318/introduction/made.
Government of United Kingdom (1990a) *Environmental Protection Act 1990*. United Kingdom. Available at: http://www.legislation.gov.uk/ukpga/1990/43/contents.
Government of United Kingdom (1990b) *The Air Quality Standards Regulations (Northern Ireland) 1990*. United Kingdom. Available at: http://www.legislation.gov.uk/nisr/1990/145/pdfs/nisr_19900145_en.pdf.
Government of United Kingdom (1990c) *The Motor Fuel (Sulphur Content of Gas Oil) (Amendment) Regulations 1990*. United Kingdom. Available at: http://www.legislation.gov.uk/uksi/1990/1097/contents/made/data.pdf.
Government of United Kingdom (1990d) *The Oil Fuel (Sulphur Content of Gas Oil) Regulations 1990*. United Kingdom. Available at: http://www.legislation.gov.uk/uksi/1990/1096/contents/made/data.pdf.
Government of United Kingdom (1993) *Clean Air Act 1993*. United Kingdom. Available at: http://www.legislation.gov.uk/ukpga/1993/11/contents.
Government of United Kingdom (1994) *The Air Quality Standards (Amendment) Regulations (Northern Ireland) 1994*. Available at: http://www.legislation.gov.uk/nisr/1994/339/pdfs/nisr_19940339_en.pdf.
Government of United Kingdom (1995) *Environment Act 1995*. United Kingdom. Available at: http://www.legislation.gov.uk/ukpga/1995/25/pdfs/ukpga_19950025_en.pdf.
Government of United Kingdom (1996) *The Air Quality Standards (Amendment) Regulations (Northern Ireland) 1996*. Available at: http://www.legislation.gov.uk/nisr/1996/23/made/data.pdf.
Government of United Kingdom (1999) *Greater London Authority Act 1999*. United Kingdom. Available at: http://www.legislation.gov.uk/ukpga/1999/29/pdfs/ukpga_19990029_en.pdf.
Government of United Kingdom (2002) *The Environment (Northern Ireland) Order 2002*. United Kingdom. Available at: http://www.legislation.gov.uk/nisi/2002/3153/pdfs/uksi_20023153_en.pdf.
Government of United Kingdom (2003) *The Pollution Prevention and Control Regulations (Northern Ireland) 2003*. United Kingdom. Available at: http://www.legislation.gov.uk/nisr/2003/46/pdfs/nisr_20030046_en.pdf.

Government of United Kingdom (2007) *Greater London Authority Act 2007*. United Kingdom. Available at: http://www.legislation.gov.uk/ukpga/2007/24/pdfs/ukpga_20070024_en.pdf.
Gross, D. S. *et al.* (2010) 'Environmental chemistry through intelligent atmospheric data analysis', *Environmental Modelling and Software*. Elsevier Ltd, 25(6), pp. 760–769. doi: 10.1016/j.envsoft.2009.12.001.
Guarieiro, L. L. N. and Guarieiro, A. L. N. (2013) 'Vehicle Emissions : What Will Change with Use of Biofuel ?', in *Biofuels - Economy, Environmental and Sustainability*, pp. 357–386.
Gundel, L. A. *et al.* (1984) 'The Relationship between optical attenuation and black carbon concentration for ambient and source particles', *Science of the Total Environment*, 36, pp. 197–202.
Hallquist, M. *et al.* (2009) 'The formation, properties and impact of secondary organic aerosol: current and emerging issues', *Atmospheric Chemistry and Physics*, 9, pp. 5155–5236.
Hansell, A. *et al.* (2016) 'Historic air pollution exposure and long-term mortality risks in England and Wales: prospective longitudinal cohort study', *Thorax*, 71, pp. 330–338. doi: 10.1136/thoraxjnl-2015-207111.
Hansen, A. D. A., Rosen, H. and Novakov, T. (1984) 'The aethalometer - An instrument for the real-time measurement of optical absorption by aerosol particles', *Science of the Total Environment, The*, 36(C), pp. 191–196. doi: 10.1016/0048-9697(84)90265-1.
Harrison, R. M. *et al.* (2001) 'Studies of the coarse particle (2.5 - 10 um) component in UK urban atmospheres', *Atmospheric Environment*, 35, pp. 3667–3679.
Harrison, R. M. *et al.* (2012) 'Comparison of methods for evaluation of wood smoke and estimation of UK ambient concentrations', *Atmospheric Chemistry and Physics*, pp. 8271–8283. doi: 10.5194/acp-12-8271-2012.
Hasunuma, H. *et al.* (2014) 'Decline of ambient air pollution levels due to measures to control automobile emissions and effects on the prevalence of respiratory and allergic disorders among children in Japan', *Environmental Research*. Elsevier, 131, pp. 111–118. doi: 10.1016/j.envres.2014.03.007.
Haywood, J. and Boucher, O. (2000) 'Estimates of the direct and indirect radiative forcing due to tropospheric aerosols: A review', *Reviews of Geophysics*, (1999), pp. 513–543.
Heal, M. R. and Beverland, I. J. (2017) 'A chronology of ratios between black smoke and PM10 and PM2.5 in the context of comparison of air pollution epidemiology concentration-response functions', *Environmental Health*. Environmental Health, 16(44). doi: 10.1186/s12940-017-0252-2.
Heal, M. R. and Quincey, P. (2012) 'The relationship between black carbon concentration and black smoke : A more general approach', *Atmospheric Environment*. Elsevier Ltd, 54, pp. 538–544. doi: 10.1016/j.atmosenv.2012.02.067.
Heal, R. M. *et al.* (2005) 'Interpretation of variations in fine, coarse and black smoke particulate matter concentrations in a Northern European city.', *Atmospheric Environment*, 39, pp. 3711–3718. doi: 10.1016/j.atmosenv.2005.03.007.
Healy, R. M. *et al.* (2010) 'Source apportionment of PM2.5 in Cork Harbour, Ireland using a combination of single particle mass spectrometry and quantitative semi-continuous measurements', *Atmospheric Chemistry and Physics*, (10), pp. 9593–9613. doi: 10.5194/acp-10-9593-2010.
Healy, R. M. *et al.* (2012) 'Sources and mixing state of size-resolved elemental carbon particles in a European megacity: Paris', *Atmospheric Chemistry and Physics*, 12, pp.

1681–1700. doi: 10.5194/acp-12-1681-2012.
Healy, R. M. *et al.* (2013) 'Quantitative determination of carbonaceous particle mixing state in Paris using single-particle mass spectrometer and aerosol mass spectrometer measurements', *Atmospheric Chemistry and Physics*, 13, pp. 9479–9496. doi: 10.5194/acp-13-9479-2013.
Healy, R. M. *et al.* (2017) 'Ambient measurements and source apportionment of fossil fuel and biomass burning black carbon in Ontario', *Atmospheric Environment*, 161, pp. 34–47. doi: 10.1016/j.atmosenv.2017.04.034.
Healy, R. M. *et al.* (2019) 'Black carbon in the Lower Fraser Valley, British Columbia: Impact of 2017 wildfires on local air quality and aerosol optical properties', *Atmospheric Environment*. Elsevier, 217. doi: 10.1016/j.atmosenv.2019.116976.
Heidorn, K. C. (1979) *A Chronology ol Important Events in the History ol Air Pollution Meteorology to 1970*, *Bullletin American Meteorological Society*.
Helin, A. *et al.* (2018) 'Characteristics and source apportionment of black carbon in the Helsinki metropolitan area, Finland', *Atmospheric Environment*. Elsevier Ltd, 190, pp. 87–98. doi: 10.1016/j.atmosenv.2018.07.022.
Hellebust, S. *et al.* (2010) 'Sources of ambient concentrations and chemical composition of PM2.5 - 0.1 in Cork Harbour, Ireland', *Atmospheric Research*. Elsevier B.V., 95(2–3), pp. 136–149. doi: 10.1016/j.atmosres.2009.09.006.
Henshaw, N. (1664) 'Aero-chanilos', pp. 1–13.
Herich, H., Hueglin, C. and Buchmann, B. (2011) 'A 2.5 year's source apportionment study of black carbon from wood burning and fossil fuel combustion at urban and rural sites in Switzerland', *Atmospheric Measurement Techniques*, 4(7), pp. 1409–1420. doi: 10.5194/amt-4-1409-2011.
Hessey, I. *et al.* (2017) *2016 Annual Report for the UK Black Carbon Network*.
Hobbs, P. V (2000) *Introduction into Atmospheric Chemistry*. Cambridge University Press.
Hoek, G. *et al.* (2013) 'Long-term air pollution exposure and cardio- respiratory mortality: a review', *Environmental Health*, (2).
IPCC (2007) *Climate Change 2007 - The Physical Science Basis*.
IPCC (2013) *Climate Change 2013: The Physical Science Basis*.
IPCC (2018) *Global Warming of 1.5°C*.
ISO (1979) 'ISO 4219:1979 Air quality - Determination of gaseous sulphur compounds in ambient air - Sampling equipment'.
ISO (1993) 'ISO 9835:1993 Ambient air - Determination of a black smoke index'.
Janssen, N. A. *et al.* (2012) *Health effects of black carbon*.
Janssen, N. A. H. *et al.* (2011) 'Black Carbon as an Additional Indicator of the Adverse Health Effects of Airborne Particles Compared with PM10 and PM2.5', *Environmental Health Perspectives*, 119(12), pp. 1691–1699.
Jennings, S. G. *et al.* (1997) 'Microphysical and Physico-chemical characterization of Atmospheric Marine and Continental Aerosol at Mace Head', *Atmospheric Environment*, 31(17), pp. 2795–2808.
Jennings, S. G. *et al.* (2003) 'Mace Head Atmospheric Research Station — characterization of aerosol radiative parameters', *Boreal Environment Research*, 8, pp. 303–314.
Jennings, S. G., McGovern, F. M. and Cooke, W. F. (1993) 'Carbon mass concentration measurements at Mace Head, on the West Coast of Ireland', *Atmospheric Environment*, 27(8), pp. 1229–1239.
Jereb, B. *et al.* (2018) 'Exposure to Black Carbon during Exposure to Black Carbon during Bicycle Commuting – Alternative Route Selection', *Atmosphere*, 9. doi:

10.3390/atmos9010021.
Johnson, T. M. *et al.* (2011) *A Review of Top-down Source Apportionment Techniques and Their Application in Developing Countries*.
Jones, G., Pye, S. and Watkiss, P. (2005) *Service contract for 'ex-post' evaluation of short-term and local measures in the CAFE context*.
Junker, C. and Liousse, C. (2008) 'A global emission inventory of carbonaceous aerosol from historic records of fossil fuel and biofuel consumption for the period 1860 - 1997', *Atmospheric Chemistry and Physics*, 8, pp. 1195–1207.
Kalogridis, A. *et al.* (2018) 'Assessment of wood burning versus fossil fuel contribution to wintertime black carbon and carbon monoxide concentrations in Athens, Greece', *Atmospheric Chemistry and Physics*, 18, pp. 10219–10236.
Karagulian, F. *et al.* (2015) 'Contributions to cities' ambient particulate matter (PM): A systematic review of local source contributions at global level', *Atmospheric Environment*. Elsevier Ltd, 120, pp. 475–483. doi: 10.1016/j.atmosenv.2015.08.087.
Katsouyanni, K. *et al.* (1996) 'Short term effects of air pollution on health : a European approach using epidemiologic time series data : the APHEA protocol', *Journal of Epidemiology and Community Health*, 50, pp. 12–18.
Katsouyanni, K. *et al.* (1997) 'Short term effects of ambient sulphur dioxide and particulate matter on mortaility in 12 European cities: results from time series data from the APHEA project', *BMJ*, 314(June).
Keary, J. *et al.* (1998) 'PM10 Concentration Measurements in Dublin City', *Environmental Monitoring and Assessment*, 52, pp. 3–18.
Kim, J. *et al.* (2015) 'Assessing Optical Properties and Refractive Index of Combustion Aerosol Particles Through Combined Experimental and Modeling Studies', *Aerosol Science and Technology*, 49, pp. 340–350. doi: 10.1080/02786826.2015.1020996.
Kim, K. E., Cho, D. and Park, H. J. (2016) 'Air pollution and skin diseases : Adverse effects of airborne particulate matter on various skin diseases', *Life Sciences*. Elsevier Inc., 152, pp. 126–134. doi: 10.1016/j.lfs.2016.03.039.
Kim, K., Kabir, E. and Kabir, S. (2015) 'A review on the human health impact of airborne particulate matter', *Environment International*. Elsevier Ltd, 74, pp. 136–143. doi: 10.1016/j.envint.2014.10.005.
Kiran, V. R. *et al.* (2018) 'Long-term observations of black carbon aerosol over a rural location in southern peninsular India: Role of dynamics and meteorology', *Atmospheric Environment*. Elsevier, 189(June), pp. 264–274. doi: 10.1016/j.atmosenv.2018.06.020.
Kirchstetter, T. W. *et al.* (2017) 'Large reductions in urban black carbon concentrations in the United States between 1965 and 2000', *Atmospheric Environment*. Elsevier Ltd, 151, pp. 17–23. doi: 10.1016/j.atmosenv.2016.11.001.
Kleefeld, S. *et al.* (2002) 'Importance of organic and black carbon in atmospheric aerosols at Mace Head, on the West Coast of Ireland', *Atmospheric Environment*, 36, pp. 4479–4490.
Klimont, Z. *et al.* (2017) 'Global anthropogenic emissions of particulate matter including black carbon', *Atmospheric Chemistry and Physics*, 17, pp. 8681–8723.
Knox, A. *et al.* (2009) 'Mass Absorption Cross-Section of Ambient Black Carbon Aerosol in Relation to Chemical Age', *Aerosol Science and Technology*, 43, pp. 522–532. doi: 10.1080/02786820902777207.
Koch, D. *et al.* (2009) 'Evaluation of black carbon estimations in global aerosol models', *Atmospheric Chemistry and Physics*, 9, pp. 9001–9026.
Koch, D. *et al.* (2011) 'Soot microphysical effects on liquid clouds, a multi-model

investigation', *Atmospheric Chemistry and Physics*, 11, pp. 1051–1064. doi: 10.5194/acp-11-1051-2011.
Kompalli, S. K. *et al.* (2013) 'Seasonal variation in the spatial distribution of aerosol black carbon over Bay of Bengal: A synthesis of multi-campaign measurements', *Atmospheric Environment*. Elsevier Ltd, 64, pp. 366–373. doi: 10.1016/j.atmosenv.2012.09.073.
Kourtchev, I. *et al.* (2011) 'The use of polar organic compounds to estimate the contribution of domestic solid fuel combustion and biogenic sources to ambient levels of organic carbon and PM2.5 in Cork Harbour, Ireland', *Science of the Total Environment*. Elsevier B.V., 409(11), pp. 2143–2155. doi: 10.1016/j.scitotenv.2011.02.027.
Krapf, M. *et al.* (2017) 'Wood combustion particles induce adverse effects to normal and diseased airway epithelia', *Environmental Science Processes & Impacts*, 19, pp. 538–548. doi: 10.1039/C6EM00586A.
Kreyling, W. G., Hirn, S. and Schleh, C. (2010) 'Nanoparticles in the lung', *Nature Publishing Group*. Nature Publishing Group, 28(12), pp. 1275–1276. doi: 10.1038/nbt1210-1275.
Kucbel, M. *et al.* (2017) 'Temporal and seasonal variations of black carbon in a highly polluted European city: Apportionment of potential sources and the effect of meteorological conditions', *Journal of Environmental Management*, 203, pp. 1178–1189. doi: 10.1016/j.jenvman.2017.05.038.
Kutzner, R. D. *et al.* (2018) 'Long-term monitoring of black carbon across Germany', *Atmospheric Environment*. Elsevier, 185(April), pp. 41–52. doi: 10.1016/j.atmosenv.2018.04.039.
Lack, D. A. *et al.* (2008) 'Bias in Filter-Based Aerosol Light Absorption Measurements Due to Organic Aerosol Loading: Evidence from Ambient Measurements', *Aerosol Science and Technology*, 6826, pp. 1033–1041. doi: 10.1080/02786820802389277.
Laeremans, M. *et al.* (2018) 'Black Carbon Reduces the Beneficial Effect of Physical Activity on Lung Function', *Journal of the American College of Sports Medicine*, (9), pp. 1875–1881. doi: 10.1249/MSS.0000000000001632.
Lamarque, J. *et al.* (2010) 'Historical (1850 – 2000) gridded anthropogenic and biomass burning emissions of reactive gases and aerosols: methodology and application', *Atmospheric Chemistry and Physics*, 10, pp. 7017–7039. doi: 10.5194/acp-10-7017-2010.
Laskin, A., Laskin, J. and Nizkorodov, S. A. (2015) 'Chemistry of Atmospheric Brown Carbon', *Chemical Reviews*, 115, pp. 4335–4382. doi: 10.1021/cr5006167.
Leonard, A. G., Crowley, D. and Belton, J. (1950) 'Atmospheric Pollution in Dublin during the Years 1944-50', in *Scientific Proceedings of the Royal Dublin Society*, pp. 166–167.
Leonard, A. G. and McVerry, B. P. (1939) 'Air Pollution in Dublin during 1938', in *Scientific Proceedings of the Royal Dublin Society*.
Leonard, A. G., McVerry, B. P. and Crowley, D. (1940) 'Air Pollution in Dublin during 1939', in *Scientific Proceedings of the Royal Dublin Society*, pp. 257–265.
Leonard, A. G., McVerry, B. P. and Crowley, D. (1941) 'Air Pollution in Dublin during 1940', in *Scientific Proceedings of the Royal Dublin Society*, pp. 399–404.
Leonard, A. G., McVerry, B. P. and Crowley, D. (1942) 'Air Pollution in Dublin during 1941', in *Scientific Proceedings of the Royal Dublin Society*, pp. 10–17.
Leonard, A. G., McVerry, B. P. and Crowley, D. (1943) 'Air Pollution in Dublin during 1942', in *Scientific Proceedings of the Royal Dublin Society*, pp. 164–170.

Lewtas, J. (2007) 'Air pollution combustion emissions: Characterization of causative agents and mechanisms associated with cancer, reproductive, and cardiovascular effects', *Mutation Research*, 636, pp. 95–133. doi: 10.1016/j.mrrev.2007.08.003.
Li, Q. *et al.* (2017) 'Impacts of household coal and biomass combustion on indoor and ambient air quality in China: Current status and implication', *Science of the Total Environment*. Elsevier B.V., 576, pp. 347–361. doi: 10.1016/j.scitotenv.2016.10.080.
Lim, S. S. *et al.* (2012) 'A comparative risk assessment of burden of disease and injury attributable to 67 risk factors and risk factor clusters in 21 regions , 1990 – 2010 : a systematic analysis for the Global Burden of Disease Study 2010', *Lancet*, 380, pp. 2224–2260. doi: 10.1016/S0140-6736(12)61766-8.
Lin, C. *et al.* (2017) 'Characterization of Primary Organic Aerosol from Domestic Wood, Peat, and Coal Burning in Ireland', *Environmental Science & Technology*, 51, pp. 10624–10632. doi: 10.1021/acs.est.7b01926.
Lin, C. *et al.* (2018) 'Extreme air pollution from residential solid fuel burning', *Nature Sustainability*. Springer US, 1(September), pp. 512–517. doi: 10.1038/s41893-018-0125-x.
Lin, C. (2019) *Chemical Nature and Sources of Particulate Matter in Urban Areas*.
Lin, C., Ceburnis, D., Huang, R., Canonaco, F., *et al.* (2019) 'Summertime Aerosol over the West of Ireland Dominated by Secondary Aerosol during Long-Range Transport', *Atmosphere*, 10. doi: 10.3390/atmos10020059.
Lin, C., Ceburnis, D., Huang, R., Xu, W., *et al.* (2019) 'Wintertime aerosol dominated by solid-fuel-burning emissions across Ireland: insight into the spatial and chemical variation in submicron aerosol', *Atmospheric Chemistry and Physics*, 5, pp. 14091–14106.
Liousse, C. *et al.* (2014) 'Explosive growth in African combustion emissions from 2005 to 2030', *Environmental Research Letters*, 9. doi: 10.1088/1748-9326/9/3/035003.
Liu, C. *et al.* (2018) 'The absorption Ångström exponent of black carbon: from numerical aspects', *Atmospheric Chemistry and Physics*, 18, pp. 6259–6273.
Liu, C. *et al.* (2019) 'Black carbon aggregates: A database for optical properties', *Journal of Quantitative Spectroscopy and Radiative Transfer*. Elsevier Ltd, 222–223, pp. 170–179. doi: 10.1016/j.jqsrt.2018.10.021.
Liu, D. *et al.* (2014) 'Size distribution, mixing state and source apportionment of black carbon aerosol in London during wintertime', *Atmospheric Chemistry and Physics*, 14, pp. 10061–10084. doi: 10.5194/acp-14-10061-2014.
Liu, H. *et al.* (2019) 'Effective densities of soot particles and their relationships with the mixing state at an urban site of the Beijing mega-city in the winter of 2018', *Atmospheric Chemistry and Physics Discussions*, pp. 1–25.
Logan, W. P. (1949) 'Fog and Mortality', *Lancet*, 253, pp. 78–79. doi: 10.1016/S0140-6736(49)90401-8.
Logan, W. P. (1952) 'Mortality in the London Fog Incident, 1952', *British Medical Journal*.
Logan, W. P. (1956) 'Mortality from Fog in London, January, 1956', *British Medical Journal*, pp. 722–725.
Longhurst, J. W. S. *et al.* (2016) 'Progress with Air Quality Management in the 60 years since the UK Clean Air Act, 1956. Lessons, Failures, Challenges and Opportunities.', *International Journal of Sustainable Development and Planning*, 11(4), pp. 491–499. doi: 10.2495/SDP-V11-N4-491-499.
Lyamani, H. *et al.* (2011) 'Black carbon aerosols over an urban area in south-eastern Spain: Changes detected after the 2008 economic crisis', *Atmospheric Environment*.

Elsevier Ltd, 45(35), pp. 6423–6432. doi: 10.1016/j.atmosenv.2011.07.063.
Macqueen, J. (1967) 'Some Methods for the Classification and Analysis of Multivaruate Observations', in *Fifth Berkeley Symposium on Mathematical Statistics and Probability*, pp. 281–297.
Magee Scientific Inc (2016) 'Aethalometer® Model AE33 User Manual', (March).
Marley, N. A. *et al.* (2001) 'An Empirical Method for the Determination of the Complex Refractive Index of Size-Fractionated Atmospheric Aerosols for Radiative Transfer Calculations', *Aerosol Science and Technology*, 34, pp. 535–549.
Mazzarella, G. *et al.* (2012) 'Inflammatory effects on human lung epithelial cells after exposure to diesel exhaust micron sub particles (PM1.0) and pollen allergens', *Environmental Pollution*. Elsevier Ltd, 161, pp. 64–69. doi: 10.1016/j.envpol.2011.09.046.
McCrillis, R. C., Watts, R. R. and Warren, S. H. (2012) 'Effects of Operating Variables on PAH Emissions and Mutagenicity of Emissions from Woodstoves', *Journal of Air & Waste Management Association*, 3289. doi: 10.1080/10473289.1992.10467021.
McGettigan, M. F. and O'Donnell, C. (1995) *Air Pollutnats in Ireland: Emissions, Depositions and Concentrations 1984 - 1994*.
McLoughlin, E. (2001) *An Economic Analysis of Air Pollution Regulations: A Case Study of the Ban on Bituminous Coal*. Dublin.
McNally, M. (2013) *Assessing the impacts of domestic solid fuel use on ambient air quality in Ireland*. Dublin Institute of Technology.
Melton, L. A. (1984) 'Soot diagnostics based on laser heating', *Applied optics*, 23(13).
Mészáros, E. (1999) *Fundamentals of atmospheric aerosol chemistry*. Budapest: Akadémiai Kiadó.
Mirabelli, M. C. *et al.* (2009) 'Respiratory Symptoms Following Wildfie Smoke Exposure - Airway Size as a Susceptibility Factor', *Epidemiology*, 20(3), pp. 451–459. doi: 10.1097/EDE.0b013e31819d128d.Respiratory.
Miyazaki, Y. *et al.* (2008) 'Performance of a newly designed continuous soot monitoring system (COSMOS)', *Journal of Environmental Monitoring*, 10, pp. 1195–1201. doi: 10.1039/b806957c.
Monks, P. S. *et al.* (2009) 'Atmospheric composition change – global and regional air quality', *Atmospheric Environment*, 43, pp. 5268–5350. doi: 10.1016/j.atmosenv.2009.08.021.
Montilla, E. *et al.* (2011) 'Absorption, scattering and single scattering albedo of aerosols obtained from in situ measurements in the subarctic coastal region of Norway', *Atmospheric Chemistry and Physics Discussions*, 11, pp. 2161–2182. doi: 10.5194/acpd-11-2161-2011.
Moosmüller, H., Chakrabarty, R. K. and Arnott, W. P. (2009) 'Aerosol light absorption and its measurement: A review', *Journal of Quantitative Spectroscopy and Radiative Transfer*, 110, pp. 844–878. doi: 10.1016/j.jqsrt.2009.02.035.
Muir, D. and Laxen, D. P. H. (1995) 'Black Smoke as a Surrogate for PM10 in Health Studies?', *Atmospheric Environment*, 29(8), pp. 959–962.
National Oceanic and Atmospheric Administation (2016) *Magee Scientific Aethalometer ® Model AE33 Standard Operation Procedures Reference Manual*.
Ng, N. L. *et al.* (2011) 'An Aerosol Chemical Speciation Monitor (ACSM) for Routine Monitoring of the Composition and Mass Concentrations of Ambient Aerosol', *Aerosol Science and Technology*, 6826. doi: 10.1080/02786826.2011.560211.
Ni, H. *et al.* (2018) 'Source apportionment of carbonaceous aerosols in Xi'an, China: insights from a full year of measurements of radiocarbon and the stable isotope 13C',

Atmospheric Chemistry and Physics, pp. 16363–16383.
Ni, M. *et al.* (2014) 'A review on black carbon emissions, worldwide and in China', *Chemosphere*. Elsevier Ltd, 107, pp. 83–93. doi: 10.1016/j.chemosphere.2014.02.052.
Novakov, T. (1984) 'The role of soot and primary oxidants in atmospheric chemistry', *Science of the Total Environment*, 36, pp. 1–10.
O'Connor, I. P. (2012) *Temporal variability of aerosols by composition within Cork Harbour*.
O'Dowd, C. D. *et al.* (1997) 'Matine Aerosol, Sea-Salt, and the Marine Sulphur Cycle: A Short Review', *Atmospheric Environment*, 31(1), pp. 73–80.
O'Dwyer, M. (2013) *Air Quality in Ireland 2013: Key Indicators of Ambient Air Quality*.
O'Leary, B. (2010) *Review of Ambient Air Quality Monitoring in Ireland*.
OECD (1964) 'Methods of Measuring Air Pollution'.
Onasch, T. B. *et al.* (2012) 'Soot Particle Aerosol Mass Spectrometer: Development, Validation, and Initial Application', *Aerosol Science and Technology*, 46, pp. 804–817. doi: 10.1080/02786826.2012.663948.
Paatero, P. (1997) 'Least squares formulation of robust non-negative factor analysis', *Chemometrics and Intelligent Laboratory Systems*, 37, pp. 23–35.
Paatero, P. and Tapper, U. (1994) 'Positive Matrix Factorization: A non-negative factor model with optimal utilization of error estimates of data values', *Environmetrics*.
Pan, X. *et al.* (2019) 'Dynamic shape factor and mixing state of refractory black carbon particles in winter in Beijing using an AAC-DMA-SP2 tandem system', *Atmospheric Chemistry and Physics Discussions*, pp. 1–31.
Pattle, R. E., Wedd, G. D. and Burges, F. (1959) 'The Acute Toxic Effects of Black Smoke', *British Journal of Inustrial Medicine*, 16, pp. 216–220.
Pearson, J. F. *et al.* (2010) 'Association Between Fine Particulate Matter and Diabetes Prevelance in the U.S.', *Diabetes Care*, 33(10), pp. 2196–2201. doi: 10.2337/dc10-0698.
Peden, D. B. (2005) 'The epidemiology and genetics of asthma risk associated with air pollution', *Journal of Allergy and Clinical Immunology*, pp. 213–219. doi: 10.1016/j.jaci.2004.12.003.
Penner, J. E., Chuang, C. C. and Grant, K. (1998) 'Climate forcing by carbonaceous and sulfate aerosols', *Climate Dynamics*, 14(June), pp. 839–851.
Penner, J. E., Eddleman, H. and Novakov, T. (1993) 'Towards the Development of a Global Inventory for Black Carbon Emissions', *Atmospheric Environment*, 27(8), pp. 1277–1295.
Perron, N. *et al.* (2010) 'Composition and sources of particulate matter in an industrialised Alpine valley', *Atmospheric Chemistry and Physics Discussions*, 10, pp. 9391–9430.
Petit, J. *et al.* (2014) 'Submicron aerosol source apportionment of wintertime pollution in Paris , France by double positive matrix factorization (PMF 2) using an aerosol chemical speciation monitor (ACSM) and a multi-wavelength Aethalometer', *Atmospheric Chemistry and Physics*, (14), pp. 13773–13787. doi: 10.5194/acp-14-13773-2014.
Petit, J. *et al.* (2017) 'Characterising an intense PM pollution episode in March 2015 in France from multi-site approach and near real time data: Climatology, variabilities, geographical origins and model evaluation', *Atmospheric Environment*. Elsevier Ltd, 155, pp. 68–84. doi: 10.1016/j.atmosenv.2017.02.012.
Petit, J. E. *et al.* (2015) 'Two years of near real-time chemical composition of

submicron aerosols in the region of Paris using an Aerosol Chemical Speciation Monitor (ACSM) and a multi-wavelength Aethalometer', *Atmospheric Chemistry and Physics*, 15(6), pp. 2985–3005. doi: 10.5194/acp-15-2985-2015.
Petzold, A. *et al.* (2013) 'Recommendations for reporting "black carbon" measurements', *Atmospheric Chemistry and Physics*, 13, pp. 8365–8379. doi: 10.5194/acp-13-8365-2013.
Petzold, A. and Schönlinner, M. (2004) 'Multi-angle absorption photometry - A new method for the measurement of aerosol light absorption and atmospheric black carbon', *Journal of Aerosol Science*, 35(4), pp. 421–441. doi: 10.1016/j.jaerosci.2003.09.005.
Pope III, C. A. *et al.* (2016) 'Lung Cancer, Cardiopulmonary Mortality, and Long-Term Exposure to Fine Particulate Air Pollution', *Journal of American Medical Association*, 287(9).
Pöschl, U. (2005) 'Atmospheric Chemistry Atmospheric Aerosols: Composition, Transformation, Climate and Health Effects', *Angewandte Chemie International Edition*, pp. 7520–7540. doi: 10.1002/anie.200501122.
Pozzer, A. *et al.* (2019) 'Long-term concentrations of fi ne particulate matter and impact on human health in Verona, Italy', *Atmospheric Pollution Research*, 10, pp. 731–738. doi: 10.1016/j.apr.2018.11.012.
Prather, K. A., Nordmeyer, T. and Salt, K. (1994) 'Real-Time Characterization of Individual Aerosol Particles Using Time-of-Flight Mass Spectrometry', *Analytical Chemistry*, 66(9), pp. 1403–1407.
Presler-jur, P. *et al.* (2017) 'An evaluation of mass absorption cross-section for optical carbon analysis on Teflon filter media Teflon filter media', *Journal of the Air & Waste Management Association*. Taylor & Francis, 67(11), pp. 1213–1228. doi: 10.1080/10962247.2017.1310148.
QUARG (1996) *Third Report of the Quality of Urban Air Review Group - Airborne Particulate Matter in the UK*.
Quincey, P. (2007) 'A relationship between Black Smoke Index and Black Carbon concentration', *Atmospheric Environment*, 41, pp. 7964–7968. doi: 10.1016/j.atmosenv.2007.09.033.
Quincey, P. *et al.* (2009) 'An evaluation of measurement methods for organic, elemental and black carbon in ambient air monitoring sites', *Atmospheric Environment*, 43(32), pp. 5085–5091.
Radney, J. G. *et al.* (2014) 'Dependence of Soot Optical Properties on Particle Morphology: Measurements and Model Comparisons', *Environmental Science & Technology*, 48, pp. 3169–3176.
Ran, L. *et al.* (2016) 'Black carbon and wavelength-dependent aerosol absorption in the North China Plain based on two-year aethalometer measurements', *Atmospheric Environment*. Elsevier Ltd, 142, pp. 132–144. doi: 10.1016/j.atmosenv.2016.07.014.
Rao, S. *et al.* (2005) 'Long-term scenarios for black and organic carbon emissions', *Environmental Sciences*, 2(2–3), pp. 205–216. doi: 10.1080/15693430500397228.
Reche, C. *et al.* (2011) 'New considerations for PM, Black Carbon and particle number concentration for air quality monitoring across different European cities', *Atmospheric Chemistry and Physics*, 11, pp. 6207–6227. doi: 10.5194/acp-11-6207-2011.
Reinard, M. S. *et al.* (2007) 'Source characterization and identification by real-time single particle mass spectrometry', *Atmospheric Environment*, 41, pp. 9397–9409. doi: 10.1016/j.atmosenv.2007.09.001.
Richter, D. and Williams, W. P. (1998) *Urban Air Quality in Europe*.
Roemer, W., Hoek, G. and Brunekreef, B. (2000) 'Pollution effects on asthmatic

children in Europe , the PEACE study', *Clinical and Experimental Allergy*, 30, pp. 1067–1075.
Rönkkö, T. and Timonen, H. (2019) 'Overview of Sources and Characteristics of Nanoparticles in Urban Traffic-Influenced Areas', *Journal of Alzheimer's Disease*, 72, pp. 15–28. doi: 10.3233/JAD-190170.
Saffari, A. *et al.* (2013) 'Increased Biomass Burning Due to the Economic Crisis in Greece and Its Adverse Impact on Wintertime Air Quality in Thessaloniki', *Environmental Science & Technology*, 47, pp. 13313–13320. doi: 10.1021/es403847h.
Sahu, S. K., Beig, G. and Sharma, C. (2008) 'Decedal growth of black carbon emissions in India', *Geophysical Research Letters*, 35. doi: 10.1029/2007GL032333.
Salameh, D. *et al.* (2015) 'PM2.5 chemical composition in five European Mediterranean cities: A 1-year study', *Atmospheric Research*. Elsevier B.V., 155, pp. 102–117. doi: 10.1016/j.atmosres.2014.12.001.
Saleh, R. *et al.* (2015) 'Contribution of brown carbon and lensing to the direct radiative effect of carbonaceous aerosols from biomass and biofuel burning emissions', *Journal of Geophysical Research: Atmospheres*, 120, pp. 10,285-10,296. doi: 10.1002/2015JD023697.Received.
Sandradewi, J., Prevot, A. S. H., Weingartner, E., *et al.* (2008) 'A study of wood burning and traffic aerosols in an Alpine valley using a multi-wavelength Aethalometer', *Atmospheric Environment*, 42, pp. 101–112. doi: 10.1016/j.atmosenv.2007.09.034.
Sandradewi, J., Prevot, A. S. H., Szidat, S., *et al.* (2008) 'Using Aerosol Light Absorption Measurements for the Quantitative Determination of Wood Burning and Traffic Emission Contributions to Particulate Matter', *Environmental Science & Technology*, 42(9), pp. 3316–3323.
Scarnato, B. V *et al.* (2013) 'Effects of internal mixing and aggregate morphology on optical properties of black carbon using a discrete dipole', *Atmospheric Chemistry and Physics*, 13, pp. 5089–5101. doi: 10.5194/acp-13-5089-2013.
Schaap, M. *et al.* (2004) 'Anthropogenic black carbon and fine aerosol distribution over Europe', *Journal of Geophysical Research*, 109. doi: 10.1029/2003JD004330.
von Schneidemesser, E., Mar, K. A. and Saar, D. (2017) *Black Carbon in Europe - Targetting an Air Pollutant and Climate Forcer*.
Schneider, J. *et al.* (2006) 'Mass spectrometric analysis and aerodynamic properties of various types of combustion-related aerosol particles', *International Journal of Mass Spectrometry*, 258, pp. 37–49. doi: 10.1016/j.ijms.2006.07.008.
Schwartz, J. and Dockery, D. W. (1992) 'Particulate Air Pollution and Daily Mortality in Steubenville , Ohio', *American Journal of Epidemiology*, 135(1), pp. 12–25.
Schwarz, J. P. *et al.* (2006) 'Single-particle measurements of midlatitude black carbon and light-scattering aerosols from the boundary layer to the lower stratosphere', *Journal of Geophysical Research Atmospheres*, 111(16), pp. 1–15. doi: 10.1029/2006JD007076.
Schwarz, J. P. *et al.* (2012) 'Assessing recent measurement techniques for quantifying black carbon concentration in snow', *Atmospheric Measurement Techniques*, 5, pp. 3771–3795. doi: 10.5194/amtd-5-3771-2012.
Sciare, J. *et al.* (2008) 'Long-term measurements of carbonaceous aerosols in the eastern Mediterranean: evidence of long-range transport of biomass burning', *Atmospheric Chemistry and Physics*, (8), pp. 5551–5563. doi: 10.5194/acp-8-5551-2008.
SEAI (2018) *Energy in ireland, 2018 Report*.
Sedlacek III, A. J. *et al.* (2012) 'Determination of and evidence for non-core-shell

structure of particles containing black carbon using the Single-Particle Soot Photometer (SP2)', *Geophysical Research Letters*, 39, pp. 2–7. doi: 10.1029/2012GL050905.
Seinfeld, J. H. and Pandis, S. N. (2006) *Atmospheric Chemistry and Physics: From Air Pollution to Climate Change*. Wiley.
Shaddick, G. and Zidek, J. V (2014) 'A case study in preferential sampling : Long term monitoring of air pollution in the UK', *Spatial Statistics*. Elsevier Ltd, 9, pp. 51–65. doi: 10.1016/j.spasta.2014.03.008.
Shupler, M. *et al.* (2018) 'Global estimation of exposure to fine particulate matter (PM 2.5) from household air pollution', *Environment International*. Elsevier, 120, pp. 354–363. doi: 10.1016/j.envint.2018.08.026.
Singh, V. *et al.* (2018) 'Trends of atmospheric black carbon concentration over the United Kingdom', *Atmospheric Environment*. Elsevier, 178, pp. 148–157. doi: 10.1016/j.atmosenv.2018.01.030.
Skyllakou, K. *et al.* (2014) 'Contributions of local and regional sources to fine PM in the megacity of Paris', *Atmospheric Chemistry and Physics*, 14, pp. 2343–2352. doi: 10.5194/acp-14-2343-2014.
Slowik, J. G. *et al.* (2010) 'Simultaneous factor analysis of organic particle and gas mass spectra: AMS and PTR-MS measurements at an urban site', *Atmospheric Chemistry and Physics*, 10, pp. 1969–1988.
Smith, J. D. and Atkinson, D. B. (2001) 'A portable pulsed cavity ring-down transmissometer for measurement of the optical extinction of the atmospheric aerosol', *Analyst*, 126, pp. 1216–1220. doi: 10.1039/b101491i.
Snelling, D. R. *et al.* (2005) 'A calibration-independent laser-induced incandescence technique for soot measurement by detecting absolute light intensity', *Applied optics*, 44(31), pp. 6773–6785.
Sorensen, C. M. (2001) 'Light Scattering by Fractal Aggregates : A Review Light Scattering by Fractal Aggregates: A Review', *Aerosol Science and Technology*, 35, pp. 648–687.
Stankovic, A. *et al.* (2019) 'Black Smoke and Sulphur Dioxide in the Air as Risk Factors for Dry Eye Disease', *Polish Journal of Environmental Studies*, 28(4), pp. 2381–2388. doi: 10.15244/pjoes/91782.
Stephens, M., Turner, N. and Sandberg, J. (2003) 'Particle identification by laser-induced incandescence in a solid-state laser cavity', *Applied optics*, 42(19), pp. 3726–36. doi: 10.1364/AO.42.003726.
Streets, D. G. *et al.* (2004) 'On the future of carbonaceous aerosol emissions', *Journal of Geophysical Research*, 109. doi: 10.1029/2004JD004902.
Sunset Laboratory Inc. (2005) *Semi-Continuous OCEC Carbon Aerosol Analyzer*.
Takemura, T. and Suzuki, K. (2019) 'Weak global warming mitigation by reducing black carbon emissions', *Nature Scientific Reports*. doi: 10.1038/s41598-019-41181-6.
The National Archives (2019) *legislation.gov.uk*. Available at: https://www.legislation.gov.uk/ (Accessed: 21 October 2019).
Thunis, P. *et al.* (2017) *Urban $PM_{2.5}$ Atlas - Air quality in European cities*. doi: 10.2760/336669.
Thunis, P. *et al.* (2018) 'PM 2.5 source allocation in European cities: A SHERPA modelling study', *Atmospheric Environment*. Elsevier, 187, pp. 93–106. doi: 10.1016/j.atmosenv.2018.05.062.
Tiwari, S. *et al.* (2013) 'Diurnal and seasonal variations of black carbon and PM 2.5 over New Delhi, India: Influence of meteorology', *Atmospheric Research*. Elsevier

B.V., 125–126, pp. 50–62. doi: 10.1016/j.atmosres.2013.01.011.
TSI (2007) *Series 3800 Aerosol Time-of-Flight Mass Spectrometers with Aerodynamic Focusing Lens Technology*.
U.S. Department of the Interior (1967) *Ringlemann Smoke Chart*.
UK Met Office (2016) *UK Storm Season 2015/16*. Available at: https://www.metoffice.gov.uk/weather/warnings-and-advice/uk-storm-centre/uk-storm-season-2015-16.
UNECE (2004) *Cleaning the Air - 25 years of the Convention on Long-range Transboundary Air Pollution*.
Vaishya, A. *et al.* (2017) 'Aerosol black carbon quanti fi cation in the central Indo-Gangetic Plain: Seasonal heterogeneity and source apportionment', *Atmospheric Research*. Elsevier B.V., 185, pp. 13–21. doi: 10.1016/j.atmosres.2016.10.001.
Vecchi, R. *et al.* (2014) 'A filter-based light-absorption measurement with polar photometer: Effects of sampling artefacts from organic carbon', *Journal of Aerosol Science*. Elsevier, 70, pp. 15–25. doi: 10.1016/j.jaerosci.2013.12.012.
Vicente, E. D. and Alves, C. A. (2018) 'An overview of particulate emissions from residential biomass combustion', *Atmospheric Research*. Elsevier, 199, pp. 159–185. doi: 10.1016/j.atmosres.2017.08.027.
Vignati, E. *et al.* (2010) 'Sources of uncertainties in modelling black carbon at the global scale', *Atmospheric Chemistry and Physics*, 2, pp. 2595–2611.
Virkkula, A. *et al.* (2007) 'A simple procedure for correcting loading effects of aethalometer data', *Journal of the Air and Waste Management Association*, 57(10), pp. 1214–1222. doi: 10.3155/1047-3289.57.10.1214.
Virkkula, A. *et al.* (2015) 'On the interpretation of the loading correction of the aethalometer', *Atmospheric Measurement Techniques*, 8, pp. 4415–4427. doi: 10.5194/amt-8-4415-2015.
Wang, R. *et al.* (2012) 'Black Carbon Emissions in China from 1949 to 2050', *Environmental Science & Technology*, 46, pp. 7595–7603. doi: 10.1021/es3003684.
Wang, R. *et al.* (2014) 'Trend in Global Black Carbon Emissions from 1960 to 2007', *Environmental Science & Technology*, 48, pp. 6780–6787. doi: 10.1021/es5021422.
Wang, X. *et al.* (2013) 'Characterization of organic aerosol produced during pulverized coal combustion in a drop tube furnace', *Atmospheric Chemistry and Physics*, 13, pp. 10919–10932. doi: 10.5194/acp-13-10919-2013.
Wang, Y., Hopke, Philip K, Rattigan, O. V and Zhu, Y. (2011) 'Characterization of ambient black carbon and wood burning particles in two', *Journal of Environmental Monitoring*, 13, pp. 1919–1926. doi: 10.1039/c1em10117j.
Wang, Y., Hopke, Philip K., *et al.* (2011) 'Characterization of ambient black carbon and wood burning particles in two urban areas', *Journal of Environmental Monitoring*, 13, pp. 1919–1926. doi: 10.1039/c1em10117j.
Wang, Y., Hopke, Philip K, Rattigan, O. V, Xia, X., *et al.* (2011) 'Characterization of Residential Wood Combustion Particles Using the Two-Wavelength Aethalometer', *Environmental Science & Technology*, 45, pp. 7387–-7393. doi: dx.doi.org/10.1021/es2013984.
Weimer, S. *et al.* (2008) 'Organic aerosol mass spectral signatures from wood-burning emissions: Influence of burning conditions and wood type', *Journal of Geophysical Research*, 113. doi: 10.1029/2007JD009309.
Weingartner, E. *et al.* (2003) 'Absorption of light by soot particles : determination of the absorption coefficient by means of aethalometers', 34, pp. 267–282. doi: 10.1016/S0021-8502(03)00359-8.
WHO (2015) *Residential heating with wood and coal: health impacts and policy*

options in Europe and North America.
WHO (2016) *Ambient Air Pollution: A global assessment of exposure and burden of disease*.
World Health Organization (2013) *Health Effects of Particulate Matter: Policy implications for countries in eastern Europe, Caucasus and central Asia*.
Wu, D. *et al.* (2013) 'Black carbon over the South China Sea and in various continental locations in South China', *Atmospheric Chemistry and Physics*, (1999), pp. 12257–12270. doi: 10.5194/acp-13-12257-2013.
Wu, J.-Z. *et al.* (2018) 'Effects of particulate matter on allergic respiratory diseases', *Chronic Diseases and Translational Medicine*. Elsevier Masson SAS, 4(2), pp. 95–102. doi: 10.1016/j.cdtm.2018.04.001.
Yang, S. *et al.* (2015) 'Climate effect of black carbon aerosol in a Tibetan Plateau glacier', *Atmospheric Environment*. Elsevier Ltd, 111, pp. 71–78. doi: 10.1016/j.atmosenv.2015.03.016.
Yap, C. *et al.* (2012) 'Association between long-term exposure to air pollution and specific causes of mortality in Scotland', *Occupational Environmental Medicine*, 69, pp. 916–924. doi: 10.1136/oemed-2011-100600.
Yin, J. *et al.* (2005) 'Major component composition of urban PM10 and PM2.5 in Ireland', *Atmospheric Research*, 78, pp. 149–165. doi: 10.1016/j.atmosres.2005.03.006.
You, R. *et al.* (2016) 'Measured Wavelength-Dependent Absorption Enhancement of Internally Mixed Black Carbon with Absorbing and Non- absorbing Materials', *Environmental Science and Technology*, 50(15), pp. 7982–7990. doi: 10.1021/acs.est.6b01473.Measured.
Zanatta, M. *et al.* (2016) 'A European aerosol phenomenology-5 : Climatology of black carbon optical properties at 9 regional background sites across Europe', *Atmospheric Environment*, 145, pp. 346–364. doi: 10.1016/j.atmosenv.2016.09.035.
Zhang, Q. *et al.* (2011) 'Understanding atmospheric organic aerosols via factor analysis of aerosol mass spectrometry: a review', *Analytical and Bioanalytical Chemistry*, 401, pp. 3045–3067. doi: 10.1007/s00216-011-5355-y.
Zhang, R. *et al.* (2008) 'Variability in morphology, hygroscopicity, and optical properties of soot aerosols during atmospheric processing', *Proceedings of the National Academy of Sciences of the United States of America*, 105(30), pp. 10291–10296.
Zhang, Y. *et al.* (2016) 'Measuring the morphology and density of internally mixed black carbon with SP2 and VTDMA: new insight into the absorption enhancement of black carbon in the atmosphere', *Atmospheric Measurement Techniques*, 9, pp. 1833–1843. doi: 10.5194/amt-9-1833-2016.
Zhang, Y. J. *et al.* (2015) 'Insights into characteristics, sources, and evolution of submicron aerosols during harvest seasons in the Yangtze River delta region, China', *Atmospheric Chemistry and Physics*, 15, pp. 1331–1349. doi: 10.5194/acp-15-1331-2015.
Zhao, X. *et al.* (2009) 'Seasonal and diurnal variations of ambient PM 2.5 concentration in urban and rural environments in Beijing', *Atmospheric Environment*. Elsevier Ltd, 43(18), pp. 2893–2900. doi: 10.1016/j.atmosenv.2009.03.009.
Zhou, X. *et al.* (2009) 'Measurement of black carbon aerosols near two Chinese megacities and the implications for improving emission inventories', *Atmospheric Environment*. Elsevier Ltd, 43(25), pp. 3918–3924. doi: 10.1016/j.atmosenv.2009.04.062.
Zotter, P. *et al.* (2017) 'Evaluation of the absorption Angstrom exponents for traffic

and wood burning in the Aethalometer-based source apportionment using radiocarbon measurements of ambient aerosol', *Atmospheric Chemistry and Physics*, 17(6), pp. 4229–4249. doi: 10.5194/acp-17-4229-2017.

Appendix I

As mentioned in Chapter 2, the analysis of all aethalometer data was carried out using the *R* programming language. The same method was used for the analysis of all data and the script is detailed below. Script 1 provides details on the averaging of the data, calculation of the α values, and the method of source apportionment. Script 2 shows the script used for the graphing of the data gathered. The scripts presented below was used to process and analyse the Killarney data. This script was adapted to analyse the data gathered in Enniscorthy, Birr, and at the UCD monitoring site.

Script 1:

```
library(openair)
library(zoo)
setwd("C:\\Users\\Paul Buckley\\Desktop\\Killarney Aeth Files")
source("C:\\Users\\Paul Buckley\\Desktop\\Killarney Aeth Files\\Killarney BC PB.r")
channels <- c("BC1.", "BC2.", "BC3.", "BC4.", "BC5.", "BC6.", "BC7.")
bc = BC[,channels]
date <- BC[,"date"]
bcmovmean <- rollmean(bc,15,na.pad=TRUE)
bcmovmean <- as.data.frame(bcmovmean, optional = FALSE, stringsAsFactors = default.stringsAsFactors())
bcmovmean <- bcmovmean[!is.na(rowSums(bcmovmean)),]
wave <- c(370, 470, 520, 590, 660, 880, 950)
sigma <- c(18.47, 14.54, 13.14, 11.58, 10.35, 7.77, 7.19)
x <- log(wave)
keep <- complete.cases(bcmovmean)
bc <- bcmovmean[keep,]
date <- date[keep]
good <- bc != 0;
use <- apply(good,1,all)
bc <- bc[use,]
date <- date[use]
columnsuse <- c(2:7)
```

```
alpha <- vector("numeric")
for(i in 1:dim(bc)[1]){
 babs = bc[i,channels[columnsuse]] * sigma[columnsuse]
 y <- as.numeric(log(babs))
 # make sure negative cases don't break the loop
 try({
  a <- lm(y ~ x[columnsuse])
  alpha[i] <- -a$coefficients[2]
 },silent=TRUE)
}
bc$alpha <- alpha
bc$date <- date
Babs880 <- bc$BC6.* 7.77
bc$Babs880 <- Babs880
AverageBC <- timeAverage(bc, avg.time = "hour", statistic = "mean", type ="default")
KValues <- c("K1.","K2.","K3.","K4.","K5.","K6.","K7.")
k = BC[,KValues]
kmovmean <- rollmean(k,15,na.pad=TRUE)
kmovmean <- as.data.frame(kmovmean, optional = FALSE, stringsAsFactors = default.stringsAsFactors())
kmovmean <- kmovmean[!is.na(rowSums(kmovmean)),]
keep <- complete.cases(kmovmean)
k <- kmovmean[keep,]
date <- date[keep]
good <- k != 0;
use <- apply(good,1,all)
k <- k[use,]
date <- date[use]
kmovmean$date <- date
bc$K1 <- kmovmean$K1.
bc$K2 <- kmovmean$K2.
bc$K3 <- kmovmean$K3.
bc$K4 <- kmovmean$K4.
bc$K5 <- kmovmean$K5.
bc$K6 <- kmovmean$K6.
bc$K7 <- kmovmean$K7.
```

```
AverageK <- timeAverage(kmovmean, avg.time = "hour", statistic = "mean", type ="default")

write.csv(AvergaeK, file = "KHour.csv")

timeVariation(AverageBC,pollutant = c("BC1.", "BC7."),ylab = "ng/m3", main = "Temporal trends BC")

AverageBC$K1<-AverageK$K1.

AverageBC$K2<-AverageK$K2.

AverageBC$K3<-AverageK$K3.

AverageBC$K4<-AverageK$K4.

AverageBC$K5<-AverageK$K5.

AverageBC$K6<-AverageK$K6.

AverageBC$K7<-AverageK$K7.

write.csv(AverageBC, file = "BCHour.csv")


#Here use the alpha values from the previous section OR standard values

alfaTR <- 0.9

alfaBB <- 1.68


# You can use any two wavelengths here, but lambda1 should be the shortest wave

lambda1 <- 470

lambda2 <- 950

Ctr <- (lambda1/lambda2)^(-alfaTR)

Cbb <- (lambda1/lambda2)^(-alfaBB)


# select BC vectors and convert to Babs using MAC values in sigma

Babsw1 <- bc[,which(wave==lambda1)] * sigma[which(wave==lambda1)]

Babsw2 <- bc[,which(wave==lambda2)] * sigma[which(wave==lambda2)]

BabsW2bb <- (Babsw1 - Babsw2*Ctr) / (Cbb - Ctr)

BabsW2tr <- (Babsw1 - Babsw2*Cbb) / (Ctr - Cbb)

EBCbb <- BabsW2bb / sigma[which(wave==lambda2)]

EBCtr <- BabsW2tr / sigma[which(wave==lambda2)]

EBC <- EBCtr + EBCbb

BB <- 100 * EBCbb / EBC

FF <- 100 * EBCtr / EBC


plot(date,BB,ylim=c(-100,100))

summary(BB)
```

```
bc$EBC <- EBC

bc$EBCsf <- EBCbb

bc$EBCtr<- EBCtr

bc$BB <- BB

bc$FF <- FF

bc$Ctr <- Ctr

bc$Cbb <- Cbb

bc$date <- date

write.csv(bc, file = "BCtest.csv")

BC <- read.csv("mydata.csv")

Average <- timeAverage(bc, avg.time = "2 hour", statistic = "mean", type ="default")

timeVariation(Average,pollutant = c("Babs880"),ylab = "ng/m3", main = "Temporal trends BC")

timePlot(bc, pollutant = c("EBCsf","EBCtr"),avg.time = "1 hour",group = TRUE, plot.type = "h", cols = c("green", "purple"),

main = "Hourly eBC Split Birr", key = TRUE, ylab = "Concentration (ug/m3)", xlab = "Date")

eBCplot = timeVariation(bc, pollutant = c("EBCsf", "EBCtr"), cols = c("green", "purple"),

ylab = "Concentration (ug/m3")

plot(eBCplot, subset = "day.hour")

plot(eBCplot, subset = "hour")

plot(eBCplot, subset = "day")

write.csv(Average, file<- "BC Killarney Full 2 Hourly Profile New MAC.csv")
```

Script 2:

```
install.packages("hexbin")

install.packages("openair")

install.packages("ggpubr")

library(openair)

library(zoo)

library(ggplot2)

library(ggpubr)

library(dplyr)

library(tidyr)

library(magrittr)

library(gridExtra)

setwd("C:\\Users\\Paul Buckley\\Desktop\\Killarney Aeth Files")
```

```
Killarney = read.csv("Killarney Data NAs.csv", header = TRUE, dec =".")

Weather = read.csv("KIllarney Weather.csv", header = TRUE, dec = ".")

names(Killarney)[1] = "date"

names(Killarney)[2] = "eBC"

names(Killarney)[3] = "eBCsf Zotter"

names(Killarney)[4] = "eBCtr Zotter"

names(Killarney)[5] = "eBCsf Sandradewi"

names(Killarney)[6] = "eBCtr Sandradewi"

names(Killarney)[7] = "eBCsf Buckley"

names(Killarney)[8] = "eBCtr Buckley"

names(Killarney)[11] = "ws"

names(Killarney)[12] = "wd"

names(Killarney)[14] = "Delta C"

names(Weather)[1] = "date"

names(Weather)[2] = "ws"

names(Weather)[3] = "wd"

summary(Killarney$Temperature)

summary(Killarney$ws)

summary(Killarney$Rainfall)

summary(Killarney$PM.2.5.mass)

summary(Killarney$eBC)

timePlot(Killarney, pollutant = c("Rainfall", "Temperature", "ws") ,avg.time = "1 hour",group = FALSE, plot.type = "h",

      cols = c("blue", "red", "green"),

      main = "Killarney", key = TRUE, ylab = NULL, xlab = "Date", par.settings=list(fontsize=list(text=14)))

windRose(Weather, ws.int = 2, angle = 15, grid.line = 2, annotate = FALSE, main = "Killarney", width = 0.5, par.settings=list(fontsize=list(text=12)))

summary(Killarney$eBC)

timePlot(Killarney, pollutant = "Killarney",avg.time = "1 hour",group = TRUE, plot.type = "h", cols = "black", main = "Killarney", key = FALSE, ylab = "eBC Concentration ( ug/m3)", xlab = "Date", par.settings=list(fontsize=list(text=14)))

eBCplot = timeVariation(Killarney, pollutant = "Killarney", main = "Killarney", cols = "black", ylab = "eBC Concentration ( ug/m3)", xlab = c("Hour", "Hour", "Month", "Weekday"), cex.axis = 1.5, cex.label = 2, par.settings=list(fontsize=list(text=14)), key = NULL, main = "Killarney")

plot(eBCplot, subset = "day.hour", key = NULL)

plot(eBCplot, subset = "hour")

plot(eBCplot, subset = "day")
```

```
timePlot(Killarney, pollutant = c("eBCsf Sandradewi","eBCtr Sandradewi"),avg.time = "1 hour",group = TRUE, plot.type = "h", cols = c("green", "purple"), main = "Hourly eBC Split Killarney", key = TRUE, ylab = "Concentration (ug/m3)", xlab = "Date")

SplitplotSandradewi = timeVariation(Killarney, pollutant = c("eBCsf Sandradewi", "eBCtr Sandradewi"), cols = c("green", "purple"), ylab = "Concentration ( ug/m3)", xlab = c("Hour", "Hour", "Month", "Weekday"), cex.axis = 1.5, cex.label = 2, par.settings=list(fontsize=list(text=14)), key = NULL, main = "Killarney")

plot(SplitplotSandradewi, subset = "day.hour")

plot(SplitplotSandradewi, subset = "hour", main = "Killarney")

plot(SplitplotSandradewi, subset = "day")

SplitplotZotter = timeVariation(Killarney, pollutant = c("eBCsf Zotter", "eBCtr Zotter"), cols = c("green", "purple"), ylab = "Concentration ( ug/m3)", xlab = c("Hour", "Hour", "Month", "Weekday"), cex.axis = 1.5, cex.label = 2, par.settings=list(fontsize=list(text=14)))

plot(SplitplotZotter, subset = "day.hour")

plot(SplitplotZotter, subset = "hour")

plot(SplitplotZotter, subset = "day")

SplitplotBuckley = timeVariation(Killarney, pollutant = c("eBCsf Buckley", "eBCtr Buckley"), cols = c("green", "purple"), ylab = "Concentration ( ug/m3)", xlab = c("Hour", "Hour", "Month", "Weekday"), cex.axis = 1.5, cex.label = 2, par.settings=list(fontsize=list(text=14)))

plot(SplitplotBuckley, subset = "day.hour")

plot(SplitplotBuckley, subset = "hour")

plot(SplitplotBuckley, subset = "day")

DeltaCplot = timeVariation(Killarney, pollutant = "Killarney", cols = "forestgreen", ylab = "Delta C (ng/m3)", xlab = c("Hour", "Hour", "Month", "Weekday"), main = "Killarney", cex.axis = 1.5, cex.label = 2, par.settings=list(fontsize=list(text=14)))

plot(DeltaCplot, subset = "day.hour")

plot(DeltaCplot, subset = "hour")

plot(DeltaCplot, subset = "day")

polarPlot(Killarney, pollutant = "eBC", x = "ws", wd = "wd", type = "default", statistic = "mean", resolution = "fine", exclude.missing = TRUE, cols = "default", weights = c(0.25, 0.5, 0.75), min.bin = 1, upper = 20, angle.scale = 315, units = "Windspeed", key.header = "Mean eBC Concentration (ug/m3)", key.footer = NULL, key.position = "bottom", ws_spread = 5, wd_spread = 4, main = "Killarney")

scatterPlot(Killarney, x = "PM.2.5.mass", y = "eBC", method = "scatter", avg.time = "default", smooth = FALSE, spline = FALSE, linear = TRUE, ci = TRUE, cols = "hue", xlab = "PM2.5 Concentration (ug/m3)", ylab = "eBC Concentration (ug/m3)", main = "Killarney eBC Concentration vs PM2.5 Concentration")

Alphaplot = timeVariation(Killarney, pollutant = "Alpha", cols = "Blue", ylab = "Alpha", main = "Killarney", ylim = c(1,1.6), xlab = c("Hour", "Hour", "Month", "Weekday"), cex.axis = 1.5, cex.label = 2, par.settings=list(fontsize=list(text=14)))

plot(Alphaplot, subset = "day.hour")

plot(Alphaplot, subset = "hour")

plot(Alphaplot, subset = "day")

mean(Killarney$Alpha, na.rm = TRUE)
```

```
ggplot(Killarney, aes(x = Alpha)) +
  geom_histogram(binwidth = 0.01,colour = "black", fill = "grey", cex.axis = 1.5,
  cex.label = 2, par.settings=list(fontsize=list(text=14))) +
  geom_vline(aes(xintercept = mean(Alpha, na.rm = TRUE)),
  colour = "red", linetype = "dashed", size = 1) +
  ggtitle("Distribution of Alpha in Killarney\n Mean = 1.24")+
  xlab("Alpha")+
  ylab("Count")+
  xlim(0.5,2.5)
```

Appendix II

While analysing data collected during the SAPPHIRE measurement campaign performed in Enniscorthy, it was discovered that the $PM_{2.5}$ mass concentration recorded by the TEOM was consistently lower than the amounts of carbonaceous aerosol (Elemental Carbon + Organic Carbon) measured. This was likely caused by a leak (detected after the campaign) in the sampling system of the TEOM. As a result, the $PM_{2.5}$ mass concentration measured by the TEOM in Enniscorthy was corrected using a factor derived from the SMPS and OPS aerosol volume concentrations, which were converted to mass, using the recommended particle density values for mixed urban aerosol (d = 1.5 g/cm^3) and sea salt (d = 2.2 g/cm^3) (Healy *et al.*, 2012, 2013; Arndt *et al.*, 2017). This approach was validated by showing that the measured and "reconstructed" $PM_{2.5}$ mass concentrations for Killarney are well correlated, *Figure A.1*. Furthermore, a comparison of the corrected TEOM daily average $PM_{2.5}$ concentration also shows an excellent correlation with daily average PM_{10} concentrations measured by a SWAM 5A monitor located at the monitoring site, *Figure A.2.*

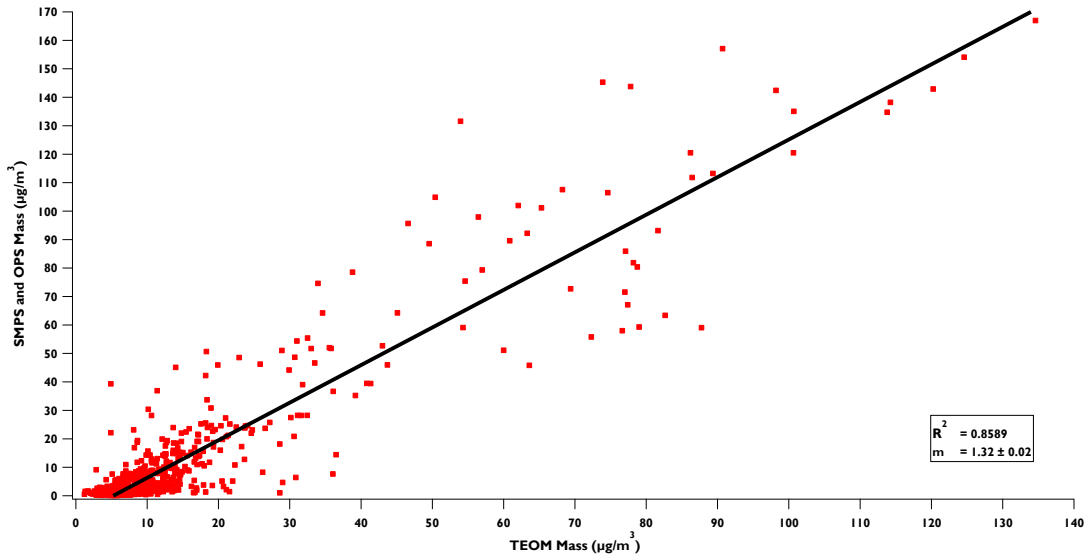

Figure A.1. Plot of "reconstructed" mass concentration (derived from SMPS (< 300 nm) and OPS (< 2.5 µm) measurements) versus the mass concentration measured by the TEOM (µg/m^3) in Killarney during the SAPPHIRE monitoring campaign, 11 November 2014 to 20 December 2014. The slope of this regression was used to correct the TEOM mass concentrations measured in Enniscorthy. Reproduced from work originally carried out by Dr Eoin McGillicuddy.

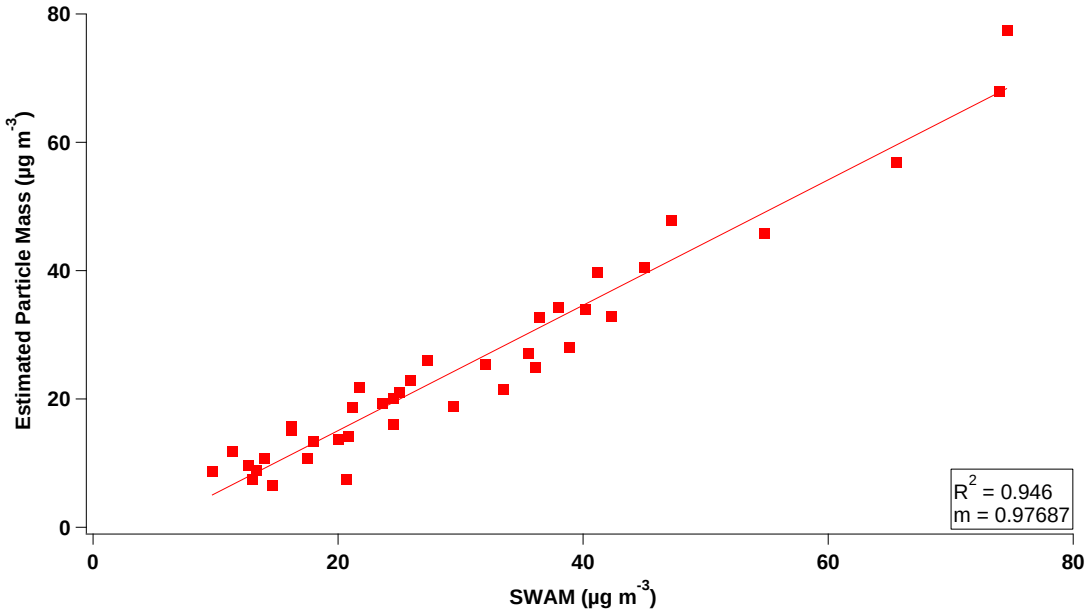

Figure A.2. Plot of estimated daily average PM2.5 mass concentration (corrected TEOM data) versus the measured daily average PM_{10} mass concentration measured using a SWAM 5A monitor in Enniscorthy during the SAPPHIRE monitoring campaign, 08 January 2015 to 17 February 2015. Reproduced from work originally carried out by Dr Eoin McGillicuddy.

Appendix III

The frequency distributions of wind directions recorded during the AEROSOURCE monitoring campaigns are presented below, in addition to the wind rose plots for each season. These distributions were used to calculate the predominant wind directions for each season. During this study, summer was defined as June, July and August, autumn was defined as September, October and November, winter was defined as December, January and February, and spring was defined as March, April and May.

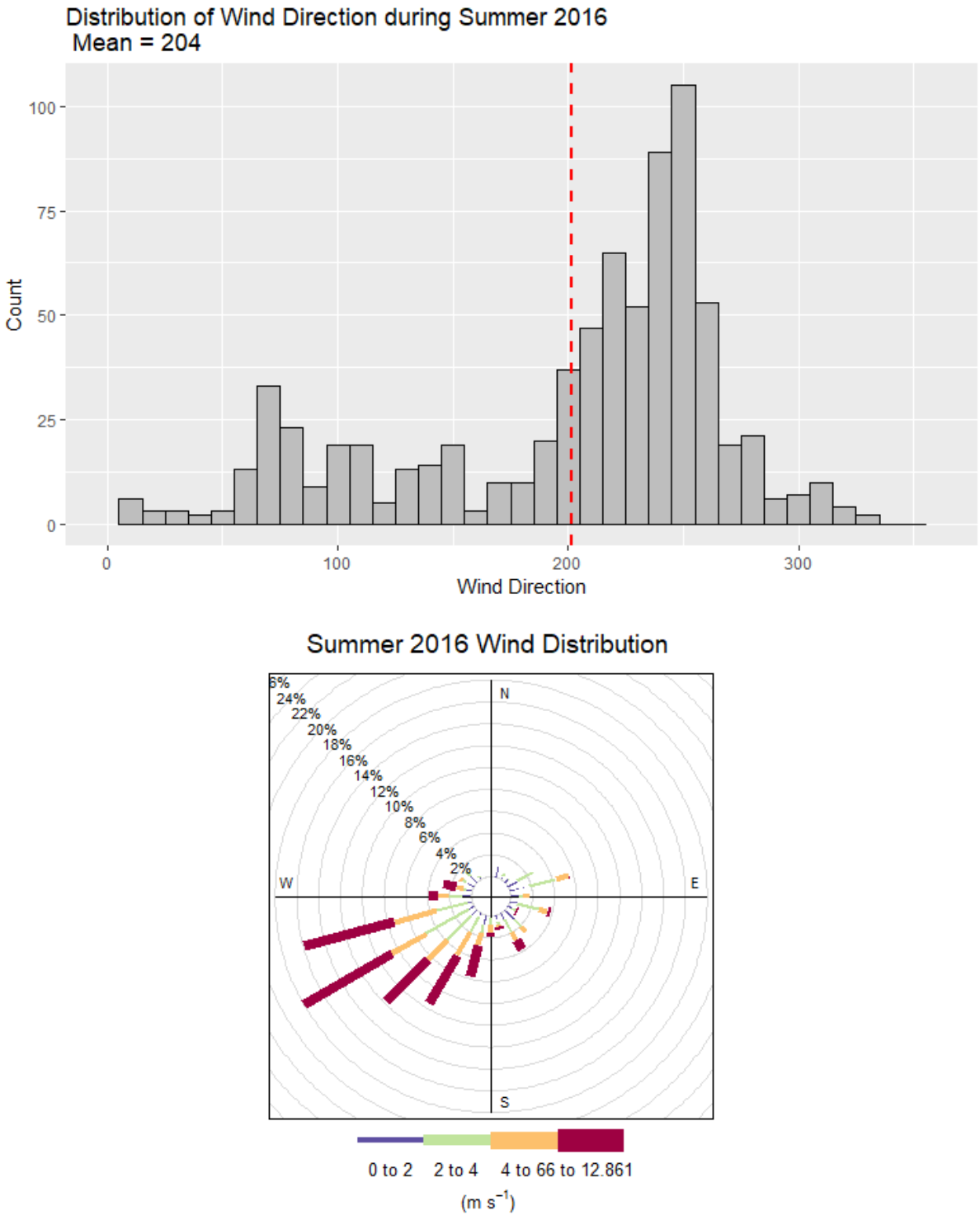

Figure A.3. Frequency distribution of recorded wind direction (top) and the wind rose distribution showing wind speed as a function of direction (bottom) for the summer 2016 period.

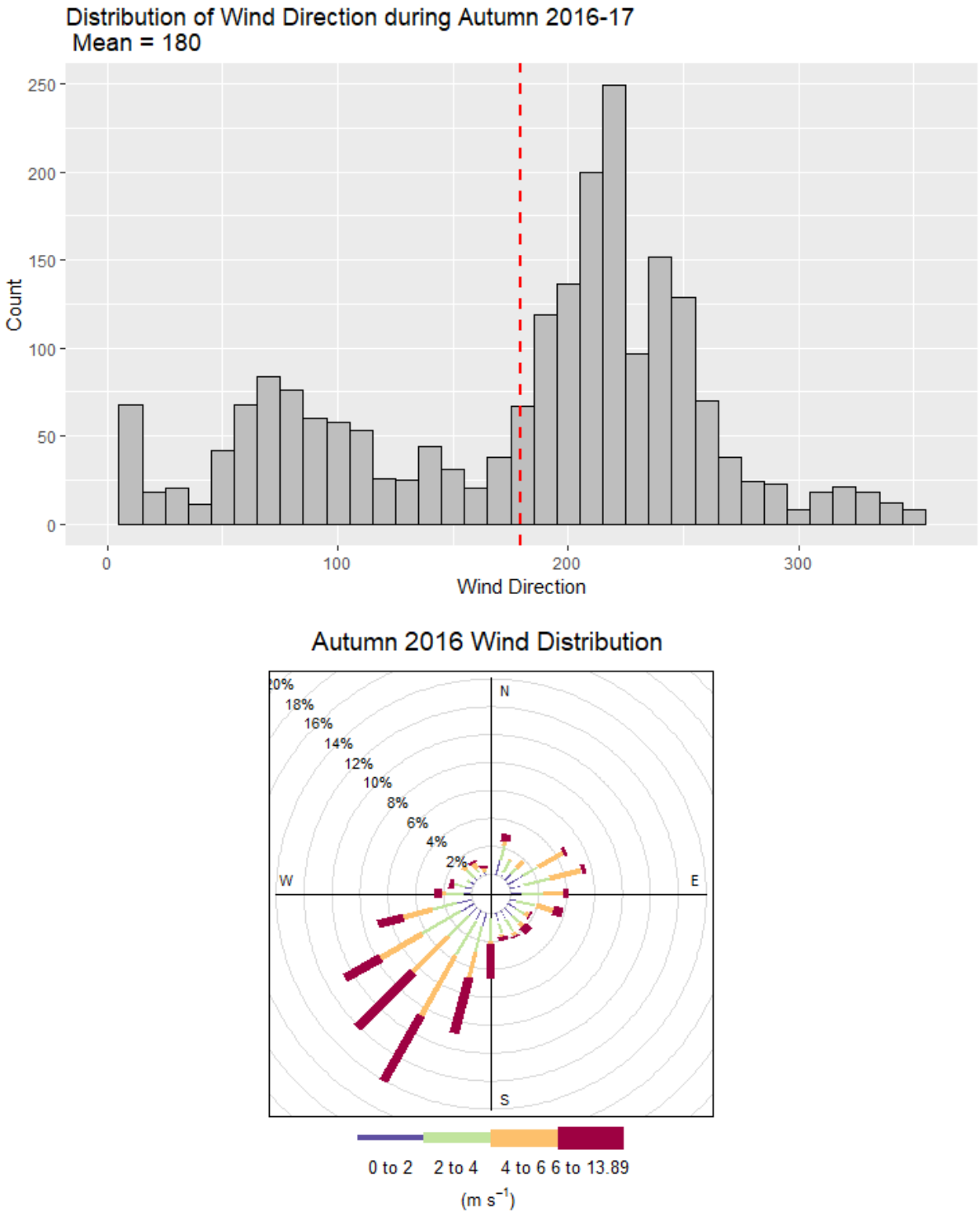

Figure A.4. Frequency distribution of recorded wind direction (top) and the wind rose distribution showing wind speed as a function of direction (bottom) for the autumn 2016 period.

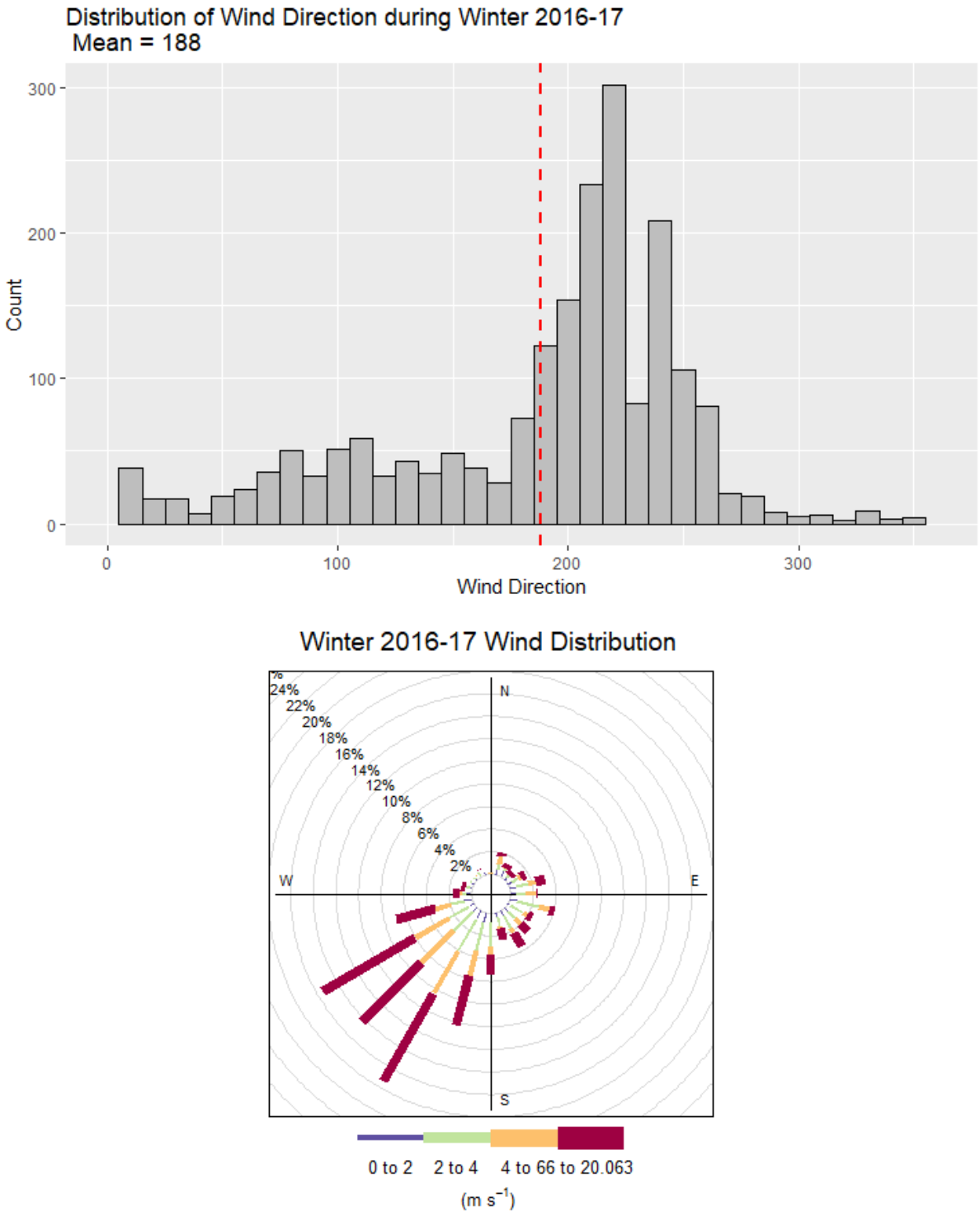

Figure A.5. Frequency distribution of recorded wind direction (top) and the wind rose distribution showing wind speed as a function of direction (bottom) for the winter 2016-17 period.

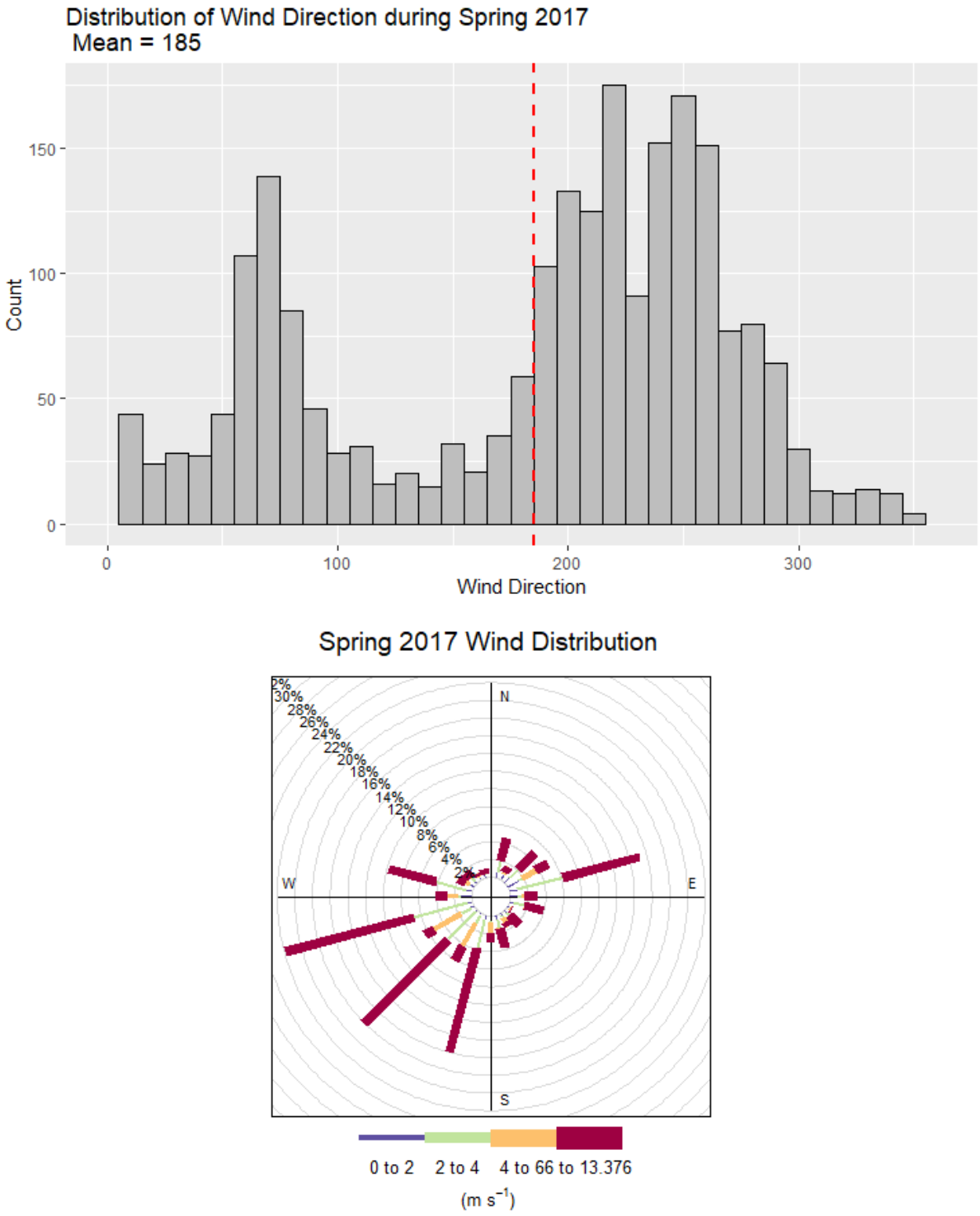

Figure A.6. Frequency distribution of recorded wind direction (top) and the wind rose distribution showing wind speed as a function of direction (bottom) for the spring 2017 period.

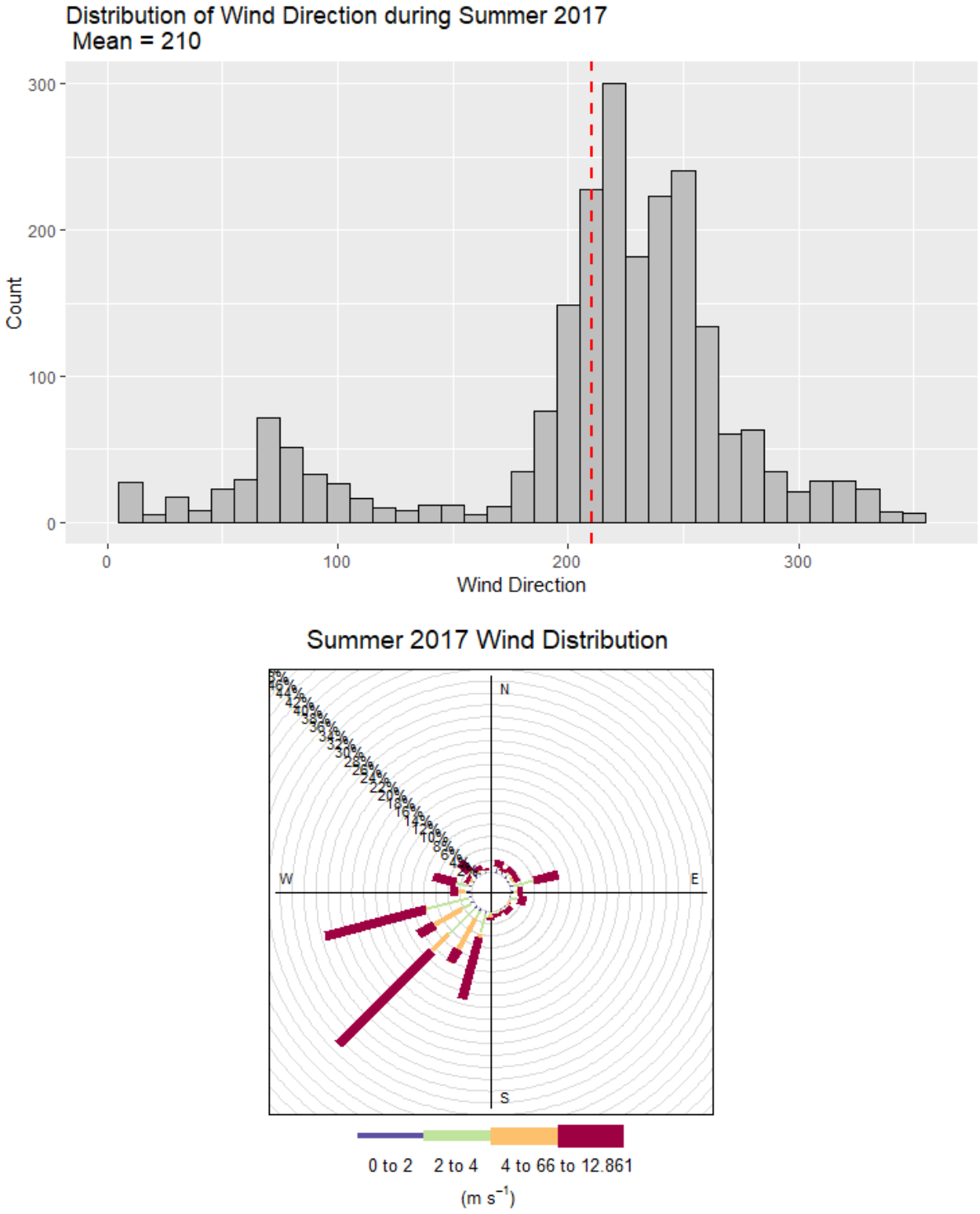

Figure A.7. Frequency distribution of recorded wind direction (top) and the wind rose distribution showing wind speed as a function of direction (bottom) for the summer 2017 period.

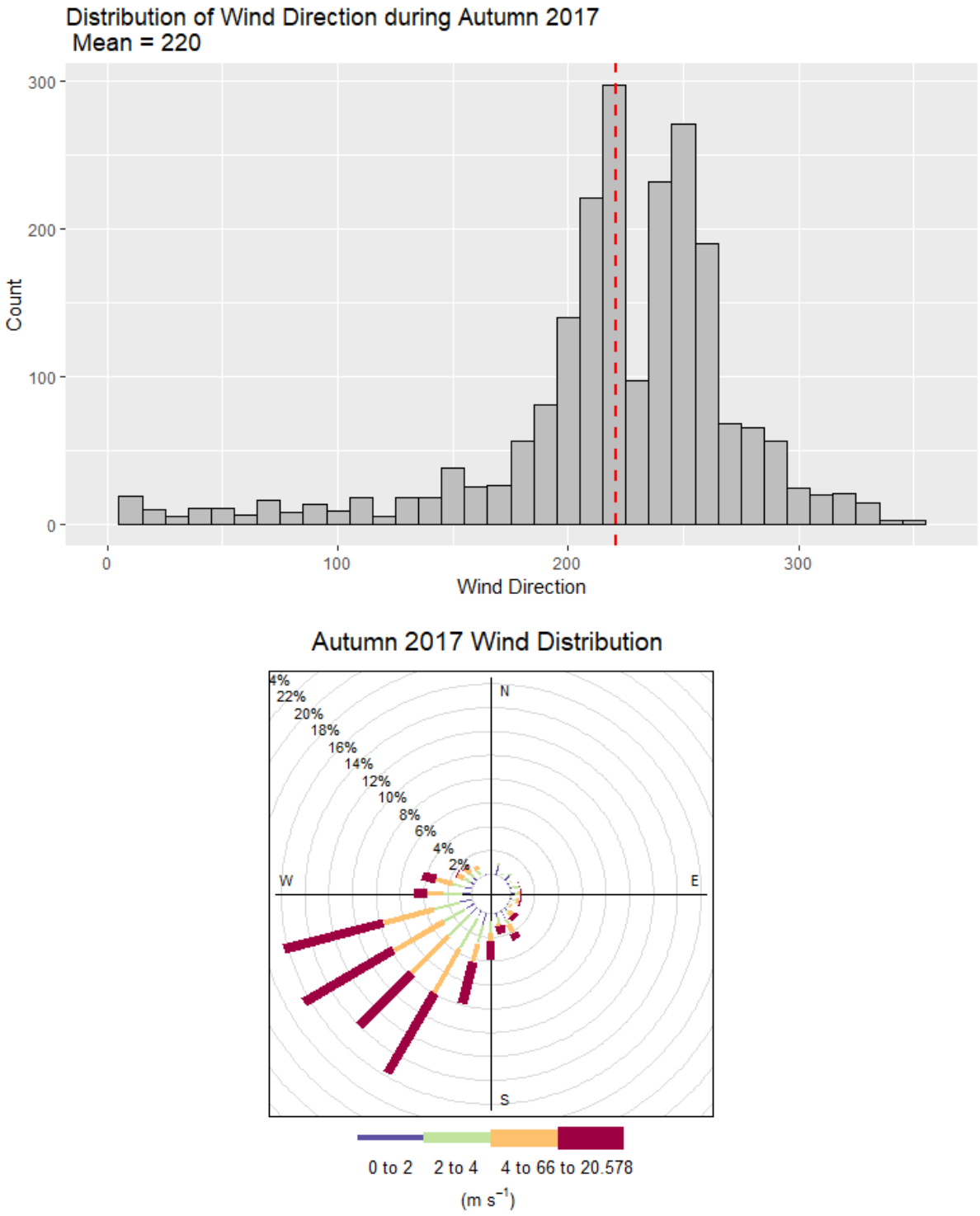

Figure A.8. Frequency distribution of recorded wind direction (top) and the wind rose distribution showing wind speed as a function of direction (bottom) for the autumn 2017 period.

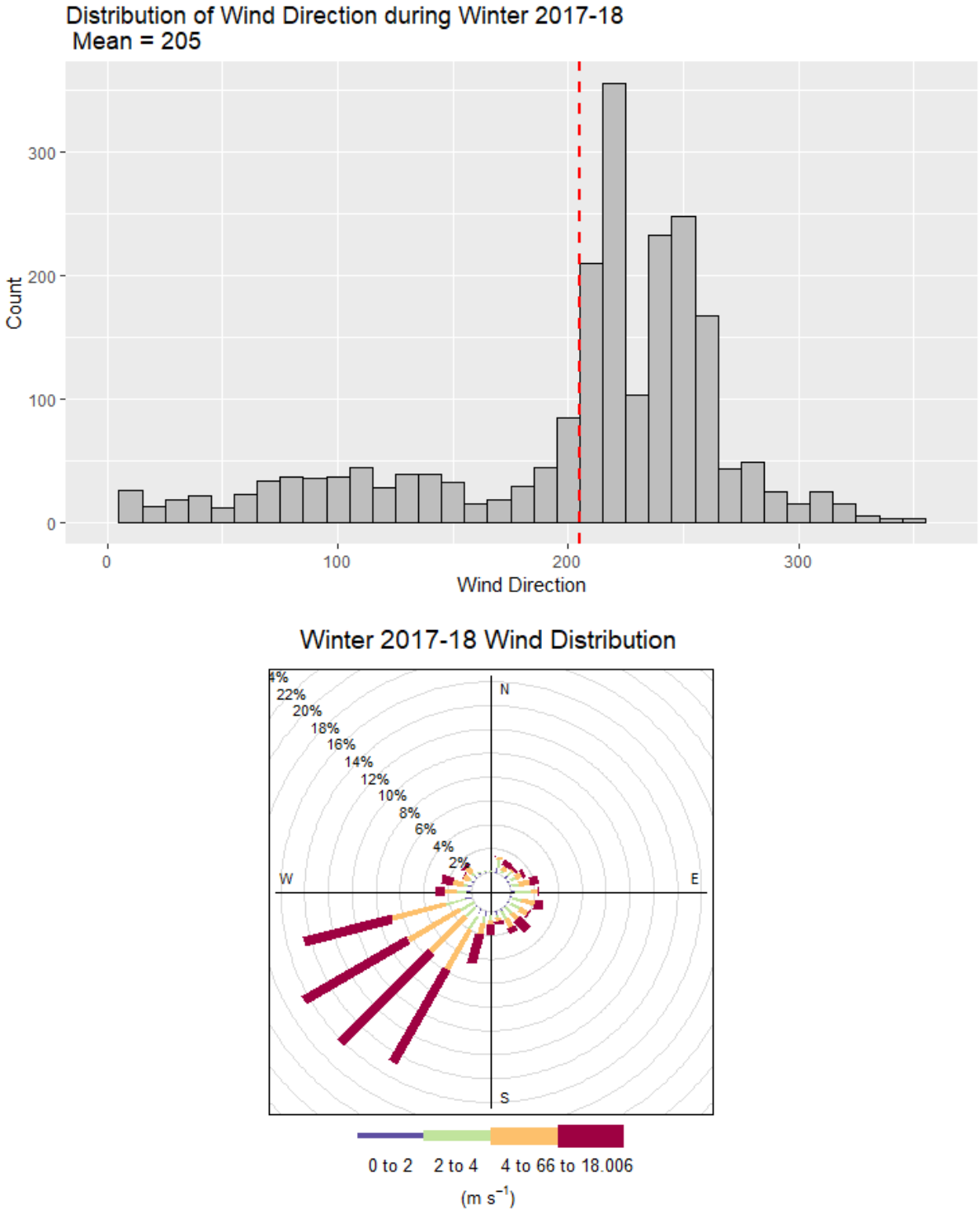

Figure A.9. Frequency distribution of recorded wind direction (top) and the wind rose distribution showing wind speed as a function of direction (bottom) for the winter 2017-18 period.

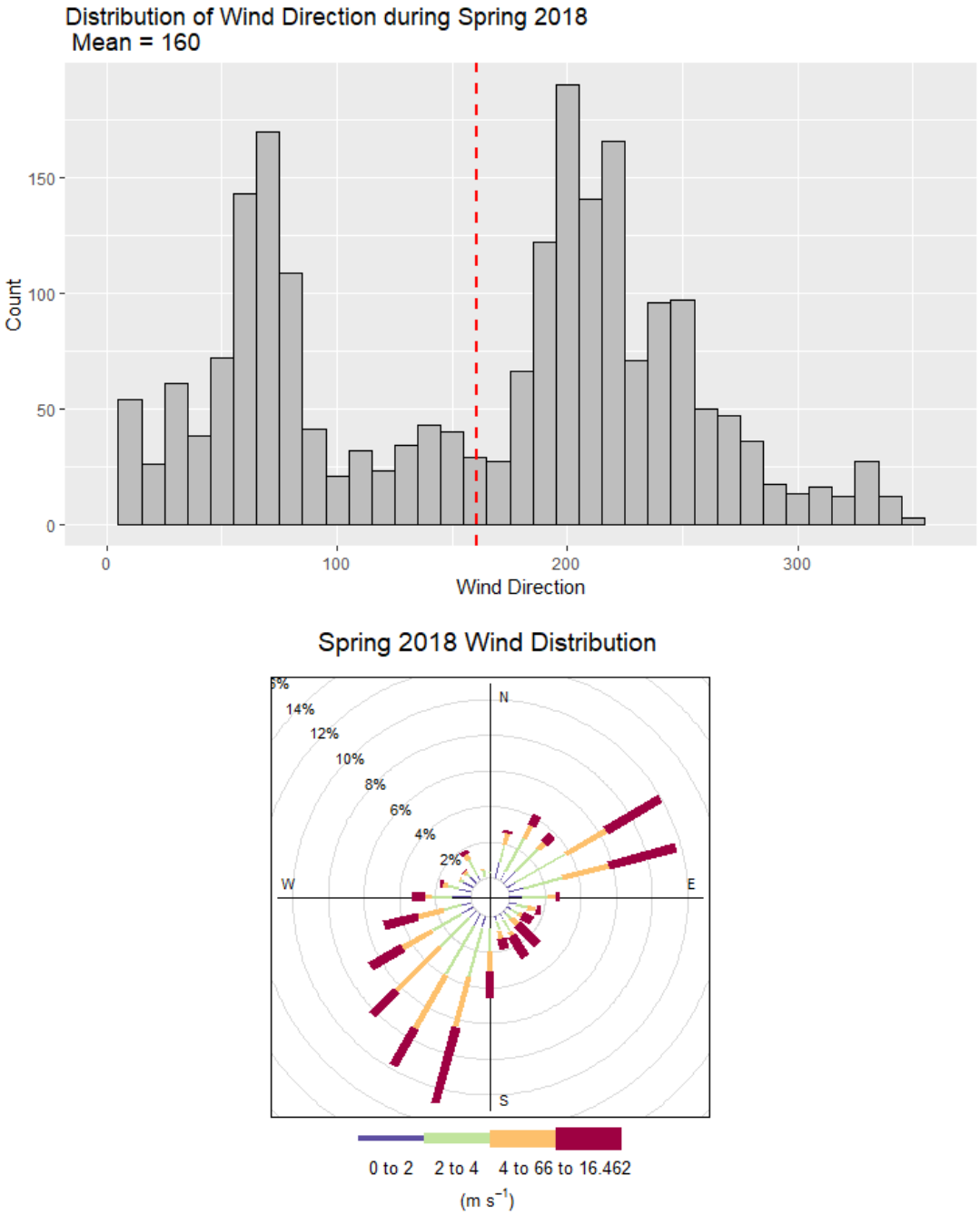

Figure A.10. Frequency distribution of recorded wind direction (top) and the wind rose distribution showing wind speed as a function of direction (bottom) for the spring 2018 period.

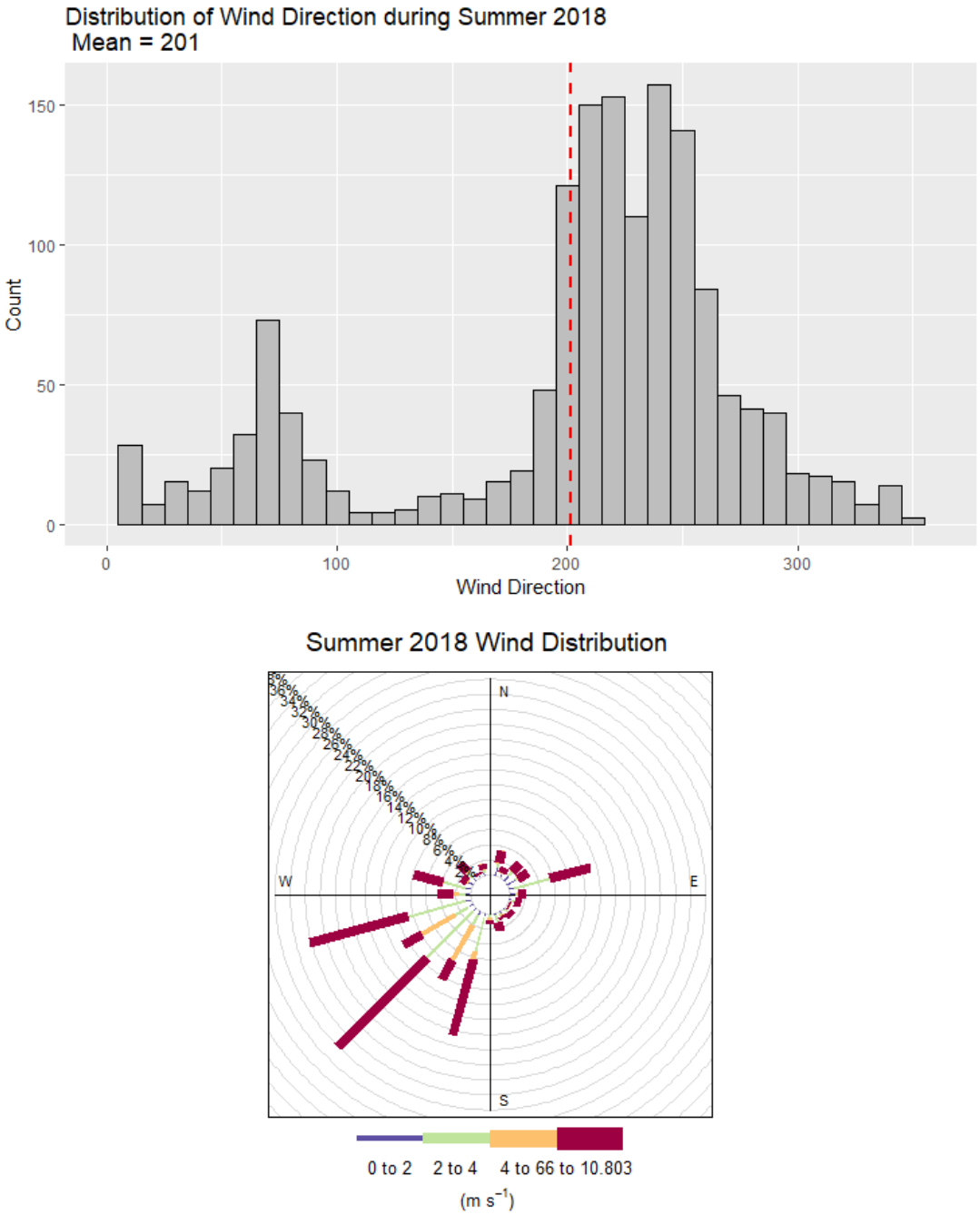

Figure A.11. Frequency distribution of recorded wind direction (top) and the wind rose distribution showing wind speed as a function of direction (bottom) for the summer 2018 period.